Investigating the role of DNA double strand break repair in determining sensitivity to radiotherapy fraction size









Thesis submitted by Dr Navita Somaiah of Wolfson College

for the degree of D.Phil Radiobiology during Hilary term, 2013

Supervised by Professor Thomas Helleday at the Gray Institute for Radiation Oncology & Biology, University of Oxford,

Professor John Yarnold at The Royal Marsden NHS Foundation Trust and

The Institute of Cancer Research, Surrey and

Dr Kai Rothkamm at the Health Protection Agency, Didcot, UK

Declaration

This work was completed under the supervision of Professor Thomas Helleday, Professor John Yarnold and Dr Kai Rothkamm.

The work was carried out at The Gray Institute for Radiation Oncology and Biology, Oxford in collaboration with The Royal Marsden NHS Foundation Trust, Surrey.

I confirm that the work presented in this thesis is my own. Where information is derived from other sources, I confirm that this has been indicated in the thesis.

Navita Somaiah

Dedication

I would like to dedicate this thesis to my parents

who are a true inspiration in every walk of life.

Acknowledgements

I would like to say a very special thank you to my brilliant supervisors Thomas Helleday, Kai Rothkamm and John Yarnold for their unfailing support and for providing me with this incredible opportunity to develop my scientific research skills. Working under their guidance has been, without a doubt, the best experience in my professional career so far.

I would like to thank Breast Cancer Campaign and Cancer Research UK for supporting me and facilitating this research.

I owe a lot to the entire Yarnold team at The Royal Marsden and Institute for Cancer Research. They have been without a doubt one of the most fantastic teams I have ever worked with. In particular, my heartfelt thanks go to Lone Gothard for her untiring support, encouragement and patience and above all for being a true friend whose advice I continue to value. My thanks also go to Ann Pearson and Sue Davies for their tremendous help with patient sample collection and data management. I would also like to mention Grace Sharp, Clair Wills and Sharon Gleeson who along with the others made the whole experience thoroughly enjoyable.

I would also like to thank the entire Helleday lab at the Gray Institute for Radiation Oncology and Biology, Oxford for being a fantastic team and making the long hours spent in the lab enjoyable. In particular, I would like to thank Cecilia Lundin, Ponnari Gottipatti, Tina Bauerschmidt and Bastiaan Evers for their help with designing the experiments, cell culture techniques, running western blots and invaluable advice. I would also like to thank Mick Woodcock for helping me with my first ever clonogenic assay and flow cytometry experiments.

I am extremely grateful to Frances Daley at the Gray Institute for Radiation Oncology and Biology (now at the Institute for Cancer Research) for patiently teaching me all the techniques involved in cellular and histopathology and for her priceless troubleshooting advice that I continue to rely on. I also gratefully acknowledge statistical input from Roger A'Hern at the Institute of Cancer Research. I am extremely thankful to all the patients who donated samples for this research, without which this work could not have been undertaken.

Finally, I would like to thank my family for their continuous encouragement and unflinching support and my little Maya for her patience.

Table of Contents

Page

Title page 1

Declaration 2

Dedication 3

Acknowledgements 4

Table of contents 6

Abstract 14

List of figures 17

List of tables 20

List of abbreviations 21

Chapter 1: Introduction 23

1.1 Fractionation in radiotherapy: From multiple doses to single fractions and back! 23

1.2 Early radiobiological research and the NSD formula 24

1.3 The linear quadratic (LQ) model 24

1.4 The 5R's of radiobiology 28

1.5 Altered fractionation schedules in clinical radiotherapy 28

1.6 Hypofractionation – the breast cancer experience 30

1.6.1 Dose escalation strategies by modifying dose per fraction as opposed to number of fractions 36

1.6.2 Benefits of hypofractionation 38

1.6.3 Concerns regarding hypofractionation 39

1.7 Clinical relevance of understanding sensitivity to radiotherapy fraction size 43

1.8 Target cell theory and the cellular basis of fractionation sensitivity 47

1.9 Fraction size sensitivity and proliferative status of normal and malignant tissues 49

1.10 Fraction size sensitivity is not a fixed property of cells or tissues 52
1.11 DSB repair capacity and kinetics are the molecular correlates of cellular recovery 54
1.12 Implications for the fractionation sensitivity of tumours 57
1.13 Testing molecular models in human skin 59
1.14 AIMS OF THE THESIS 60

Chapter 2: Materials and Methods 61

2.1 Materials 61
2.1.1 Chemicals & common buffers 61
2.1.2 Reagents used in histology and immunohistochemistry 62
2.1.3 Primary antibodies used in immunohistochemistry and immunofluorescence 63
2.1.4 Secondary antibodies used in immunohistochemistry and immunofluorescence 64
2.1.5 Cell lines 64
2.1.6 Reagents and plastics used in tissue culture 65
2.1.7 DNA repair inhibitors 65
2.1.8 Reagents used in FACS analysis 66
2.2 Methods 66
2.2.1 Ethics approval 66
2.2.2 Patients 66
2.2.3 Radiotherapy 66
2.2.4 Human tissue work 67
2.2.4.1 Tissue collection 67
2.2.4.2 Tissue processing 67
2.2.4.2.1 Cutting paraffin sections 67
2.2.4.2.2 Cutting frozen sections 68
2.2.4.2.3 Haematoxylin and eosin protocol 68
2.2.4.3 Immunohistochemistry 68

2.2.4.4	Scoring methods for immunohistochemistry	70
2.2.4.5	Immunofluorescence technique	70
2.2.4.6	Scoring methods for immunofluorescence	71
2.2.5	Mammalian cell culture	71
2.2.5.1	Cell culture conditions	71
2.2.5.2	Thawing liquid nitrogen stocks	72
2.2.5.3	Freezing cell stocks	72
2.2.5.4	*Mycoplasma* testing	73
2.2.6	Preparation and quantification of mammalian cell extracts	73
2.2.6.1	Whole cell extracts	73
2.2.6.2	Bradford assay	74
2.2.7	Visualisation of proteins by Western Blotting and chemiluminescent detection	74
2.2.7.1	Electrophoresis	74
2.2.7.2	Nitrocellulose transfer	75
2.2.7.3	Immunodetection	75
2.2.7.4	Chemiluminescence	76
2.2.7.5	PARP activity assay	77
2.2.8	Cell-based assays	78
2.2.8.1	Clonogenic survival assay	78
2.2.8.1.1	Acute dose survival assays	78
2.2.8.1.2	Fractionated dose survival assays	78
2.2.8.1.3	Fractionated dose survival assays with inhibitors	79
2.2.8.2	Irradiation	80
2.2.8.3	Flow Cytometry: Cell-cycle analysis	80
2.2.8.4	Immunocytochemistry: IN Cell analysis	81
2.2.8.4.1	DNA DSB induction and repair in each of the 4 CHO cell lines	81
2.2.8.4.2	DNA DSB induction and repair analysis in wild type cells with or without DNA repair inhibitors	84
2.2.9	Statistical analysis and sample size	88

Chapter 3: Results-1 **89**

The relationship between homologous recombination repair and the sensitivity of human epidermis to the size of daily doses over a 5-week course of breast radiotherapy

3.1 Introduction 89

3.2 Results 91

3.2.1 Patient characteristics 91

3.2.2 Proliferation kinetics of human basal epidermis during 5 weeks of radiotherapy 93

3.2.3 Cell cycle checkpoint responses during radiotherapy 95

3.2.4 Homologous recombination repair in basal epidermis during radiotherapy 98

3.2.5 DNA DSB repair kinetics in cycling vs non-cycling cells 101

3.2.6 Epidermal stem cells 104

3.2.6.1 Identifying basal epidermal stem cells 104

3.2.6.2 Variation in the β-1Integrin positive population during a course of RT 106

3.2.6.3 DNA DSB repair in β-1Integrin positive cells during RT 108

3.3 Discussion 111

Chapter 4: Results-2 **116**

The relationship between DNA double strand break repair, cellular radioresistance and fraction size sensitivity in CHO cell lines

4.1 Introduction 116

4.2 Results 117

4.2.1 Clonogenic cell survival in wild type and DNA repair defective CHO cell lines 117

4.2.1.1 Acute radiation dose survival curves 117

4.2.1.2 Fractionated irradiation survival curves – 1 Gy/day, 4 Gy/day, 0.1 Gy/day 118
4.2.1.3 Sensitivity to changes in dose per fraction as measured by clonogenic survival in wild type and DNA repair defective CHO cells 121
4.2.2 Cell cycle changes in response to fractionated irradiation 123
4.2.2.1 Cell line reliant on HR accumulates in S/G2 phase of the cell cycle 123
4.2.3 DNA DSB repair kinetics during fractionate IR in wild type and DNA defective CHO cells 126
4.2.3.1 DNA DSB repair kinetics with 1 Gy/day 126
4.2.3.2 DNA DSB repair kinetics with 4 Gy/day 129
4.2.4 Homologous recombination repair kinetics in wild type and DNA repair defective CHO cell during fractionated IR 131
4.2.4.1 RAD51 foci kinetics after 1 Gy/day 131
4.2.4.2 RAD51 foci kinetics after 4 Gy/day 133
4.3 Discussion 135

Chapter 5: Results-3 139

The effect of different small molecule inhibitors of DNA repair on fractionated radiation responses

5.1 Introduction 139
5.1.1 DNA Double-Strand Break Response: DNA Repair and Cell Cycle Checkpoints 140
5.2 ATM as a Target for Radiosensitisation 141
5.2.1 Inhibitors of ATM 143
5.2.2 Results 144
5.2.2.1 Western blot testing the ATM inhibitor KU55933 144
5.2.2.2 Clonogenic cell survival following radiation in wild type CHO cells (AA8) with or without ATM inhibitor 146
5.2.2.2.1 Single radiation dose clonogenic survival curves 146

5.2.2.2.2 Fractionated irradiation clonogenic survival curves – 1 Gy/day 148
5.2.2.3 Sensitivity to changes in dose per fraction as measured by clonogenic survival in AA8 cells with or without ATMi 150
5.2.2.4 DNA DSB repair kinetics during fractionated IR in AA8 cells with or without ATMi 152
5.2.2.5 Homologous recombination repair kinetics in AA8 cells with or without ATMi during fractionated IR 157
5.2.3 Discussion 162
5.3 DNA-PK as a Target for Radiosensitisation 165
5.3.1 Inhibitors of DNA-PK 166
5.3.2 Results 166
5.3.2.1 Western blot testing the DNA-PK inhibitor NU7026 (KU51777) 166
5.3.2.2 Clonogenic cell survival following radiation in wild type CHO cells (AA8) with or without DNAPKcs inhibitor 169
5.3.2.2.1 Single radiation dose clonogenic survival curves 169
5.3.2.2.2 Fractionated irradiation clonogenic survival curves – 1 Gy/day 171
5.3.2.3 Sensitivity to changes in dose per fraction as measured by clonogenic survival in AA8 cells with or without DNA-PKi 173
5.3.2.4 DNA DSB repair kinetics during fractionated IR in AA8 cells with or without DNA-PKi 175
5.3.2.5 Homologous recombination repair kinetics in AA8 cells with or without DNAPKcsi during fractionated IR 180
5.3.3 Discussion 185
5.4 PARP as a target for radiosensitisation 189
5.4.1 PARP-1 and DNA repair 189
5.4.1.1 PARP inhibition as a therapeutic strategy 190
5.4.1.2 PARP inhibitors as radiosensitisers 191
5.4.2 Results 192
5.4.2.1 PARP inhibitor activity assay 192

5.4.2.2 Clonogenic cell survival following radiation in wild type CHO cells (AA8) with or without PARP inhibitor 193
5.4.2.2.1 Acute dose clonogenic survival 193
5.4.2.2.2 Fractionated irradiation clonogenic survival curves – 1 Gy/day 195
5.4.2.2.3 Sensitivity to changes in dose per fraction as measured by clonogenic survival in AA8 cells with or without PARPi 197
5.4.2.3 DNA DSB repair kinetics during fractionated IR in AA8 cells with or without PARPi 199
5.4.2.4 Homologous recombination repair kinetics in AA8 cells with or without PARPi during fractionated IR 204
5.4.3 Discussion 209

Chapter 6: Final discussion 211

6.1 Cell and molecular basis of fractionation sensitivity 211
6.2 The proposed model of fractionation sensitivity 213
6.3 Deregulation of cell cycle controls and DNA damage responses modify the fractionation sensitivity of cancer 214
6.4 Influence of hypoxia on fractionation sensitivity 215
6.5 Modelling the change in fractionation sensitivity with time during radiotherapy 216

Chapter 7: Future directions - Biomarkers of sensitivity to fraction size in curative radiotherapy 219

7.1 Aims and Objectives 219
7.2 Hypotheses 220
7.2.1 Hypothesis 1 220
7.2.2 Hypothesis 2 220
7.3 Future translational research plan 222
7.3.1 *In vitro* studies 222
7.3.1.1 Testing hypothesis 1 222
7.3.1.2 Testing hypothesis 2 222

7.3.1.3 Testing the effect of small molecule inhibitors on radiotherapy fractionation response 223
7.3.2 Implications for translational research 223
7.3.3 Molecular pathology 224
7.3.3.1 Identification of human tumour biomarkers 224
7.3.4 Clinical evaluation- prospective randomised trial 224

Publications arising from this work 226

References 229

Abstract

The dose of curative radiotherapy (RT) for cancer is commonly limited by adverse effects presenting years later. Late reacting normal tissues are, on average, more sensitive to the size of daily doses (fractions) than early reacting normal tissues and cancers. Clinical trials have shown breast cancers to be one exception to this rule, in that they are as sensitive to fraction size as the late reacting normal tissues. This has led to the adoption of hypofractionation (use of fractions >2.0 Gy) in the UK for the adjuvant therapy of women with early breast cancer. An understanding of the molecular basis of fraction size sensitivity is necessary to improve radiotherapy outcome. In this respect, it is relevant that late reacting normal tissues have lower proliferative indices than early reacting normal tissues and most cancers. Here, we test the hypothesis that tissue sensitivity to fraction size is determined by the DNA repair systems activated in response to DNA double strand breaks (DSB), and that these systems vary according to the proliferative status of the tissue.

Clinical data suggest that sensitivity of epidermis to fraction size varies over a 5-week course of RT. It resembles a late reacting normal tissue in its sensitivity to fraction size in the first week of RT and loses fractionation sensitivity by weeks 4 & 5. We used this feature of human epidermis to test how fractionation sensitivity and DNA repair changed over 5 weeks of RT. Breast skin biopsies were collected 2 h after the 1^{st}, 5^{th} and last fractions from 30 breast cancer patients prescribed 50 Gy/25fractions/5weeks. Sections of epidermis were co-stained for Ki67, cyclin A, p21, RAD51, 53BP1 and β1-Integrin**.** After 5 weeks of radiotherapy, the mean basal Ki67 density increased from 5.72 to 15.46 cells per mm of basement membrane ($p=0.002$), of which the majority were in S/G2 phase as judged by cyclin A staining ($p<0.0003$). The p21 index rose from 2.8% to 87.4% ($p<0.0001$) after 25 fractions, indicating cell cycle arrest in the basal epidermis. By week 5, there was a 4-fold

increase (p=0.0003) in the proportion of Ki67-positive cells showing RAD51 foci, confirming an association between activation of homologous recombination (HR) and loss of tissue fractionation sensitivity.

Subsequently, CHO cell lines deficient in specific DNA repair genes were used to test molecular pathways involved in sensitivity to fraction size. We irradiated AA8 (WT), irs-1SF (XRCC3-), V3-3 (DNA-PK-) and EM9 (XRCC1-) with 16 Gy gamma-rays in 1 Gy daily fractions over 3 weeks or 16 Gy in 4 Gy daily fractions over 4 days, and studied clonogenic survival, DNA double-strand break (DSB) repair kinetics (RAD51 & 53BP1 staining) and cell cycle analysis using flow cytometry. We found that wild-type and DNA repair defective cells acquire resistance to fractionated radiotherapy by accumulation in the late S/G2 phase of the cell cycle and increased use of HR. In contrast, the irs1SF cells, defective in HR, failed to acquire radioresistance and remained equally sensitive to ionizing radiation throughout the 3-week treatment. We also demonstrated that sensitivity to fraction size is associated with functional NHEJ. It was undetectable in V3-3 cells lacking NHEJ and thereby likely relying on HR. The high fidelity of HR, which is independent of induced DNA damage levels and hence, of fraction size, may explain the low fractionation sensitivity of cells using HR to repair radiation induced DSBs.

We then wanted to investigate the modifying effects of small molecule inhibitors of DNA repair on fractionation responses. To this end we tested the effects of adding selected ATM, PARP, and DNAPK inhibitors to fractionated radiotherapy in WT CHO cells. Our results showed that the ATM inhibitor had a significant radiosensitising effect when combined with fractionated RT and resulted in loss of sparing effect of fractionation in wild type CHO cells, an observation that may be

clinically relevant. We also examined DNA DSB repair kinetics (RAD51 & 53BP1 foci) with these drugs in the context of fractionated IR.

List of figures

		Page
Chapter 1		
Fig. 1.1	Dose response curves - Classical model faces a challenge	45
Chapter 2		
Fig. 2.1	96 well plate lay out for fractionated IR experiments comparing 4 different CHO cell lines	83
Fig. 2.2	96 well plate lay out for fractionated IR experiment (1 Gy/day) with AA8 cells with or without inhibitor drugs	86
Fig. 2.3	96 well plate lay out for control experiment (no IR) with AA8 cells	87
Chapter 3		
Fig. 3.1	Changes in Ki67 expression in human epidermis during RT	94
Fig. 3.2	p21 expression in human epidermis	96
Fig. 3.3	A & B. Serial 3 µm sections of epidermis stained with Cyclin A and p21	97
Fig. 3.4	Changes in RAD51 expression during a course of RT	99
Fig. 3.5	Changes in RAD51 expression during a course of RT	100
Fig. 3.6	Identifying DNA DSB in human epidermis	102
Fig. 3.7	DNA DSB repair in proliferating vs non-proliferating cells during RT	103
Fig. 3.8	Identifying basal epidermal stem cells	105
Fig. 3.9	Changes in β1 integrin expression with RT	107
Fig. 3.10	DNA DSB repair in β-1Integrin positive cells during RT	109
Fig. 3.11	Triple staining with β1 integrin, Ki67 and 53BP1	110
Chapter 4		
Fig. 4.1	Acute dose survival curves (semi-log) for all 4 cell lines (AA8 (WT), EM9 (XRCC1-), V3-3 (DNA-PKcs-), irs1SF (XRCC3-)) at doses of 0, 1, 2, 3, 4, 6 and 8 Gy	118
Fig. 4.2	Clonogenic survival (semi-log) following fractionated IR in 4 CHO cell lines: AA8 (WT), EM9 (XRCC1-), V3-3 (DNA-PKcs-), irs1SF (XRCC3-)	120

Fig. 4.3 Comparison of survival between high dose per fraction vs low dose per fraction 122
Fig. 4.4 Cell cycle changes with fractionated IR 1 Gy/day over 2 weeks with a weekend gap 124
Fig. 4.5 53BP1 foci analysis with 1 Gy/day over 2 weeks with a weekend gap: measured as % positive cells with >5 53BP1 foci 127
Fig. 4.6 53BP1 foci analysis with 1 Gy/day over 2 weeks with a weekend gap: measured as mean 53BP1 foci per cell 128
Fig. 4.7 53BP1 foci analysis with 4 Gy/day 130
Fig. 4.8 RAD51 foci analysis with 1 Gy/day over 2 weeks with a weekend gap 132
Fig. 4.9 RAD51 foci analysis with 4 Gy/day 134

Chapter 5

Fig. 5.1 Western Blot testing the ATM inhibitor KU55933 145
Fig. 5.2 Acute dose clonogenic survival curves (semi-log) comparing WT AA8 cells with or without the ATMi and HR mutant irs-1SF cells (XRCC3-) 147
Fig. 5.3 Fractionated IR clonogenic survival curves (semi-log) testing 1 Gy/day in WT AA8 cells with or without the ATMi and HR mutant irs-1SF 149
Fig. 5.4 Comparison of survival between high dose per fraction vs low dose per fraction with or without ATMi 151
Fig. 5.5 DNA DSB repair kinetics using 53BP1 foci analysis during fractionated IR in AA8 cells with or without ATMi 153
Fig. 5.6 Homologous recombination repair kinetics in AA8 cells with or without ATMi during fractionated IR 158
Fig. 5.7 Western Blot testing the DNA-PK inhibitor NU7026 168
Fig. 5.8 Acute dose clonogenic survival curves (semi-log) comparing WT AA8 cells with or without the DNA-PKi and NHEJ mutant V3-3 cells 170
Fig. 5.9 Fractionated IR clonogenic survival curves testing 1 Gy/day in WT AA8 cells with or without the DNA-PKi and NHEJ mutant V3-3 cells 172
Fig. 5.10 Comparison of survival between high dose per fraction vs low dose per fraction with or without DNA-PKcsi 174

Fig. 5.11 DNA DSB repair kinetics using 53BP1 foci analysis during fractionated IR in AA8 cells with or without DNAPKcsi 176
Fig. 5.12 Homologous recombination repair kinetics in AA8 cells with or without DNAPKi during fractionated IR 181
Fig. 5.13 Acute dose clonogenic survival curves comparing WT AA8 cells with or without the PARPi and BER mutant EM9 cells 194
Fig. 5.14 Fractionated IR survival curves testing 1 Gy/day in WT AA8 cells with or without the PARPi and BER mutant EM9 cells 196
Fig. 5.15 Comparison of survival between high dose per fraction vs low dose per fraction without without PARPi 198
Fig. 5.16 DNA DSB repair kinetics using 53BP1 foci analysis during fractionated IR in AA8 cells with or without PARPi 200
Fig. 5.17 Homologous recombination repair kinetics in AA8 cells with or without PARPi during fractionated IR 205

Chapter 6

Fig. 6.1 Model of fractionation sensitivity 213

List of tables

		Page
Chapter 1		
Table 1.1	Fractionation sensitivities of various early and late reacting tissues as denoted by their α/β ratios	27
Table 1.2	Main characteristics of the conventional and altered fractionation schedules	29
Table 1.3	Selected characteristics of randomised trials of breast hypofractionation	32
Table 1.4	Cosmesis and normal tissue effects of hypofractionated compared to standard breast radiation therapy	33
Table 1.5	Rates of Local recurrence in the altered fractionation trials	34
Table 1.6	UK FAST Forward Trial (N=4000), primary end point of local tumour control	42
Table 1.7	Average α/β ratios of various tumours	46
Table 1.8	Potential doubling times (T_{pot}) and volume doubling times (T_d) for various tumours and consequent fractionation regimens	51
Chapter 2		
Table 2.1	Chemical reagent information	61
Table 2.2	Common buffer information	62
Table 2.3	Primary antibodies used in immunohistochemistry and immunofluorescence	63
Table 2.4	Secondary antibodies used in immunohistochemistry and immunofluorescence	64
Table 2.5	Antibodies used in western blotting	76
Chapter 3		
Table 3.1	Patient characteristics	92
Chapter 7		
Table 7.1	Possible biomarkers of fractionation sensitivity	221

List of abbreviations

53bp1	p53 binding protein 1
γ-H2AX	Phosphorylated histone H2AX
ATM	Ataxia telangiectasia mutated
ATR	Ataxia telangiectasia and Rad3 related
BER	Base excision repair
BRCA1	Breast cancer 1 early onset
BRCA2	Breast cancer 2 early onset
BSA	Bovine serum albumin
CHK1	Checkpoint homolog 1
CHO	Chinese hamster ovarian
DAB	diaminobenzadine
DAPI	4,6 diamidino-2-phenylindole
DMSO	Dimethyl sulfoxide
DNA	Deoxyribonucleic acid
DNA-PK	DNA-dependent protein kinase
DNA-PKcs	DNA-dependent protein kinase, catalytic subunit
DSB	DNA double strand breaks
Gy	Gray
HIF-1α	Hypoxia inducible factor 1
HR	Homologous recombination
HRP	Horse radish peroxidise
ICRU	International Commission on Radiation Units and Measurements
IMRT	Intensity modulated radiotherapy
IR	Irradiation
LQ	Linear quadratic

MCSP	Melanoma chondroitin sulphate proteoglycan
MV	Megavoltage
NHEJ	Non-homologous end joining
NSD	Nominal standard dose
p53	Tumour protein 53
PARP	Poly ADP-ribose polymerase
PARP1	Poly (adenine diphosphate-ribose) polymerase 1
PARP2	Poly (adenine diphosphate-ribose) polymerase 1
PCNA	Proliferating cell nuclear antigen
PI3K	Phosphoinositide 3-kinase
PBS	Phosphate-buffered saline
RAD51	Radiation sensitivity abnormal 51
RNA	Ribonucleic acid
RNAi	Ribonucleic acid interference
RPA	Replication protein A
shRNA	Short hairpin ribonucleic acid
siRNA	Small interfering ribonucleic acid
RT	Radiotherapy
SEM	Standard error of mean
SSB	Deoxyribonucleic acid single-strand break
TBS	Tris buffer saline
WT	Wild type
XRCC1	X-ray repair cross complementing protein 1
XRCC3	X-ray repair cross complementing protein 3

CHAPTER ONE

Introduction

1.1 Fractionation in radiotherapy: From multiple doses to single fractions and back!

Fractionation was originally introduced to cope with over-heating of early x-ray therapy machines (Kogelnik 1997). With more advanced equipment, single fraction treatments could be tested, but it became evident that “therapia magna sterilans” was clinically ineffective. Radiobiological experiments conducted in the 1920s introduced the concept of fractionation, when it was observed that rams were sterilised without scrotal skin moist desquamation by dividing a single radiation dose into multiple daily fractions (Regaud and Ferroux 1919; Regaud 1923); (Regaud 1977). Regaud, Coutard and Baclesse developed fractionated regimens for clinical use, and in the 1920s Coutard demonstrated uncomplicated cure of laryngeal cancer using daily fractions of 200-250 Rad lasting 2-3 hours over 4-6 weeks to total doses of 7,000 Rad (Coutard 1937). Questions of economics and resources arose early. German radiotherapists were, because of cost, unable to adopt Coutard’s protracted, low dose-rate approach. Instead they used fractionated radiotherapy at high dose-rates per fraction, including multiple fractions per day. By the mid 1930s, daily fractions for 4-6 weeks to total doses of up to 6,500 Rad were being widely used. In the late 1930s, due to a shortfall in machine capacity in Manchester, Paterson reduced the number of fractions to 16 and the dose to 5,000 Rad delivered over 3.2 weeks (Paterson 1936). Over the years this has proved a safe and effective treatment regimen.

1.2 Early radiobiological research and the NSD formula

In the 1930s work by Reisner and Miescher on human and rabbit skin respectively highlighted the importance of dose per fraction on tissue tolerance to radiation (Reisner 1933; Miescher 1935). However, due to Strandqvist's publication in 1944, which placed total dose and treatment duration as the main determinants of both tumour response and normal tissue damage, the already detected impact of dose per fraction on normal tissue reactions fell into oblivion (Strandqvist 1944). Ellis built on the work of Reisner, Mischer, Strandqvist and Cohen and introduced the concept of Nominal Standard Dose (NSD) into clinical radiotherapy as an attempt to enable clinicians to change from one fractionation regimen to another (Ellis 1969).

$$\text{Total dose} = \text{NSD}\ N^{0.24} T^{0.11}$$

The NSD formula seemed to work well for acute reactions when relatively small changes in overall time (T) or fraction number (N) were involved. Unfortunately the original NSD model underestimated the importance of dose per fraction in determining late effects in normal tissues, and early clinical adoption led to unacceptable rates of late adverse effects (Singh 1978; Thames, Withers et al. 1982; Fowler 1984; Fletcher 1991).

1.3 The linear quadratic (LQ) model

The development of technology that permitted evaluation of the proliferative capacity of individual mammalian cells after exposure to ionizing radiation (Puck & Marcus 1956)(Puck, Morkovin et al. 1957) introduced a completely new way of thinking about radiation isoeffect data, namely as manifestations of target cell killing characterised by specific survival curves (Elkind 1960; Fowler & Stern 1960, 1963; Munro & Gilbert 1961; Lajtha & Oliver 1961). Elkind and Sutton demonstrated that recovery from sub-lethal damage occurred when a single radiation dose was split into two doses separated by several hours (Elkind and Sutton 1959). The initial

shoulder on the in vitro survival curve was restored after each of five fractionated doses with increasing total dose required for a given level of cell kill for increasing fractionation (Elkind and Sutton 1960). This was clearly a major milestone in the history of radiobiology.

The concept 'isoeffect equals isosurvival' was applied using several types of survival models. This led to the development of the linear quadratic (LQ) equation, a model employed by Douglas and Fowler for interpretation of skin isoeffect doses with fractionated radiation (Douglas and Fowler 1976).

$$E = n(\alpha d + \beta d^2)$$

Where E is the measured effect, n is the number of fractions and d is the dose per fraction. Following on from this, Thames *et al* showed that the fractionation sensitivity of tissues can be classified according to the ratio α/β, which can be derived from tissue isoeffect doses (Thames, Withers et al. 1982). The α/β ratio is the dose of radiation (in Gy) at which the amount of cell killing that is directly proportional to dose is equal to the amount of cell killing proportional to dose squared. It is an indication of the curviness of the cell survival curve. The greater the curvature, the lower the α/β ratio and higher the sparing effect of fractionation on tissue damage. Acutely responding tissues which express their damage within days/weeks after irradiation have a high α/β ratio in the range of 7-20 Gy (Fowler 1989; Thames, Bentzen et al. 1989; Thames, Bentzen et al. 1990), whereas for late responding tissues, which express their damage months/years after irradiation, the α/β ratio generally ranges from 0.5-6 Gy (Barendsen 1982; Bentzen, Saunders et al. 1999; Stuschke and Thames 1999) **(Table 1.1)**. It has been suggested that the α component represents the intrinsic radiosensitivity of the cells and the β component represents the extent to which damage can be repaired (Steel 1991). Although the parameters α and β were taken as representing survival parameters of the

presumptive target cells, it was changes in tissue response with changes in dose per fraction that was actually measured (Douglas and Fowler 1976; Fowler 1983).

Currently, the LQ model dominates the field of mathematical radiobiology (Withers, Thames et al. 1983; Fowler 1989). This model incorporates the effect of dose per fraction and can, by making additional assumptions, also incorporate the effects of repopulation during a course of fractionated radiotherapy. For fraction sizes in the range of 1 to 6 Gy, the LQ model is the model that, for now at least, is considered best at providing a rational basis for comparisons between different regimens of treatment assuming an appropriate value of α/β ratio is used (Withers, Thames et al. 1983; Fowler 1989). It has been widely developed, discussed and interpreted particularly with respect to the use of the biologically effective dose (BED) concept. The distinct fractionation sensitivities of early and late responding normal tissues are well described using the LQ model in which the α/β ratio offers a reliable way of describing these differences (Withers, Thames et al. 1983; Fowler 1989). For example, assuming a typical α/β value of 3.0 Gy for late normal tissue responses, a 15-fraction regimen reproducing the effects of 25 fractions of 2.0 Gy requires a reduction in total dose from 50 Gy to 42.8 Gy in fractions of 2.85 Gy (Jones, Dale et al. 2001). There is, therefore, nothing intrinsically unsafe about doses >2 Gy per fraction, but the total dose must be reduced in order to maintain the same level of normal tissue effect. Demonstrating equivalence in dose-limiting adverse effects is not enough to make the schedule useful: tumour control must be maintained or improved as well.

Table 1.1. Fractionation sensitivities of various early and late reacting normal tissue effects as denoted by their α/β ratios

Tissue/organ	Endpoint	α/β (Gy)	95% CL (Gy)	Source
Early reactions				
Skin	Erythema	8.8	6.9; 11.6	(Turesson and Thames 1989)
	Erythema	12.3	1.8; 22.8	(Bentzen, Christensen et al. 1988)
	Desquamation	11.2	8.5; 17.6	(Turesson and Thames 1989)
Oral mucosa	Mucositis	9.3	5.8; 17.9	(Denham, Walker et al. 1996)
	Mucositis	15	- 15; 45	(Rezvani, Alcock et al. 1991)
Late reactions				
Skin/vasculature	Telangiectasia	2.8	1.7; 3.8	(Turesson and Thames 1989)
	Telangiectasia	2.8	- 0.1; 8.1	(Bentzen and Overgaard 1991)
Subcutis	Fibrosis	1.7	0.6; 2.6	(Bentzen and Overgaard 1991)
	Cosmetic change in breast appearance	3.4	2.3; 4.5	(Bentzen, Agrawal et al. 2008)
	Induration (fibrosis)	3.1	1.8; 4.4	(Yarnold, Ashton et al. 2005)
Muscle/vasculature/ cartilage	Impaired shoulder movement	3.5	0.7; 6.2	(Bentzen, Overgaard et al. 1989)
Nerve	Brachial plexopathy	~ 2	N/A	(Powell, Cooke et al. 1990)
	Optic neuropathy	1.6	- 7; 10	(Jiang, Tucker et al. 1994)
Spinal cord	Myelopathy	< 3.3	N/A	(Dische, Martin et al. 1981)
Bowel	Various late effects	4.3	2.2; 9.6	(Dische and Saunders 1999)
Lung	Pneumonitis	4.0	2.2; 5.8	(Bentzen, Skoczylas et al. 2000)
	Lung fibrosis (radiological)	3.1	- 0.2; 8.5	(Dubray, Henry-Amar et al. 1995)
Head and neck	Various late effects	3.5	1.1; 5.9	(Rezvani, Alcock et al. 1991)
Head and neck	Various late effects	4.0	3.3; 5.0	(Stuschke and Thames 1999)
Supraglottic larynx	Various late effects	3.8	0.8; 14	(Maciejewski, Taylor et al. 1986)

CL, confidence limit

1.4 The 5R's of radiobiology

Nowadays, we comfortably base our clinical practice on the rational foundations provided by the five Rs of radiobiology namely intrinsic **R**adiosensitivity, **R**e-oxygenation, **R**epair, **R**epopulation and **R**edistribution (Withers 1975; Steel, McMillan et al. 1989). Fractionation in clinical radiotherapy was initiated in order to spare normal tissue by repair of sublethal damage and repopulation from surviving cells and also to increase the damage to the tumour by re-oxygenation of hypoxic cells and redistribution of cells along the cell cycle. Repair and repopulation confer resistance to tissue between two radiation doses, while redistribution and re-oxygenation are expected to make the tissue more sensitive to a subsequent dose. These four factors modify the response of a tissue to repeated doses of radiation.

1.5 Altered fractionation schedules in clinical radiotherapy

All the fractionation regimens that have been used throughout 100 years of clinical radiotherapy represent some form of compromise between as many fractions as possible to maximise therapeutic ratio between tumour cells and late reacting normal tissues and avoidance of undue protraction of treatment so as to minimise the opportunities for tumour cell repopulation during treatment **(Table 1.2)**. Clinical innovation and experience have been consistently followed by attempts to explain the underlying biology. One of the important lessons that history taught us is that fractionation cannot be considered in isolation. There is a complex interdependence between total dose, dose per fraction, overall treatment time, treated volume, beam parameters, prescribing conventions and quality control procedures (Thames, Withers et al. 1982; Fowler 1984; Bentzen, Turesson et al. 1990; Fletcher 1991).

Table 1.2. Main characteristics of the conventional and altered fractionation schedules

Fractionation regimen	Conventional	Hyperfractionated	Accelerated	Hypofractionated
Aim	To control the tumour through redistribution and reoxygenation at the same time as sparing normal tissue through repair and repopulation	To exploit the differences in radiosensitivity of tumour and healthy cells	To overcome tumour repopulation during treatment	To improve therapeutic ratio in tumours with low α/β ratio. Patient convenience with fewer fractions (especially palliative setting)
Dose/fraction	2 Gy	$<$1.8 Gy	$\geq$2 Gy	$>$2 Gy
Number of fractions/day	1	$\geq$1, usually 2-3	$\geq$1	1
Days of treatment/week	5	5	5-6	5
Overall dose (examples only)	70 Gy	≥70 Gy	$<$70 Gy	$<$60 Gy
Overall treatment time	7 weeks	7 weeks	5 weeks	$\leq$5 weeks

Conventional radiotherapy schedules use fractions of 1.8-2.0 Gy, a choice reflecting historical observations that late reacting normal tissues are, on average, more sensitive to fraction size than malignant tissues (Williams, Denekamp et al. 1985). Attempts to reduce the number of fractions in the 1970s made inadequate downward adjustments to total dose, resulting in unacceptable rates of late complications (Fletcher 1991). Interest in fewer larger fractions (>2 Gy) delivered over a shorter overall treatment time has been rekindled by randomised clinical trials based on a better understanding of normal tissue and tumour responses.

1.6 Hypofractionation – the breast cancer experience

An α/β value of 4-5 Gy was first estimated for locally advanced and recurrent breast cancer by Douglas in the mid-1980s based on clinical data published by Cohen in the early 1950s (Cohen 1952; Douglas and Castro 1984). Over the last 20 years, several randomised trials involving a combined total of around 8,000 women have compared hypofractionated adjuvant radiotherapy to a standard regimen of 50 Gy in 25 fractions **(Table 1.3)** (Whelan, MacKenzie et al. 2002; Yarnold, Ashton et al. 2005; Owen, Ashton et al. 2006; Bentzen, Agrawal et al. 2008; Bentzen, Agrawal et al. 2008; Whelan, Pignol et al. 2010; 2011). The UK Royal Marsden Hospital/Gloucestershire Oncology Centre (RMH/GOC) and Standardisation of Breast Radiotherapy Trial A (START A) trials tested two dose levels of a 13- fraction regimen in terms of late adverse effects and tumour control. The study design allowed direct estimates of α/β for each trial (Yarnold, Ashton et al. 2005; Owen, Ashton et al. 2006; Bentzen, Agrawal et al. 2008). Based on a combined total of 278 local-regional tumour relapses in the two trials, the adjusted α/β value for tumour control was 4.6 Gy (95% confidence interval [CI], 1.1-8.1), comparable to 3.4 Gy (95% CI, 2.3-4.5) for late change in photographic breast appearance. The two trials' results suggested that a 13-fraction regimen delivered over 5 weeks can be as safe and effective as 50 Gy in 25 fractions.

Results from the Canadian and START B trials are consistent with this interpretation. The Ontario trial compared 42.5 Gy in 16 fractions of 2.66 Gy (3.2 weeks) with 50 Gy in 25 fractions over 5 weeks (Whelan, MacKenzie et al. 2002; Whelan, Pignol et al. 2010). Schedules are expected to be equivalent in terms of late normal tissue and tumour responses assuming an α/β value of 3.0 Gy for each and no influence of treatment time. Rates of breast cosmesis at a median follow-up of >11 years were virtually identical in both treatment arms, consistent with this

expectation **(Table 1.4)**. Given that tumour control might be sensitive to a 2-week difference in treatment duration, it is not possible to estimate tumour fractionation sensitivity from these two trials. The UK START B trial compared 40 Gy in 15 fractions of 2.67 Gy (3.0 weeks) to 50 Gy in 25 fractions and recorded a lower rate of change in breast appearance after the 15-fraction regimen (hazard ratio [HR] = 0.83; 95% CI, 0.66–1.04; p = 0.06) (Bentzen, Agrawal et al. 2008). An HR of <1 for late adverse effects is likely to be real, since 40 Gy in 15 fractions is equivalent to 45.5 Gy in 2.0 Gy fractions if the α/β ratio = 3.0 Gy. In other words, 40 Gy in 15 fractions is gentler on late reacting normal tissues than 50 Gy in 25 fractions. The next important question is whether it is also gentler on breast cancer. If the α/β value for tumour control is ≥10 Gy, tumour control should be inferior after such a large reduction in total dose (from 50 Gy to 40 Gy), unless there is a major effect of shortening overall time, but tumour control does not appear to be worse **(Table 1.5)**. Although there were only 65 local-regional tumour relapses in START B at the time of reporting, the HR for this endpoint was 0.79 (95% CI, 0.48–1.29), indicating similar rates of local-regional relapse after 40 Gy in 15 fractions compared with the control arm. The residual imprecision indicated by the upper and lower 95% CI limits for the absolute difference between 40 Gy in 15 fractions and the control schedule in START B suggests that local-regional tumour relapse is unlikely to be more than 1% higher, and perhaps 1% or 2% lower, than after 50 Gy in 25 fractions.

Table 1.3. Selected characteristics of randomised trials of breast hypofractionation

	RMH/GOC (Yarnold, Ashton et al. 2005; Owen, Ashton et al. 2006)	START A (Bentzen, Agrawal et al. 2008)	START B (Bentzen, Agrawal et al. 2008)	Canadian (Whelan, MacKenzie et al. 2002; Whelan, Pignol et al. 2010)	FAST (2011)
Years accrual	1986-1998	1998-2002	1999-2001	1993-1996	2004-2007
Total number of patients	1410	2236	2215	1234	915
Standard arm (Gy/fractions/weeks)	50/25/5	50/25/5	50/25/5	50/25/5	50/25/5
Test arm A (Gy/fractions/weeks)	42.9/13/5	41.6/13/5	40.0/15/5	42.5/16/3.1	30/5/5
Test arm B (Gy/fractions/weeks)	39/13/5	39/13/5	n/a	n/a	28.5/5/5
Mean age (years)	54.5	57.2	57.4	not reported	62.5
Node+ (%)	32.7	28.8	22.8	0	0
Mastectomy (%)	0	15	8	0	0
Tumour size ≥T2 (%)	42.5*	48.6	35.9	20	17.8
Boost (%)	74.5	60.6	42.6	0	0
Chemotherapy (%)	13.9	35.5	22.2	11	0
Regional radiotherapy (%)	20.6	14.2	7.3	0	0

*Clinical T stage

Table 1.4. Cosmesis and normal tissue effects of hypofractionated compared to standard breast radiation therapy

Trial	Total dose (Gy/ fractions)	Excellent/good cosmesis or no change (%)		Moderate/marked change (% or HR*)		Moderate/marked induration (% or HR*)	
		5 yr	10 yr	5 yr	10 yr	5 yr	10 yr
RMH/GOC (Yarnold, Ashton et al. 2005; Owen, Ashton et al. 2006)	50/25	60.4	46.6	6.4	9.8	23.1	36.3
	42.9/13	54.3	42.0	11.2	15.6	35.6	51.1
	39/13	69.7	43.9	3.9	6.6	16.0	27.7
START A (Bentzen, Agrawal et al. 2008)	50/25	57.1		1.0*		1.0*	
	41.6/13	56.4		1.05*		1.09*	
	39/13	67.9		0.86*		0.81*	
START B (Bentzen, Agrawal et al. 2008)	50/25	57.8		1.0*		1.0*	
	40/15	63.5		0.83*		0.89*	
Canadian (Whelan, MacKenzie et al. 2002; Whelan, Pignol et al. 2010)	50/25	79.2	71.3			6.1	10.4
	42.5/16	77.9	69.8			4.7	11.9
FAST (2011)	50/25	98.3♣		7.6♦		1.9♦	
	30/5	90.7♣		13.7♦		4.0♦	
	28.5/5	96.2♣		7.9♦		2.6♦	

*Hazard ratio (HR)
♣2 years post randomisation
♦3 years post randomisation (breast shrinkage only)

Table 1.5. Rates of Local recurrence in the altered fractionation trials

Trial	Total dose (Gy/fraction)	3 yr local recurrence (%)	5 yr local recurrence (%)	10 yr local recurrence (%)
RMH/GOC (Yarnold, Ashton et al. 2005; Owen, Ashton et al. 2006)	50/25		7.9	12.1
	42.9/13		7.1	9.6
	39/13		9.1	14.8
START A (Bentzen, Agrawal et al. 2008)	50/25		3.2	
	41.6/13		3.2	
	39/13		4.6	
START B (Bentzen, Agrawal et al. 2008)	50/25		3.3	
	40/15		2.0	
Canadian (Whelan, MacKenzie et al. 2002; Whelan, Pignol et al. 2010)	50/25		3.2	6.7
	42.5/16		2.8	6.2
FAST (2011)	50/25	0.7		
	30/5	0		
	28.5/5	0		

A 15-fraction schedule is now the UK standard recommended by the National Institute for Health and Clinical Excellence (NICE), but it is unlikely to represent the useful limits of hypofractionation for whole breast radiotherapy. There is a history of prescribing once-weekly fractions of whole breast radiotherapy for women too frail or otherwise unable to attend for conventional schedules. In a French series of 115 patients undergoing primary radiotherapy without surgery for non-metastatic breast cancer from 1987 to 1999, the whole breast received 5 once-weekly fractions of 6.5 Gy (Courdi, Ortholan et al. 2006). 101 were given additional tumour bed boost doses, 7 with 1 fraction, 69 with 2 fractions and 25 with 3 once-weekly fractions of 6.5 Gy using electrons. Kaplan-Meier estimates of late effects in the breast were 24% grade 1, 21% grade 2 and 6% grade 3 at 48 months. The 5-year local progression-free rate was 78% (95% CI: 66.6-88.4). In a separate French series, 5 once-weekly fractions of 6.5 Gy to the whole breast with no boost were given to 50 women after local tumour excision (Kirova, Campana et al. 2009). Grade 1 or 2 induration was reported in 33% of the patients at a median follow up of 93 months (range 9-140). The 7-year local relapse free survival was 91%. Five fractions of 6.5 Gy are equivalent to 62 Gy in 31 fractions assuming α/β=3.0 Gy, a significantly higher dose intensity than conventional schedules deliver.

The recently reported UK FAST Trial tested two dose levels of a 5-fraction regimen delivering 1 fraction per week against a control schedule of 50 Gy in 25 fractions, defining radiotherapy adverse effects as the primary endpoint (2011). Once-weekly fractions were chosen to minimise confounding of treatment outcome measures by differences in overall treatment time. The two test dose levels delivered 5 fractions of 5.7 Gy or 6.0 Gy (total dose 28.5 Gy or 30 Gy), estimated to be iso-effective with the control regimen assuming α/β values of 3.0 Gy or 4.0 Gy, respectively. Seven hundred and twenty nine patients had 2-year photographic assessments. Risk ratios

for mild/marked change were 1.70 (95% CI 1.26–2.29, p <0.001) for 30 Gy and 1.15 (0.82–1.60, p = 0.489) for 28.5 Gy versus 50 Gy. Three-year rates of physician-assessed moderate/marked adverse effects in the breast were 17.3% (13.3–22.3%, p<0.001) for 30 Gy and 11.1% (7.9–15.6%, p=0.18) for 28.5 Gy compared with 9.5% (6.5–13.7%) after 50 Gy. With a median follow-up of 37.3 months, 2 local tumour relapses and 23 deaths have occurred. Change in photographic breast appearance, the primary endpoint, gave an estimate of α/β of 2.6 Gy (95% CI 1.4-3.7). Using this estimate, the isoeffect doses expressed in 2 Gy equivalents for 30 Gy and 28.5 Gy in 5 fractions are 56.3 and 51.6 Gy, respectively. Therefore, at 3 years median follow-up, 28.5 Gy in 5 fractions is comparable to 50 Gy in 25 fractions, and significantly milder than 30 Gy in 5 fractions, in terms of adverse effects in the breast.

All the evidence so far suggests that the α/β value for breast tumour control is around 4 Gy, comparable to values for late responding normal tissues, meaning that small fractions are as gentle on the cancer as on the healthy tissues (Yarnold, Ashton et al. 2005; Owen, Ashton et al. 2006; Bentzen, Agrawal et al. 2008; Bentzen, Agrawal et al. 2008). Despite a 10 Gy reduction in total dose, from 50 Gy to 40 Gy, introduced in UK trials to compensate for the increase in fraction size from 2.0 to 2.67 Gy, no inferiority in tumour control was reported. This observation suggests that breast cancer responded strongly to this modest increase in fraction size.

1.6.1 Dose escalation strategies by modifying dose per fraction as opposed to number of fractions

Improvements in RT techniques with intensity modulated radiotherapy (IMRT), 3D conformal RT and image guided RT (IGRT) can be used to test hypofractionation as

a dose escalation strategy. In other words, the tumour bed (high risk areas requiring a boost) can be treated to a higher equivalent total dose by increasing the dose per fraction, while the rest of the breast (low risk areas) can be treated to a lower equivalent dose by decreasing the dose per fraction in a single phase plan using IMRT. There are 3 recent phase I/II trials showing the safety and short-term efficacy of hypofractionated radiation therapy with a concurrent boost (Formenti, Gidea-Addeo et al. 2007; Freedman, Anderson et al. 2007; Chadha, Woode et al. 2009). The integrated boost doses per fraction used were 2.8 Gy in 20 fractions, 3.17 Gy in 15 fractions and 3 Gy in 15 fractions, respectively. With a median follow up ranging from 12 to 54 months across the 3 trials there were no reports of unusual acute or late toxicity.

There are now at least 2 randomised phase III trials currently underway comparing standard sequential boost with a simultaneous integrated boost in high risk women after breast conservation surgery and appropriate adjuvant systemic therapy . The RTOG-1005 trial tests standard sequential boost (12 Gy in 6 fractions or 14 Gy in 7 fractions) after 50 Gy in 25 fractions or 42.5 Gy in 16 fractions to whole breast versus the same dose to whole breast delivered with a concurrent tumour bed boost to 48 Gy in 15 fractions of 3.2 Gy . This represents an equivalent tumour bed dose (assuming an α/β ratio of 4, and correcting for proliferation effects) in 2 Gy per fraction of approximately 63-66 Gy in 2 Gy fractions.

The UK IMPORT HIGH trial (activated in 2009), also tests advanced techniques of dose intensity modulation to adjust fraction size across the breast as a way of matching dose to tumour relapse risk. The control arm delivers 40 Gy in 15 fractions to the whole breast followed by 16 Gy in 8 fractions to the tumour bed. Two test arms deliver 36 Gy in 15 fractions to whole breast, 40 Gy in 15 fractions to partial

breast and 48 Gy (test arm 1) or 53 Gy (test arm 2) in 15 fractions concomitant boost to tumour bed. Assuming an α/β ratio of 3 Gy, the total tumour bed doses in the control arm, test arm 1 and test arm 2 are equivalent to 62 Gy, 60 Gy and 69 Gy in 2 Gy fractions, respectively. The modest dose reduction to whole breast in the test arms, equivalent to a reduction from 46 Gy in 23 fractions (control) to 40 Gy in 23 fractions (test 1 & 2) assuming α/β=3 Gy, is intended to reduce late adverse effects and allow safe dose escalation to the tumour bed.

1.6.2 Benefits of hypofractionation

Immediate advantages of hypofractionation include increased patient convenience, lower treatment costs and lower radiotherapy waiting times, especially important in countries where these resources are restrained (Lievens 2010). The lower total dose delivered in fewer, larger fractions means shorter overall treatment duration (accelerated hypofractionation), which may be more effective in subsets of patients with high proliferative indices (a hypothesis that needs testing). Shorter treatment times may also have scheduling advantages, in that radiotherapy can be delivered straight after surgery when the residual tumour burden is likely to be lowest, as in current accelerated partial breast conformal radiotherapy techniques (Orecchia, Ciocca et al. 2005; Vaidya, Baum et al. 2010). A benefit of the lower total dose delivered using hypofractionation is a lower rate of moist desquamation, often developing in the inframammary fold of large breasted women. This was demonstrated in the UK FAST Trial, in which the rate of moist desquamation fell from 12/110 (10.9%) after 50 Gy in 25 fractions to 2/106 (1.9%) after 28.5 Gy in 5 fractions (2011). One of the benefits expected from lower rates of moist desquamation are lower rates of consequential late effects, including cutaneous atrophy, telangiectasia and subcutaneous induration, the direct consequences of severe epidermal denudation and delayed healing.

1.6.3 Concerns regarding hypofractionation

Most of the apprehension regarding accelerated hypofractionated schedules is based on the memory of severe late toxicities from schedules based on misapplication of dose algorithms in the 1960s and 1970s (Thames, Withers et al. 1982; Fowler 1984; Bentzen, Turesson et al. 1990; Fletcher 1991). Other factors contributing to poor historical results of hypofractionated breast radiotherapy included poor dosimetry, high skin doses delivered by low-energy beams, use of nonstandard reference points, and position errors causing overlap at field junctions (Dewar, Benhamou et al. 1988; Bates and Evans 1995).

With regards to stochastic and non-stochastic adverse effects from radiotherapy, these continue to develop over the whole lifetime of a patient, so that many decades are needed for a complete description. The important question for interpreting trials of hypofractionation is whether the ratio of dose-limiting adverse effects in experimental and control arms, at the time of reporting, predicts the ratio of relevant adverse effects at later time-points. Comparisons of 5-and 10-year results for a range of late adverse effects scored in the RMH/GOC trial are consistent with this requirement for the safe adoption of hypofractionation (Yarnold, Ashton et al. 2005). Also persuasive are the 14-year follow up data of the EORTC 22881-10882 tumour bed boost trial, in which the relative risk of breast induration 14 years after randomisation to boost versus no boost could be accurately quantified within 5 years of treatment (Collette, Collette et al. 2008).

Where the heart is concerned, even 10 years is insufficient to estimate the relative risk of heart disease. However, the issue of fractionation is lessrelevant for this organ once a threshold dose is exceeded. An excess risk of ischaemic heart disease is apparent after cardiac doses <10 Gy, so the priority is to exclude the

heart from the treatment volume whatever fractionation regimen is used (McGale and Darby 2005; Taylor, Nisbet et al. 2007). Fractionation issues are also less relevant where the lung is concerned, since lung tolerance of 20 Gy in 2.0 Gy fractions is exceeded whatever fractionation is used. Radiation pneumonitis risk is more closely related to volume, so that an increased risk is unlikely to be seen with hypofractionation in the absence of higher volume of lung irradiated (Ragaz, Olivotto et al. 2005; Lind, Wennberg et al. 2006; Rancati, Wennberg et al. 2007).

Another concern is the implication of 'double trouble', a term describing the clinical effects of higher total doses and higher doses per fraction in partial volumes (hotspots) receiving more than 100% prescribed dose (Withers 1992). Due to the mathematical form of the linear-quadratic dose effect relationship, hotspots are penalised more severely in a hypofractionated treatment, so-called 'triple trouble' (Jones, Dale et al. 2000). In practice, triple trouble is of little clinical significance if hot spots are limited in volume and dose gradients are restricted to between 95% and 107% of the reference isodose (Yarnold, Ashton et al. 2005). Despite this reassurance, full dose compensation is recommended as standard practice for patients prescribed breast radiotherapy regardless of fractionation regimen, since it has been shown in a randomised trial to reduce the incidence and severity of late adverse effects (Donovan, Bleakley et al. 2007). With improved dose homogeneity there should be no concern about treating large breast size with hypofractionation.

After irradiation of the axilla and/or supraclavicular fossa in over 400 patients within hypofractionated arms of the RMH/GOC, START A and START B trials, there was no increase in reports of brachial plexopathy at a median follow up of ≥6 years (Yarnold, Ashton et al. 2005; Owen, Ashton et al. 2006; Bentzen, Agrawal et al. 2008; Bentzen, Agrawal et al. 2008). The 40 Gy in 15 fractions regimen is equivalent

to 47 Gy in 2 Gy fractions if the α/β value for brachial plexus is 2 Gy, or 49 Gy in 2 Gy fractions if α/β is 1 Gy. In other words, this hypofractionated regimen is actually gentler than 50 Gy in 25 fractions with respect to late effects in all normal tissues. If radiotherapy centres are confident that their techniques are safe when prescribing 50 Gy in 25 fractions, there is a reduced risk of late adverse effects after 40 Gy in 15 fractions using the same treatment position, field arrangement, dosimetry and reference points.

In conclusion, it is fair to say that after decades of resistance to evaluating larger radiotherapy fraction sizes in breast cancer, expert opinion is responding to an accumulating body of evidence supporting the safety and effectiveness of this approach. The standard UK schedule of 40 Gy in 15 fractions is gentler on normal tissues than 50 Gy in 25 fractions, without evidence of inferior local tumour control. This schedule, or 42.5 Gy in 16 fractions, can be recommended as safe and effective alternatives to 50 Gy in 25 fractions for whole-breast, postmastectomy chest wall and lymphatic radiotherapy. Future challenges will involve testing the limits of hypofractionation for whole and partial breast RT. Experience gained with accelerated partial breast irraditaion cannot be translated to the context of whole breast radiotherapy due to a strong volume effect. A phase III randomised trial in the UK is currently testing a 5-fraction schedule of adjuvant whole breast radiotherapy delivered in 1 week against a 15-fraction schedule in women with early breast cancer **(Table 1.6)**.

Table 1.6. UK FAST Forward Trial (N=4000), primary end point of local tumour control

	Total Dose (Gy)	Fractions	Dose per fraction (Gy)	Time
Control arm 1	40.0	15	2.67	3 weeks
Test arm 1	27.0	5	5.4	5 days
Test arm 2	26.0	5	5.2	5 days

1.7 Clinical relevance of understanding sensitivity to radiotherapy fraction size

There is strong evidence of a radiation dose response for tumour control (UKCRN, *ART DECO* study). However, it has long been recognised that safe and effective dose escalation must take account of the differential sensitivities of normal and malignant tissues to the size of daily doses (Williams, Denekamp et al. 1985). The assumption that cancers are, on average, relatively insensitive to fraction size holds true for human squamous carcinomas ($\alpha/\beta \geq 10$ Gy) (Stuschke and Thames 1999; Bourhis, Overgaard et al. 2006) but now there is high quality evidence that some adenocarcinomas are significantly more sensitive to fraction size than previously thought **(Figure 1.1) (Table 1.7)** (Fowler 1989; Thames, Bentzen et al. 1989; Thames, Bentzen et al. 1990). The evidence for breast cancer has been discussed in detail above. In addition there is strong evidence that the α/β ratio for prostate tumours is likely to be very low (Fowler, Chappell et al. 2001; Fowler 2005). A recently published article analysing the dose-fractionation sensitivity of prostate cancer from radiotherapy outcomes of 5,969 patients in seven international institutional datasets estimated a consistently low α/β ratio of 1.4 Gy (95% CI=0.9-2.2) (Miralbell, Roberts et al. 2012). Importantly, this low value of α/β ratio for prostate cancer appears to be significantly less than the α/β of 3 Gy for late complications in rectal tissues (Fowler, Chappell et al. 2001; Fowler 2005). This means that radiotherapy schedules using $\leq$2.0 Gy fractions spare tumour as much or even more than the dose limiting healthy tissues. This has stimulated a resurgent interest in the potential benefits of hypofractionation as described above. In addition, with advanced radiotherapy techniques such as IMRT and IGRT it is possible to modulate total dose delivered by altering dose per fraction across the radiation field to reflect the different fractionation sensitivities of the tissues irradiated (IMPORT HIGH study protocol ISRCTN47437448). It is important to understand that

population-based estimates of the α/β value represent averages, which are likely to vary within tumour types as well as between them. At present we do not have enough evidence to exclude clinically relevant differences in fractionation sensitivity between primary tumours arising from the same site, but this may not be surprising given the wide tumour heterogeneity that exists within tumour types (Stephens, Tarpey et al. 2012). A better understanding of the molecular basis of fraction size sensitivity is highly relevant to these above initiatives, and necessary if this important therapeutic variable is to be exploited for the benefit of patients. Identifying biomarkers of fractionation sensitivity would allow more effective stratification of our patients for this important treatment parameter in curative radiotherapy.

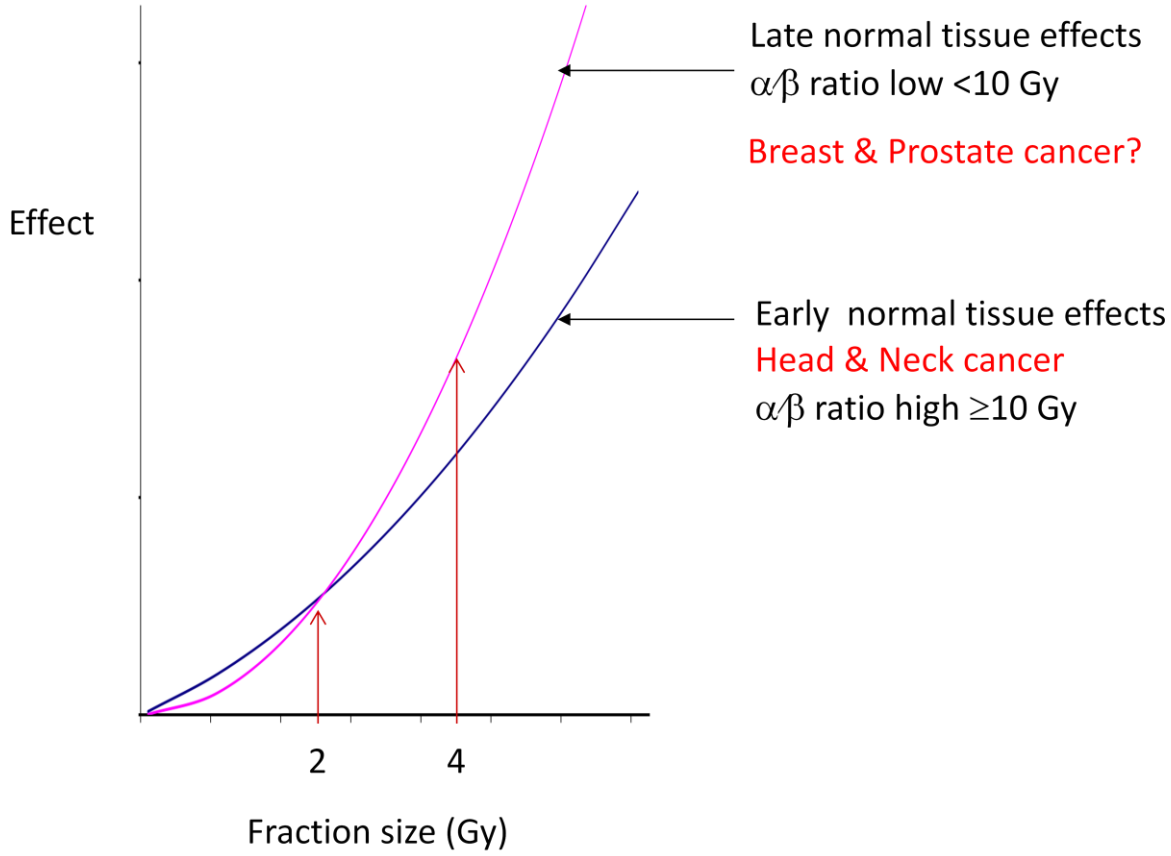


Figure 1.1: Dose response curves - Classical model faces a challenge. Sensitivity is described in terms of a linear-quadratic model, in which low values (up to 10) of alpha/beta ratio indicate sensitivity to fraction size, typical of late reacting normal tissues, and high values (10 or more) indicate insensitivity, typical of squamous carcinomas. The units of alpha/beta are Gy. X-axis shows dose per fraction.

Table 1.7. Average α/β ratios of various tumours

Tumours	α/β (Gy)	95% CL (Gy)	Source
Head and neck			
Various	10.5	6.5; 29	(Stuschke and Thames 1999)
Larynx	14.5*	4.9; 24	(Rezvani, Fowler et al. 1993)
Buccal mucosa	6.6	2.9; ∞	(Maciejewski, Withers et al. 1989)
Tonsil	7.2	3.6; ∞	(Maciejewski, Withers et al. 1989)
Nasopharynx	16	11; 43	(Lee, Leu et al. 1995)
Skin	8.5*	4.5; 11.3	(Trott, Maciejewski et al. 1984)
Prostate	1.1	- 3.3; 5.6	(Bentzen and Ritter 2005)
Breast	4.6	1.1; 8.1	(Bentzen, Agrawal et al. 2008)
Oesophagus	4.9	1.5; 17	(Geh, Bond et al. 2006)
Melanoma	0.6	- 1.1; 2.5	(Bentzen, Overgaard et al. 1989)
Liposarcoma	0.4	- 1.4; 5.4	(Thames and Suit 1986)

CL, confidence limit
*Re-analysis of original published data

1.8 Target cell theory and the cellular basis of fractionation sensitivity

The introduction in the 1980s of the LQ model to predict normal tissue isoeffect relationships had as an implied assumption that normal tissue response was primarily controlled by the radiosensitivity of the parenchymal (or target) cells in that tissue as mentioned earlier. This assumption is reinforced by the common interpretation of the differences in early vs. late normal tissue responses in terms of differences in the curvature of the underlying survival curves for the target cells (Thames and Hendry 1987; Withers 1989). The success of the LQ formula in such prediction and its widespread use as a starting point for comparison or calculation of the effects of different fractionation schedules has largely proceeded in the absence of formal proof of this underlying assumption. Under the target-cell hypothesis, the main effect of ionizing radiation on tissues and organs was thought to be a direct consequence of cell killing, resulting in the depopulation of crucial cell populations and subsequent functional deficiency (Thames and Hendry 1987). The finding that patients with ataxia telangiectasia had an unusually severe response to irradiation and that fibroblasts taken from these patients reflected this increased sensitivity was an early indication that cellular radiosensitivity could reflect tissue sensitivity (Taylor, Harnden et al. 1975). Ionizing radiation was thought to create complex DNA lesions that were difficult to manipulate precisely, and the main route to improve the therapeutic ratio of radiotherapy in the early 1980s seemed to be to devise modified dose-fractionation schedules to exploit differences in the shape of the target-cell survival curve for tumours and late-responding normal tissues, for example by reducing the dose per fraction (Bentzen 2006). Such altered fractionation trials conducted in the 1990 were largely successful in squamous-cell carcinoma of the head and neck which lent support to this target cell concept (Bernier and Bentzen 2003; Bernier 2005).

The ability of the same empirical LQ model to describe cell and tissue responses to fraction size implies that cellular responses are critical determinants of tissue fractionation sensitivity of normal tissues even if it does not prove causality (Fowler 1983). Human skin provides a good example of the relationships between the fractionation sensitivity of cells and tissue. Target theory postulates that the fractionation sensitivity of acute skin reactions can be considered in relation to a single population of target stem cells in the basal epidermis (Jones, Harper et al. 1995). The low sensitivity of moist desquamation to fraction size (high α/β value) has been accurately quantified, and there is a very close association between desquamation and depletion of basal epidermal cells (Turesson and Thames 1989; Nyman and Turesson 1994). If moist desquamation is severe, permanent epidermal stem cell depletion explains healing by secondary intention with atrophy, scarring and telangiectasia, a so-called consequential late effect, which shares the high α/β value of epidermis (Dorr and Hendry 2001). Assuming healing of moist desquamation without scarring, late epidermal atrophy represents an indirect response to hypoxia secondary to endothelial cell depletion in the dermis, and shares the same low α/β value as endothelium.

The target cell theory is also useful for understanding the early response (high α/β) of the haematopoietic system, the spermatogenic system (Meistrich, Hunter et al. 1978; Judas, Bentzen et al. 1996) and epithelial tissues such as the mucosa lining the gastrointestinal tract where direct parenchymal cell killing or depletion is the dominant effect (Dorr 1997). However, the relationship for late normal tissues effects such as fibrosis, atrophy, vascular damage and neural damage is more complex due the involvement of multiple target cells and intercellular interactions. Various studies have shown that the “target cell” view of parenchymal or vascular cells as passive bystanders dying when they attempt mitosis is too simple, and that radiation-induced

late normal tissue effects involves complex interactions among parenchymal, stromal and endothelial cells and inflammatory cytokines (Moulder, Robbins et al. 1998; Bentzen 2006).

However, these results suggesting the contribution of inflammatory cytokines and tumour microenvironment in radiation effects, do not rule out the importance of damaging or killing of parenchymal and/or vascular cells as the triggering event. For example, the role of nonirradiated bone marrow cells in the rescue of animals and humans from death due to bone marrow failure following irradiation is well recognized. It has also been reported by a number of groups that wound healing in irradiated tissue can be enhanced by the injection of nonirradiated fibroblasts into the wound site (Gorodetsky, McBride et al. 1991; Ferguson, Boynton et al. 1999). Another study has reported that injection of nonirradiated hepatocytes into an irradiated liver via the spleen can significantly modify the development of radiation-induced liver damage and improve animal survival (Guha, Sharma et al. 1999). These examples clearly show that target cell killing mediates radiation damage such that introduction of non-irradiated target cells can modify the damage response and rescue the tissue. Therefore, interventions that aim to reduce the initial cell killing would reduce the cellular and tissue-damage response and although much of the emphasis over the past decade has been placed on tissue remodelling as a crucial element in radiation pathogenesis, the damage-induction step i.e. the initial cellular processing of damage remains relevant for tissue fractionation effects.

1.9 Fraction size sensitivity and proliferative status of normal and malignant tissues

There is a strong inverse association between the proliferative indices of normal tissues and their fractionation sensitivities. Self-renewal tissues have high

proliferative indices and low sensitivity to fraction size (high α/β value), and vice versa for late responding tissues. These relationships have been recognised for many decades, and similar relationships appear to apply in human tumours **(Table 1.8)**. Incorporation of BrdU identifies tumour cells in S phase and generates a labelling index (LI), which is the percentage of cancer cells taking up the radiolabelled nucleotide. LI can be measured in human cancers following pre-surgical injection or ex vivo if sections of fresh tumour are incubated with radiolabelled nucleotide. Such studies have shown that head and neck tumours have a small potential doubling time (Tpot) of 4.5 days (Rew and Wilson 2000), which is the time for the tumour to double its size when there is no cell loss. At the same time, direct measurements of cellular proliferation in prostate tumours suggests a slow growth rate, with a potential doubling time ranging from 16-61 days, the largest Tpot measured in human tumours (Haustermans, Hofland et al. 1997). Similarly, tumour volume doubling time measurements of breast cancer cells indicate wide variations (44-295 days), suggesting very different pretreatment patterns of tumour kinetics (Peer, van Dijck et al. 1993). The age-dependent volume doubling time as reported by Peer et al (Peer, van Dijck et al. 1993) indicates smaller doubling times for women less than 50 years of age, suggesting that accelerated radiotherapy schedules may be suitable for this patient category. However, an association between proliferation index and the fractionation sensitivity of a tissue is not evidence of a causal relationship, particularly in cancers, which contain multiple genetic and epigenetic modifications expected to impact on radiation response.

Table 1.8. Potential doubling times (T_{pot}) and volume doubling times (T_d) for various tumours and consequent fractionation regimens

Tumour type	(T_{pot} (days)	T_d (days)	Radiobiological/clinical properties	Treatment indication
Head and neck	4.5 (1.8-5.9) (Rew and Wilson 2000)	45 Rew, 2000 #5511}	Rapid regrowth during treatment High hypoxic content	Hyperfractionaton Accelerated radiotherapy
Prostate	28 (16-61) (Haustermans, Hofland et al. 1997)	1100 (Lee, Hanks et al. 1995)	Slow proliferation Very low α/β ratio	Hypofractionation
Glioblastoma	3.9-7.5 (Hlatky, Olesiak et al. 1996) 2.3-13.3 (Nakajima, Nakasu et al. 1998)	3.3-29.2 (Nakajima, Nakasu et al. 1998)	High hypoxic content Poor differentiation; radioresistance High proliferation	Hyperfractionation Accelerated radiotherapy Hyperfractionation
Breast	10.4 (8.2-12.5) (Rew and Wilson 2000)	82 (Spratt, Meyer et al. 1996) 44-295 (Peer, van Dijck et al. 1993)	Age-dependent proliferation α/β ratio similar to the normal tissue one	Hypofractionation Accelerated radiotherapy
Lung (non-small cell lung cancer – NSCLC	7.1 (Shimomatsuya, Tanigawa et al. 1991) 8.2 (Shibamoto, Ike et al. 1998)	46 (El Sharouni, Kal et al. 2003) 67.5 (Arai, Kuroishi et al. 1994) 81 (Lindell, Hartman et al. 2007)	Small volume doubling time Rapid regrowth during treatment NCSLC higher radioresistance than other histologic types	Hyperfractionation Accelerated radiotherapy

1.10 Fraction size sensitivity is not a fixed property of cells or tissues

The sensitivity of normal and malignant tissues to fraction size has long been understood to have a basis in the process of cellular recovery, one of the 4 R's of classical radiobiology as described above (Withers 1975). However, recovery capacity varies with the experimental conditions. Human fibroblasts show more recovery (sublethal damage repair) from split dose or low dose rate exposure if irradiated in plateau phase than in exponential growth phase (Deschavanne, Fertil et al. 1980; Badie, Alsbeih et al. 1996; Lambin P 2004). Additional sparing (potentially lethal damage repair) can be gained by delayed plating rather than immediate plating of human fibroblasts irradiated at high dose rate in plateau phase (Fertil, Deschavanne et al. 1988).

Since fraction size sensitivity is not a fixed property of cells, it should not be a fixed property of a tissue if the proliferative properties of stem cell compartments change during radiotherapy. Skin serves to show how sensitivity to radiotherapy fraction size changes according to changes in overall treatment time. In the 1970s carefully conducted experiments by Turesson *et* al demonstrated this in breast cancer patients irradiated postoperatively to the internal mammary nodes exposed to various dose schedules (Turesson and Thames 1989). Skin erythema was measured by reflectance spectrophotometry and photographs were taken twice a week during the acute reactions, every 3 months for 5 years and then 6 monthly and scored blindly by 2 observers. They showed that if overall treatment time is less than 14 days, acute human epidermal responses are more sensitive to fraction size (α/β value ~4 Gy) than when radiotherapy is delivered over longer periods (α/β values >10 Gy) (Trott 1986; Turesson and Thames 1989), and the clue lies in changes to the proliferation kinetics of stem cells during fractionated radiotherapy. For example, a dose-dependent fall in basal epidermal cell density reaches its minimum level in

human skin one week into the delivery of 50 Gy in 25 fractions, with a mean nadir of 38% (SD 10) of baseline density (86 cells/mm SD 10) in 6 patients (Nyman and Turesson 1994). The nadir is followed by a phase of accelerated repopulation, documented as a rapid increase in basal cell density and a return to baseline levels over several weeks. Accelerated repopulation is preceded by a switch from asymmetric to symmetric division in basal stem cells, whereby a stem cell divides to create two stem cells, rather than one stem cell and one transit cell, in order to replenish the stem cell compartment. In mouse epidermis, the switch to symmetric division is triggered when stem cell numbers have fallen to 1% of control levels (Dorr 1997). In pig skin, which strongly resembles human skin in its responses to ionising radiation, rapid proliferation is seen in discrete colonies of normal-looking cells in the basal layer 14 days after the start of radiotherapy (50 Gy in 2.0 Gy fractions over 5 weeks), even while overall basal cell density is still falling (Morris and Hopewell 1986). In specific experiments, the tritiated thymidine labelling index fell from 10% at baseline to immeasurably low levels, after which it rose to a peak of 20% by the end of 50 Gy in 25 fractions over 5 weeks (Hopewell, Nyman et al. 2003). It is also relevant that colonies of normal looking basal cells with labelling indices of 40–50% were seen 21 days after a single dose of 15–20 Gy in pigs. If these colonies represent stem cells in a phase of accelerated proliferation, they provide the basis for predicting a fall in the fractionation sensitivity of epidermis during radiotherapy lasting >14 days.

The tritiated thymidine labelling index cannot be applied easily in humans, but alternative markers have been used, including p53, Ki67, p21 and cyclin A (Turesson, Bernefors et al. 2001). In patients exposed to 50 Gy in 2.0 Gy fractions over 5 weeks, the proportion of Ki67+ basal cells fell from 10% at baseline to 5% at 2 weeks, after which it rose to 30% by the end of treatment (Hopewell, Nyman et al.

2003). Over the first four weeks, the number of cyclin A+ basal cells increased from 4% at baseline to >10%. Since cyclin A is expressed only between late G1 and mid M phases, the paucity of Ki67+ cyclin A- cells suggests virtual abolition of the G1 phase with shortening of cell turnover time. These data are consistent with DNA labelling studies in pigs that confirm shortening of cell turnover time in the basal epidermis from 130 hours at baseline to around 20 hours once accelerated proliferation is underway (Morris and Hopewell 1986). In pig skin, shortening of cell cycle time during accelerated proliferation coincides with a fall in the total radiation dose required for a given level of acute skin response to two doses separated by intervals of 10–14 days compared to 22 hours (Rezvani, Hopewell et al. 1998). This observation has clinical correlates, which are relevant to proposed links between cell proliferation and fractionation sensitivity. In a comparison of 50 Gy in 2.0 Gy fractions given 8 hours or 24 hours apart (2.5 versus 5 weeks), the nadir basal cell density in the 2.5 weeks schedule was higher, against expectation, than after the 5-week schedule, roughly equivalent to 40 Gy in 2.0 Gy fractions over 4 weeks (Nyman and Turesson 1994). The postulated explanation is that during a 5-week schedule, sublethal and/or potentially lethal damage repair capacity is attenuated during the phase of accelerated proliferation, causing enhanced cellular radiosensitivity and tissue response. The association between the fractionation sensitivity and the proliferative indices of normal tissues and cancers forms the basis of subsequent discussions of molecular mechanisms of fractionation sensitivity.

1.11 DSB repair capacity and kinetics are the molecular correlates of cellular recovery

Molecular processes relevant to cellular recovery in vitro and to fraction size sensitivity in vivo include recognition and processing of DNA double strand breaks

(DSB) (Jackson 2002). The 2 most common pathways of repair of DSBs in eukaryotes are NHEJ (where the 2 broken ends rejoin), and HR repair (in which breaks are repaired through genetic exchanges with homologous DNA strands). NHEJ is an error prone method of repair that is important in all phases of the cell cycle whilst HR is active only in the S and G2 phases of the cell cycle and has a high fidelity for repair (Rothkamm, Kruger et al. 2003). NHEJ is particularly important, and is expected to be the system predominantly used by vascular and parenchymal cells in late reacting normal tissues (Collis, DeWeese et al. 2005). NHEJ is a rapid repair process as it does not require homology search and strand invasion, which makes HR a slower process. A significantly longer repair half-time for homologous recombination repair compared to NHEJ has been proposed as a basis for the reduced radiotherapy fractionation sensitivity of rapidly proliferating tissues (Lambin P 2004). Mammalian fibroblast lines genetically defective in components of the NHEJ pathway, and presumably relying on HR, lose LDR sparing, suggesting that HR may not be fraction size dependent (Thacker and Wilkinson 1995). There is no evidence for HR as the predominant form of repair in the stem cells of rapidly proliferating tissues, including phases of accelerated repopulation, but whatever role it has is expected to be more relevant in rapidly proliferating cells than in slowly proliferating ones. This suggests a model of clinical fractionation sensitivity based on the predominance of NHEJ (sensitive to fraction size) in slowly proliferating tissues and the predominance of HR (insensitive to fraction size) in rapidly proliferating ones. When using once daily fractions as in the clinic, one assumes repair is complete by 24 h. Any DSB unrepaired after that time is unlikely to be repairable. Decreasing the interval between fractions or giving higher doses per fraction is likely to cause more IR induced DSBs before repair is complete thereby increasing the likelihood of mis-repair with NHEJ whereas HR will repair with high fidelity independent of DNA damage levels.

An alternative model for the association between fraction size dependency and proliferative status focuses on the shorter time period that proliferating cells have available compared to non-proliferating cells for the repair of DSBs, regardless of putative differences in DNA DSB repair processes. There is an extensive literature based on normal tissue responses, cellular responses and pulse field gel electrophoresis (PFGE) consistent with a slow component to recovery, repair and rejoining, respectively, having a $T^{1/2}$ of several hours (Hendry 1992; van den Aardweg and Hopewell 1992; Nyman and Turesson 1995; Bentzen, Saunders et al. 1999; Orton 2001). The kinetics of rejoining of chemical- or radiation-induced DSBs can be assayed after high doses by pulse field gel electrophoresis or by IHC against γ-H2AX or 53BP1 after very low doses (Gauter, Zlobinskaya et al. 2002; Banath and Olive 2003; Qvarnstrom, Simonsson et al. 2004). The clinical literature is also consistent with a slow component to tissue recovery (Hendry 1992; van den Aardweg and Hopewell 1992; Nyman and Turesson 1995; Bentzen, Saunders et al. 1999; Orton 2001). For example, in breast cancer patients treated via direct electron fields to right and left internal mammary chains (sternum) to 50 Gy in 25 fractions using once daily (24 hours interval) or twice daily (8 hours interval) fractions to right and left sides, respectively, the increased incidence and severity of cutaneous telangiectasia developing over 7 years of follow up in the skin irradiated with 8 hour intervals were equivalent to a 10% increase in total dose (Nyman and Turesson 1995). Overall, the data are consistent with a model in which rapidly proliferating cells have less time than slowly proliferating ones to complete the repair of complex DSB prior to DNA replication and mitosis, regardless of fraction size. A significant degree of incomplete repair prior to cell division in rapidly cycling cells would account for a reduction in clinical fractionation sensitivity. However, this model is not obviously applicable to normal tissues which have effective cell cycle controls. The

induction of DSB by ionising radiation activates checkpoints at several positions in the cell cycle (Fei and El-Deiry 2003; Pawlik and Keyomarsi 2004). Exponential phase primary human fibroblasts exposed to high doses of x-rays in vitro remain in predominantly G1 arrest, perhaps for months, unless stimulated to resume passage through the cell cycle (Di Leonardo, Linke et al. 1994). It may be possible to envisage loss of fractionation dependency in acutely responding tissues, where depletion of cells in the epidermis, for example, becomes a powerful stimulus of stem cell division despite incomplete repair (Dorr 1997; Trott 1999).

1.12 Implications for the fractionation sensitivity of tumours

The association between fraction size sensitivity and the proliferative status of stem cell compartments has been discussed in relation to normal tissues, but there is no reason why it should not apply to tumours too. As discussed previously, squamous carcinomas have high proliferative indices, and display, on average, low fraction size sensitivity (Thames, Bentzen et al. 1989). Breast and prostate cancers have relatively low proliferative indices, and there is recent evidence that they are substantially more sensitive to fraction size than hitherto assumed (Rew and Wilson 2000; Fowler, Chappell et al. 2001; Owen, Ashton et al. 2006).

The second model of fractionation sensitivity may be more relevant in tumours, which are commonly defective for cell cycle control proteins such as p53, p21 and pRb through gene mutation (Vogelstein, Lane et al. 2000; Bartek and Lukas 2003) or by high-risk human papillomavirus (HPV) infections (Ganguly and Parihar 2009). Radiation induced G1/S arrest and subsequent non-homologous end joining repair is a p53-dependent process and, thus, is lacking in many tumour cells (Ferguson, Sekiguchi et al. 2000). Therefore, tumours with high growth fractions and/or defective checkpoints are expected to have less time than tumours with low growth

fractions and/or competent checkpoints to repair complex DSB before DNA replication and cell division.

In addition, many tumours acquire defects in one or more DNA repair pathways for example up to 30% of sporadic breast cancers harbour defects in the HR pathway (Turner, Tutt et al. 2004). Differences between different healthy and malignant tissues in how they handle DNA DSB repair are but one of several potential modulators of fractionation sensitivity. If these differences are quantitatively significant, they offer a satisfactory hypothesis for differences in clinical fraction size sensitivity.

1.13 Testing molecular models in human skin

As described above, skin serves to show how sensitivity to radiotherapy fraction size changes with time. The epidermis in patients undergoing radiotherapy for breast cancer is a readily accessible system for investigating proliferation and double strand break (DSB) repair. Acute human epidermal responses are more sensitive to fraction size (α/β value ~4 Gy) at the beginning of radiotherapy but lose this sensitivity when radiotherapy is delivered over longer periods (α/β values >10 Gy) (Trott 1986; Turesson and Thames 1989). Thus the epidermis serves as a model for late reacting normal tissues (during the first 2 weeks of radiotherapy) and early reacting normal tissues towards the end of treatment. At baseline, basal epidermal stem cells are predominantly in G0 phase, but switch to proliferative phase during the third week before accelerated proliferation gets underway. The regional distribution of stem cells and transit cells can be imaged using IHC against β1-integrin to identify the former and Ki67 or specific anti-keratin antibodies to identify the latter (Jensen, Lowell et al. 1999). This offers a powerful system for studying the kinetics of DSB rejoining in subpopulations of cells with markedly different proliferative indices. It also opens the possibility of investigating changes in DSB repair kinetics coinciding with accelerated proliferation in response to radiotherapy. DSB rejoining can be monitored in tissue sections using antibodies against 53BP1 as a surrogate for DSB and antibodies against RAD51 as a bio-marker of HR (Thompson and Schild 2001).

1.14 Aims of the thesis

The aims of this study were to identify cell and molecular processes accounting for sensitivity to radiotherapy fraction size using basal epidermis as a model for early and late responding normal tissues in patients undergoing radiotherapy for early breast cancer. For mechanistic studies, CHO cell lines deficient in specific DNA repair genes were used to test molecular pathways involved in sensitivity to fraction size. Subsequently, the effect of adding various DNA repair inhibitors (ATM, PARP, DNAPKcs and CHK1 inhibitors) to fractionated radiotherapy in CHO cell lines was evaluated.

The hypotheses under test are

1. Loss of fraction size sensitivity observed in human epidermis during a course of high dose fractionated radiotherapy is associated with use of HR for repair of radiation induced DSB
2. Cells reliant on HR lose fractionation sensitivity

CHAPTER TWO

Materials and methods

2.1 Materials

2.1.1 Chemicals & common buffers (Table 2.1 and 2.1)

Table 2.1. Chemical reagent information

Chemical	Supplier	Solvent	Stock concentration	Sterility	Storage
Dimethyl sulfoxide (DMSO)	Sigma-Aldrich	-	100%	Sterile-filtered (0.2 µM)	RT
Phosphate buffered saline (PBS)	Oxoid	Millipore H_2O	1x	Autoclaved	RT
Para-formaldehyde	Agar Scientific	PBS	4%	Autoclaved	RT
Citric Acid	VWR	H_2O	10mM	N/A	RT
Sodium Chloride	VWR	H_2O	8%	N/A	RT
Hydrochloric Acid	VWR	H_2O	1M	N/A	RT
Trizma base	VWR	H_2O	0.5M		RT
Calcium Chloride	VWR	H_2O	0.1%		RT
Alpha Chymotrypsin	Sigma	H_2O	0.1%		-20^{o}C

Unless otherwise stated, all chemicals were obtained from Sigma-Aldrich, UK.

Table 2.2. Common buffer information

Chemical	Contents	Stock concentration	Sterility	Storage	Stability
Lysis buffer	25 mM Tris (pH 7.6), 150 mM NaCl, 1% NP-40 (v/v), 1% sodium deoxycholate (v/v), 0.1% SDS, 10 mM NaF, 5 mM NaPPi, 1 mM Na_3VO_4, and 1x 'Complete-mini' protease inhibitor cocktail (Roche)	1x	Non-sterile	4°C	1 day
TBE buffer	108 g Tris base and 55 g boric acid dissolved in 980 ml deionised water and 20 ml 0.5 M EDTA (pH 8)	10x	Non-sterile	RT	>1 year
TBS buffer	61 g Trizma base and 81 g NaCl dissolved in 1 L deionised water. pH adjusted to pH 7.6 with addition of 1 M HCl	10x	Non-sterile	RT	>1 year
TBS-T buffer	As TBS buffer but with addition of 10 ml Triton X-100	10x	Non-sterile	RT	>1 year

2.1.2 Reagents used in histology and immunohistochemistry

Superfrost Plus Micro Slide, VWR International (#631-0108)

Coverglass (24x50), VWR International (#631-0146)

Protein block, serum free, DAKO (#X0909)

Vector avidin/biotin blocking kit, Vector Laboratories Peterborough, UK (#SP-2001)

EnVision detection systems peroxidise/DAB, Rabbit/Mouse, DAKO (#K5007)

(#K4006)

Vectastain ABC kit (Universal), Vector laboratories, (#PK-7200)

Antibody diluent DAKO (S2022)

Peroxidase blocking reagent DAKO (S2023

DAB substrate kit Vector laboratories (SK-4100)

Resin Pen Dako (S2002)

2.1.3 Primary antibodies used in immunohistochemistry and immunofluorescence

Primary antibodies used in immunohistochemistry and immunofluorescence along with their source and dilution are listed in **Table 2.3** below

Table 2.3. Primary antibodies used in immunohistochemistry and immunofluorescence

Marker	Source	Clone	Species	Cat.No.	Dilution
B1 Integrin	Novocastra	7F10	mouse	NCL-CD29	1:150-1:300 (tissues)
MCSP	Abcam	LHM2	mouse	Ab20156	1:400-1:800 (tissues)
Ki67	Novocastra	polyclonal	rabbit	NCL-Ki67p	1:100 (tissues)
Ki67	Dako	MIB-1	mouse	M7240	1:50 (tissues)
Cyclin A	Novocastra	6E6	mouse	NCL-CyclinA	1:25-1:50 (tissues)
P21	Novocastra	4D10	mouse	NCL-L-WAF-1	1:30 (tissues)
RAD51	Abcam	51RAD01	mouse	Ab1837	1:25 (tissues)
RAD51	Santa Cruz	polyclonal	rabbit	sc-8349	1:1000 (cells)
γH2AX	Millipore	JBW301	mouse	05-636	1:1000 (cells)
53BP1	Bethyl Labs	polyclonal	rabbit	A300-272A	1:100-1:300 (tissues) 1:500 (cells)

2.1.4 Secondary antibodies used in immunohistochemistry and immunofluorescence

Details of the secondary antibodies used in immunohistochemistry and immunofluorescence are listed in **Table 2.4** below.

Table 2.4. Secondary antibodies used in immunohistochemistry and immunofluorescence

Antibody	Supplier	Species	Dilution
Goat anti-rabbit Alexa Fluor 488 (green)	Invitrogen	Rabbit	1:200
Donkey anti-mouse Cy3 (red)	Donation from MRC	Mouse	1:200
Goat anti-mouse Alexa Fluor 568 (red)	Invitrogen	Mouse	1:200
Goat anti-rabbit Alexa Fluor 555	Invitrogen	Rabbit	1:500
Dako EnVision horse radish peroxidase	Dako (K4006)	Mouse/Rabbit	Not applicable

2.1.5 Cell lines

CHO cells were obtained from Larry H Thompson's lab, tested and authenticated at source. The parent wild type AA8 (Thompson, Fong et al. 1980) and its derivatives irs1SF (defective in XRCC3) (Fuller and Painter 1988; Liu, Lamerdin et al. 1998), V3-3 (defective in DNA-PKcs) (Blunt, Finnie et al. 1995) and EM9 (defective in XRCC1) (Thompson, Brookman et al. 1982) have been well characterised previously and have been used extensively in radiobiological experiments. These cell lines provided a system for testing mammalian cells derived from the same parent wild type cell line deficient in HR, NHEJ and base excision repair (BER)

respectively, representing the most important repair pathways for radiation-induced single strand breaks & DSB, respectively.

2.1.6 Reagents and plastics used in tissue culture

Dulbecco's modified Eagle Medium (DMEM)

DMSO, Sigma

Foetal calf serum (FCS), Invitrogen

Cell freezing medium, 10% DMSO, 90% FCS

Trypsin, Sigma

Normal saline, Sigma

Tissue culture plastics from Corning

2.1.7 DNA repair inhibitors

- **ATMi (KU55933)**

Chemical name: 2-morpholin-4-yl-6-thianthren-1-yl-pyran-4-one.

KU55933 was synthesised by KuDOS pharmaceuticals Ltd, Cambridge Science Park, Milton Road, Cambridge and was a kind gift from the Stephen Jackson laboratory.

- **DNAPKcsi (KU51777/NU7026)**

Chemical name: 2-(morpholin-4-yl)-benzo[h]chromen-4-one.

NU7026 was synthesised in the Department of Chemistry, University of Newcastle upon Tyne, United Kingdom and was a kind gift from Professor Nicola Curtin.

- **PARPi (AG-14699/PF 01367338)** Rucaparib, Axon Medchem

Chemical name: 8-Fluoro-2-(4-methylaminomethyl-phenyl)-1,3,4,5-tetrahydro-azepino[5,4,3-cd]indol-6-one phosphate. This molecule was a kind gift from Pfizer.

2.1.8 Reagents used in FACS analysis

Propidium iodide, Molecular probes, Invitrogen (#P1304MP)

RNAse A, Sigma (#R6513)

Triton X100, Sigma (#T9284)

EDTA, Sigma (#E5134)

Ethanol, VWR International, Leicestershire, UK (#101077Y)

2.2 Methods

2.2.1 Ethics approval

Ethical and scientific approval for the study was granted by the Royal Marsden Hospital Research Ethics Committee (REC No: 06/Q0801/73) and Committee for Clinical Research (CCR 2900). All patients received a patient information sheet and gave written informed consent.

2.2.2 Patients

30 patients prescribed radiotherapy to a dose of 50 Gy in 25 fractions (2.0 Gy per fraction) over 5 weeks to the breast after tumour excision of early breast cancer were recruited. No concurrent chemotherapy was allowed and endocrine therapy was started after completion of radiotherapy where appropriate.

2.2.3 Radiotherapy

Radiotherapy was delivered to the whole breast using tangential 6-10 MV X-ray beams. We adhered to the ICRU (International Commission on Radiation Units and Measurements) recommendations to keep dose inhomogeneity between 95% and 105% in the target volume and three-dimensional dose compensation was used to achieve homogeneity. The estimated dose to the skin was 1.6 Gy per fraction. Radiotherapy treatment was not started on Tuesday so that the interval between

fractions 4 and 5 (i.e. prior to biopsy on day 5) would not exceed 24 hours. In view of bank holidays 2 patients had biopsies taken after their 4th fraction instead of the 5th.

2.2.4 Human tissue work

2.2.4.1 Tissue collection

Single 4 mm punch biopsies of breast skin were collected at the following time-points and locations:

a) 2 hours (h) after the 1st fraction from irradiated and contralateral breasts.

b) 2 h after the 5th fraction from irradiated breast.

c) 1 h before and 2 h after the final (25th) fraction from irradiated breast.

Local anaesthetic (0.5–1 ml lidocaine) was infiltrated subcutaneously prior to biopsies. Biopsies were taken at least 2 cm inside the lateral border of the breast volume and at least 1 cm apart. Steri-strips plus dry non-adhesive gauze were applied to approximate the wound edges. No problems with healing or infection were encountered.

2.2.4.2 Tissue processing

Biopsies were fixed in 10% neutral buffered formalin for at least 24 hours and then embedded in paraffin. Four punch biopsies, 2 from the irradiated breast and 2 from the unirradiated breast, were collected immediately after the 25th fraction of radiotherapy in 3 patients. One paired sample from each of the 3 patients was snap frozen in liquid nitrogen and the other fixed in formalin.

2.2.4.2.1 Cutting paraffin sections

3-4 µm sections were cut from formalin-fixed paraffin embedded blocks. To avoid loss of tissue section adherence following antigen retrieval, all sections were picked

up onto either superfrost plus or superfrost gold slides. Sections were dried overnight at 37ºC.

2.2.4.2.2 Cutting frozen sections

The skin biopsies snap frozen in liquid nitrogen were embedded in cryogel. 4-5 µm sections were cut and fixed in cold acetone for 10 minutes.

2.2.4.2.3 Haematoxylin and eosin protocol

Sections were stained in Harris's haematoxylin for 5 minutes and dipped in 1% acid alcohol prior to washing in running tap water for 5 minutes. Sections were then stained in 1% aqueous eosin for 5 minutes prior to further washing in running tap water. Sections were subsequently dehydrated through a series of graded ethanols and xylene before mounting in DPX.

2.2.4.3 Immunohistochemistry

To improve adherence of tissue sections following antigen retrieval, all sections were picked up onto either superfrost plus or superfrost gold slides and placed on a hot plate at 60 degrees for 10 minutes before starting. De-paraffinised & rehydrated samples were then microwaved at 850 W in 250 ml of 10 mM citric acid (pH adjusted to 6.0) for 12 minutes (3 X 4 minutes). They were then left to stand at room temperature for 20 min, before being washed in running tap water, rinsed in Tris buffer saline (TBS) and the section circled with a resin pen. We performed double staining in layers as described before (Hoskin, Sibtain et al. 2004) **(For all antibody details please refer to Table 2.3 and 2.4)**. Briefly, after treating with DAKO peroxidase & protein block for 5 minutes each, the sections were incubated with β1 Integrin (CD29) for 1 hour at room temperature. After washing with TBS, mouse/rabbit Dako EnVision horse radish peroxidase (HRP) was applied for 30

minutes. Following further washing in TBS, diaminobenzadine (DAB) solution was applied for 2 min. For the second layer of staining, 250 ml of 10mM citric acid (pH adjusted to 6.0) was brought to the boil by microwaving at 850 W for 4 minutes and the slides immersed in it for 1-2 minutes (to remove any unbound antibody) before cooling down to room temperature. Dako protein block was again applied for 5 minutes, and the sections were incubated for 1 hour at room temperature with Ki67 (MIB-1) or 53BP1 antibody. Similar to the first layer, mouse/rabbit Dako EnVision HRP was applied for 30 minutes followed by Vector SG (Vector laboratories) for 5-10 minutes. Counterstaining was performed using methyl green (Surgipath) for 20 seconds followed by dehydration, clearing in xylene & mounting in DPX.

Cyclin A and p21 single staining was done on serial 4 µm sections of epidermis as described above for the first layer. In order to compare β1 Integrin staining with melanoma chondroitin sulphate proteoglycan (MCSP), which works best on fresh frozen skin samples, we obtained paired biopsies from 3 patients, one of which was fixed in formalin and the other snap frozen. For MCSP staining, the snap frozen skin biopsies were embedded in cryogel, sectioned & fixed in cold acetone for 10 minutes. No antigen retrieval was required. After peroxidase & protein block the sections were incubated with the MCSP antibody for 60 minutes at room temperature followed by EnVision HRP & DAB as described above. Haematoxylin was used as the counterstain.

2.2.4.4 Scoring methods for immunohistochemistry

The entire interfollicular basal compartment was analysed in each section. Analysis of the immunohistochemical data was undertaken by visual inspection and counting of the slides at high power (X60) and was facilitated for some of the analyses by capturing digital images using an Axioscope trans-illumination microscope (Zeiss) connected to a 3CCD colour camera (JVC) connected to a PC with a Matrox Meteor frame grabber in a PCI bus. The basement membrane length was measured using a calibrated line tool developed in Visilog 5.02 software (Noesis Vision Inc.). β1 integrin and p21 staining was scored as negative (-), weak (+), moderate (++) or strong (+++) depending on intensity of staining. Only cells that were attached to the basement membrane and had moderate to strong uptake of β1 integrin along the entire cell membrane were considered to be positive (putative stem cells). Any nuclear uptake of Ki67 (positive in all phases of cell cycle except G0) or cyclin A (S-G2 phase marker) was scored as positive.

2.2.4.5 Immunofluorescence technique

For double fluorescent staining, the sections were deparaffinised, rehydrated & heat mediated antigen retrieval performed as above. After 5 minutes in Dako protein block the sections were incubated with RAD51 (51RAD01) and Ki67 (NCL-Ki67p) antibody for 60 minutes at room temperature. After washing with 3% fetal calf serum (FCS) in PBS, Alexa Fluor 488-conjugated goat anti-mouse IgG (Invitrogen,1:200) and TRITC-conjugated donkey anti-rabbit IgG (1:200) was applied for 60 minutes in the dark at room temperature. This was followed by washing with 3% FCS & staining with DAPI (1:200) for 5 minutes. The slides were air dried and mounted in Vectashield. Double staining with 53BP1 and Ki67 (MIB-1) as well as Ki67 (NCL-Ki67p) and cyclin A was done in a similar fashion. Secondary antibody combinations

(conjugated with Alexa Fluor 488 or 555, all at 1:200 dilutions) were applied as appropriate.

2.2.4.6 Scoring methods for immunofluorescence

All analysis was done manually at 100X in oil using a Nikon Eclipse TE200 epifluorescence microscope. Digital images were obtained with a cooled analog camera via a video frame grabber and PC. To study the DNA double strand break repair pathways in the proliferating versus non-proliferating cell population of the basal epidermis, we looked at RAD51 & 53BP1 foci numbers in all Ki67 positive versus negative cells along the basement membrane. To assess what proportion of proliferating cells were in S-G2 phase of the cell cycle, all Ki67+ cells in the section were analysed for cyclin A uptake by co-staining.

2.2.5 Mammalian cell culture

2.2.5.1 Cell culture conditions

CHO cells were obtained from Larry H Thompson's lab, tested and authenticated at source. The parent wild type (AA8), XRCC1 deficient (EM9), XRCC3 deficient (irs-1SF) and DNA-PK deficient (V3-3) cells were grown in Dulbecco's Modified Eagle Medium (D-MEM) (1X) containing 1000 mg/L glucose, 4mM L-glutamine and 110 mg/L sodium pyruvate with 10% fetal bovine serum, 100 U penicillin, and 0.1 mg/ml streptomycin (termed here, 'complete media'). All cells were maintained in T175 flasks (Corning) with 20 ml D-MEM in a well-humidified incubator at 37°C with 5% CO2. Exponentially growing cultures were used for all experiments. Cells were split every 3-4 days (at approximately 80% confluency) at a ratio of 1:10 (AA8, EM9) and 2:10 (V3-3, irs-1SF). They were split by aspirating the existing media and washing the flask twice with 10 ml warm 1x phosphate buffered saline (PBS) and once with 5 ml warm 1x trypsin-EDTA solution. Following 5 minutes incubation at 37°C, the cells

were re-suspended in complete media and transferred into a sterile 50 ml tube (Corning). Vigorous pipetting was used to ensure a single-cell suspension before cells were diluted by the appropriate ratio in fresh complete media and returned to the flask.

2.2.5.2 Thawing liquid nitrogen stocks

Liquid nitrogen stocks were rapidly thawed at 37°C for 2 minutes, and the cell suspension diluted in a drop-wise fashion with 10 ml complete media. The cells were spun into a pellet by centrifugation at 800 rpm for 5 minutes, the DMSO-containing media aspirated off, and the cells re-suspended with 10 ml fresh complete media. The cell suspension was then transferred to a T75 flask (Corning) and cells allowed to revive for 2 passages before they were used for experimentation.

2.2.5.3 Freezing cell stocks

Early passage cell lines to be frozen were grown to 80% confluency in T175 flasks (Corning) and trypsinised as described above. The cells were re-suspended in 10 ml complete DMEM containing 10% Hybrid-max sterile-filtered DMSO (v/v) and a single-cell suspension obtained. 1 ml aliquots were prepared in cyrotubes and placed directly into -80°C overnight before being transferred into liquid nitrogen. These ‘primary’ stocks were subsequently tested for *Mycoplasma* infection and used to create ‘secondary’ frozen stocks from which cells could be obtained for experimentation. The primary stocks were thus kept to replenish secondary stocks with early passage cells as needed.

2.2.5.4 *Mycoplasma* testing

Liquid nitrogen stocks of all cell lines used were shown to be *Mycoplasma* negative, and thawed cultures were maintained for a maximum of one month before being discarded and replaced. Growing cultures were subjected to periodic *Mycoplasma* testing, which involved seeding a 96-well plate at a density of 4,000 cells per well and allowing the cells to grow in antibiotic-free but otherwise complete media for 48 hours. The media was then replaced with 100 µl PBS containing 70% methanol (v/v), and incubated at room temperature for 20 minutes, before staining the DNA in a similar incubation with 100 µl PBS containing 1 µg/ml DAPI for 5 minutes. This solution was then replaced with 100 µl PBS and the cells imaged under 20x magnification using an InCell Analyser (GE Healthcare, UK). *Mycoplasma*-infected cultures were identified by the presence of a halo and/or shading around the outside of the nucleus and within the cytoplasm. Cellular morphology was also checked daily and if any significant changes were detected the culture was discarded.

2.2.6 Preparation and quantification of mammalian cell extracts

2.2.6.1 Whole cell extracts

Unless otherwise stated, whole cell extracts were prepared from cells growing 75 cm^2 flasks (Corning). Wild type CHO cells were grown in D-MEM (1X) alone or in D-MEM (1X) with specific DNA repair inhibitors. The ATM inhibitor KU55933 and the DNAPKcs inhibitor KU51777 were added at a concentration of 10 µM at least 1 hour before irradiating the cells with 10 Gy. Lysis buffer was prepared on the day of use. Cells were washed once with 200 µl aliquots of warm 1x PBS before 10 µl aliquots of 1x lysis solution were incubated on the cells for 5 minutes on ice, with occasional swirling of the plate to ensure equal coverage. Pipette tips were used to scrape the wells and collect the lysate, which was subsequently incubated in an ice-cold sonicating water bath for 15 minutes, prior to centrifugation at 14,000 g for 15

minutes to pellet cellular debris. The supernatant was collected, protein concentration estimated by Bradford assay, and aliquots stored at -20°C.

2.2.6.2 Bradford assay

Bradford assays were carried out in 96-well plate format. A protein standard consisting of 0, 10, 20, 30, 40, 50, 60, 70, 80, 90, and 100 µg/ml bovine serum albumin was first created, and duplicate 5 µl aliquots transferred to a 96-well plate. The experimental sample was next diluted 1:10 by adding 1 µl sample to 9 µl 1x PBS, and 5 µl aliquots of the diluted sample added to the 96-well plate. 250 µl aliquots of shaken Coomassie Plus protein assay reagent (Thermo Scientific) was transferred to each well and the plate incubated in the dark at room temperature for 10 minutes, before reading the absorbance of each well at 595 nm using an Envision 2103 multi-label plate reader (Perkin Elmer). To obtain an estimate of protein concentration from the data, the blank control was first subtracted from all wells, and a standard curve of BSA concentration against absorbance was plotted. A linear regression was performed and the equation, y = slopex + intercept, solved. Each experimental sample value was subtracted from the intercept and divided by the slope, before dividing by 10 to account for the dilution factor, and finally dividing by 1000 to give a protein concentration estimate in µg/µl.

2.2.7 Visualisation of proteins by Western Blotting and chemiluminescent detection

2.2.7.1 Electrophoresis

Pre-cast 4-12% graduated Bis-Tris gels (for smaller molecular weight proteins) (Invitrogen) or 3-8% Tris-acetate gels (for larger molecular weight proteins) were prepared by removal of the comb and non-conducting strip, and rinsing the wells with Millipore H_2O (mH_2O) to remove air bubbles. These were loaded into tanks and

both chambers filled with 1x NuPAGE MOPS SDS running buffer (Invitrogen). 500 µl antioxidant (Invitrogen) was added to the inner chamber. 10 µg protein was diluted in 1x LDS sample buffer (Invitrogen) and 1x reducing agent (Invitrogen), and the proteins denatured by incubation at 70°C for 10 minutes. Samples were subseqeuently loaded onto the gel, alongside a Seagate Blue Plus (Invitrogen) ladder. The gel was run at 180 V for one hour.

2.2.7.2 Nitrocellulose transfer

The gel was removed from its casing, rinsed with mH_2O, and the leading edge cut away and discarded. A transfer 'sandwich' was created by overlaying a 1x transfer buffer soaked sponge, with 3 similarly soaked pieces of Whatman paper, which were rolled smooth to ensure a flat surface for even protein transfer. The gel was next placed onto the sandwich, and covered with a nitrocellulose membrane on which the orientation had been marked. The sandwich was completed by an additional 3 pieces of Whatman paper and second sponge. The whole apparatus was inserted into a transfer tank containing 1x transfer buffer and ice block, and ran at 100 V for 1 hour. The nitrocellulose membrane was subsequently rinsed in 1x TBS-T, and non-specific binding blocked by overnight incubation at 4°C in 1x TBS-T containing 5% skimmed milk (w/v, Fluka).

2.2.7.3 Immunodetection

The nitrocellulose membrane was incubated at room temperature on a shaking board in 1x TBS-T containing 5 % milk (w/v) and an appropriate dilution of primary antibody **(Table 2.5)** for 1 hour. After three 10 minute washes with 1x TBS-T, the membrane was similarly incubated in 1x TBS-T containing 5 % milk (w/v) and a 10,000x dilution of either mouse, rabbit, or goat secondary antibody (table 2.4). The membrane was again washed three times with 1x TBS-T for 10 minutes.

Table 2.5. Antibodies used in western blotting.

Antibody	Supplier	Dilution	Species
Anti-DNA-PKcs (phospho Ser2056)	Abcam	1:500	Rabbit polyclonal
Anti-ATM (phospho Ser1981)	Abcam	1:5000	Rabbit monoclonal
Anti-actin	Abcam	1:40,000	Mouse
Anti-Tubulin	Abcam	1:5,000	Mouse
Mouse secondary (HRP)	Abcam	1:10,000	Mouse
Rabbit secondary (HRP)	Abcam	1:10,000	Rabbit

2.2.7.4 Chemiluminescence

Protein chemiluminescence was achieved using the BM Chemiluminescence ELISA Substrate kit (Roche) according to the manufacturer's instructions. Briefly, 100 µl starting reagent B (stabilized H_2O_2) was added to 10 ml substrate reagent A (buffered solution containing Horseradish peroxidase, luminol and 4-iodophenol) and mixed, immediately before use. The nitrocellulose membrane was coated with the mixed solution and incubated at room temperature for 1 minute, before blotting off the excess fluid. Under dark room conditions, the membrane was transferred into a Hypercassette (Amersham Biosciences) and overlaid with X ray film (Fujifilm). The X ray film was exposed for between 1-10 minutes and subsequently fixed using a film processor (Konica Minolta SRX-101A, USA). Quantification of protein expression was completed using Quantity One software (Version 4, Bio-Rad Laboratories).

2.2.7.5 PARP activity assay

To assay cellular PARP activity in cells, cells were grown in 10-cm tissue culture dishes in medium alone or in medium with 10 μmol/L AG14699 for 4 hours. Cells were washed once with ice-cold PBS, lysed in 50 μL of PARP buffer containing 0.5 mol/L NaCl, 1% (v/v) NP40, and Complete protease inhibitors (Roche) on ice for 30 minutes with occasional vortexing. The lysates were clarified by centrifugation at 14,000 rpm, at 4°C for 10 minutes. The protein concentration of the extracts was quantified using Bradford protein dye reagent (Bio-Rad), and PARP activity was assayed using the Trevigen Universal chemiluminescent PARP assay kit according to the manufacturer's instructions, with modifications. The lysate (30 μg/well) was added in duplicates to the wells containing PARP buffer and PARP cocktail, followed by incubation at room temperature for 1 hour. Activated DNA was added to the standards but was omitted from the extracts. The wells were washed thrice with PBS and thrice with PBS and 0.1% Triton X-100, followed by incubation with a 1:1,000 dilution of streptavidin-horseradish peroxidase in strep diluent buffer for 1 hour. The wells were washed again thrice with PBS and thrice with PBS and 0.1% Triton X-100. Chemiluminescent detection was performed per the manufacturer's instructions. The background reading was subtracted from the readings of the samples, and PARP activity was calculated using the standard curve obtained from readings of the standards.

2.2.8 Cell-based assays

2.2.8.1 Clonogenic survival assay

2.2.8.1.1 Acute dose survival assays

All cell lines were grown in 8 ml D-MEM (1X) at 37°C and 5% CO_2 in a well-humidified incubator. Cells were incubated for four hours followed by treatment with IR doses of 1, 2, 3, 4, 6 and 8 Gy. The control flask was sham irradiated. Four hours after irradiation cells were counted and plated in triplicate onto 10 cm^2 tissue culture petri dishes (Corning) in appropriate numbers optimised by cell line and day of IR (ranging from 250 to 100,000 cells). Once plated for survival, the cells were incubated in fresh D-MEM (1X) for a minimum of 10 days to allow colony outgrowth. Colonies were fixed and stained by replacing media with a solution of 70% methanol (v/v) and 0.5% methylene blue (w/v) for 1 hour. Plates were then rinsed with tap water and allowed to dry overnight. Colonies of more than 50 cells were counted and plating efficiency calculated from the untreated controls. Clonogenic survival was expressed as a fraction of the untreated control using the formula 'Surviving fraction = Plating efficiency $_{(treated)}$/Plating efficiency $_{(control)}$.

2.2.8.1.2 Fractionated dose survival assays

The experiments were initiated by seeding of 50,000-100,000 (depending on cell line) cells in 25 cm^2 flasks (Corning) which were cultivated in 8 ml D-MEM (1X) at 37°C and 5% CO_2. Six flasks were seeded for all groups including the control. The flasks were incubated for four hours followed by treatment with 1 Gy IR (or 4 Gy). The control was sham irradiated. Four hours after irradiation cells were counted and plated in triplicate onto 10 cm^2 tissue culture petri dishes (Corning) in appropriate numbers optimised by cell line and day of IR. This procedure was repeated for 16 days with 1 Gy exposure each day (or 4 days for the 4 Gy experiment).

On every Friday the AA8 and EM9 cell lines required reseeding to avoid overgrowth for the following week, which was done at the same concentration as in the beginning. Irs-1SF required reseeding in the first week only, whereas V3-3 cells did not require to be reseeded. No irradiation or plating for survival was done over the weekend. When reseeding and seeding for survival all the cultivation media and washes were retained, centrifuged and the cell pellet pooled with the trypsinized ones. This was done to reduce any loss of cells that may have detached during IR. Once plated for survival, the cells were incubated in fresh D-MEM (1X) for a minimum of 10 days to allow colony outgrowth. Colonies were fixed and stained by replacing media with a solution of 70% methanol (v/v) and 0.5% methylene blue (w/v) for 1 hour. Plates were then rinsed with tap water and allowed to dry overnight. Colonies of more than 50 cells were counted and plating efficiency calculated from the untreated controls. Clonogenic survival was expressed as a fraction of the untreated control as described above.

2.2.8.1.3 Fractionated dose survival assays with inhibitors

For every drug tested, 50,000 AA8 cells each were seeded in six 25 cm^2 flasks (Corning) and cultivated in 8 ml D-MEM (1X) at 37°C and 5% CO_2. These served as controls, one for each day of the week from Monday to Friday. The controls received only DMSO at the same concentration as the inhibitors (i.e. <1% final concentration). For the test flasks 100,000 AA8 cells were seeded in six 25 cm^2 flasks (Corning) for each drug. The drugs were used at the following concentrations

1. ATM inhibitor KU55933: 10 µM
2. DNAPKcs inhibitor KU51777: 10 µM
3. PARP inhibitor AG-14699: 0.4 µM; PARP inhibitor KU58948: 2 µM

All the flasks were incubated for four hours followed by treatment with 1 Gy IR. All the drugs were added at least 1 hour before the first fraction of IR. Four hours after irradiation cells were counted and 200 cells plated in triplicate onto 10 cm^2 tissue culture petri dishes (Corning) for clonogenic survival. An extra flask was seeded for the 0 and 1 Gy dose which was allowed overnight recovery following IR before plating out for survival to check that reseeding the same day did not affect survival. This procedure was repeated for 16 days with 1 Gy exposure each day with cells being plated for clonogenic survival 4 hours after each exposure.

On every Friday the AA8 cells were reseeded into six new flasks for each day of the following week and fresh drugs/DMSO added accordingly. 50,000 cells were seeded for the control flasks and 100,000–250,000 cells for the flasks with inhibitors. No irradiation or plating for survival was done over the weekend. As above, when reseeding and seeding for survival all the cultivation media and washes were retained, centrifuged and the cell pellet pooled with the trypsinised ones. This was done to reduce any loss of cells that may have detached during IR. Once plated for survival, the cells were incubated in fresh D-MEM (1X) for a minimum of 10 days to allow colony outgrowth. Colonies were fixed and stained by replacing media with a solution of 70% methanol (v/v) and 0.5% methylene blue (w/v) for 1 hour. Plates were then rinsed with tap water and allowed to dry overnight. Colonies of more than 50 cells were counted and plating efficiency calculated from the untreated controls. Clonogenic survival was expressed as a fraction of the untreated control.

2.2.8.2 Irradiation

γ-irradiations were performed at room temperature using a GSR D1 137Cs γ-irradiator (Gamma-Service Medical GmbH, Leipzig, Germany) at a dose rate of ~1.9 Gy/min. Cells were either irradiated with 1 Gy each weekday to a total of 16 Gy over

3 weeks or at a higher dose per fraction of 4 Gy daily for 4 days to the same total dose. Before and after irradiation, cells were incubated in a well-humidified incubator at 37°C with 5% CO2, situated next to the irradiator room in order to minimise detachment during transportation. No irradiation was done on weekends.

2.2.8.3 Flow Cytometry: Cell-cycle analysis

Cells were harvested with trypsin from columns 2, 4, 6, 8, 10 and 12 of duplicate 96 well plates (**Fig 2.1),** 24 h after the previous dose of RT for each cell line separately. The cells were fixed in ice-cold ethanol (70%) at 4°C for a minimum of 30 min or at -20°C overnight. For cell cycle analysis the fixative was removed by centrifugation at 250 g and the cells were resuspended in PBS containing propidium iodide (Sigma, Dorset, UK) at a final concentration of 10 µg/ml. The samples were subjected to fluorocytometric analysis using a Becton-Dickinson FACScan. Analyses were carried out using Modfit (Verity Software House, ME, USA).

2.2.8.4 Immunocytochemistry: IN Cell analysis

2.2.8.4.1 DNA DSB induction and repair in each of the 4 CHO cell lines

Twenty three 96 well plates were seeded with optimised cell numbers for each of the 4 CHO cell lines and allowed to attach for at least 4 hours prior to IR (as per the template in **Fig 2.1**). 3 plates served as controls (sham irradiated) and were fixed 24 h, 1 week and 2 weeks after seeding. The remaining twenty 96 well plates were irradiated each day with 1 Gy from Monday to Friday for 2 weeks (total of 10 Gy) with 2 plates removed each day for fixing cells and studying DSB repair kinetics at each 1 Gy incremental dose level. For each cell line alternate columns were fixed at 0.5 h, 1 h, 2 h, 4 h, 6 h and 24 h after irradiation (**Fig 2.1**). Whilst each column was being fixed the remaining wells were covered with adhesive plate sealing film (BD Falcon, Catalogue number 353073) so that the cells would be protected from

paraformaldehyde (PFA). The plates were placed on a hot plate at 36°C whilst fixing so as not to slow DSB repair. The cells from the desired column were washed with phosphate-buffered saline (PBS), fixed with 4% PFA for 15 minutes and then washed with PBS. The plates were returned back to the incubator after removing the adhesive film till the next time point. After all the columns in the plates were fixed, the cells were permeabilised with 0.3% TritonX-100 in PBS for 10 minutes followed by blocking with 3% bovine serum albumin (BSA) in PBS for 40 minutes. RAD51 antibody (Santa Cruz) was added at 1:1000 in 3% BSA and incubated at 4°C overnight. For dual staining with γH2AX, the RAD51 antibody was removed and γH2AX antibody (Millipore) added at 1:1000 for 1.5 h at room temperature. Single staining with 53BP1 antibody (Bethyl labs) was done at 1:500 for 1.5 h at room temperature. (**For antibody details please see Table 2.3 and 2.4**). After washing thrice with PBS, appropriate secondary antibodies Alexa Fluor 488-conjugated goat anti-rabbit IgG (Invitrogen, 1:500) and Alexa Fluor 555-conjugated goat anti-mouse IgG (Invitrogen, 1:500) was applied for 1 h in the dark at room temperature. Cells were counterstained with 4,6 diamidino-2-phenylindole (DAPI), for 5 minutes and washed in PBS.

Fluorescence images were captured with the IN Cell Analyzer 1000 automated epifluorescence microscope (GE Healthcare) using a 40X objective. Fifteen images were taken per well and at least 100 cells were analysed for each time point. Automated foci analysis for percentage positive cells and mean foci number per cell was carried out using the IN Cell analyser 1000 workstation software (v3.5) as previously described (Prevo, Deutsch et al. 2008; Higgins, Prevo et al. 2010). The cut-off for 53BP1 positivity was taken as >5 foci and for RAD51 as >4 foci based on the control un-irradiated levels and previous optimisation studies (Higgins, Prevo et al. 2010).

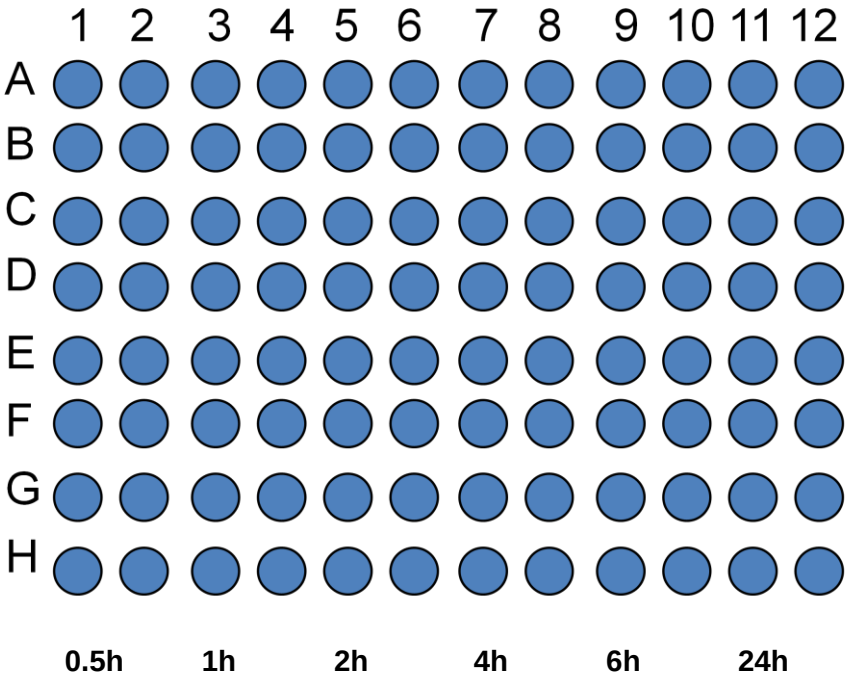


Figure 2.1: 96 well plate lay out for fractionated IR experiments comparing 4 different CHO cell lines.

Rows A&B: AA8 cells plated

Rows C&D: EM9 cells plated

Rows E&F: V3-3 cells plated

Rows G&H: irs1SF cells plated

Columns 2, 4, 6, 8, 10, 12: Cells harvested for cell cycle analysis just prior to next fraction of IR

Columns 1, 3, 5, 7, 9, 11: Cells fixed and stained for RAD51, 53BP1 and γH2AX at various time points after each fraction of IR as shown in the figure

2.2.8.4.2 DNA DSB induction and repair analysis in wild type cells with or without DNA repair inhibitors

Twenty three 96 well plates were seeded with AA8 cells optimised for each dose level and allowed to attach for at least 4 hours prior to IR (as per the template in **Fig 2.2 and 2.3**). The drugs were used at the following concentrations

1. ATM inhibitor KU55933: 10 µM
2. DNAPKcs inhibitor KU51777: 10 µM
3. PARP inhibitor AG-14699: 0.4 µM

3 plates served as controls (sham irradiated) and were fixed 24 h, 1 week and 2 weeks after seeding. The remaining twenty 96 well plates were irradiated each day with 1 Gy from Monday to Friday for 2 weeks (total of 10 Gy) with 2 plates removed each day for fixing cells and studying DSB repair kinetics at each 1 Gy incremental dose level. The media and drug were changed every Monday, Wednesday and Friday. For each cell line alternate columns were fixed at 0.5 h, 1 h, 2 h, 4 h, 6 h and 24 h after irradiation (**Fig 2.2 and 2.3**). Whilst each column was being fixed the remaining wells were covered with adhesive plate sealing film (BD Falcon, Catalogue number 353073) so that the cells would be protected from paraformaldehyde (PFA). The plates were placed on a hot plate at 36°C whilst fixing so as not to slow DSB repair. The cells from the desired column were washed with phosphate-buffered saline (PBS), fixed with 4% PFA for 15 minutes and then washed with PBS. The plates were returned back to the incubator after removing the adhesive film till the next time point. After all the columns in the plates were fixed, the cells were permeabilised with 0.3% TritonX-100 in PBS for 10 minutes followed by blocking with 3% bovine serum albumin (BSA) in PBS for 40 minutes. RAD51 antibody (Santa Cruz) was added at 1:1000 in 3% BSA and incubated at 4°C overnight. For dual staining with γH2AX, the RAD51 antibody was removed and γH2AX antibody (Millipore) added at 1:1000 for 1.5 h at room temperature. Single

staining with 53BP1 antibody (Bethyl labs) was done at 1:500 for 1.5 h at room temperature. (**For antibody details please see Table 2.3 and 2.4**). After washing thrice with PBS, appropriate secondary antibodies Alexa Fluor 488-conjugated goat anti-rabbit IgG (Invitrogen, 1:500) and Alexa Fluor 555-conjugated goat anti-mouse IgG (Invitrogen, 1:500) was applied for 1 h in the dark at room temperature. Cells were counterstained with 4,6 diamidino-2-phenylindole (DAPI), for 5 minutes and washed in PBS.

Fluorescence images were captured with the IN Cell Analyzer 1000 automated epifluorescence microscope (GE Healthcare) using a 40X objective. Fifteen images were taken per well and at least 100 cells were analysed for each time point. Automated foci analysis for percentage positive cells and mean foci number per cell was carried out using the IN Cell analyser 1000 workstation software (v3.5) as previously described (Prevo, Deutsch et al. 2008; Higgins, Prevo et al. 2010). The cut-off for 53BP1 positivity was taken as >5 foci and for RAD51 as >4 foci based on the control un-irradiated levels and previous optimisation studies (Higgins, Prevo et al. 2010).

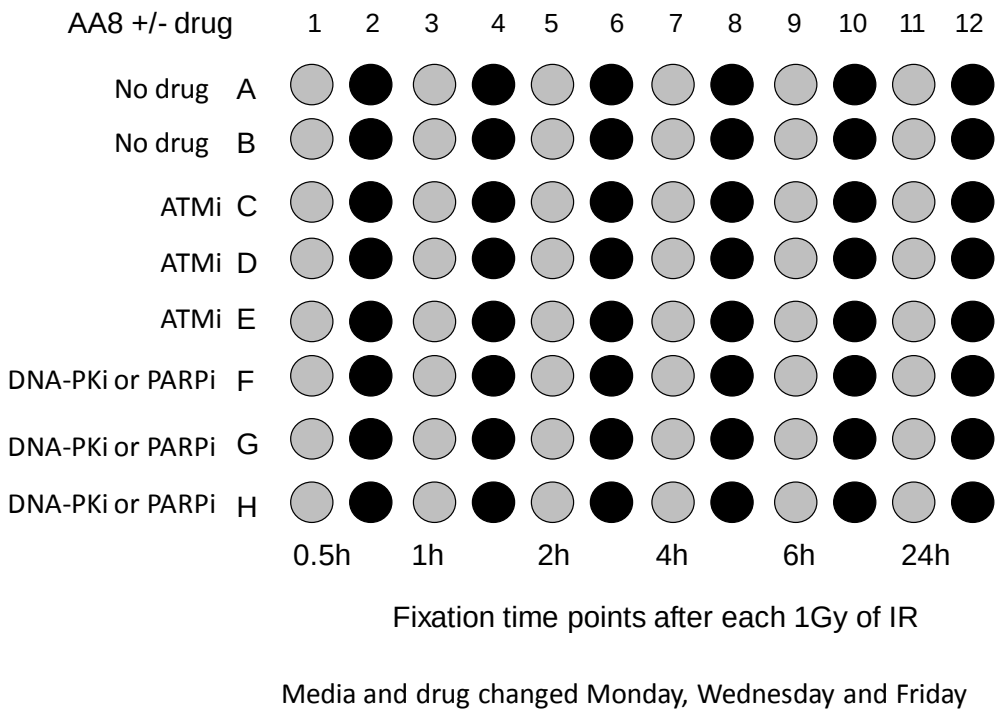


Figure 2.2: 96 well plate lay out for fractionated IR experiment (1 Gy/day) with AA8 cells with or without inhibitor drugs.

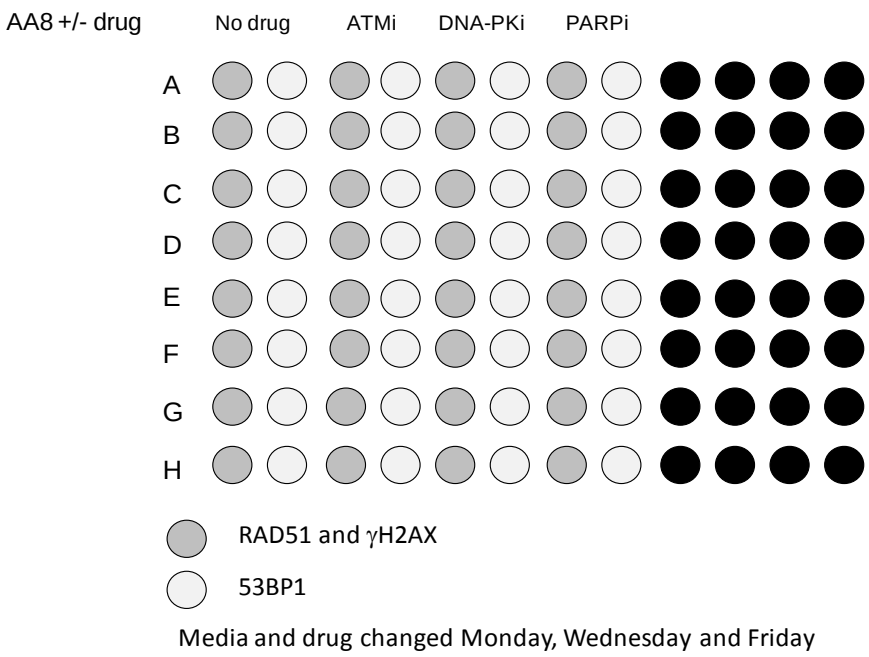


Figure 2.3: 96 well plate lay out for control experiment (no IR) with AA8 cells.

2.2.9 Statistical analysis and sample size

Standard errors of the mean were calculated by dividing the standard deviation of the mean of more than two experiments (or patient data set) by the square root of the number of experiments (or patients). Unless otherwise stated, error represents standard error calculated from three independent experiments in triplicate. Student's T-test (2-tailed) was applied to generate statistical significance. The level of significance was taken as $p<0.05$. One star refers to a p value <0.05, two stars <0.01, and three stars <0.001, whereas the abbreviation 'NS' means 'not significantly different'.

For the primary analysis the number of RAD51 foci present after the first fraction was compared with the number present after the final fraction using a paired t-test. A sample size of 30 patients would enable a standardised difference of 0.6 to be detected with 88% power (5% significance level). If the within patient variation observed is too high to undertake a reliable analysis the sample size would be increased. For the secondary endpoints (tissue sections), similar methods of analysis were employed. A sample size of 30 patients would enable a standardised difference of 0.75 to be detected with 90% power (1% significance level for multiple testing).

CHAPTER THREE

Results-1

The relationship between homologous recombination repair and the sensitivity of human epidermis to the size of daily doses over a 5-week course of breast radiotherapy.

3.1 Introduction

Clinical radiotherapy is delivered as a sequence of fractional, usually daily, doses. Normal and malignant tissues differ in their responses to several treatment-related variables, including total dose, fraction size, inter-fraction interval and overall treatment time (Thames, Bentzen et al. 1989; Turesson, Nyman et al. 1996). The α/β ratio describes the shape of the fractionation response. On average, most cancers have a high α/β ratio and are less sensitive to fraction size than the normal tissues responsible for dose-limiting adverse effects presenting months or years later (Thames, Bentzen et al. 1989; Thames, Bentzen et al. 1990; Stuschke and Thames 1999). In this setting, high total doses (>60 Gy) delivered using small (≤2 Gy) fractions spare the cancer less than the dose-limiting normal tissues, thereby increasing therapeutic gain (Thames, Bentzen et al. 1989). Recent evidence suggests that breast and prostate cancers show, on average, comparable sensitivity to fraction size as the dose-limiting normal tissues (Owen, Ashton et al. 2006; Bentzen, Agrawal et al. 2008; Whelan, Pignol et al. 2010). If so, small fractions spare the cancer as much as the normal tissues, and there is no disadvantage in giving fewer, larger fractions to a lower total dose. This strategy is increasingly adopted for the adjuvant radiotherapy of women with early breast cancer, for example (Holloway, Panet-Raymond et al. 2010; Yarnold and Haviland 2010). Given

the evidence for variation in fraction size sensitivity between tumour types, it is also possible that significant variation in sensitivity exists within tumour types. An understanding of molecular mechanisms is, therefore, needed to ensure effective selection of fractionation schedule in individual patients.

Fraction size sensitivity is a cellular property reflecting, the ability to repair otherwise lethal DNA double-strand breaks (DSB) prior to the next fraction of radiotherapy (Steel 1991). DSB are rapidly repaired by non-homologous end-joining (NHEJ) in all phases of the cell cycle, in addition to which, homologous recombination (HR) requiring an intact sister chromatid, repairs a proportion of DSB in S and G2 phases of the cell cycle (Rothkamm, Kruger et al. 2003; Saleh-Gohari and Helleday 2004; Beucher, Birraux et al. 2009). Fractionation sensitivity is associated with the proliferative status of a tissue, being higher in tissues with low proliferative indices, and vice versa (Hopewell, Nyman et al. 2003). Rodent cell lines deficient in NHEJ are very radiation sensitive, relying disproportionately on HR to repair DSB and showing no dose-rate sparing, an indicator of insensitivity to fraction size (Thacker and Wilkinson 1995). On the other hand, wild type and HR defective cell lines show typical sparing from low dose-rate compared to high dose-rate radiation (Thacker and Wilkinson 1995). Furthermore Rothkamm *et al*, based on Southern Hybridisation techniques, have shown that NHEJ-proficient cells show a high rate of incorrectly rejoined DSB at high dose-rate radiation and this is significantly reduced at low dose-rate. This frequency of DSB misrepair is considerably reduced in NHEJ-deficient cells and not affected by dose-rate alterations (Rothkamm, Kuhne et al. 2001; Kruger, Rothkamm et al. 2004). It has also been shown that restriction fragment reconstitution is more efficient in G2 than in G1 phase suggesting that structural characteristics of G2 phase chromatin such as the cohesion of sister chromatids enhances the fidelity of DSB rejoining. We postulated that the high

fidelity of DSB repair in replicated chromatin (Rothkamm, Kuhne et al. 2001; Kruger, Rothkamm et al. 2004), which is independent of DNA damage levels (fraction sizes), may explain the low fractionation sensitivity of tissues with high proliferative indices, including self-renewal normal tissues and many cancers.

The epidermis in patients undergoing radiotherapy for breast cancer offers a readily accessible system for investigating DSB repair in different proliferative states. Early in the course of treatment, clinical data suggest that the epidermis is more sensitive to fraction size than at the end of a 5-week schedule of radiotherapy (Turesson and Thames 1989; Hopewell, Nyman et al. 2003). Prior to RT, basal epidermal cells are predominantly in non-proliferative phase, but proliferative markers and cell cycle checkpoints change over the course of 5 weeks radiotherapy (Turesson, Bernefors et al. 2001; Turesson, Nyman et al. 2010). DSB rejoining can be monitored in tissue sections using antibodies against 53BP1 as a surrogate for DSB and antibodies against RAD51 as a bio-marker of HR (Thompson and Schild 2001).

3.2 Results

3.2.1 Patient characteristics (Table 3.1)

The mean age of patients recruited was 58 years. Three patients experienced grade 3 erythema and 3 had moist desquamation in the inframammary fold towards the end of RT. None of the patients recorded severe late toxicities after 5 years of follow up. To our knowledge, none of these patients had BRCA1/2 associated familial cancers.

Table 3.1: Patient characteristics

Trial no	Age (yrs)	Day 1 of Radio-therapy	Day 5 of Radio-therapy	Hormone therapy	Chemo-therapy	Her-ceptin	Erythema	Moist desqua-mation
100	70	Mon	n/a♣	Yes	No	No	n/a♣	n/a♣
101	70	Thu	Wed	Yes	No	No	mild	none
102	46	Mon	Thu*	Yes	No♦	No	moderate	none
103	55	Mon	n/a♣	Yes	No	No	n/a♣	n/a♣
104	53	Mon	Fri	Yes	No	No	moderate	none
105	39	Mon	Thu*	Yes	Yes	No	mild	none
106	79	Tue	Fri*	Yes	No	No	mild	none
107	63	Mon	Fri	Yes	No	No	moderate	mild
108	56	Tue	Fri*	No	No	No	mild	none
109	46	Mon	n/a♣	Yes	No	No	n/a♣	n/a♣
110	73	Fri	Thu	No	No	No	moderate	mild
111	54	Fri	Thu	No	Yes	No	none	none
112	59	Mon	Fri	Yes	No	No	severe	mild
113	51	Fri	Thu	No	Yes	Yes	moderate	mild
114	57	Mon	Fri	Yes	No	No	moderate	none
115	58	Thu	Thu	Yes	No	No	moderate	none
116	37	Fri	Thu	Yes	Yes	No	mild	moderate
117	53	Thu	Wed	Yes	No	No	moderate	none
118	73	Wed	Wed	Yes	No	No	mild	none
119	55	Mon	Fri	Yes	No	No	moderate	mild
120	46	Wed	Tue	Yes	Yes	No	moderate	moderate
121	54	Tues	Fri*	Yes	Yes	No	moderate	none
122	48	Thu	Wed	Yes	No	No	n/a♠	n/a♣
123	52	Mon	Fri	Yes	No	No	mild	none
124	63	Mon	Fri	Yes	No	No	severe	none
125	60	Thu	Wed	Yes	Yes	No	mild	none
126	58	Mon	Fri	Yes	Yes	No	moderate	mild
127	56	Mon	Thu*	Yes	No	No	mild	none
128	60	Wed	Tue	Yes	Yes	No	severe	none
129	80	Mon	Fri	No	Yes	No	moderate	none
130	45	Thu	Wed	Yes	No	No	mild	none
131	58	Mon	n/a♣	Yes	No	No	n/a♣	n/a♣
132	69	Mon	Fri	Yes	Yes	No	mild	none
133	75	Wed	Tue	Yes	No	No	moderate	mild
134	60	Wed	Tue	Yes	Yes	No	n/a♣	n/a♣
135	52	Mon	Fri	No	Yes	No	mild	none
136	67	Tues	Fri*	No	No	No	mild	none
Mean age	58							

***** Second biopsy collected on 4th day of radiotherapy rather than 5th

♦Patient received one cycle FEC only

♣Patient withdrawn due to: personal reasons (100, 109); reaction to dressing (103); infection (131); psychiatric breakdown during RT (134)

♠Data missing

A total of 15 patients were analysed (from 101 to 117 excluding those that withdrew). The first 10 of patients analysed were used for the p21 analysis.

3.2.2 Proliferation kinetics of human basal epidermis during 5 weeks of radiotherapy

Most of the basal cells showed increased Ki67 expression towards the end of radiotherapy (**Figure 3.1A**). The mean basal Ki67 density (cells per mm of basement membrane (BM)) increased from 5.72 to 15.46 per mm of BM by the end of the week 5 (p=0.002) (**Figure 3.1B)**. Immunostaining for cyclin A protein identified the proportion of cells in the late S and G2 phases of the cell cycle. Basal cyclin A index (number of positive cells/total number of cells in basal layer) rose from 3.7% at baseline to 12.8% at 5 weeks. To accurately analyse cell cycle stage, we co-stained with Ki67 and cyclin A **(Figure 3.1A)**, revealing a significantly higher proportion of cycling cells in S or G2 phases of the cell cycle by the end of week 1 of RT (48%) as compared to baseline (29%), and the increase was maintained at the end of 5 weeks (p<0.0003, 95%CI 47.7-50.2) **(Figure 3.1C)**. These findings are consistent with other reports of human epidermis in response to fractionated RT, detected using single staining with Ki67 and cyclin A (Turesson, Bernefors et al. 2001).

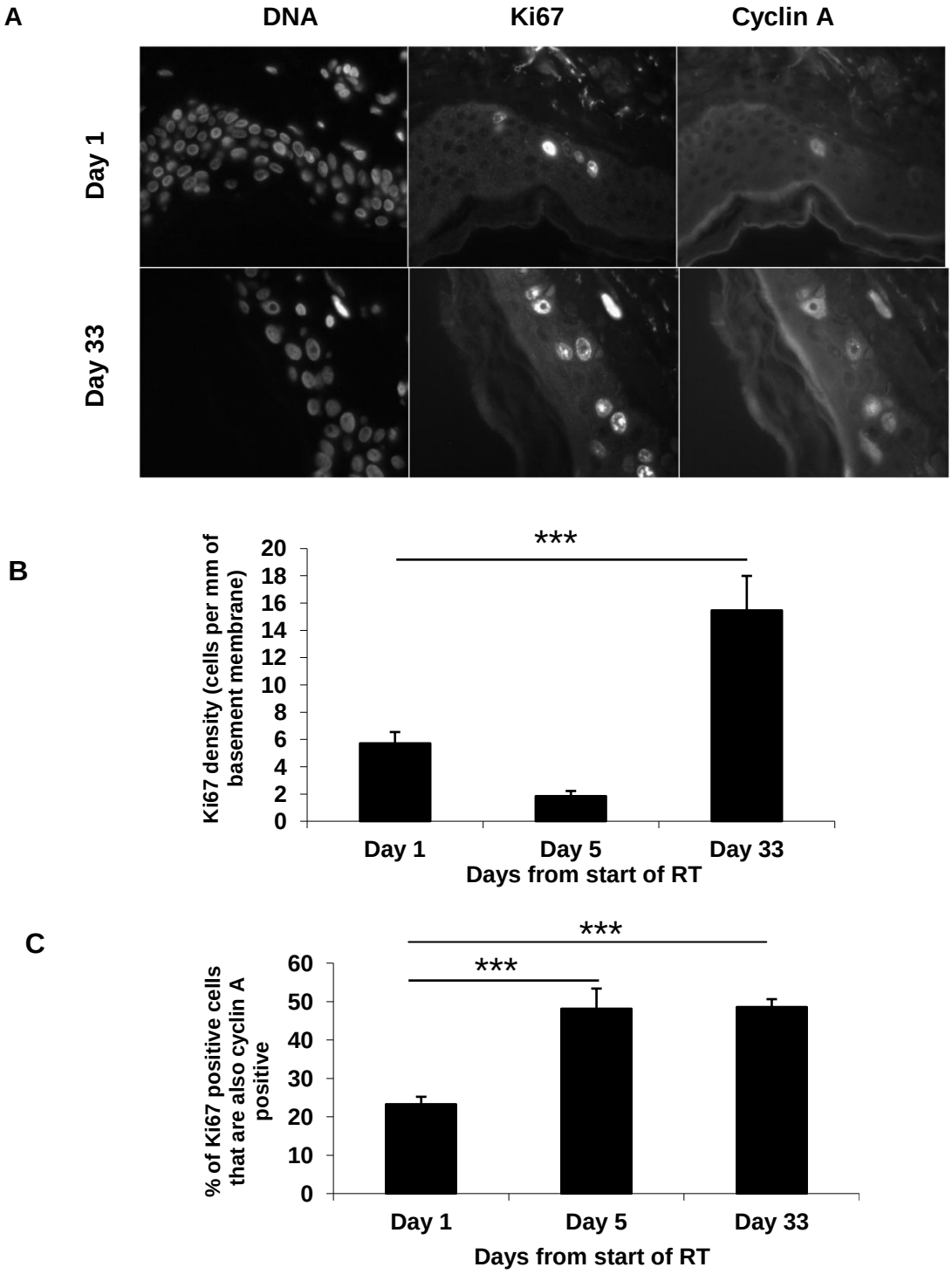


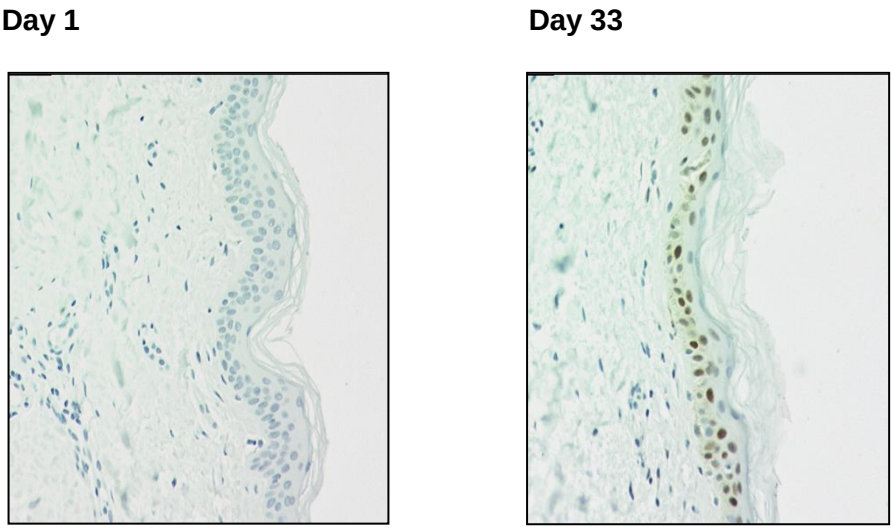
Fig. 3.1: Changes in Ki67 expression in human epidermis during RT. A Double immunofluorescent staining of human epidermis with Ki67 (panel 2), cyclin A (panel 3) and DAPI counterstain (panel 1) at the beginning and end of RT (100X). **B** The variation of mean basal Ki67 density during the course of radiotherapy. **C** The percentage of cycling cells (Ki67 positive) that were in S-G2 phase of the cell cycle (cyclin A positive) increased significantly by week 1 of RT (48%) and this increase was maintained at the end of 5 weeks (49%, $p<0.0003$). Error bars show standard error of mean (SEM) in 15 patients.

3.2.3 Cell cycle checkpoint responses during radiotherapy

It is well established that IR triggers cell cycle arrest, and it was initially surprising to observe a higher proportion of cycling cells after 5 weeks of RT. One explanation is that cells accumulate in cell cycle phases with enhanced capacity to survive IR-induced damage. We immunostained for the cyclin dependent kinase inhibitor p21, which activates several DNA damage induced cell cycle checkpoints including the G1-S and G2-M transitions (Abbas and Dutta 2009). In our study, there was virtually no expression of p21 at baseline, and only 2.8% of cells showed mild (+) staining 2 hours after the first fraction of RT (95%CI 2-3.5). The p21 index subsequently rose to 26.3% by the end of 1 week of RT ($p=0.01$) and to 87.4% by the end of 5 weeks of RT ($p<0.0001$, 95%CI 84.1-90.6) **(Figures 3.2 A & B)**. When serial sections stained for cyclin A & p21 were overlaid using MATLAB 7.9 R2009b software, the cyclin A positive nuclei overlapped with strong p21 uptake (**Figure 3.3 A, B & C**).

Ki67 and cyclin A staining was seen only in the basal or first suprabasal layer, but nuclear staining of p21 was seen dispersed in all layers of the epidermis with strongest uptake in the basal compartment. The upregulated p21 in Ki67 negative (i.e. G0) cells, coupled with a decrease in the proportion of G1 cells is likely to be related to a radiation induced G0 block as suggested by Turesson et al (Turesson, Bernefors et al. 2001). Our data suggests that although a significantly high proportion of basal cells enter the cell cycle in response to radiation induced cell depletion, effective cell cycle check point activation prevents them from entering mitosis whilst RT is ongoing. Staining with the mitosis marker phospho-Histone H3 does not show an increase until after the end of a 5-week course of RT (Turesson, Nyman et al. 2010).

A



B

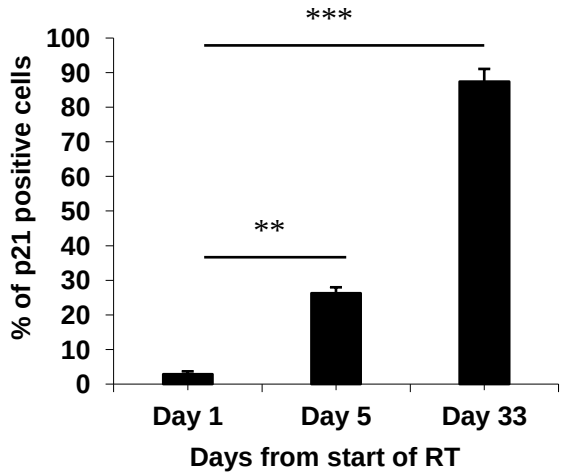
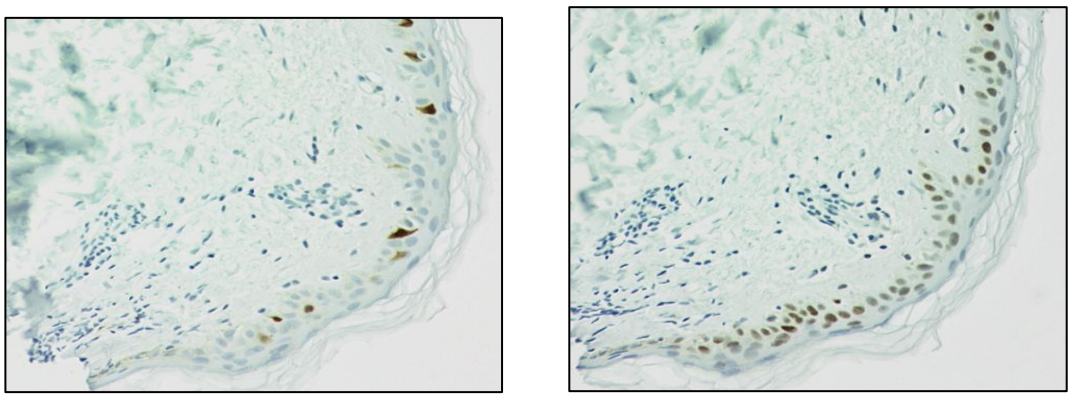


Fig 3.2: p21 expression in human epidermis. A. p21 staining (brown) of human epidermis with haematoxylin counterstain (blue) (20X). At the start of RT there was virtually no uptake of p21 staining. However by the 25th fraction of RT there was a dramatic increase throughout the epidermal layers. **B.** p21 index scored in 10 patients. Only 2.8% of cells showed mild staining 2 h after the first fraction of RT. However, the p21 index rose dramatically to 87.4% (any positivity) at day 33 of RT ($p<0.00002$). Error bars show SEM in 10 patients.

A **B**

Cyclin A (Day 33) **P21 (Day 33)**



C **Cyclin A and P21 serial section overlay (Day 33)**

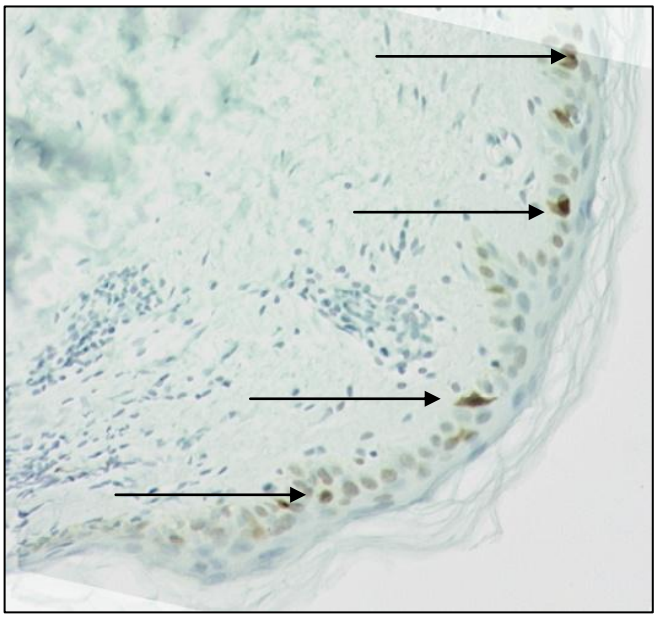


Fig 3.3: A & B. Serial 3 µm sections of epidermis stained with Cyclin A and p21 (brown) and counterstained with haematoxylin (blue). **C.** Overlay of serial sections using MATLAB 7.9 R2009b software shows strong uptake of p21 in Cyclin A positive cells.

3.2.4 Homologous recombination repair in basal epidermis during radiotherapy

Next, we stained for RAD51 foci formation as a measure of active HR (Thompson and Schild 2001). As expected, RAD51 foci were seen only in Ki67 positive cells **(Figure 3.4)**, consistent with HR activation in S/G2 phase cells (Rothkamm, Kruger et al. 2003; Saleh-Gohari and Helleday 2004; Beucher, Birraux et al. 2009). Ki67 positive cells arrested in S/G2 phase are able to trigger Chk1 DNA damage response and HR repair (Jazayeri, Falck et al. 2006). Dual staining with Ki67 helped to identify RAD51 foci more easily as this protein is expressed only in cycling cells (Yamamoto, Taki et al. 1996). RAD51 foci have been previously visualised in human tissue after ex vivo radiation (Willers, Taghian et al. 2009) and in vivo chemotherapy (Graeser, McCarthy et al. 2010). However, to our knowledge this is the first demonstration of RAD51 foci formation in human tissue following in vivo RT. The inherent background noise in tissue sections needed to be optimised to accomplish this (**Figure 3.4**).

The number of Ki67 positive nuclei in the basal epidermis containing RAD51 foci increased 3.9 fold between day 1 and 33 (range 2.6-7.2, p=0.0003) (**Figure 3.5A**). Taking into account the increased number of Ki67 positive cells during the course of fractionated RT, the total RAD51 positive cell density (per mm of basement membrane) increased 9.7 fold (**Figure 3.5B**). The mean RAD51 foci count per foci-containing cell two hours after the first fraction was 2.5 compared to 3.8 after the last fraction of RT (p=0.01) (**Figure 3.5C)**. We also observed that the foci seen on day 33 were on average larger and brighter than those seen on day 1 (not quantified).

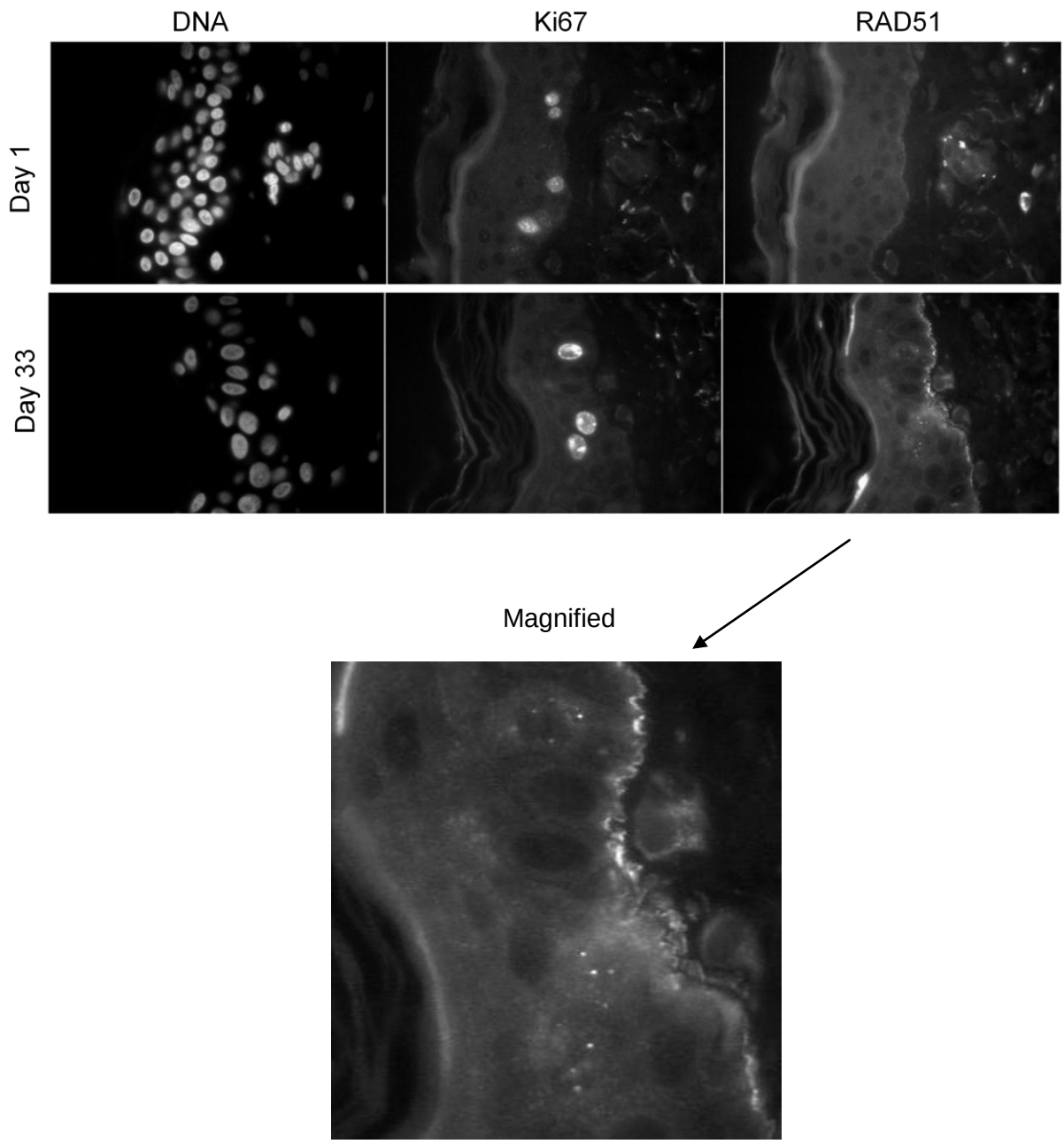


Fig. 3.4: Changes in RAD51 expression during a course of RT. Co-staining by immmunofluorescence with Ki67, RAD51 and DAPI counterstain (100X). The top panel represents the epidermis 2 h after the first fraction of RT where no RAD51 foci can be seen in the Ki67 positive cells. Lower panel shows the picture 2 h after the 25th fraction of RT and all three Ki67 positive cells in the field demonstrate RAD51 foci.

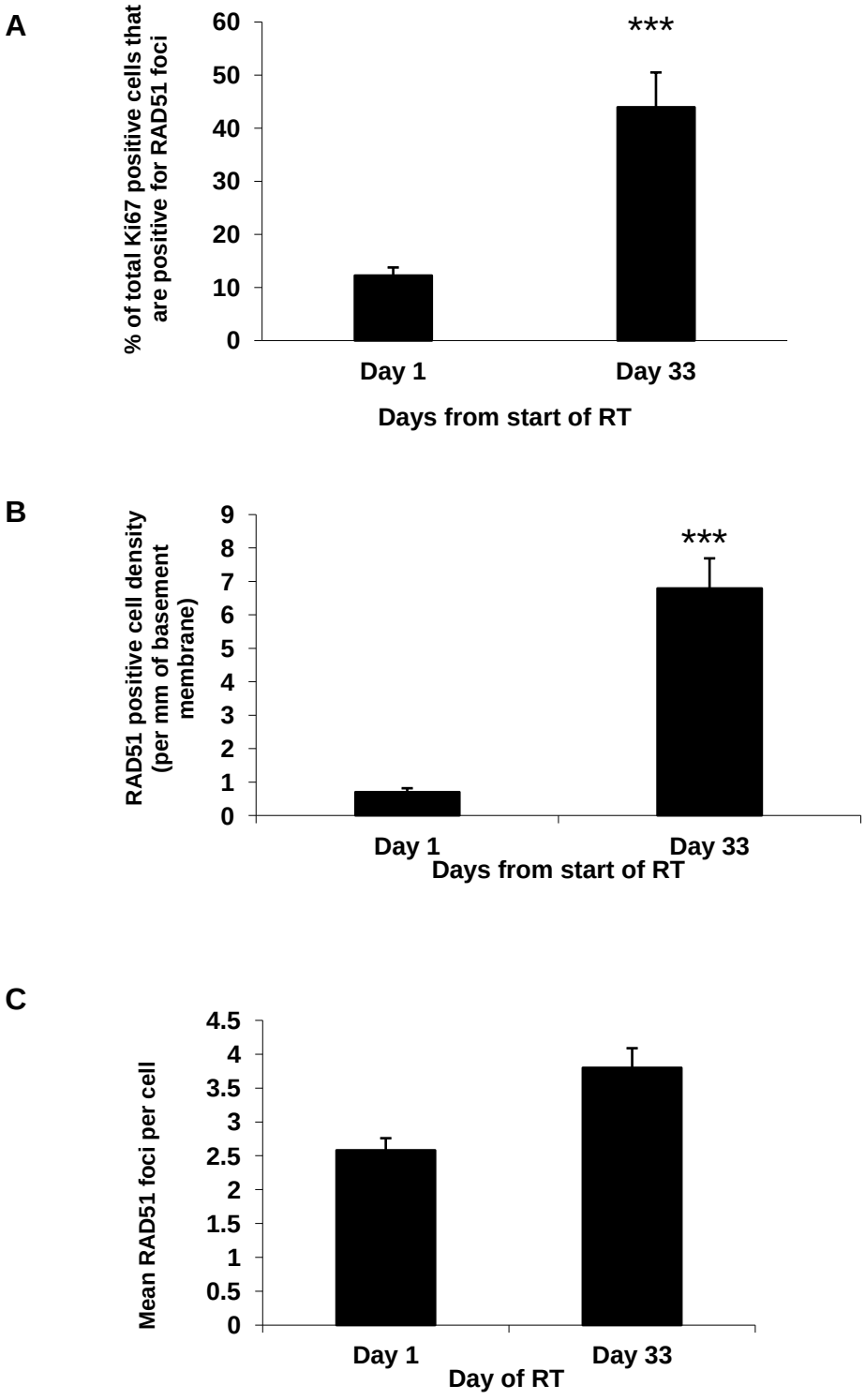


Fig. 3.5: Changes in RAD51 expression during a course of RT. A Between day 1 & 33, the percentage of cycling cells (Ki67 positive) containing RAD51 foci increased from 12.25% to 44.5% (p=0.0003). **B** RAD51 positive cell density per mm of BM increased 9.7 fold by the end of RT. **C** Mean RAD51 foci count per foci-containing cell two hours after the first fraction was 2.5 compared to 3.8 after the last fraction of RT (p=0.01). Error bars represent SEM in 15 patients.

3.2.5 DNA DSB repair kinetics in cycling vs non-cycling cells

It is well established that cells present in the late S/G2 phases are more resistant to IR as compared to other phases, pointing to HR as a possible mechanism for minimising residual DSBs (Wilson, Hinz et al. 2010). The 53BP1 protein accumulates in discrete nuclear foci at DSB (Schultz, Chehab et al. 2000), which can be used as a marker for DSB (**Figure 3.6 A&B)**. To analyse DSB repair in cycling versus non-cycling cells during 5 weeks of fractionated RT, we co-stained with Ki67 & 53BP1 **(Figure 3.7A)**. At baseline (un-irradiated controls) there was no significant difference in the number of 53BP1 foci seen in Ki67 positive (mean 0.6) versus Ki67 negative cells (mean 0.7, p=0.1) **(Figure 3.7B)**. Interestingly, the mean number of residual foci remaining just before the last fraction of RT was 1.6 and 2.0 in Ki67 positive and negative cells, respectively (p=0.01). Overall, there was a 2.6 fold (p=0.001) increase in the number of residual 53BP1 foci remaining prior to the last fraction. However, it is not possible to say if residual foci just prior to the last fraction represented an accumulation of unrepaired DSB over weeks, or residual foci from the previous day's dose.

When examining 53BP1 foci 2 h after the first fraction of RT, we found that the average foci numbers were significantly higher in Ki67 negative (5.82) vs. Ki67 positive (3.48) nuclei (p<0.0001) **(Figure 3.7C)**. A similar finding was seen 2 hours after the last fraction with Ki67 negative cells having a mean foci number of 7.24 as compared to 4.59 in Ki67 positive cells (p=0.0002) **(Figure 3.7C)**. In the Ki67 positive population around 20-30% of nuclei failed to show distinct 53BP1 foci, but rather a diffuse staining pattern (similar to unirradiated nuclei) suggesting completion of DSB repair. Cells with diffuse staining pattern were scored as negative. This diffuse staining pattern was not observed in any of the Ki67 negative cells counted along the basal layer 2 h after treatment.

A. Control unirradiated **B. 2hours after first fraction of RT**

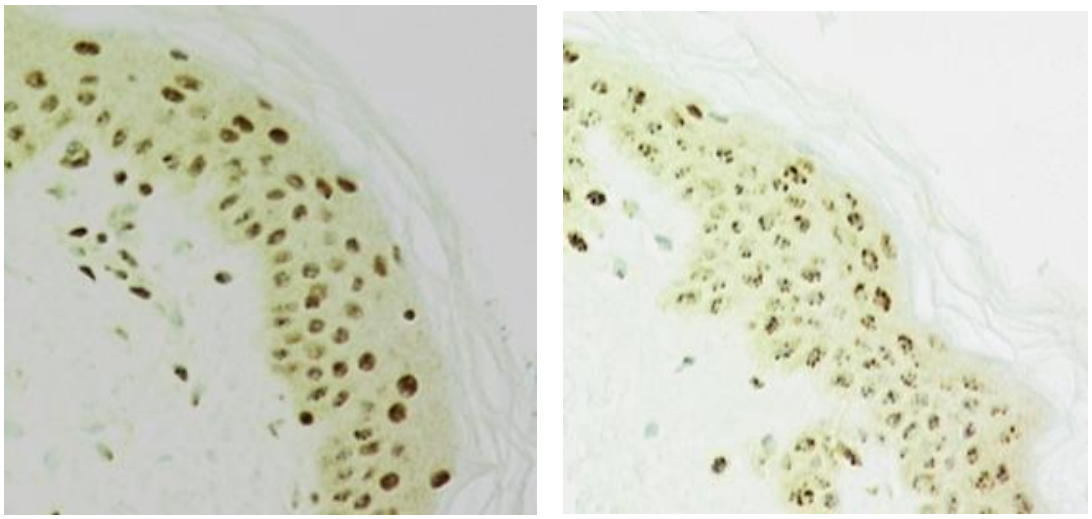


Figure 3.6: Identifying DNA DSB in human epidermis. Section of human breast epidermis stained immunohistochemically for the DNA DSB marker 53BP1 (nuclear staining) with haematoxylin counter stain (10X). A. Control unirradiated cells show constitutive expression of 53BP1 protein as a diffuse (brown) nuclear uptake. B. After IR 53BP1 protein accumulates in discrete nuclear foci which can be easily detected on IHC.

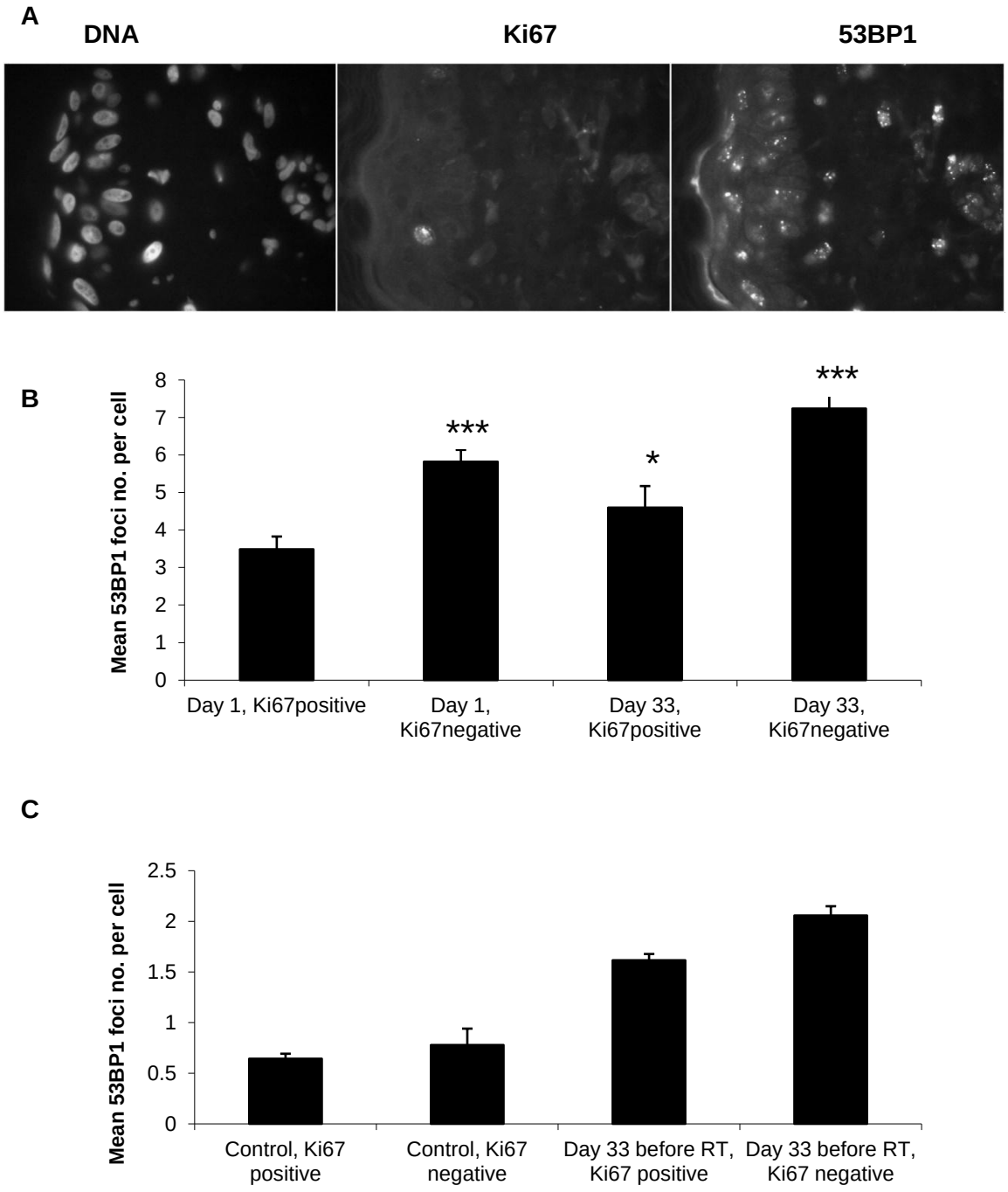


Fig. 3.7: DNA DSB repair in proliferating vs non-proliferating cells during RT.

A Double immunofluorescent staining with Ki67, 53BP1 and DAPI counterstain after the 1st fraction (100X). **B** shows the mean residual 53BP1 foci numbers 2 h after the 1st and last fractions of RT in cycling vs non-cycling cells. Mean foci numbers were significantly higher in Ki67 negative cells compared to Ki67 positive cells at both time points ($p<0.0001$ day1, $p=0.0002$ day 33). **C** plots the mean 53BP1 foci number per cell at baseline before the 1st fraction and before the last fraction of RT in cycling vs non-cycling cells. There was no significant difference in unirradiated cells, however, there were higher residual foci in non-cycling cells prior to the last fraction ($p=0.01$). Error bars represent SEM in 15 patients.

3.2.6 Epidermal stem cells

3.2.6.1 Identifying basal epidermal stem cells

The human epidermis consists of quiescent stem cells and cycling progenitors/transit-amplifying cells that amplify the number of differentiated daughters resulting from each stem cell division (Ambler and Maatta 2009). Several research groups have made extensive efforts to define a set of stem cell specific markers in the epidermis. Much of this research has used a combination of cell adhesion molecules such as α6 or β1 Integrin and the absence of cell proliferation markers such as Ki67 (Li, Simmons et al. 1998; Jensen, Lowell et al. 1999; Ambler and Maatta 2009). In our study a combination of β1 integrin and Ki67 were used to identify putative epidermal stem cells (β1integrin ++/+++ & Ki67 negative) **(Figure 3.8)**. Only cells that were attached to the basement membrane and had moderate to strong uptake of β1 integrin along the entire cell membrane were considered to be positive.

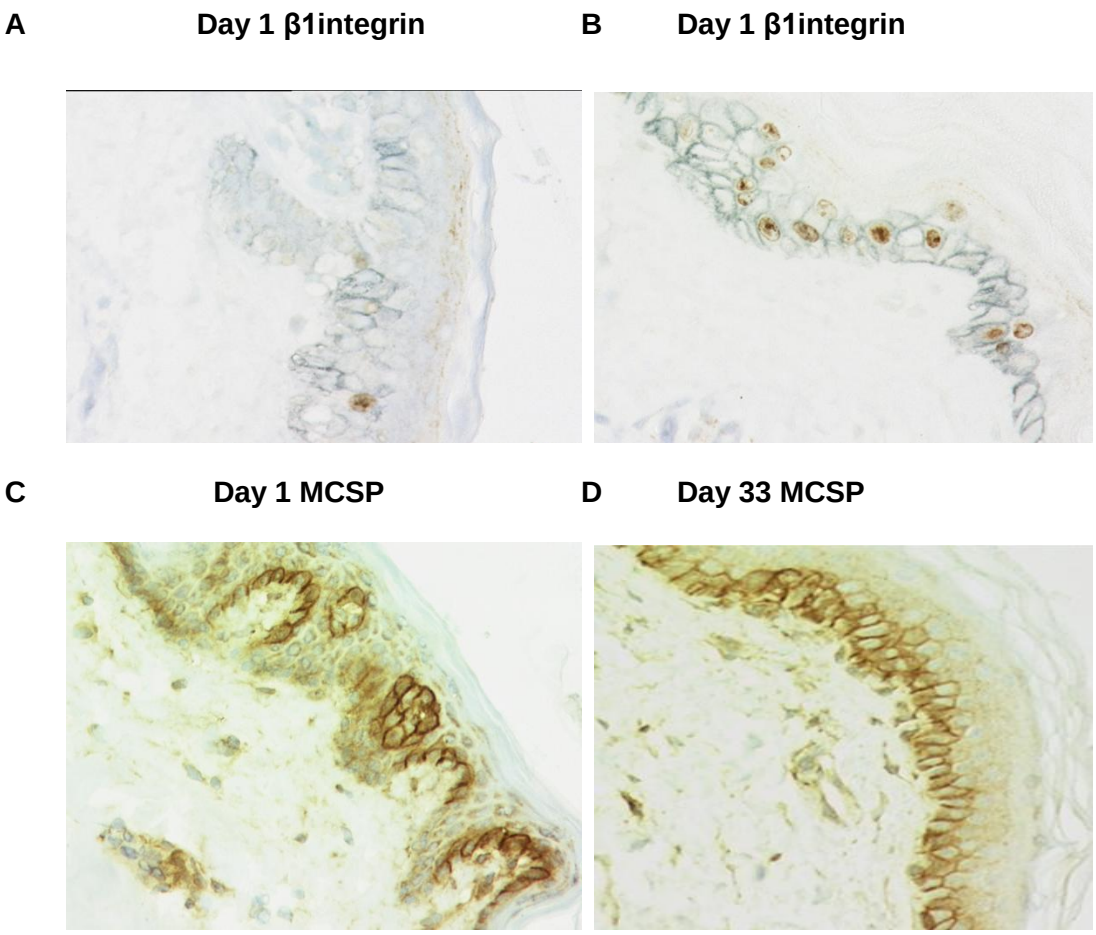


Fig. 3.8: Identifying basal epidermal stem cells. Section of human breast epidermis stained immunohistochemically for the epidermal stem cell marker β1integrin (membrane staining) and the proliferation marker Ki67 (nuclear staining) with methyl green counter stain (40X). The weak clustered pattern of β1integrin staining at baseline (**A)** changed to an intense staining by week 5 of RT **(B)** with majority of basal cells being positive. There was also a significant RT induced proliferation as quantified in figure 3.9. **C.** Frozen section of human breast epidermis at day 1 of RT, stained immunohistochemically for the epidermal stem cell marker MCSP (membrane staining) with haematoxylin counter stain (20X) shows a distinct clustered pattern of uptake mainly in the tips of the dermal papillae which becomes diffuse after 5 weeks of RT **(D)**, with most of the basal layer cells staining positive

3.2.6.2 Variation in the β-1Integrin positive population during a course of RT

At baseline in un-irradiated skin sections, only 20% of proliferating cells were β1 integrin positive, whereas 84% were β1 integrin positive by the end of 5 weeks of RT ($p<0.00001$) **(Figure 3.8 & 3.9)**. By week 5, the distinct dermal papillae had disappeared and the clustered pattern of β1 integrin staining was lost. Not only did the fraction of basal cells expressing β1 integrin increase dramatically from 5-10% at baseline to around 85% at week 5, the intensity of staining increased as well **(Figure 3.8)**. Using a more specific stem cell marker MCSP (Legg, Jensen et al. 2003) we found a similar change in staining pattern with RT. In the snap frozen sections, at baseline, MCSP uptake was highly clustered in a few basal cells (3-5%), but became diffuse after 5 weeks of RT, with most of the basal layer cells staining positive (**Figure 3.8C,** not quantified).

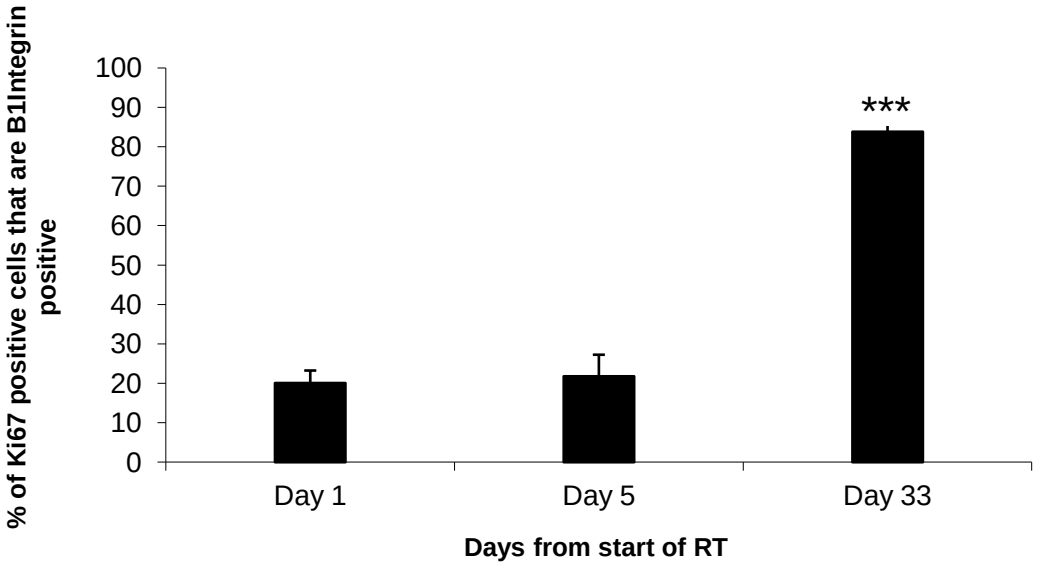
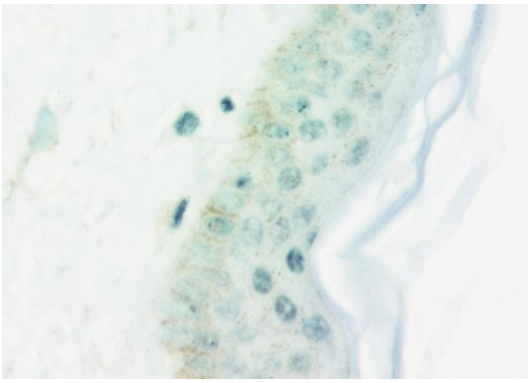


Fig. 3.9: Changes in β1 integrin expression with RT. Percentage of Ki67 positive cells expressing β-1Integrin showed a significant increase from baseline to the end of 5weeks of RT ($p<0.00001$). Error bars represent SEM in 15 patients.

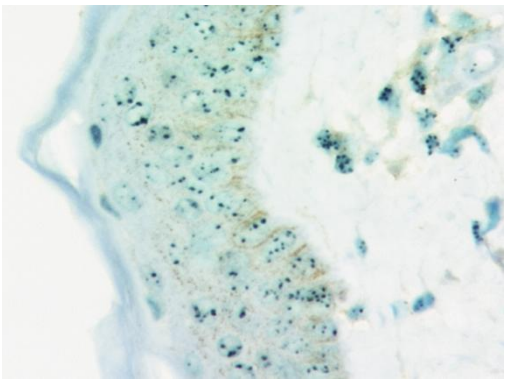
3.2.6.3 DNA DSB repair in β-1Integrin positive cells during RT

We tried to study DNA DSB repair in the putative epidermal stem cell population by double staining with β-1Integrin and 53BP1 **(Figure 3.10).** As described above only cells that were attached to the basement membrane and had moderate to strong uptake of β1 integrin along the entire cell membrane were considered as positive and the β1 integrin negative cells were analysed from the basal and first suprabasal layers of the epidermis. We were not able to demonstrate any significant difference in the residual 53BP1 foci levels 2 h after the first and last fraction of RT in β1 integrin positive versus β1 integrin negative cell populations **(Figure 3.10D)**. Despite several attempts we were not able to successfully co-stain for RAD51 and β1 integrin, therefore HR repair could not be studied in this population of cells. Triple staining with β1 integrin, Ki67 and RAD51 or 53BP1 was also attempted but was not of sufficient quality for analysis **(Figure 3.11)**.

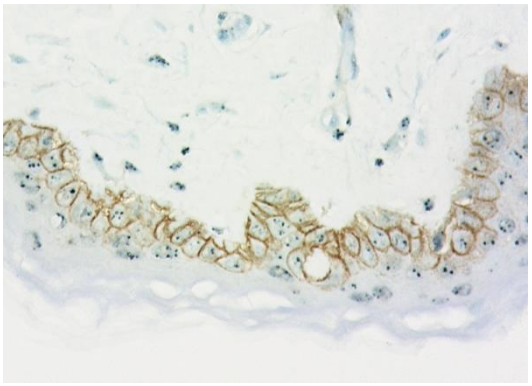
A Control Day 1 (unirradiated)



B Day 1 (after 1st fraction)



C Day 33 (after 25th fraction)



D

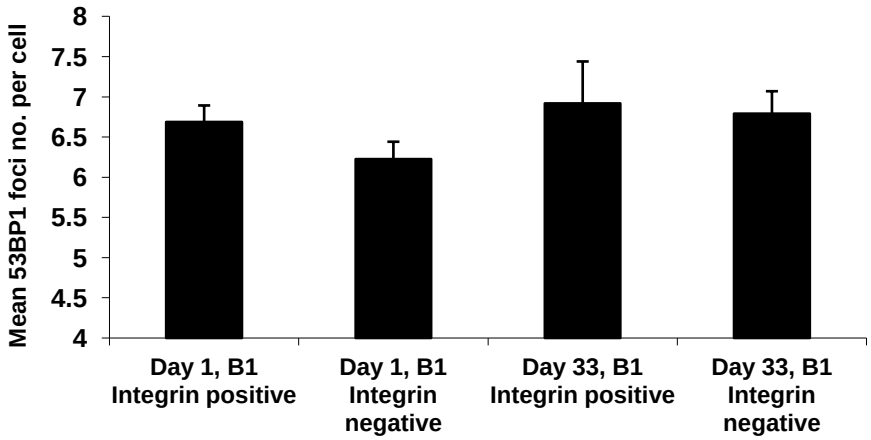
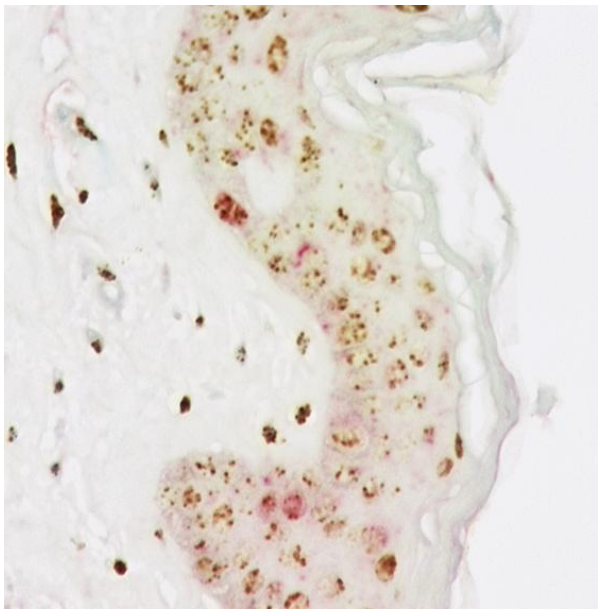


Fig 3.10: DNA DSB repair in β-1Integrin positive cells during RT. A, B, C Section of human breast epidermis stained immunohistochemically for the epidermal stem cell marker β1integrin (membrane staining) and the DNA DSB marker 53BP1 (nuclear staining) with haematoxylin counter stain (40X). **D.** No significant difference was identified when 53BP1 foci were scored in β1integrin positive versus β1integrin negative cells at the beginning and end of RT. Error bars represent SEM in 15 patients.

A. Day 1 (after 1st fraction)



B. Day 33 (after 25th fraction)

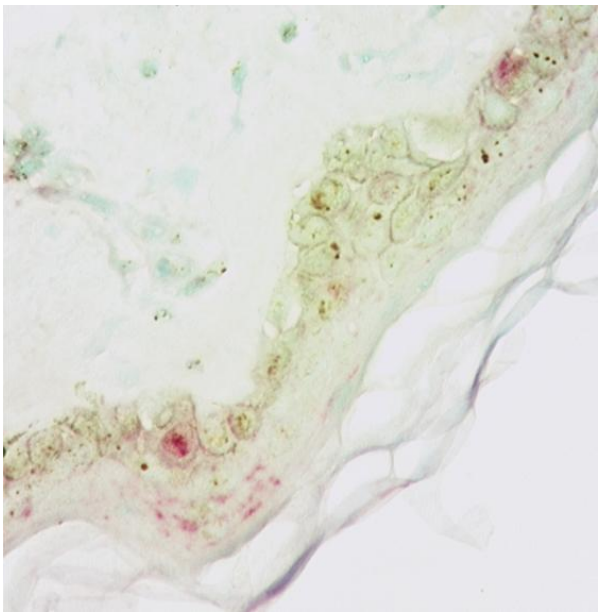


Figure 3.11: Triple staining with β1 integrin, Ki67 and 53BP1. Section of human breast epidermis stained immunohistochemically for the epidermal stem cell marker β1integrin (membrane staining- Vector blue grey), Ki67 (nuclear- Vector Red) and the DNA DSB marker 53BP1 (nuclear foci- DAB brown) with methyl green counter stain (20X).

3.3 Discussion

Clinical data suggest that sensitivity of epidermis to fraction size varies over a 5-week course of radiotherapy, being sensitive to fraction size at the beginning of radiotherapy, and losing sensitivity during weeks 4 & 5 (Hopewell, Nyman et al. 2003). Our data suggests that activation of HR to repair DSB towards the end of RT correlates with this loss of fractionation sensitivity seen clinically. NHEJ is an error prone method of repair whilst HR has a high fidelity for repair that is independent of DNA damage levels (fraction size) (Rothkamm, Kruger et al. 2003). Another mechanism contributing to loss of fraction size sensitivity in S/G2 could be via cohesin, which facilitates more efficient DSB repair in replicated chromatin (Bauerschmidt, Arrichiello et al. 2010) and may enhance correct DSB repair at high doses in S/G2 in an HR-independent manner (Kruger, Rothkamm et al. 2004). The tightly bound chromatid in S/G2 might serve as a scaffold to hold break ends in place and thus avoid loss or rearrangement of chromosome material. Without such a scaffold (i.e. in G0/G1), break ends would be able to move more freely, repair would be slower and more frequently result in 'wrong' ends being joined, especially at higher doses (or dose per fraction) when breaks are in close proximity. Whatever mechanisms are involved, cells in S-G2 appear to have a high fidelity for repair that is independent of DNA damage levels, explaining insensitivity to fraction size and mediating resistance to radiation (Utsumi and Elkind 2001; Rothkamm, Kruger et al. 2003). Thus a higher proportion of cells in S/G2 phase of the cell cycle (allowing greater use of high fidelity DSB repair) is more likely to influence fractionation sensitivity than proliferation per se (as determined by Ki67 staining).

The 53BP1 protein accumulates in discrete nuclear foci at DSB (Schultz, Chehab et al. 2000), which can be used as a marker for DSB. We have been cautious in not interpreting the RAD51 and 53BP1 data in terms of relative use of HR and NHEJ for

several reasons. It was technically challenging to triple stain with Ki67, RAD51 and 53BP1 and the 2 hour time point may underestimate NHEJ repair. We have therefore used 53BP1 to study the total remaining DSB and found that the number of residual DSB is lower in Ki67 positive cells as compared to Ki67 negative cells 2 hours after RT **(Figure 3.7)**. This is surprising, as it previously has been shown that cells in G2 acquire almost twice as many DSB as those in G1 after a 2 Gy ionising radiation (IR) treatment, which is explained by the increased DNA content in G2 cells (Rothkamm, Kruger et al. 2003; Beucher, Birraux et al. 2009). Thus, our finding that there are overall fewer 53BP1 foci in Ki67 positive cells suggests an increased DSB repair capacity of late S/G2 cells, probably obtained by activated HR. This is consistent with the findings of Rothkamm *et al* in rodent cell lines (Rothkamm, Kruger et al. 2003). Residual 53BP1 foci observed before the last fraction, following 5 weeks of RT **(Figure 3.7)** may not just reflect unrepaired damage directly induced by radiation. It is possible that stress/senescence associated 53BP1 foci may contribute (Rodier, Coppe et al. 2009). Recent evidence suggests a preferential association of such foci with telomeres (Hewitt, Jurk et al. 2012).

Supiot et al have shown upregulation of p21 with a decreased Ki67 after 5 days of prostate radiotherapy suggesting that terminal growth arrest rather than apoptosis maybe the dominant mode of radiation induced cell death in prostate epithelium (Supiot, Shubbar et al. 2008). In our study, after the initial drop in Ki67 staining after 5 days there was a significant increase in the Ki67 staining in the basal epithelium after 5 weeks of continuous RT. This was accompanied by increased p21 staining which indicates not just G1 arrest but also G2 arrest as shown by overlaying serial sections stained for cyclin A and p21 (**Figure 3.3**). As shown by Turesson et al, the mitosis marker phospho-Histone H3 starts to increase significantly in the basal epithelial cells after the end of RT (Turesson, Nyman et al. 2010). Thus it appears

that these basal epithelial cells are likely to be composed of stem/progenitor cells that have not undergone permanent cell cycle arrest/senescence. The increased p21 reflects checkpoint activation preferably in S-G2 which allows the cells to repair their DSB most efficiently. After RT these basal cells proliferate to replenish the epithelium. Our study suggests that a high proportion of cells in (or arrested in) S-G2 may influence the fractionation sensitivity of the tissue as a whole.

It is suggested that normal and cancer stem cells display a radioresistant phenotype due to activation of a DNA damage response (DDR) that enhances repair of radiation-induced DNA damage (Bao, Wu et al. 2006). The hypothesis is that stem cells make up an increasing proportion of surviving cells after each fraction of RT. In this study we found that the number of cells positive for the putative epidermal stem cell marker β1 Integrin, (Li, Simmons et al. 1998; Jensen, Lowell et al. 1999; Ambler and Maatta 2009), increased during RT, in line with the notion that stem cells are radioresistant (Bao, Wu et al. 2006; Rachidi, Harfourche et al. 2007) **(Figure 3.8 & 3.9)**. The β1 Integrin positive cells were to a high degree also Ki67 positive, suggesting that many of the stem cells have entered the cell cycle. Altogether, our data may suggest that the cells persisting after 5 weeks of RT are epidermal stem cells that have arrested in the late S-G2 phase of the cell cycle and activated HR. However, we remain very uncertain of such a conclusion as our study suggests that integrins and MCSP may not be the best markers to study stem cells in the setting of RT due to radiation induced up-regulation. Cell-extracellular matrix contact mediated via integrins is thought to have an impact on cellular mechanisms resulting in increased cell survival upon exposure to ionising radiation (Cordes and Meineke 2004; Nam, Chung et al. 2009). Several human tumour cell lines and normal human fibroblastic cell strains have shown to increase β1integrin expression in a dose dependent manner following IR (Cordes and Meineke 2003). We could not find other

reports describing this in skin in vivo. It is difficult to comment if β1integrin positivity after 5 weeks of RT is representative of true stemness or inherent radioresistance. However the finding that Ki67 positive cells (the majority of which are β1integrin positive at 5 weeks) show increased DSB repair capacity, suggest that these are surviving RT and are likely to play a role in repopulating the epidermis after RT.

Are the responses to RT in skin tissue reported here also relevant to cancer? Here, we find that epidermal cells accumulate in late S/G2 phases of the cell cycle, allowing them to trigger HR. It is widely accepted that normal fibroblast cultures with intact p53 arrest at the G1/S checkpoint, which is thought to be less leaky than the G2 checkpoint. However, there is evidence that human epidermal cells (keratinocytes) may have a differential response compared to fibroblasts, in that they predominantly arrest at the G2 checkpoint following radiation (Flatt, Price et al. 1998). The attenuated G1 arrest in keratinocytes correlated with reduced p53 accumulation compared with G1 arrested fibroblasts (Flatt, Price et al. 1998). Cancer cells often lose cell cycle checkpoints such as the p53 pathway and accumulate in the G2 phase of the cell cycle after DNA damage (Kastan, Onyekwere et al. 1991). Thus, it is highly likely that the increase in HR reported here in skin epithelial cells also extends to many cancer cells, especially those with a high proliferative index.

In conclusion, although it is known that most of the IR induced DSB are repaired by NHEJ in mammalian cells, our results suggest that HR plays an important role in DSB repair in the human epidermis by the end of a 5-week course of fractionated RT as cells accumulate in S/G2 phase of the cell cycle. Adoption of HR, due to its high fidelity, offers a mechanism explaining loss of fractionation sensitivity in rapidly

cycling normal and malignant tissues, and suggests a potential approach to individualisation of radiotherapy dose prescription.

CHAPTER FOUR

Results- 2

The relationship between DNA double strand break repair and radiation fraction size sensitivity in CHO cell lines

4.1 Introduction

The sensitivity of normal and malignant tissues to fraction size has long been understood to have a basis in the process of cellular recovery, one of the 4 R's of classical radiobiology as described above (Withers 1975) (Chapter 1). Molecular processes relevant to cellular recovery in vitro and to fraction size sensitivity in vivo include recognition and processing of DNA double strand breaks (DSB) prior to the next fraction of radiotherapy (Steel 1991) (Jackson 2002). DSB are rapidly repaired by non-homologous end-joining (NHEJ) in all phases of the cell cycle, in addition to which, homologous recombination (HR) requiring an intact sister chromatid, repairs a proportion of DSB in S and G2 phases of the cell cycle (Rothkamm, Kruger et al. 2003; Saleh-Gohari and Helleday 2004; Beucher, Birraux et al. 2009). The relatively high radioresistance of NHEJ-defective mutants in the S-G2 portion of the cell cycle further suggests that HR promotes survival when sister chromatids are present (Stamato, Weinstein et al. 1983; Whitmore, Varghese et al. 1989). Rodent cell lines that are deficient in NHEJ and that rely disproportionately on HR to repair DSB, show no dose-rate sparing, an indicator of insensitivity to fraction size (Thacker and Wilkinson 1995). We postulate that the high fidelity of DSB repair in replicated chromatin (Rothkamm, Kuhne et al. 2001; Kruger, Rothkamm et al. 2004) explains the low fractionation sensitivity of cells reliant on HR.

Having shown in Chapter 3 that clinical loss of fractionation sensitivity in human epidermis is associated with the increased use of HR to repair radiation induced DSB, we wanted to conduct further mechanistic experiments. Therefore, we chose Chinese hamster ovarian (CHO) cell lines in order to study the fractionation sensitivity of specific DNA repair pathways. This provided a system for testing mammalian cells derived from the same parent wild type cell line deficient in base excision repair (BER), NHEJ and HR, representing the most important repair pathways for radiation-induced single strand breaks & DSB, respectively. The parent wild type AA8 (Thompson, Fong et al. 1980) and its derivatives irs1SF (XRCC3-) (Fuller and Painter 1988; Liu, Lamerdin et al. 1998), V3-3 (DNA-PKcs-) (Blunt, Finnie et al. 1995) and EM9 (XRCC1-) (Thompson, Brookman et al. 1982) were irradiated with different fractionated schedules and tested for clonogenic survival, DNA DSB repair kinetics and cell cycle profiles.

4.2 Results

4.2.1 Clonogenic cell survival in wild type and DNA repair defective CHO cell lines

4.2.1.1 Acute radiation dose survival curves

We conducted single dose clonogenic survival assays on all 4 CHO cell lines i.e. wild type (AA8), BER defective (EM9), NHEJ defective (V3-3) and HR defective (irs-1SF) with doses ranging from 0 to 8 Gy. These confirmed the increased radiosensitivities of the mutant cell lines consistent with previous literature (Rothkamm, Kruger et al. 2003) **(Figure 4.1)**. Survival data (S) after a radiation dose (D) were fitted by a weighted, stratified linear regression according to the linear-quadratic formula $S(D)/S(0)=\exp(\alpha D+\beta D^2)$ using SPSS software (Franken, Rodermond et al. 2006). We were thus able to calculate dose-modifying factors

(DMF=$D_{wild\ type}/D_{mutant}$) at 10% survival. Thus for EM9, V3-3 and irs-1SF the dose modifying factor at 10% survival compared to AA8 was 1.36, 4.75 and 2.14 respectively.

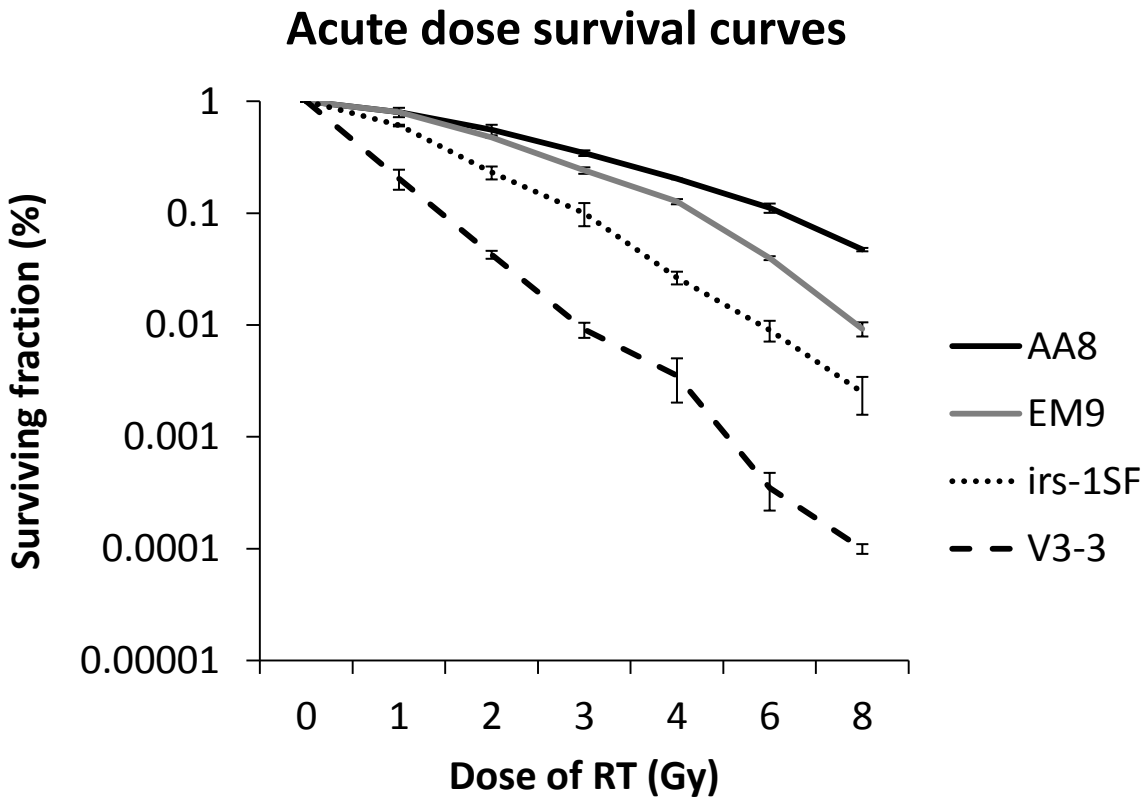


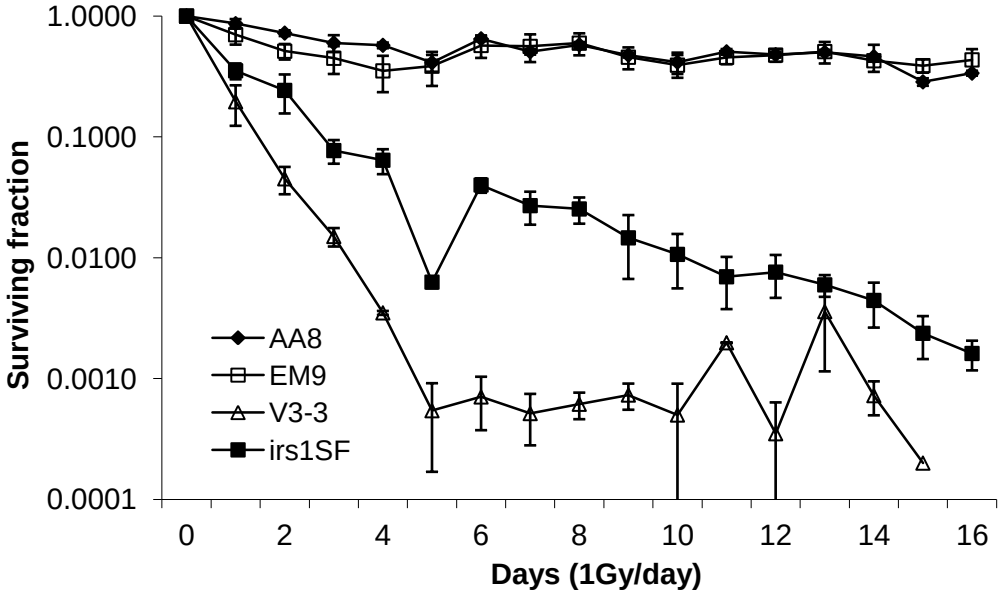
Figure 4.1: Acute dose survival curves (semi-log) for all 4 cell lines at doses of 0, 1, 2, 3, 4, 6 and 8 Gy. AA8 (WT), EM9 (XRCC1-), V3-3 (DNA-PKcs-), irs1SF (XRCC3-). Error bars represent SEM of 3 repeats in triplicate.

4.2.1.2 Fractionated irradiation survival curves – 1 Gy/day, 4 Gy/day, 0.1 Gy/day

In order to elucidate the fraction size sensitivity of different DNA repair pathways we irradiated AA8 (WT), irs1SF (XRCC3-), V3-3 (DNA-PKcs-) and EM9 (XRCC1-) to a total dose of 16 Gy using 2 different fractionation schedules. **Figure 4.2A** shows the

survival curves with daily fractions of 1 Gy. The wild type AA8 cell line showed well above 50% survival throughout this low dose fractionated regimen. The cell line defective in base excision repair (EM9) showed around 20% decreased survival compared to AA8 cells in the first week but returned to wild type levels thereafter. This suggests that intact NHEJ & HR pathways process unrepaired damage caused by loss of the BER pathway and prevent the accumulation of lethal DNA DSB. Cell lines deficient in DNA DSB repair pathways showed much higher radiosensitivity, with the NHEJ defective cells (V3-3) worst affected. This is consistent with the literature showing NHEJ to be the most important pathway for rapid repair of IR induced DSB in all phases of the cell cycle (Rothkamm, Kruger et al. 2003). However, whilst irs1SF (defective in HR) continued to show increased cell kill with increasing total IR doses, V3-3 showed a pronounced biphasic survival curve, becoming relatively radioresistant after the first week of fractionated IR. All 4 cell lines showed some recovery after the first weekend gap (i.e. between the 5^{th} & 6^{th} dose of IR), but this was most dramatic with irs1SF. When comparing **Figure 4.2A** with **Figure 4.2B,** AA8, EM9 and irs1SF all show a steeper curve with the 4 Gy/day schedule consistent with increased sensitivity to higher levels of DNA damage each day.

A



B

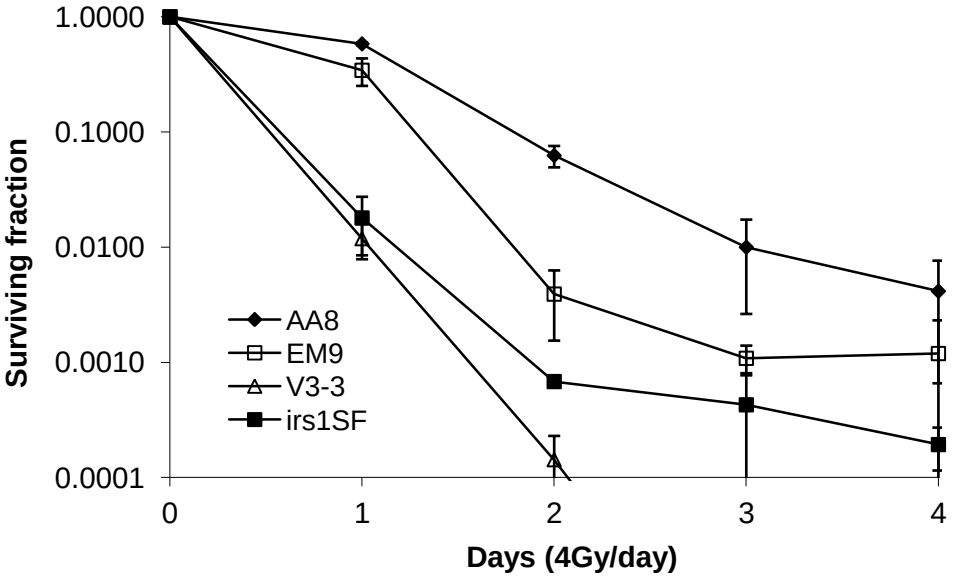


Figure 4.2: Clonogenic survival (semi-log) following fractionated IR in 4 CHO cell lines: AA8 (WT), EM9 (XRCC1-), V3-3 (DNA-PKcs-), irs1SF (XRCC3-). A. 1 Gy given daily Monday to Friday with weekend breaks to a total of 16 Gy. **B.** A higher dose per fraction of 4 Gy given daily to the same total dose. Error bars represent standard error of mean (SEM) of 3 experiments each in triplicate.

4.2.1.3 Sensitivity to changes in dose per fraction as measured by clonogenic survival in wild type and DNA repair defective CHO cells

In order to study the fractionation sensitivity of cell lines, we compared survival following 2 Gy as a single fraction (high dose per fraction) versus 2 fractions of 1 Gy each (low dose per fraction); 1x4 Gy versus 4x1 Gy and 1x8 Gy versus 2x4 Gy versus 8x1 Gy **(Figure 4.3)**. As predicted, the cell line relying on HR to repair DSB (V3-3) was insensitive to changes in dose per fraction (p=NS) in contrast to the cell line (irs1SF) relying on NHEJ, which showed a 1.4 and 3.5 fold increase in sensitivity when the total radiation dose was given in fractions of 2 Gy (p=0.10) and 4 Gy (p=0.04), respectively **(Figure 4.3 A & B)**. AA8 and EM9, cell lines with intact NHEJ, also showed increased sensitivity to higher dose per fraction with significantly higher cell kill with 8 Gyx1 versus 1 Gyx8 (AA8 $p<0.0001$, EM9 $p=0.001$) and with 4 Gyx2 versus 1 Gyx8 (AA8 $p=0.001$, EM9 $p=0.01$) **(Figure 4.3 C & D)**.

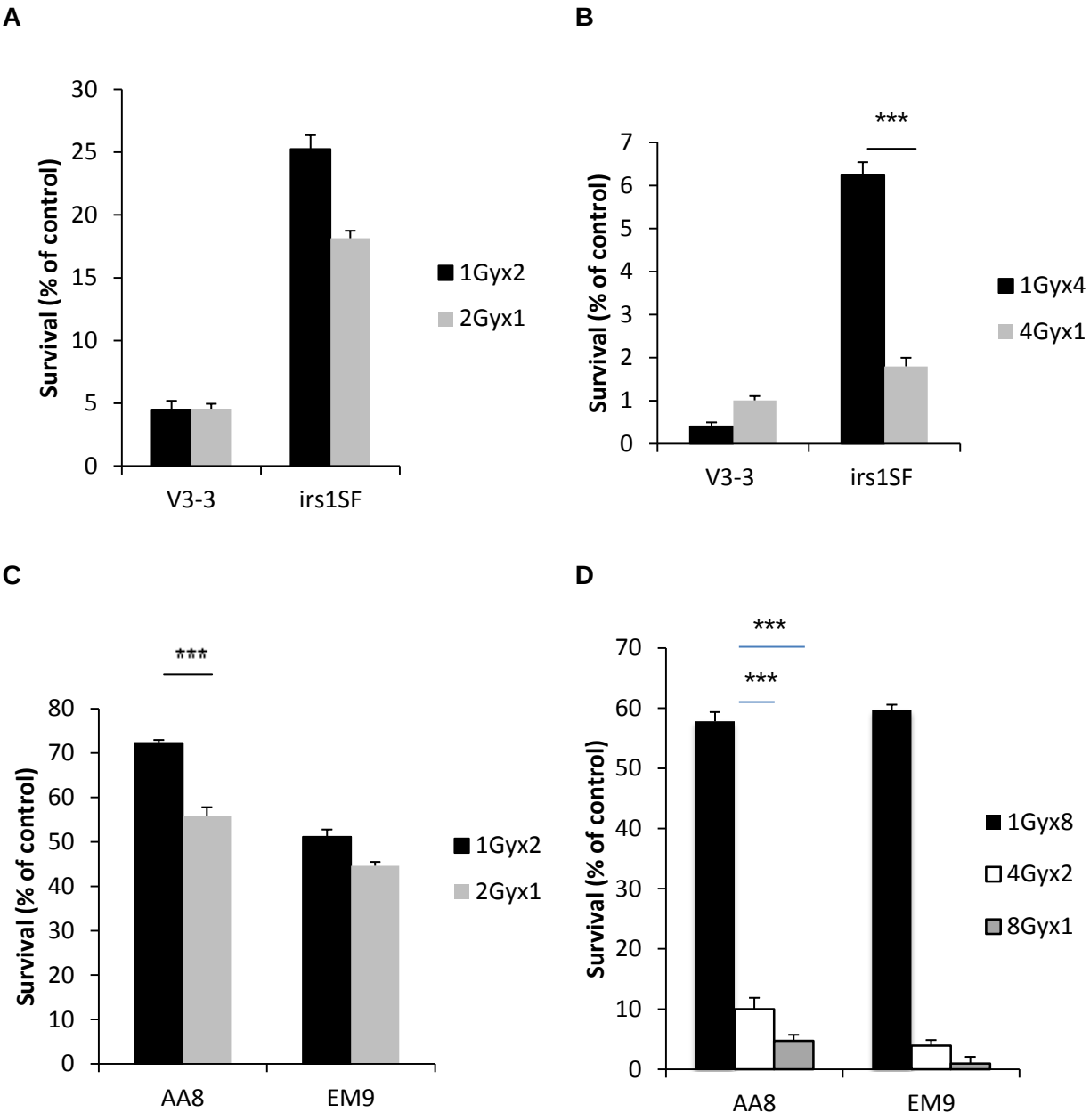


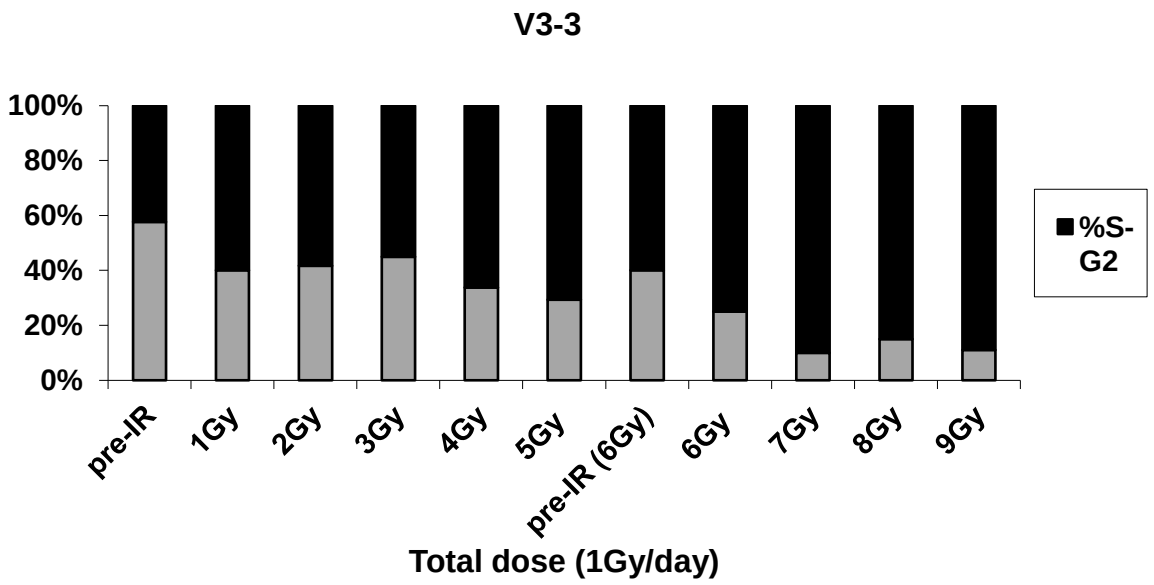
Figure 4.3: Comparison of survival between high dose per fraction vs low dose per fraction. A & B. The irs1SF cell line showed increased sensitivity to higher dose per fraction whereas V3-3 showed loss of sensitivity to changes in fraction size, when comparing 2 Gy in a single fraction vs 1 Gy in 2 fractions or 4 Gyx1 vs 1 Gyx4. **C & D.** Both AA8 & EM9 cells showed higher cell kill with higher dose per fraction. Time interval between each fraction for all experiments was 24 h. Error bars show SEM of 3 repeats in triplicate.

4.2.2 Cell cycle changes in response to fractionated irradiation

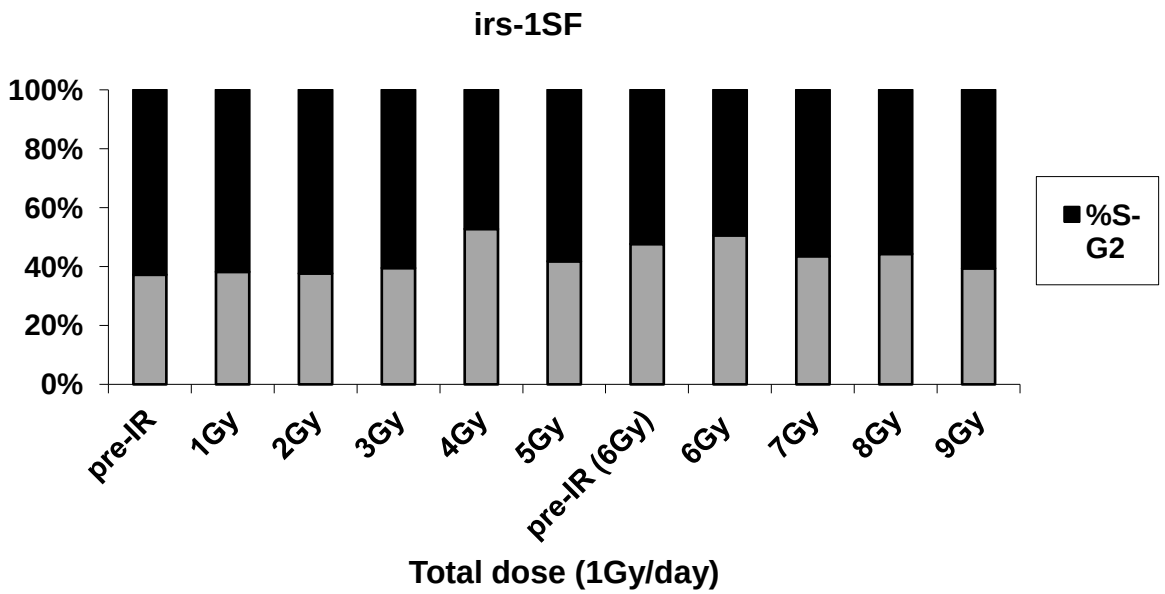
4.2.2.1 The cell line reliant on HR accumulates in S/G2 phase of the cell cycle in response to fractionated IR

Flow cytometric analysis of cell cycle distribution during a course of fractionated IR (1 Gy per day) over 2 weeks (with a weekend gap) confirmed gradual accumulation of V3-3 cells in the S-G2 phase of the cell cycle, more pronounced in the 2nd week of IR **(Figure 4.4A)** and coinciding with flattening of the V3-3 survival curve **(Figure 4.2A)** in week 2. This emergent radioresistance might reflect error-free repair of DSB in the S-G2 phase of the cell cycle. On the other hand, irs1SF cells relying on NHEJ to repair DSB did not show any significant change in cell cycle profile during the 2 weeks of IR **(Figure 4.4B)**. This most likely reflects NHEJ being equally effective throughout the cell cycle. The cell cycle profiles of AA8 and EM9 reflected progression through the cell cycle during a course of fractionated IR **(Fig 4.4 C&D)**.

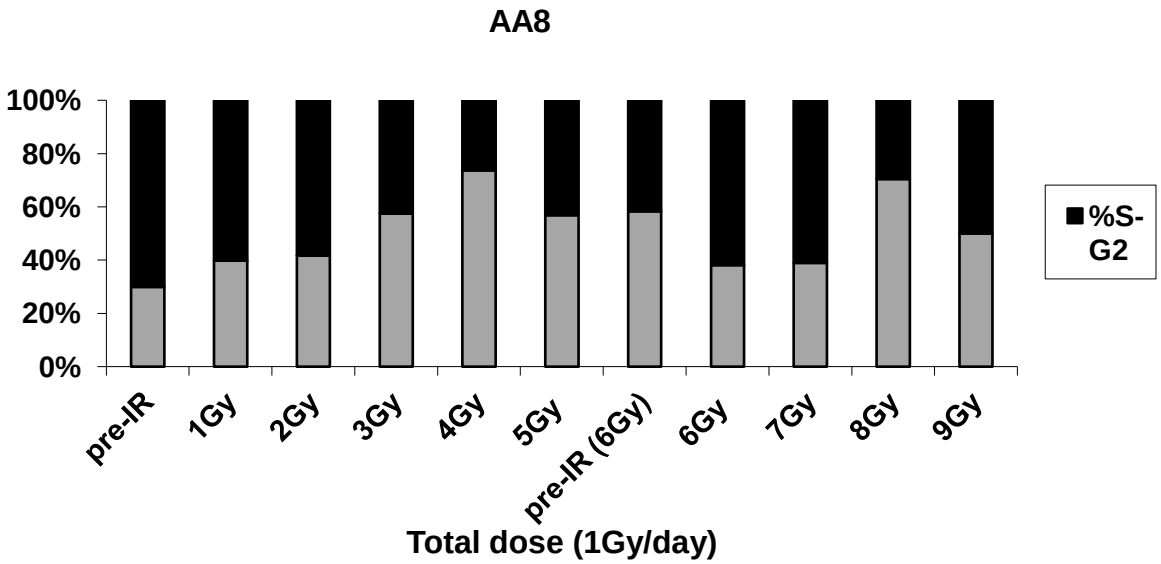
A


V3-3
100%
80%
60%
40%
20%
0%
pre-IR
1Gy
2Gy
3Gy
4Gy
5Gy
pre-IR (6Gy)
6Gy
7Gy
8Gy
9Gy
%S-G2
Total dose (1Gy/day)

B


irs-1SF
100%
80%
60%
40%
20%
0%
pre-IR
1Gy
2Gy
3Gy
4Gy
5Gy
pre-IR (6Gy)
6Gy
7Gy
8Gy
9Gy
%S-G2
Total dose (1Gy/day)

C



D

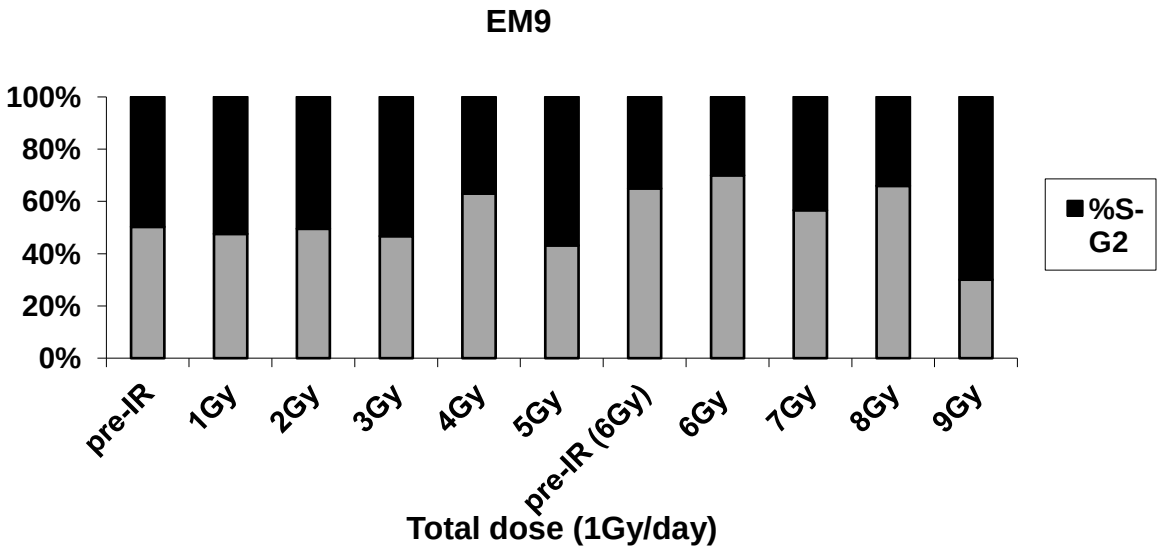


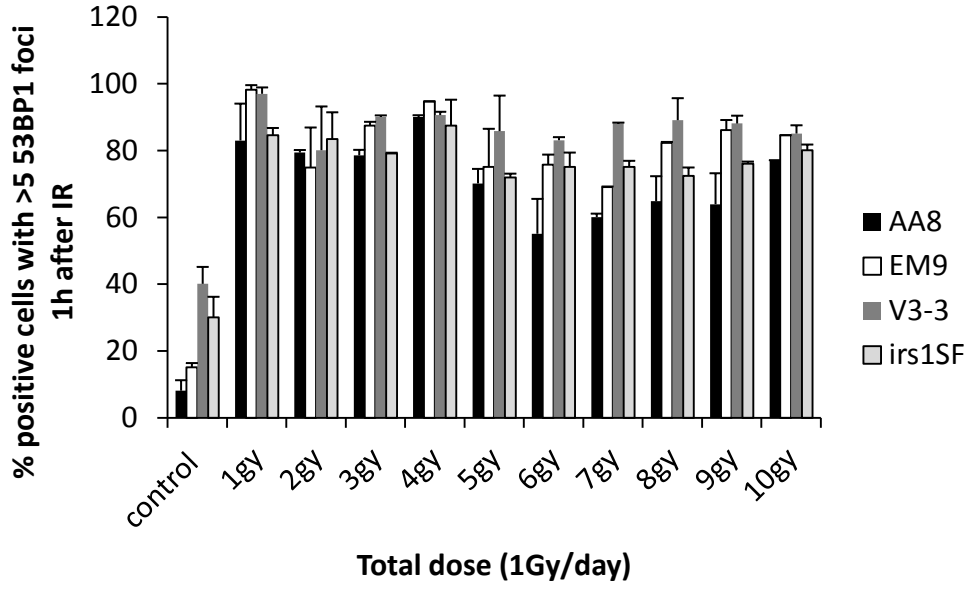
Figure 4.4: Cell cycle changes with fractionated IR 1 Gy/day over 2 weeks with a weekend gap. A. V3-3 cells gradually accumulated in the S/G2 phase of the cell cycle. **B.** The irs1SF cells did not show any change in cell cycle profile during the course of IR. **C.** AA8 cells and **D.** EM9 cells did not show any particular trend.

4.2.3 DNA DSB repair kinetics during fractionated IR in wild type and DNA defective CHO cells

4.2.3.1 DNA DSB repair kinetics with 1 Gy/day

The 53BP1 protein accumulates in discrete nuclear foci at DNA DSB (Schultz, Chehab et al. 2000). Hence, to study DSB repair kinetics we analysed 53BP1 foci at various time points after each 1 Gy fraction of IR to a total dose of 10 Gy **(Figure 4.5)**. The mutant cell lines, especially V3-3 and irs1SF, had 30% and 20% higher baseline levels of 53BP1 positive cells (>5 foci) compared to WT cells respectively, in keeping with a defect in DSB repair. The maximum induction of DSB was detected 0.5 (data not shown) to 1 h after IR in all 4 cell lines with comparable levels throughout the 2 week period **(Figure 4.5A)**. The mean percentage of positive cells (>5 foci) at 1 h, over the 2 week period, was 72% for AA8 but higher for EM9 (82% p=0.03), V3-3 (88% p=0.0007) and irs1SF cells (79% p=0.07). Similarly, the percentage of cells with >5 residual 53BP1 foci remaining 24 h after each fraction of IR varied considerably between cell lines **(Figure 4.5B)**. WT cells demonstrated the most efficient DSB repair, with foci levels returning almost to baseline before successive 1 Gy fractions (19% mean residual positive cells over the 2 week period). EM9 cells followed a similar trend (30% mean residual positive cells, p=0.004). However, V3-3 cells had the highest number of unrepaired DSB (58% mean residual positive cells, p<0.0001), consistent with a lack of NHEJ. Relative to WT, irs1SF cells also showed high residual foci, which increased during the first week, fell after the weekend gap and increased again in the second week (50% mean residual positive cells, p<0.0001). The variation in the mean 53BP1 foci levels per cell mirrored the variation in the percentage of positive cells for all cell lines during the 2 week course of fractionated IR (**Figure 4.5C&D).**

A



B

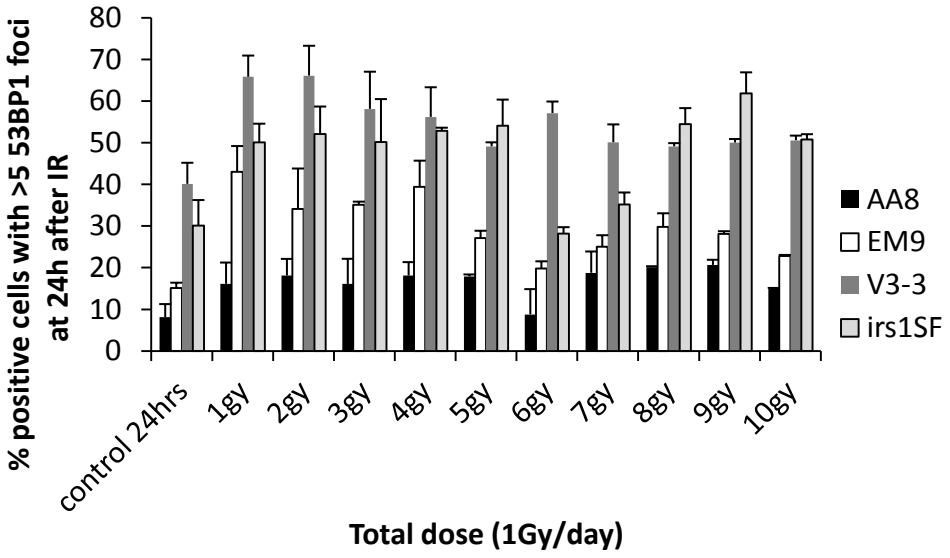
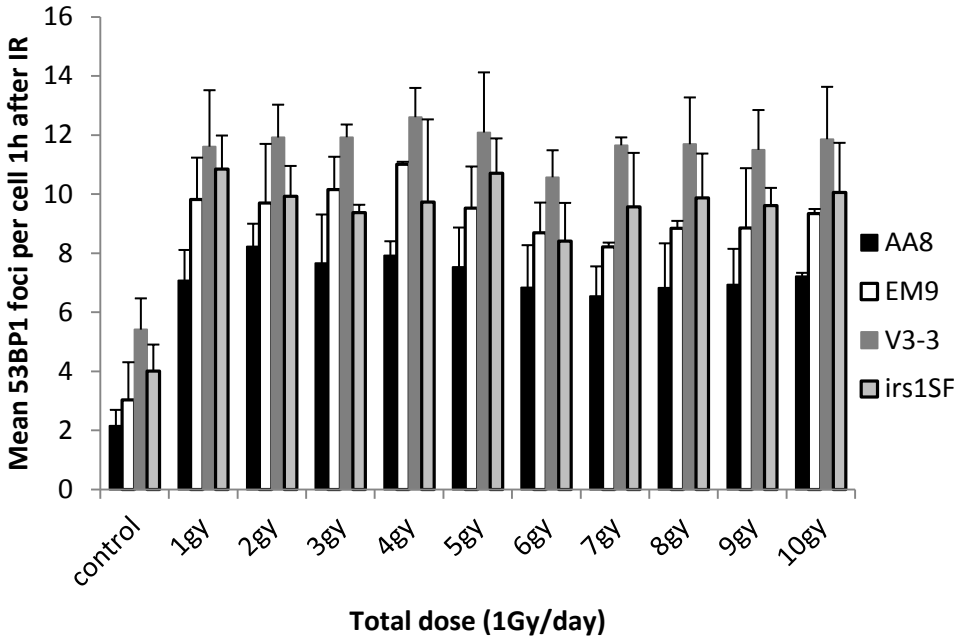


Figure 4.5: 53BP1 foci analysis with 1 Gy/day over 2 weeks with a weekend gap: measured as % positive cells with >5 53BP1 foci. A. Maximum 53BP1 foci induction at 1 hour in all 4 cell lines with fractionated daily IR. **B.** Residual 53BP1 positive cells (with >5 foci) 24 h after each fraction. Error bars represent SEM of 3 experiments in duplicate.

A.



B.

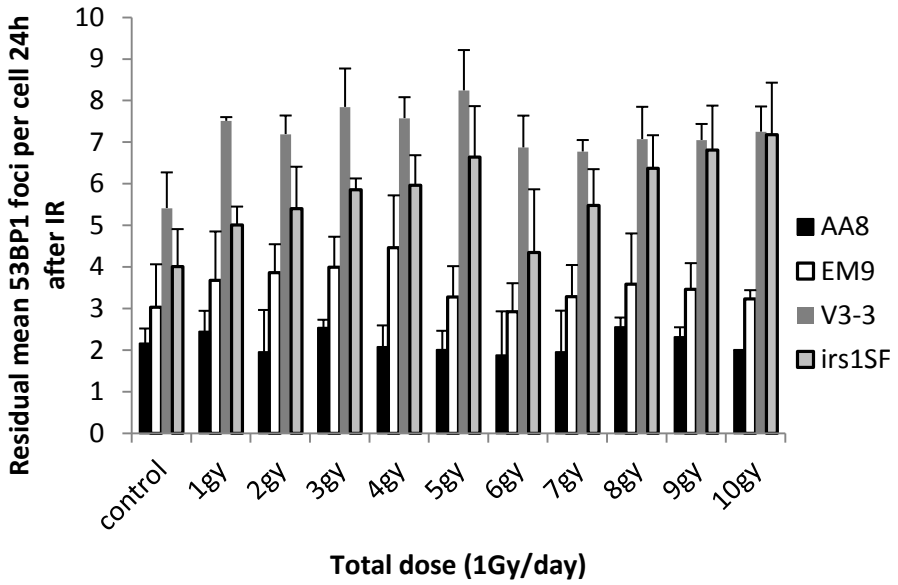
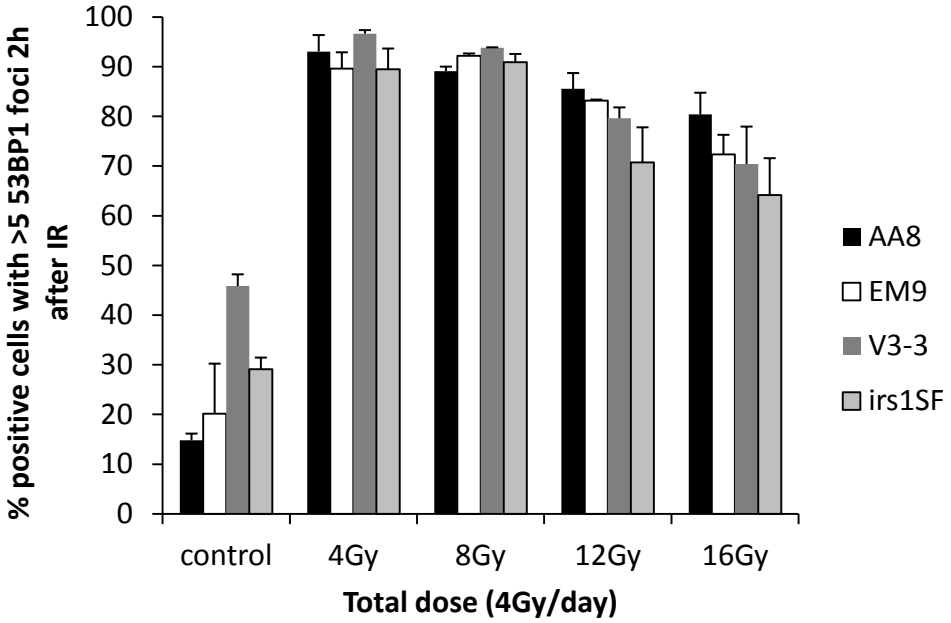


Figure 4.6: 53BP1 foci analysis with 1 Gy/day over 2 weeks with a weekend gap: measured as mean 53BP1 foci per cell. A. Maximum 53BP1 foci induction at 1 hour in all 4 cell lines with fractionated daily IR. **B.** Residual mean 53BP1 foci levels 24 h after each fraction. The variation in the mean 53BP1 foci levels per cell mirrored the variation in the percentage of positive cells for all cell lines during the 2 week course of fractionated IR. Error bars represent SEM of 3 experiments in duplicate.

4.2.3.2 DNA DSB repair kinetics with 4 Gy/day

We also analysed 53BP1 repair kinetics after daily fractions of 4 Gy to a total dose of 16 Gy **(Figure 4.6)**. The maximum percentage of positive cells with >5 53BP1 foci was slightly higher in all cell lines following the higher dose per fraction at 4 Gy and 8 Gy total doses with mean percentage of positive cells at 91%, 90%, 95% and 90% for AA8, EM9, V3-3 and irs1SF respectively **(Figure 4.6A)**. However, the percentage of positive cells was lower after total doses of 12 Gy & 16 Gy compared to 4 and 8 Gy. The decreased survival seen after the 4 Gy/day fractionated regimen **(Figure 4.2B)** was not reflected in the DSB foci remaining 24 h after successive fractions. This may represent misrepair of DNA DSB resulting in resolution of 53BP1 foci, but poorer survival. Another explanation is that DSB numbers in each cell got so high that only few copies of the 53BP1 protein relocated to each DSB, resulting in lower signal to noise levels and 'undercounting' of foci by the analysis software.

A



B

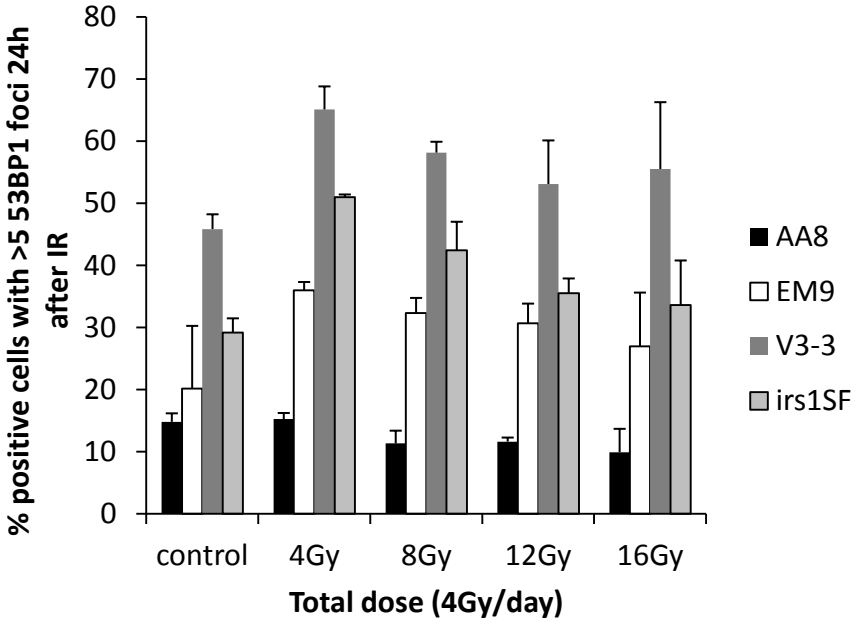


Figure 4.7: 53BP1 foci analysis with 4 Gy/day. A. Maximum 53BP1 foci induction (percentage of positive cells with >5 foci). **B.** Residual 53BP1 positive cells (with >5 foci) 24 h after each fraction. The variation in the mean foci levels per cell (data not shown) mirrored the variation in the percentage of positive cells for all cell lines. Error bars represent SEM of 3 experiments in duplicate.

4.2.4 Homologous recombination repair kinetics in wild type and DNA repair defective CHO cell during fractionated IR

4.2.4.1 RAD51 foci kinetics after 1 Gy/day

We used RAD51 foci as a marker for homologous recombination (Thompson and Schild 2001). The percentage of RAD51 positive cells (defined as cells with >4 foci) peaked 2 h after IR for most of the cell lines **(Figure 4.7A)**, approximately an hour later than 53BP1 foci levels. Spontaneous HR is increased in DNA-PKcs defective cells (Allen, Kurimasa et al. 2002) in keeping with our findings in V3-3 cells at baseline. V3-3 had the maximum number of RAD51 positive cells at baseline, 2 h and 24 h after each fraction of 1 Gy **(Figure 4.7 A & B)**. The maximum induction was seen after the 1st fraction, and from the 4th day onwards there was a gradual increase in the number of RAD51 positive cells at 2 h **(Figure 4.7A)** in keeping with the accumulation of V3-3 cells in S-G2 phase **(Figure 4.4A)**. The percentage of RAD51 positive cells (unrepaired foci) at 24 h was higher during the first week compared to the lower almost constant level during week 2 in V3-3 cells **(Figure 4.7B)**. As expected, the irs1SF cells showed a deficiency in RAD51 foci formation. The AA8 cells (and to a slightly lesser extent the EM9 cells) showed a pattern of RAD51 foci induction consistent with the cell cycle distribution during the course of fractionated 1 Gy/day IR **(Figure 4.7A & Figure 4.4C)**. WT cells also cleared their RAD51 foci most effectively 24 h after each 1 Gy dose **(Figure 4.7B)**.

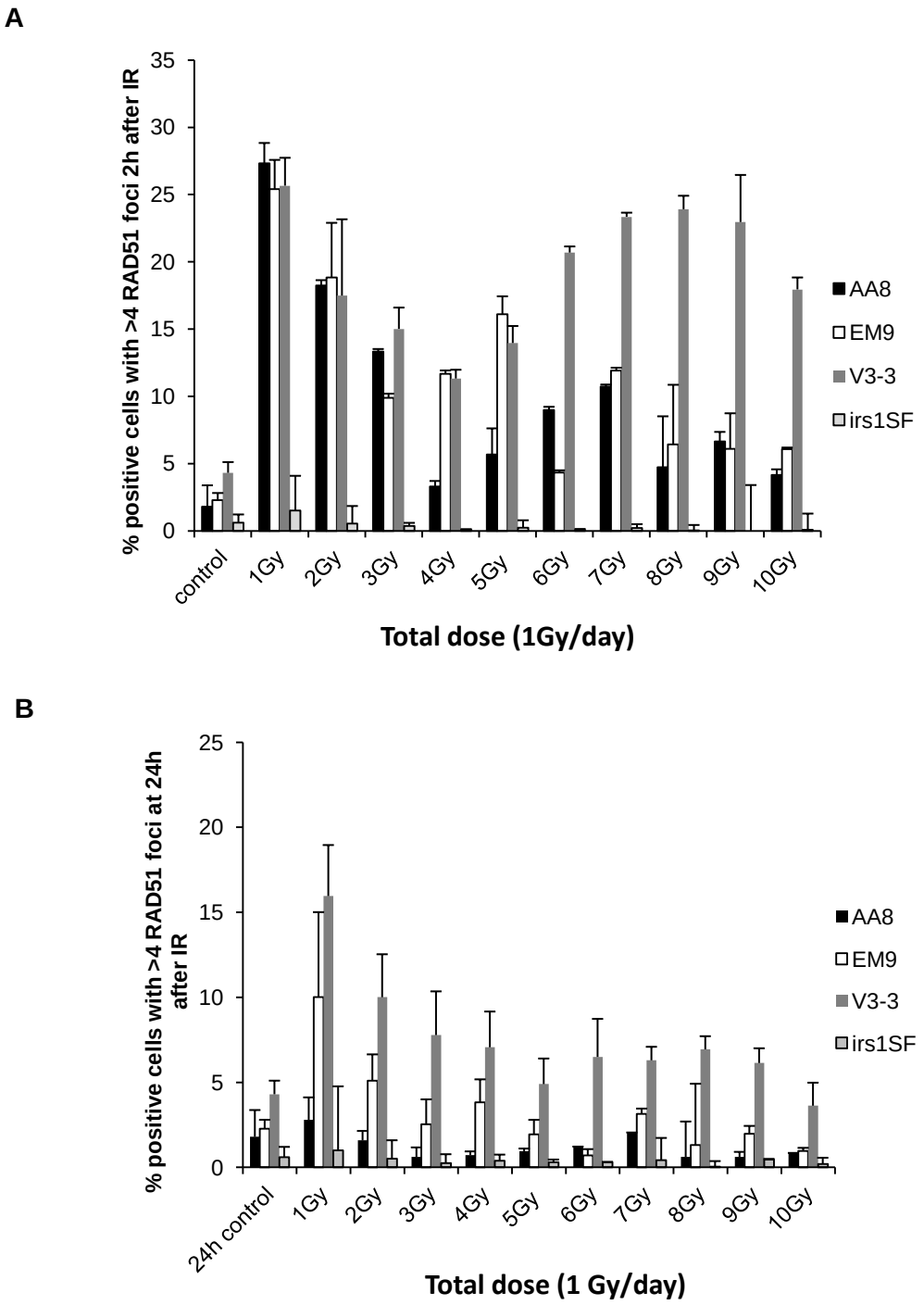
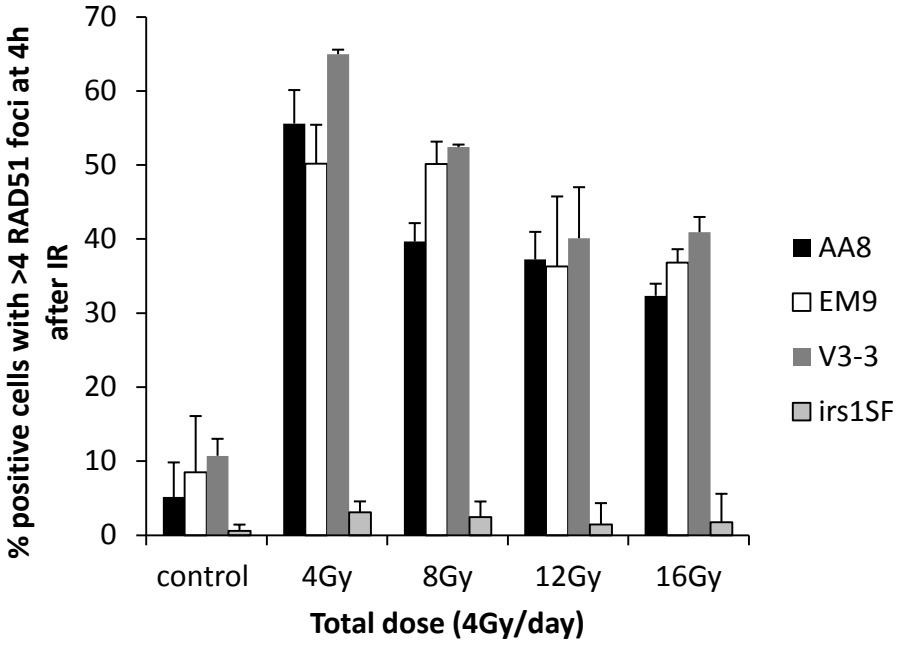


Figure 4.8: RAD51 foci analysis with 1 Gy/day over 2 weeks with a weekend gap. A. Maximum RAD51 foci induction (percentage of positive cells with >4 foci) in all 4 cell lines with fractionated daily IR. **B.** Residual RAD51 positive cells (with >4 foci) 24 h after each fraction. The variation in the mean foci levels per cell (data not shown) mirrored the variation in the percentage of positive cells for all cell lines. Error bars represent SEM of 3 experiments in duplicate.

4.2.4.2 RAD51 foci kinetics after 4 Gy/day

In response to 4 Gy/day, there was a 28% and 40% higher peak incidence of RAD51 positive cells in AA8 and V3-3 cells respectively **(Figure 4.8A)**. Similarly the residual RAD51 positive cells at 24 h was higher in all cell lines (except irs1SF) compared to the 1 Gy/day regimen **(Figure 4.8B)**. One possible explanation is that the higher damage levels inflicted each day resulted in more complex or difficult to repair DNA breaks in the heterochromatin for instance, that required involvement of HR (Jeggo, Geuting et al. 2011). The maximum percentage of RAD51 positive cells (>4 foci) was seen slightly later at 4 h after a 4 Gy dose compared to 2 h after a 1 Gy dose.

A



B

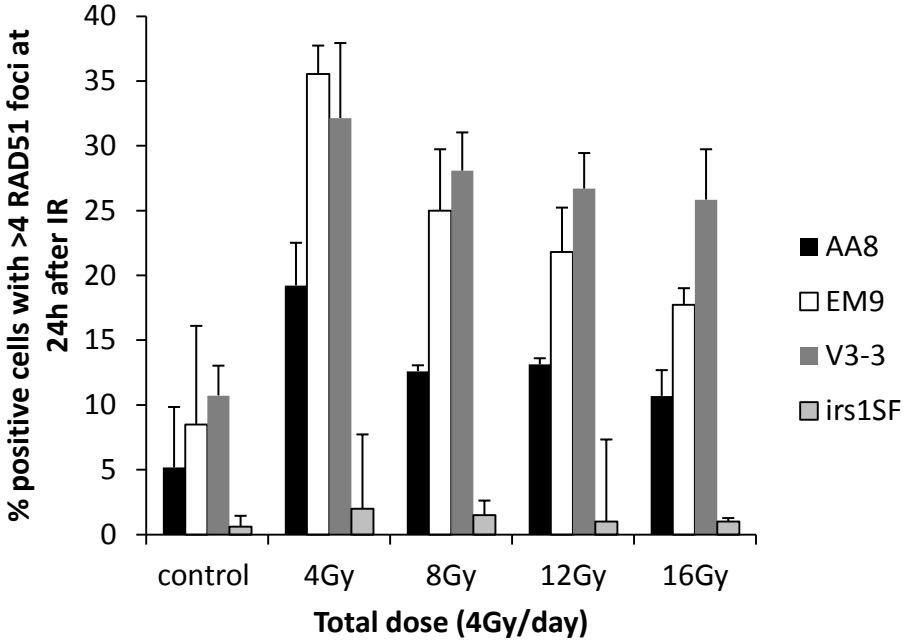


Figure 4.9: RAD51 foci analysis with 4 Gy/day. A. Maximum RAD51 foci induction (percentage of positive cells with >4 foci). **B.** Residual RAD51 positive cells (with >4 foci) 24 h after each fraction. The variation in the mean foci levels per cell (data not shown) mirrored the variation in the percentage of positive cells for all cell lines. Error bars represent SEM of 3 experiments in duplicate.

4.3 Discussion

To examine the link between DNA DSB repair pathways and fraction size sensitivity, we studied the response of mutant CHO cells defective in different DNA repair pathways. We find that sensitivity to fraction size is associated with functional NHEJ. It is undetectable in cells that lack functional NHEJ and make greater use of HR. This is consistent with the findings of Thacker *et al* (Thacker and Wilkinson 1995) who showed that the cell line relying on HR showed no difference in cell kill with high dose rate compared to low dose rate irradiation. In addition, split dose recovery has been observed under a variety of experimental conditions in many cell systems and is believed to be the result of the repair of sublethal damage (SLD) (Elkind and Sutton 1959; Elkind, Sutton-Gilbert et al. 1967; Frankenberg, Frankenberg-Schwager et al. 1984). SLD repair between fractions has long been established as a critical factor for the sparing effect of fractionated radiotherapy. It has been shown previously that XRCC3 and XRCC2 (HR) deficient chicken B lymphocyte (DT40) cell lines show a substantial recovery with split dose as opposed to single dose experiments, in keeping with our findings in irs1SF (XRCC3 deficient) (Rao, Tano et al. 2007). Our data also show that cells defective in NHEJ accumulate in the S/G2 phase of the cell cycle with fractionated IR enabling them to make greater use of HR. These findings in V3-3 cells are consistent with previously published studies showing an interactive competition between NHEJ and HR whereby DSBs destined for repair by NHEJ are shunted to HR in the absence of DNA-PKcs (Allen, Kurimasa et al. 2002; Allen, Halbrook et al. 2003) . It has also been shown that cells exposed to the DNA-PK inhibitor AMA37, DNA-PK deficient cells and NHEJ deficient cells all enter a prolonged G2 arrest after exposure to doses of 2 to 6.5 Gy (Sturgeon, Knight et al. 2006).

NHEJ is prone to generating rearrangements in the DNA through misrejoining of DSB ends when these are in close proximity, for example at high acute doses (Rothkamm, Kruger et al. 2003). Reducing the dose per fraction reduces the chance of DSB coinciding, resulting in reduced misrejoining using NHEJ (Kuhne, Rothkamm et al. 2000; Lobrich, Kuhne et al. 2000; Rothkamm and Lobrich 2002). The linear quadratic (LQ) model for chromosome aberration induction assumes that at low doses, rearrangements arise from multiple DSB induced in the same electron track (typically by track-end electrons), giving rise to a linear induction. At higher doses, DSB from separate tracks increasingly form sufficiently close to each other to interact. In this model, both the linear and quadratic components of damage can arise by NHEJ. HR, in contrast, uses the intact sister chromatid as a template for repair, thus avoiding any risk of rejoining break ends that originated from different DSB. Therefore, the high fidelity of HR, independent of DNA damage levels, may explain its insensitivity to fractionation.

Another mechanism contributing to loss of fraction size sensitivity in S/G2, independent of the use of HR, could involve cohesin. This protein facilitates accurate DSB repair in replicated chromatin (Bauerschmidt, Arrichiello et al. 2010) and may enhance high fidelity DSB repair after high doses (Kruger, Rothkamm et al. 2004). The tightly bound chromatid in S/G2 might serve as a scaffold to hold break ends in place and thus avoid loss or rearrangement of chromosome material. Without such a scaffold (i.e. in G0/G1), break ends would be able to move more freely, repair would be slower and more frequently result in ‘wrong’ ends being joined, especially at higher doses (or dose per fraction) when breaks are in close proximity .

Although most IR-induced DSB are repaired by NHEJ in mammalian cells, our results demonstrate that HR plays an important role in resistance to fractionated RT by virtue of accumulation of cells in late S and G2 phases of the cell cycle. It is well established that radioresistance in *D radiodurans* bacterium is mediated by increasing the ploidy (White, Eisen et al. 1999), thereby offering substrates for HR repair. In analogy, it appears that increasing the ploidy to 4n rather than 2n offers cells a significant advantage to mediate resistance to fractionated RT *in vitro* and *in vivo*. We have shown previously using normal human breast epidermal tissue in patients undergoing 5 weeks of fractionated RT that there is an accumulation of cells in the S-G2 phase of the cell cycle towards the end of RT (Chapter 3) (Somaiah, Yarnold et al. 2012). Our data shows that there is a significant increase in the use of HR to repair DSB by 5 weeks of RT. This correlates with loss of fractionation sensitivity seen clinically (Turesson and Thames 1989; Hopewell, Nyman et al. 2003). In fact CHO cells have been shown to harbour mutations in p53 that abrogates their ability to arrest in G1 without affecting the G2 checkpoint (Lee, Larner et al. 1997). This finding may also be relevant to cancer cells in that most have lost cell cycle checkpoints such as the p53 pathway and accumulate in the G2 phase of the cell cycle after DNA damage (Kastan, Onyekwere et al. 1991). Many tumours acquire defects in one or more DNA repair pathways, and up to 30% of sporadic breast cancers harbour defects in the HR pathway (Turner, Tutt et al. 2004). There is emerging evidence that competent HR is associated with poorer outcomes with chemotherapy (Asakawa, Koizumi et al. 2010; Graeser, McCarthy et al. 2010). Our data suggest that inhibition of HR may also be a useful target to exploit fractionated RT and has implications for tumour radioresistance and adverse normal tissue responses. Tumours characterised by slowly cycling cells (G0/G1 phase) reliant on NHEJ and those lacking HR (even if rapidly proliferating) are expected be more sensitive to fraction size. This opens the possibility for

individualisation of radiotherapy dose prescription, moving away from the ‘one fraction size fits all’ approach that has characterised the field of radiotherapy for decades.

CHAPTER FIVE

Results- 3

The effect of different small molecule inhibitors of DNA repair on fractionated radiation responses

5.1 Introduction

Radiotherapy is one of the standard treatment options for various malignant cancers and is often combined with surgical resection and/or chemo therapy as a part of multidisciplinary treatment. More than 50% of patients with cancer receive radiotherapy at some point during their treatment process. Modern advances in technology such as IMRT, IGRT and Cyberknife mean that we can now target the tumour more precisely than ever before whilst sparing the dose limiting critical structures, thereby allowing dose escalation strategies to be tested. However radioresistance, both acquired and inherent, continues to be a problem in clinical practice which can only be overcome by understanding the underlying biology (Bentzen, Harari et al. 2007) (Bentzen, Harari et al. 2007; Begg, Stewart et al. 2011). Over the recent years there has been great interest in molecular targets for radiosensitisation with several new drugs entering clinical trials with radiotherapy (Bentzen, Harari et al. 2007). Currently we do not know how these drugs modulate fraction size sensitivity and this needs to be evaluated further if we want to exploit the interaction between drugs and radiation for maximum therapeutic gain.

5.1.1 DNA Double-Strand Break Response: DNA Repair and Cell Cycle Checkpoints

Following DNA double strand-breaks (DSBs) induced by ionizing radiation, DNA repair and cell cycle checkpoints are the main mechanisms of maintenance of genomic stability (Krempler, Deckbar et al. 2007). Cells have several checkpoints that function at various phases of the cell cycle. Specifically, the G1/S and intra-S checkpoints prevent inappropriate DNA replication, whereas the G2/M checkpoint prevents cells with DNA damage from entering mitosis. When these checkpoints detect DNA damage at each phase, they induce cell cycle arrest and make time for repair of DNA damage. ATM plays a central role in the DNA damage response pathway by controlling the checkpoints via effector proteins such as Chk1, Chk2, p53 and BRCA1 (Kuroda, Urata et al. 2012).

Homologous recombination (HR) and nonhomologous end joining (NHEJ) are the major DNA DSB repair pathways, and cells use them according to the phase of the cell cycle and condition of the DSB ends (Helleday, Lo et al. 2007). HR provides accurate genetic recombination using a sister chromatid as a template, which is essential for maintenance of genomic stability. Although HR is a desirable method of DNA DSB repair, it is limited in cells during the S and G2 phases because of the need for a sister chromatid. NHEJ is a simple method of directly connecting the DSB ends. Although NHEJ is not as accurate as HR, it plays an important role in minimizing DNA damage, especially in cells in the G0 and G1 phases, in which HR is not available. Ku70/80, the DNA-dependent protein kinase, catalytic subunit, and DNA ligase IV are major contributors to NHEJ.

DNA repair and cell cycle checkpoints must cooperate closely to repair DNA damage and maintain genomic stability. Defects in this network produce dysfunction

in the repair of DNA damage induced by ionizing radiation, which results in enhancement of the cytotoxic activity of radiation. Thus, molecules involved in these mechanisms can be suitable targets for radiosensitisation. We therefore wanted to study the pre-clinical effects of small molecule inhibitors of ATM, DNA-PKcs and PARP in the context of fractionated irradiation as it is delivered in the clinical setting and study DNA DSB repair kinetics with each fraction. In addition, given our findings in chapters 3 and 4 we wanted to study their effects on fraction size sensitivity.

5.2 ATM as a Target for Radiosensitisation

As described above, the cellular response to DNA damage is a complex process that includes recognition of the DNA damage, activation of signalling pathways including cell cycle checkpoints, and repair of the damage. An important protein in the cellular response to DNA damage is the ataxia telangiectasia mutated (ATM) protein. Studies originally identified the ATM gene in the genomic instability syndrome termed Ataxia-Telangiectasia (A-T), a disease that causes several severe disabilities, such as cerebellar degeneration, immunodeficiency, hypersensitivity to radiation and genomic instability, and increased incidence of malignancies (Savitsky, Bar-Shira et al. 1995). All patients with A-T have mutations in the ATM gene, and intensive investigation of such patients and A-T cells has contributed to the elucidation of ATM function. ATM belongs to the phosphatidylinositol 3-kinase (PI3K)-related kinase family. The construction of the ATM protein is similar to that of ATM- and RAD3-related (ATR), the DNA-dependent protein kinase catalytic subunit and mammalian target of rapamycin (mTOR). The increased sensitivity of A-T cells to ionizing radiation is not associated with defective repair of DNA single-strand breaks or in the removal of base damage from DNA (Fornace and Little 1980). Instead, after exposure to ionizing radiation, A-T cells have been reported to display residual chromosomal breaks (Cornforth and Bedford 1985), slower DNA DSB

rejoining than wild-type cells (Coquerelle, Weibezahn et al. 1987), and a failure to repair all DNA DSBs (Foray, Priestley et al. 1997), which could account for the radiosensitivity and genome instability associated with A-T.

Following DNA damage, ATM immediately activates signalling pathways for DNA repair and cell cycle checkpoints (Kastan and Lim 2000). Although recent studies have shown that downstream signalling of ATM is becoming increasingly complicated, p53 and Chk2 are undoubtedly the main targets of ATM and control the G1/S and G2/M checkpoints while interacting with each other (Banin, Moyal et al. 1998; Matsuoka, Rotman et al. 2000). Also, inhibition of these checkpoints allows damaged cells to move to the mitotic phase without undergoing proper DNA repair, leading to mitotic catastrophe, which is currently considered a main cause of cell death induced by radiotherapy (Eriksson and Stigbrand 2010; Postiglione, Chiaviello et al. 2010). Moreover, ATM is known to affect HR repair by directly or indirectly phosphorylating at least 12 targets, such as BRCA1/2 and NBS1, and defects in ATM function lead to dysfunction in HR repair (Shrivastav, De Haro et al. 2008; Morgan, Parsels et al. 2010). After DNA damage, a number of proteins localize to the DSB and DSB-flanking chromatin including ATM, MDC1, the MRN complex, 53BP1 and BRCA1 (Bekker-Jensen, Lukas et al. 2006). Phosphorylated H2AX (γH2AX) plays an important role in anchoring these proteins to the DSB and DSB-flanking chromatin (Stucki and Jackson 2006). ATM phosphorylates H2AX and MDC1 binds through its BRCT domain to the phosphorylated tail of γH2AX (Burma, Chen et al. 2001; Lou, Minter-Dykhouse et al. 2006). It has been proposed that amplification of ATM signaling results from a cyclic process in which ATM phosphorylates H2AX and γH2AX subsequently recruits MDC1, which stabilizes ATM further at the DSB and DSB-flanking chromatin, resulting in expanded H2AX phosphorylation over mega bases of DNA flanking the DSB (Stucki and Jackson

2006). These findings indicate that targeted ATM inhibition is an attractive approach to enhancing tumour radiosensitivity.

5.2.1 Inhibitors of ATM

Caffeine and wortmannin, which are nonspecific PI3K inhibitors, have been widely used in studies related to ATM/ATR functions (Sarkaria, Tibbetts et al. 1998; Alao and Sunnerhagen 2009). However some of the effects of caffeine and wortmannin in cells, such as apoptosis and checkpoint abrogation, are caused not only by ATM/ATR inhibition but also by other factors in the PI3K family (Sarkaria, Tibbetts et al. 1998; Zhou, Chaturvedi et al. 2000). Recently, researchers have developed several more specific ATM and ATM/ATR inhibitors—KU-55933, KU-60019, CGK733, and CP466722—and tested their potential as radiosensitisers in preclinical studies. KU-55933 was found to exhibit a specific inhibitory effect on ATM but not on other PI3K-family proteins, such as PI3K, DNA-PK, ATR, and mTOR, and sensitized cells to ionizing radiation by blocking phosphorylation of γH2AX, NBS1, and Chk1 (Hickson, Zhao et al. 2004). KU-60019, a more potent inhibitor of the ATM kinase, was shown to compromise insulin, AKT and ERK prosurvival signalling and inhibit migration and invasion of glioma cells in addition to its radiosensitising properties (Golding, Rosenberg et al. 2009). CGK733 demonstrated selective inhibition of ATM and ATR, which led to blockage of the checkpoint signaling pathways, and researchers showed that its inhibitory effects were more beneficial than its small interfering RNA-mediated inhibition (Won, Kim et al. 2006). CP466722 exhibited inhibition of ATM and its downstream signaling pathways in the same way that KU-55933 did, and investigators emphasized that transient (4 h or less) inhibition of ATM expression was sufficient to increase the radiosensitivity of tumour cells (Rainey, Charlton et al. 2008). Small interfering RNAs and antisense DNA for ATM

also exhibited potent radiosensitising effects (Guha, Guha et al. 2000; Collis, Swartz et al. 2003).

Based on this evidence, ATM inhibitors are expected to be promising candidate radiosensitisers. We therefore wanted to study the effects of ATM inhibition in the context of fractionated irradiation as it is delivered in the clinical setting and study DNA DSB repair kinetics with each fraction. We used KU-55933 which is an ATP-competitive inhibitor, 2-morpholin-4-yl-6-thianthren-1-yl-pyran-4-one that has been shown to specifically inhibit ATM with an IC_{50} of 13 nmol/L and a Ki of 2.2 nmol/L (Hickson, Zhao et al. 2004).

5.2.2 Results

5.2.2.1 Western blot testing the ATM inhibitor KU55933

ATM is rapidly phosphorylated at multiple residues in response to ionizing radiation (IR) (Bakkenist and Kastan 2003; Kozlov, Graham et al. 2006; Matsuoka, Ballif et al. 2007). In human cells, serines 367, 1893, and 1981 have been shown to be autophosphorylated in response to IR (Kozlov, Graham et al. 2006). The best characterised of these sites is serine 1981 (S1981). Autophosphorylation at this site leads to dissociation of ATM from a dimer into an active monomer (Bakkenist and Kastan 2003). After activation, the phosphorylated ATM monomers are recruited to DNA breaks where they phosphorylate various substrates (Lukas, Falck et al. 2003). Autophosphorylation at serine 1981 is widely considered a sign of ATM activation and is required for stabilising ATM at sites of DSBs for a proper DNA damage response (So, Davis et al. 2009). Using an anti-ATM (phospho S1981) antibody, we confirmed that the ATM inhibitor KU 55933 at 10 µM concentration for 1 h effectively abolishes the phosphorylation of ATM at this site in response to 10 Gy of irradiation in wild type CHO cells **(Figure 5.1).**

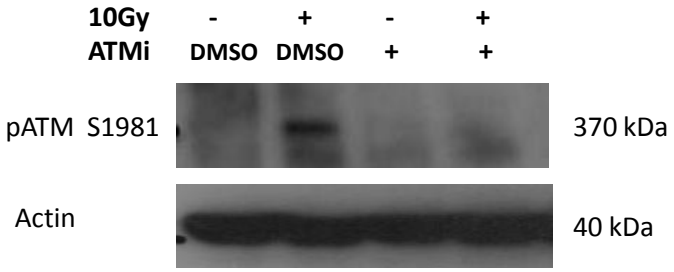


Figure 5.1: Western Blot testing the ATM inhibitor KU55933. The ATM inhibitor KU 55933 at 10 µM concentration for 1 h effectively abolishes the phosphorylation of ATM at serine 1981 in response to 10 Gy of irradiation in wild type CHO cells

5.2.2.2 Clonogenic cell survival following radiation in wild type CHO cells (AA8) with or without ATM inhibitor

5.2.2.2.1 Single radiation dose clonogenic survival curves

It has been shown previously that KU55933 increases ionising radiation-induced cytotoxicity as studied by single dose in vitro clonogenic assays (Hickson, Zhao et al. 2004). It was found to maximally potentiate radiation-induced cell killing at a concentration of 10 μM and hence was used at this dose in our experiments. At this concentration the drug alone does not reduce clonogenic survival (Hickson, Zhao et al. 2004). In line with published data we found that KU55933 sensitises AA8 cells to the effect of ionising radiation **(Figure 5.2)**. Survival data were fitted by a weighted, stratified linear regression according to the linear-quadratic formula using SPSS software as described in Chapter 4 (Franken, Rodermond et al. 2006). We were thus able to calculate the radiation dose at a certain survival level after radiation alone to that for the combined treatment with ATMi. Thus the dose-modifying factor ($DMF=D_{control}/D_{treated}$) at 10% and 1% survival was 1.2 and 1.5 respectively. As ATM is known to mainly affect the HR repair pathway we compared it to the HR defective AA8-derived cell line, irs-1SF. However, the radiosensitisation was not the same, with the irs-1SF cells (XRCC3 defective) much more radiosensitive compared to ATM inhibited wild type cells with a DMF of 2.14 at 10% survival (**Figure 5.2)**.

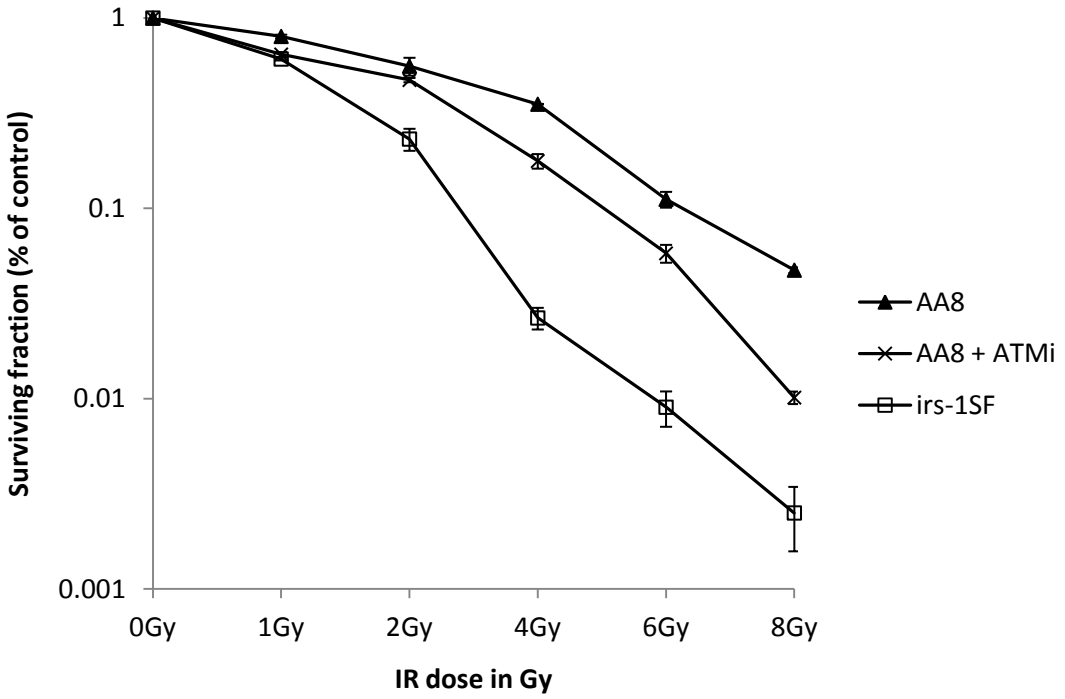


Figure 5.2: Acute dose clonogenic survival curves (semi-log) comparing WT AA8 cells with or without the ATMi and HR mutant irs-1SF cells (XRCC3-) at doses of 0, 1, 2, 3, 4, 6 and 8 Gy. Error bars show SEM of 3 repeats in triplicate.

5.2.2.2.2 Fractionated irradiation clonogenic survival curves – 1 Gy/day

As clinical radiotherapy is given in small fractional doses each day (usually 1.8-2 Gy per day) over several weeks with a gap over the weekend, we wanted to test the effect of adding an ATMi to fractionated IR. We tested 1 Gy/day given from Monday to Friday for 3 weeks to a total dose of 16 Gy. We found significant radiosensitisation with the addition of the ATMi to AA8 cells as seen in **Figure 5.3** increasing with each additional fraction of IR. However, significant recovery was seen after each weekend gap. Although all media and washings were saved and added to the final trypsinised pellet, it is possible that reseeding of the cells on Friday resulted in some loss of non-viable cells contributing to higher survival after the weekend. Similar recovery was also seen in the irs-1SF cells, but this was mainly after the first weekend gap. As with acute dose survival curves, radiosensitivity was greater in the genetically deficient HR mutant compared to the ATM inhibited WT cells.

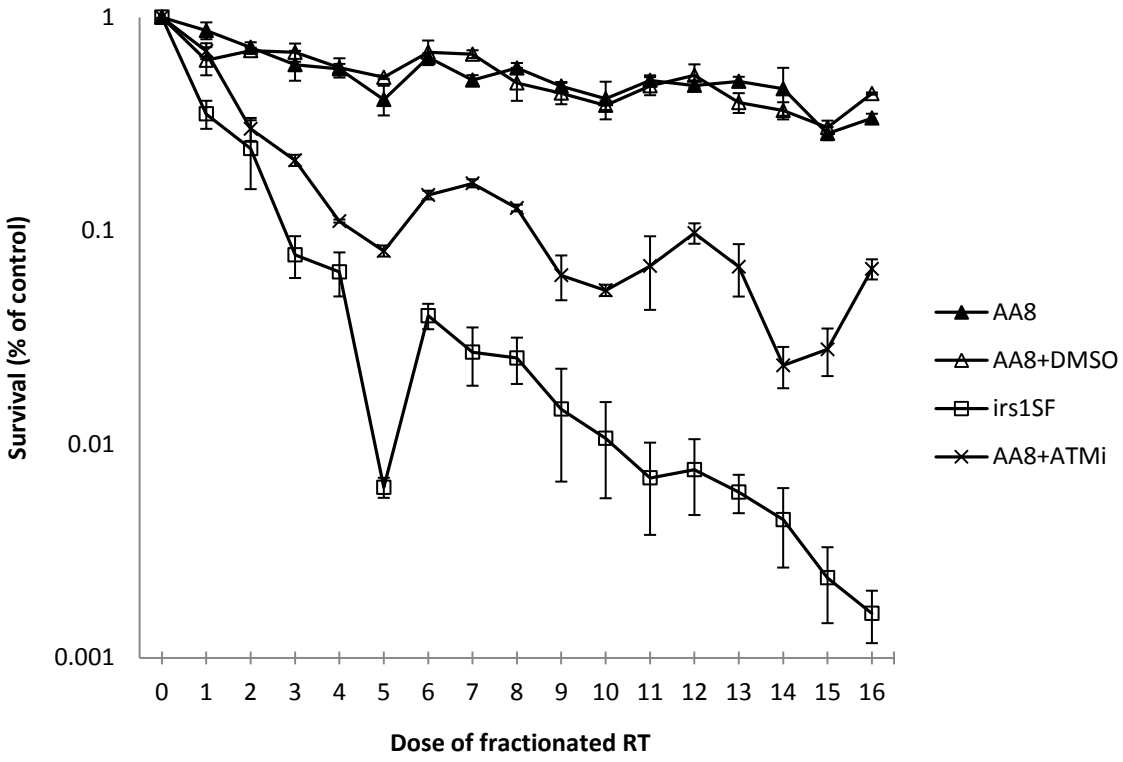


Figure 5.3: Fractionated IR clonogenic survival curves (semi-log) testing 1 Gy/day in WT AA8 cells with or without the ATMi and HR mutant irs-1SF cells. 1 Gy given daily Monday to Friday with weekend breaks to a total of 16 Gy. Error bars show SEM of 3 repeats in triplicate.

5.2.2.3 Sensitivity to changes in dose per fraction as measured by clonogenic survival in AA8 cells with or without ATMi

In order to see if addition of ATMi altered the fraction size sensitivity of the WT cell line, we compared survival following 2 Gy as a single fraction (high dose per fraction) versus 2 fractions of 1 Gy each (low dose per fraction) and 1x4 Gy versus 4x1 Gy **(Figure 5.4)**. We found that the addition of ATMi to AA8 reversed its sensitivity to fractionation. In other words, whilst AA8 and the HR mutant irs-1SF show increased sensitivity to higher dose per fraction (2.8 and 2.4 fold decrease after 4 Gyx1 versus 1 Gyx4 respectively), when ATMi was added to AA8 there was no sparing effect of smaller fractions (2.5 fold increase in survival after 4 Gyx1 versus 1 Gyx4).

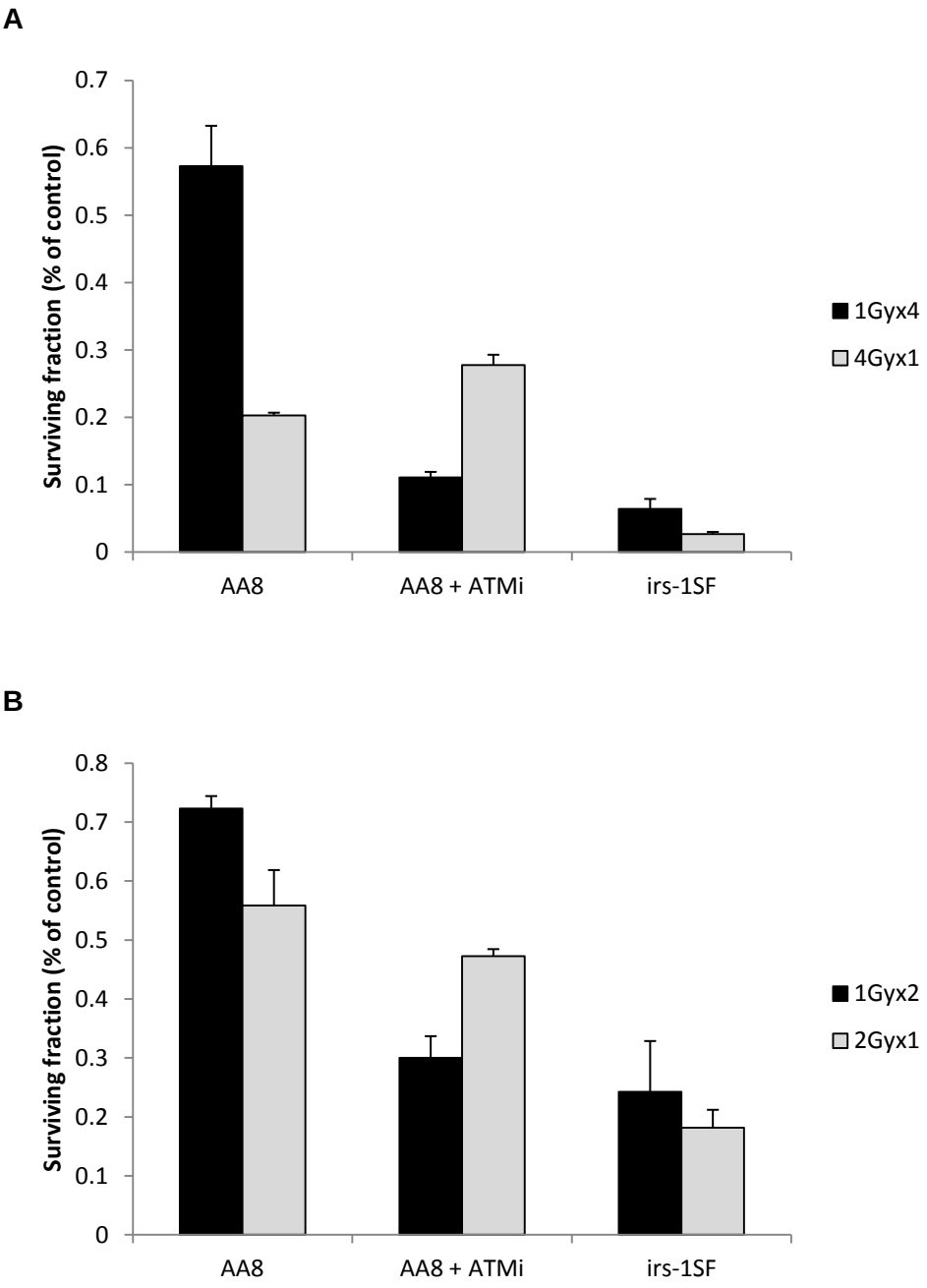
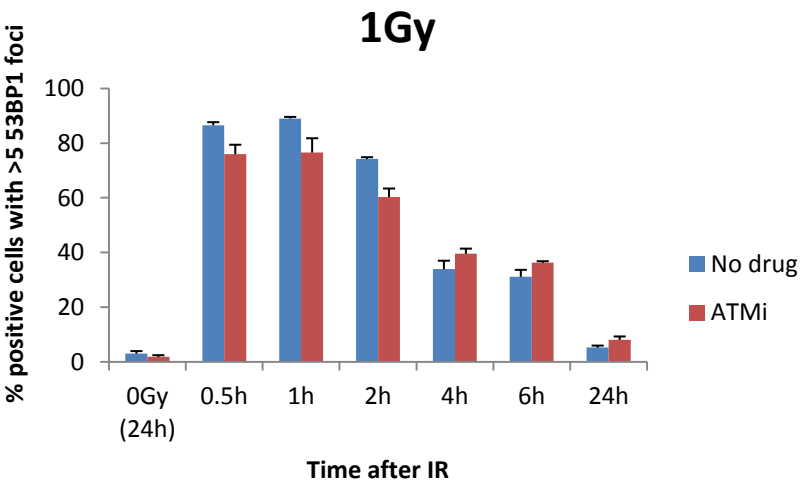
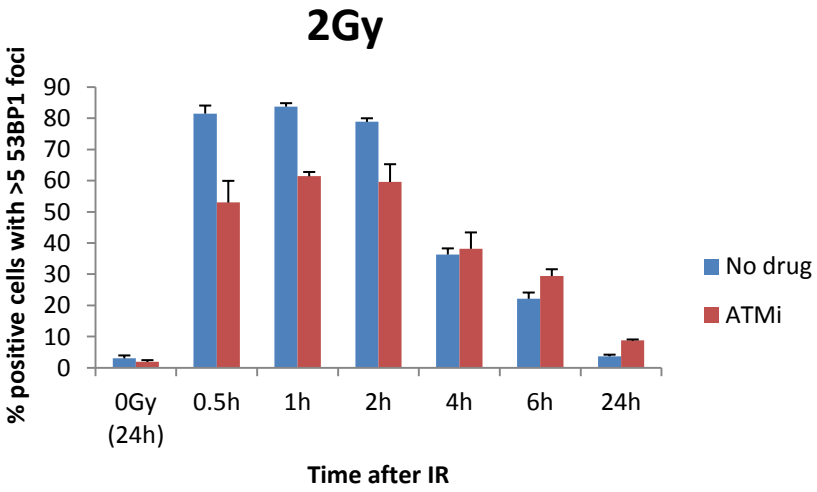


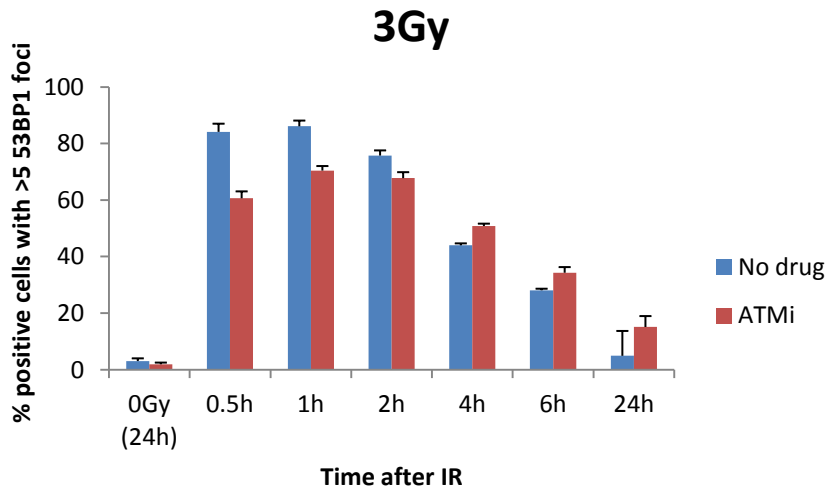
Figure 5.4: Comparison of survival between high dose per fraction vs low dose per fraction with or without ATMi. A & B. The WT AA8 and irs1SF (HR-) cell lines showed increased sensitivity to higher dose per fraction whereas addition of ATMi to WT cells showed loss of sparing effect with fractionation, when comparing 2 Gy in a single fraction vs 1 Gy in 2 fractions or 4 Gyx1 vs 1 Gyx4. Error bars show SEM of 3 repeats in triplicate.

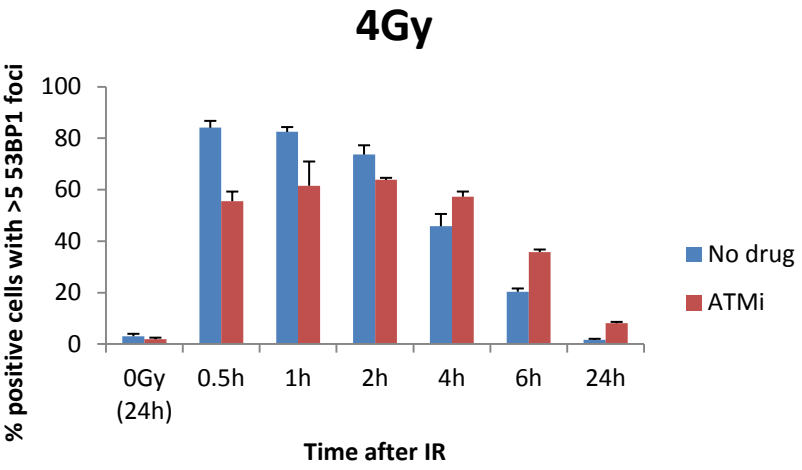
5.2.2.4 DNA DSB repair kinetics during fractionated IR in AA8 cells with or without ATMi

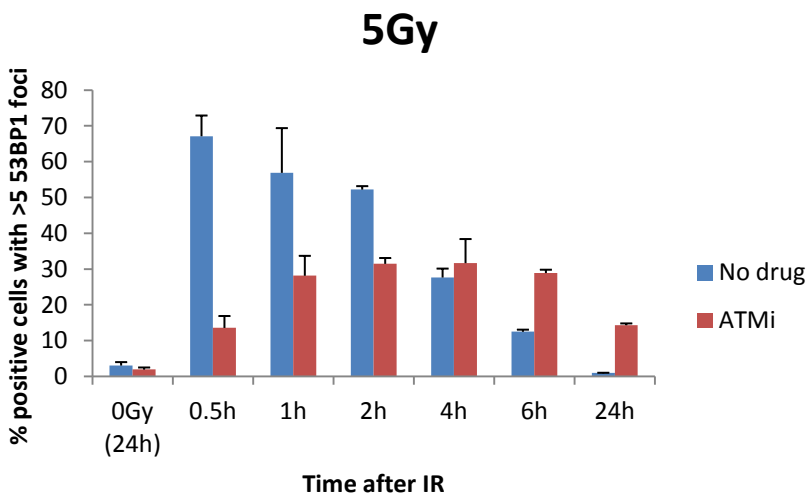
It has been shown previously that KU55933 inhibits DNA DSB repair using the neutral comet assay in p65+/+ and p65−/− mouse embryonic fibroblasts exposed to a single fraction of 10 Gy (Veuger and Durkacz 2011). We wanted to study DSB repair kinetics using 53BP1 foci analysis at various time points (0.5, 1, 2, 4, 6 and 24 hours) after each daily 1 Gy fraction of IR to a total dose of 10 Gy over 2 weeks with or without the ATMi **(Figure 5.5).** The 96 well plate format was used as described earlier and percentage of cells with >5 53BP1 foci were analysed as positive. There was no increase in 53BP1 foci in the control unirradiated cells with addition of ATMi alone. As seen in **Figure 5.5** the initial 53BP1 foci induction was lower in the presence of ATMi and this was significantly impaired as IR progressed. The peak 53BP1 foci levels were always seen at the 0.5 h time point in WT cells, but this was progressively delayed in the presence of ATMi as IR continued. The residual unrepaired 53BP1 foci at 24 h were higher in the presence of ATMi with a steady increase after each fraction of IR.

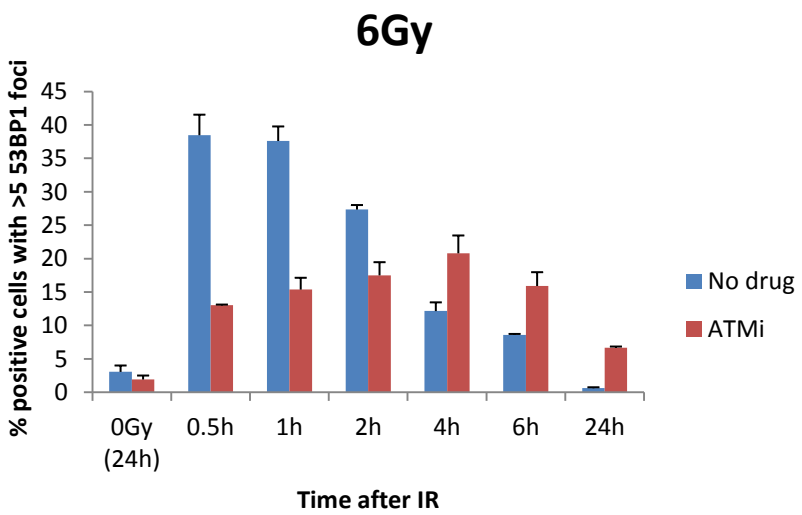

1Gy
% positive cells with >5 53BP1 foci
100
80
60
40
20
0
0Gy (24h)
0.5h
1h
2h
4h
6h
24h
Time after IR
No drug
ATMi

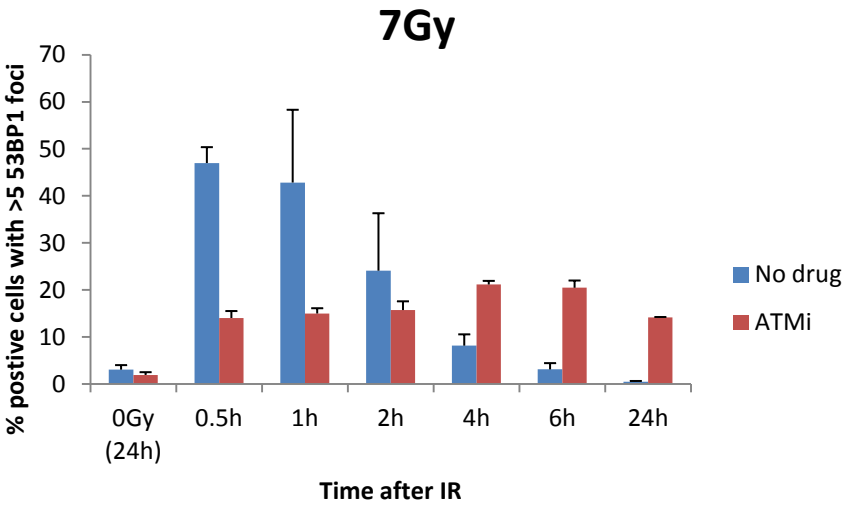

2Gy
% positive cells with >5 53BP1 foci
90
80
70
60
50
40
30
20
10
0
0Gy (24h)
0.5h
1h
2h
4h
6h
24h
Time after IR
No drug
ATMi

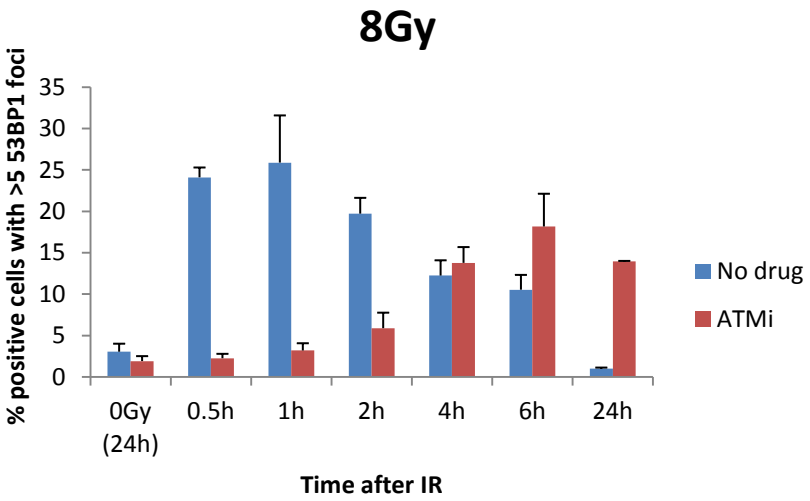

3Gy
% positive cells with >5 53BP1 foci
100
80
60
40
20
0
0Gy (24h)
0.5h
1h
2h
4h
6h
24h
Time after IR
No drug
ATMi

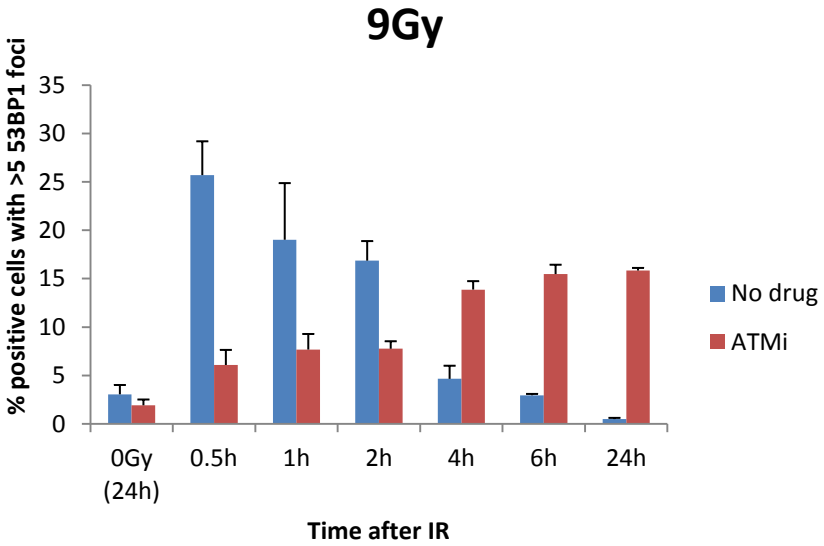

4Gy
% positive cells with >5 53BP1 foci
100
80
60
40
20
0
0Gy (24h)
0.5h
1h
2h
4h
6h
24h
Time after IR
No drug
ATMi


5Gy
% positive cells with >5 53BP1 foci
80
70
60
50
40
30
20
10
0
0Gy (24h)
0.5h
1h
2h
4h
6h
24h
Time after IR
No drug
ATMi


6Gy
% positive cells with >5 53BP1 foci
45
40
35
30
25
20
15
10
5
0
0Gy (24h)
0.5h
1h
2h
4h
6h
24h
Time after IR
No drug
ATMi


7Gy
% postive cells with >5 53BP1 foci
70
60
50
40
30
20
10
0
0Gy (24h)
0.5h
1h
2h
4h
6h
24h
Time after IR
No drug
ATMi


8Gy
% positive cells with >5 53BP1 foci
35
30
25
20
15
10
5
0
0Gy (24h)
0.5h
1h
2h
4h
6h
24h
Time after IR
No drug
ATMi


9Gy
% positive cells with >5 53BP1 foci
35
30
25
20
15
10
5
0
0Gy (24h)
0.5h
1h
2h
4h
6h
24h
Time after IR
No drug
ATMi

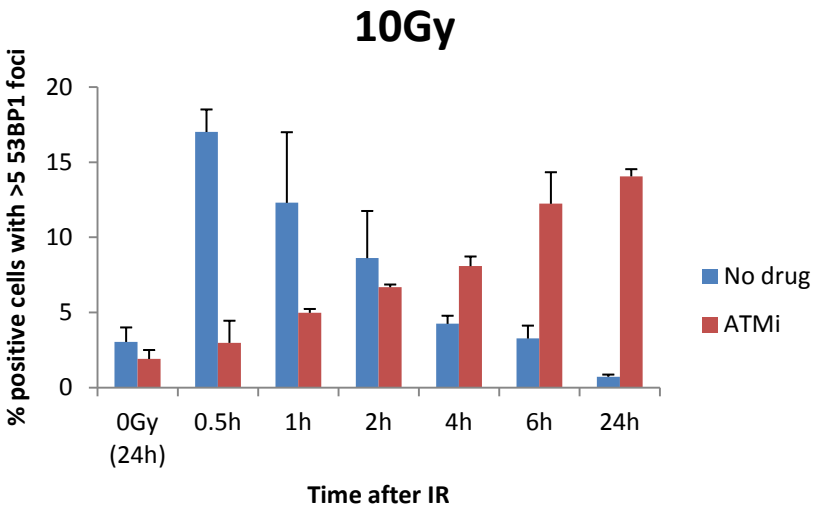
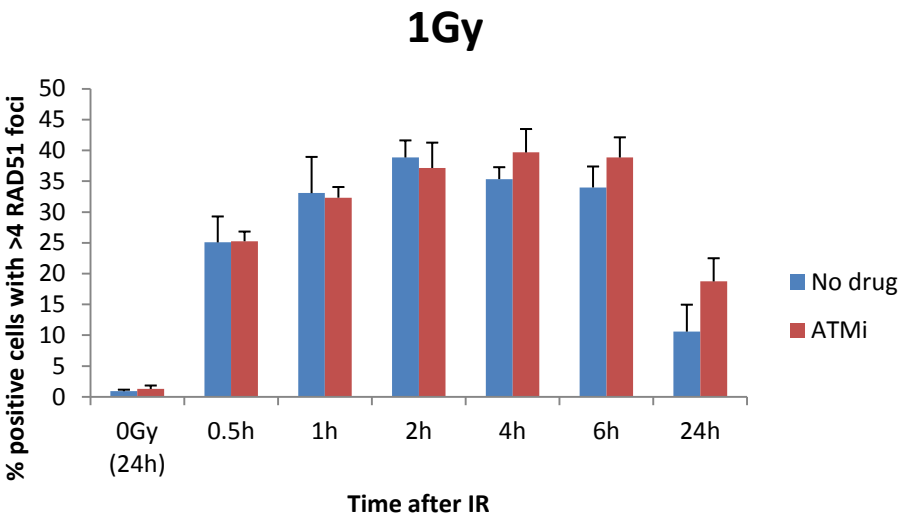
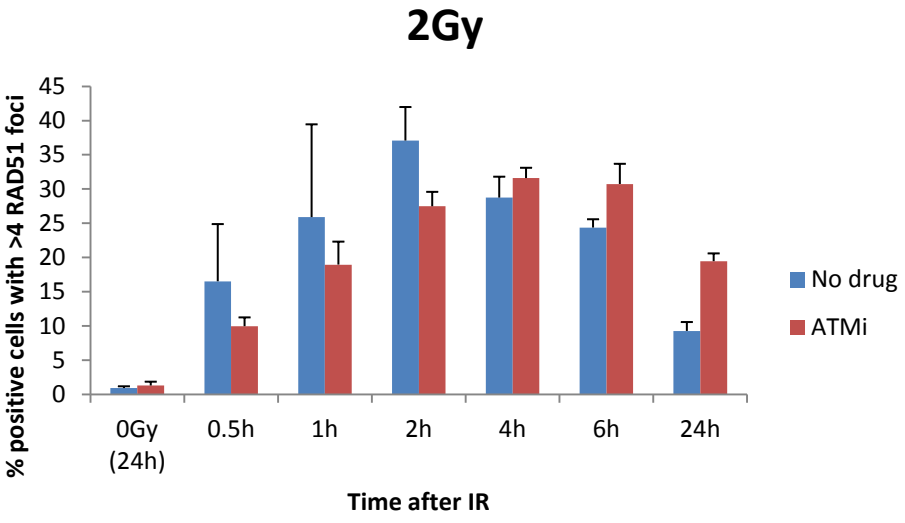


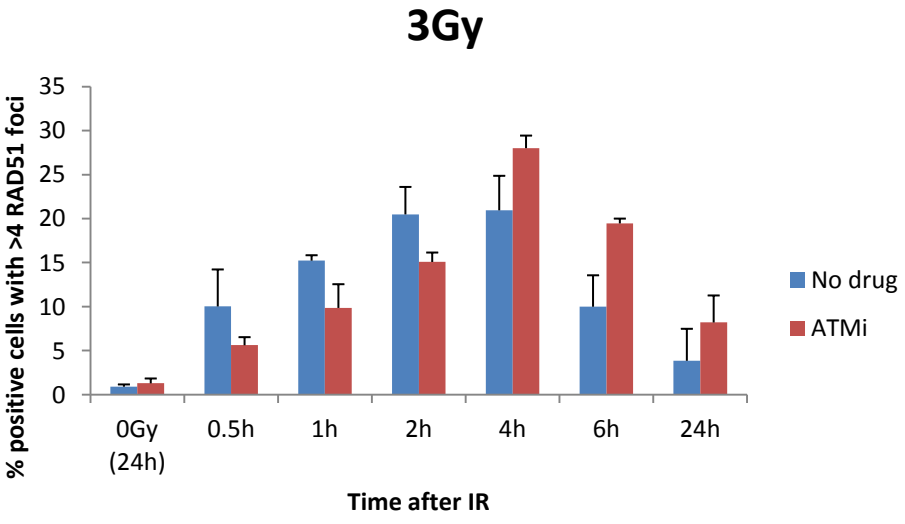
Figure 5.5: DNA DSB repair kinetics using 53BP1 foci analysis during fractionated IR in AA8 cells with or without ATMi. Measured as percentage positive cells with >5 53BP1 foci at 0.5, 1, 2, 4, 6 and 24 h after each fraction of 1 Gy given daily over 2 weeks (with a weekend gap), to a total dose of 10 Gy. Error bars represent SEM of 3 experiments in duplicate.

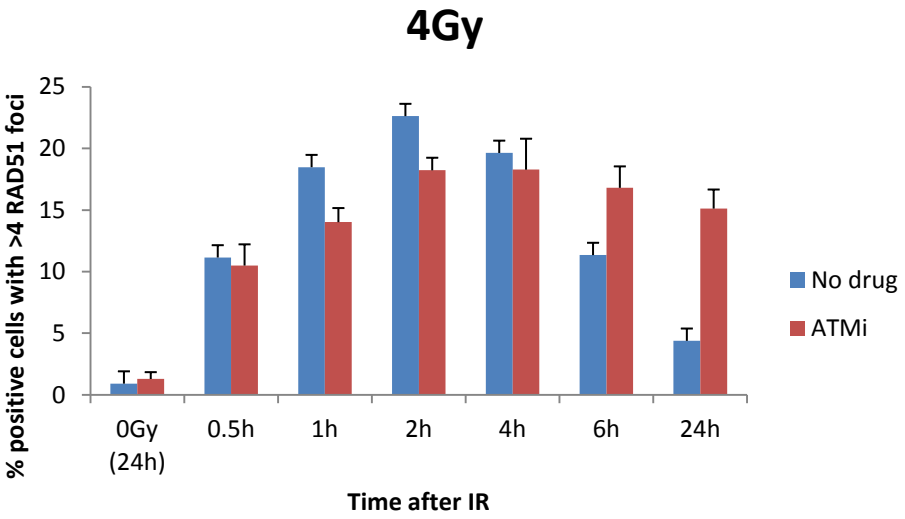
5.2.2.5 Homologous recombination repair kinetics in AA8 cells with or without ATMi during fractionated IR

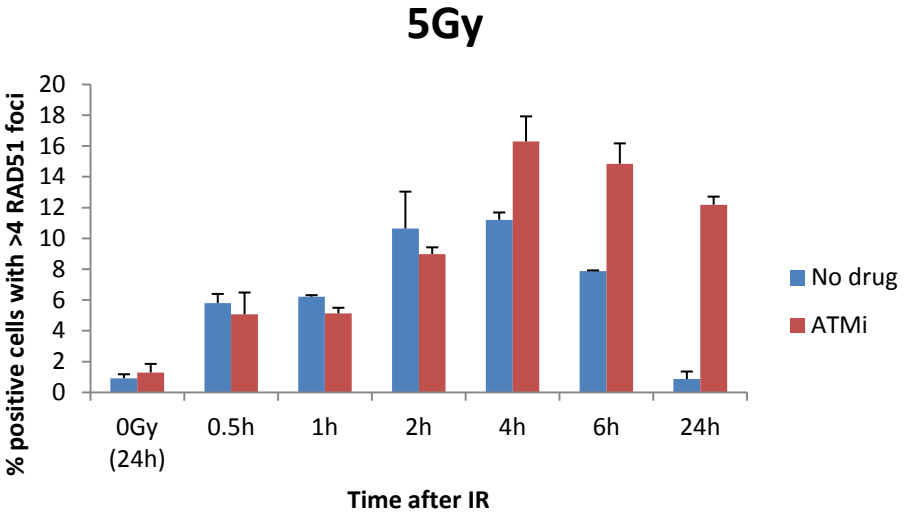
To study the effect of KU55933 on HR repair we analysed RAD51 foci levels at various time points (0.5, 1, 2, 4, 6 and 24 hours) after each daily 1 Gy fraction of IR to a total dose of 10 Gy with or without the ATMi **(Figure 5.6).** The peak induction of RAD51 foci was usually seen at the 2 h time point in WT cells, whereas this was later in the presence of ATMi especially during the first week of IR. Subsequently there was an increased accumulation of RAD51 positive cells at all time points after IR with ATMi compared to without confirming that ATMi interferes with HR repair.

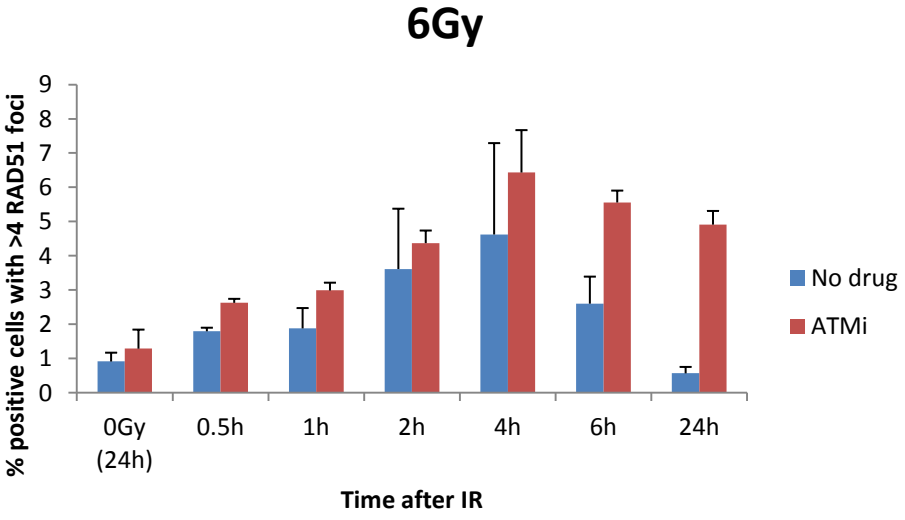

1Gy
% positive cells with >4 RAD51 foci
50
45
40
35
30
25
20
15
10
5
0
0Gy (24h)
0.5h
1h
2h
4h
6h
24h
Time after IR
No drug
ATMi

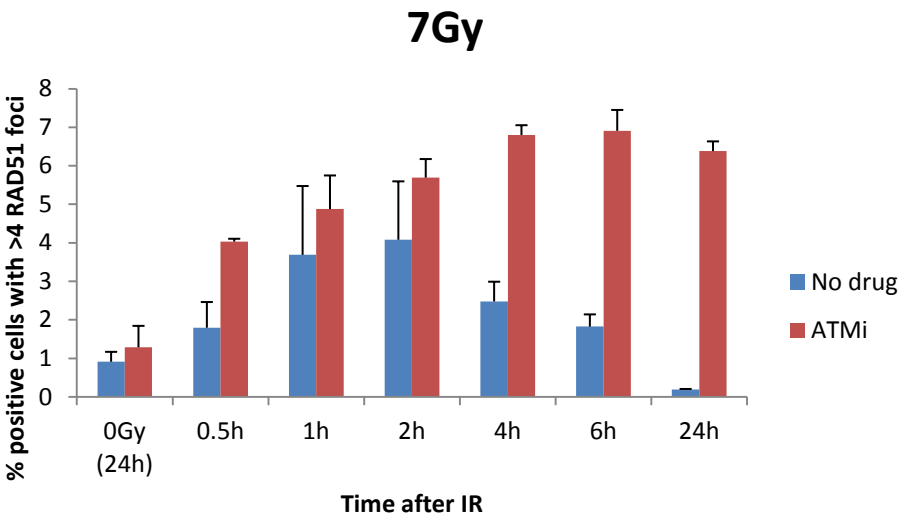

2Gy
% positive cells with >4 RAD51 foci
45
40
35
30
25
20
15
10
5
0
0Gy (24h)
0.5h
1h
2h
4h
6h
24h
Time after IR
No drug
ATMi

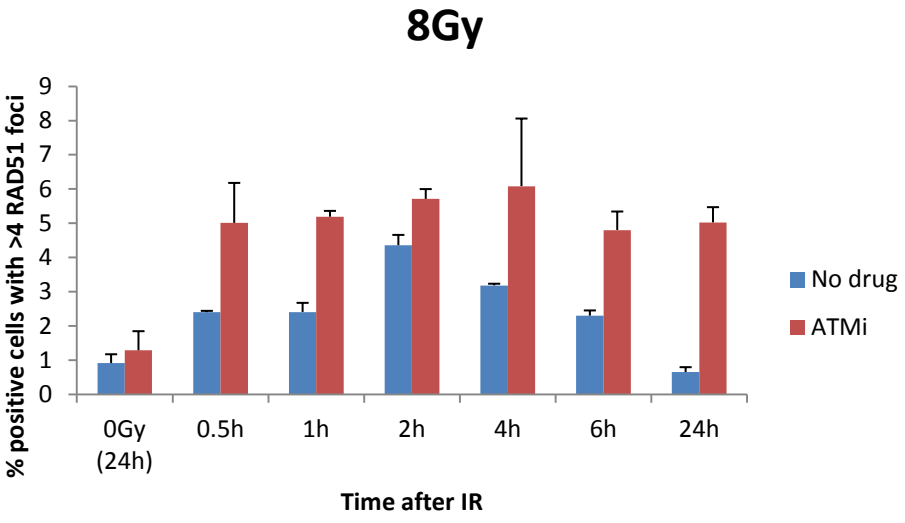

3Gy
% positive cells with >4 RAD51 foci
35
30
25
20
15
10
5
0
0Gy (24h)
0.5h
1h
2h
4h
6h
24h
Time after IR
No drug
ATMi

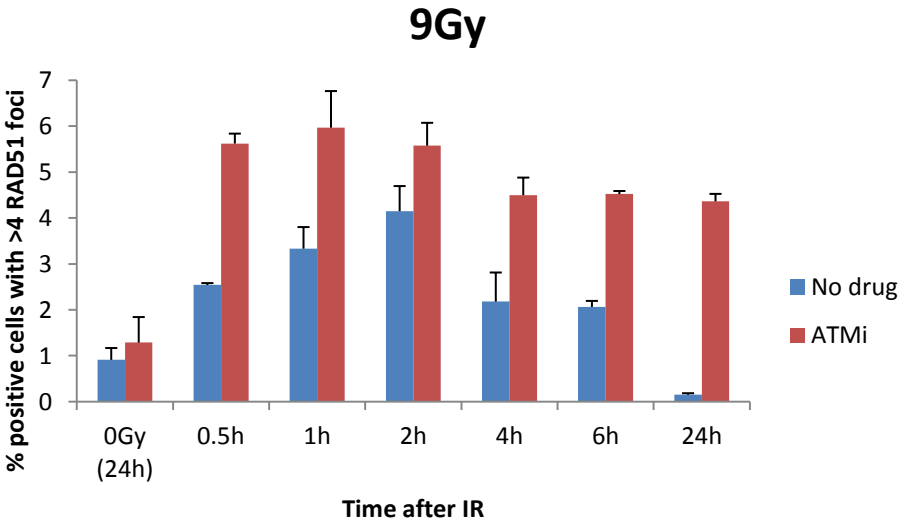

4Gy
% positive cells with >4 RAD51 foci
25
20
15
10
5
0
0Gy (24h)
0.5h
1h
2h
4h
6h
24h
Time after IR
No drug
ATMi


5Gy
% positive cells with >4 RAD51 foci
20
18
16
14
12
10
8
6
4
2
0
0Gy (24h)
0.5h
1h
2h
4h
6h
24h
Time after IR
No drug
ATMi


6Gy
% positive cells with >4 RAD51 foci
9
8
7
6
5
4
3
2
1
0
0Gy (24h)
0.5h
1h
2h
4h
6h
24h
Time after IR
No drug
ATMi


7Gy
% positive cells with >4 RAD51 foci
0
1
2
3
4
5
6
7
8
0Gy (24h)
0.5h
1h
2h
4h
6h
24h
Time after IR
No drug
ATMi


8Gy
% positive cells with >4 RAD51 foci
0
1
2
3
4
5
6
7
8
9
0Gy (24h)
0.5h
1h
2h
4h
6h
24h
Time after IR
No drug
ATMi


9Gy
% positive cells with >4 RAD51 foci
0
1
2
3
4
5
6
7
0Gy (24h)
0.5h
1h
2h
4h
6h
24h
Time after IR
No drug
ATMi

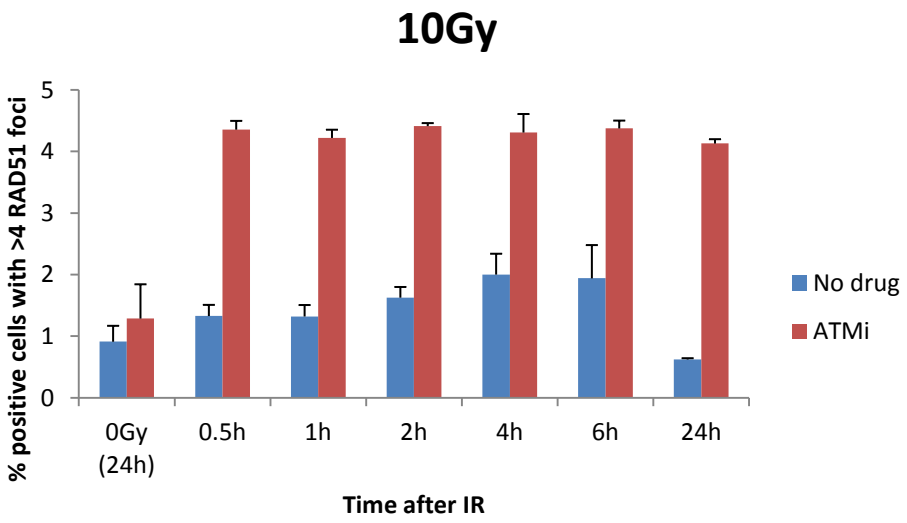


Figure 5.6: Homologous recombination repair kinetics in AA8 cells with or without ATMi during fractionated IR. Measured as percentage positive cells with >4 RAD51 foci at 0.5, 1, 2, 4, 6 and 24 h after each fraction of 1 Gy given daily over 2 weeks (with a weekend gap), to a total dose of 10 Gy. Error bars represent SEM of 3 experiments in duplicate.

5.2.3 Discussion

Our data show that the ATMi KU55933 results in significant radiosensitisation with fractionated IR with progressively impaired overall DNA DSB repair as well as HR repair. It has been shown previously that KU55933 results in higher residual γH2AX foci in glioma cells, 24 h after a 2 Gy dose of IR (Chalmers, Ruff et al. 2009). Veuger et al using the neutral comet assay in p65+/+ and p65−/− mouse embryonic fibroblasts exposed to a single fraction of 10 Gy reported a greater inhibition of DNA DSB repair at the 1 h time point compared to the 4 h and 24 h time points in both cell lines (Veuger and Durkacz 2011). We found lower levels of 53BP1 positive cells at the initial time points of 0.5, 1 and 2 h with gradual accumulation thereafter in the presence of KU55933. The WT cells always had maximum induction of 53BP1 foci at 0.5h with resolution of DNA DSB to baseline levels by 24 h after each fraction of IR, reflected in the improved clonogenic survival following fractionated IR. It has previously been demonstrated that ATM has a role in phosphorylating H2AX to γH2AX, which binds to MDC1 that mediates RNF8 recruitment of 53BP1 to DSBs. Hence, ATM inhibition may delay the recruitment of 53BP1 to radiation induced DSBs. It has also been argued previously that inhibitors of repair enzymes have a greater effect on repair than deficiency of enzyme alone and this is likely to be a result of competing for or blocking of damaged sites for other enzymes. Furthermore, as well as interfering with the access and activation of other enzymes, these protein bound termini could hinder assembly of enzyme complexes required for successful execution of NHEJ or HRR (Veuger, Curtin et al. 2003). It is therefore likely that the low levels of 53BP1 foci positive cells seen initially represent impaired formation of 53BP1 foci in the presence of KU55933 rather than more efficient repair. The persistent 53BP1 foci at later time points reflects impaired DSB repair in ATM inhibited cells.

Recent reports describe a requirement for ATM in the repair of DSBs both by NHEJ and HR pathways (Chen, Yuan et al. 1999; Morrison, Sonoda et al. 2000; Kuhne, Riballo et al. 2004; Riballo, Kuhne et al. 2004). Although ATM is known to play a major role in the slow phase of repair (HR), it responds rapidly to DNA DSBs by signalling to key effector cell cycle and DNA repair components to elicit checkpoint arrest or activation of apoptosis. Here, we demonstrate that RAD51 foci are formed normally after fractionated IR treatment with persisting RAD51 foci at later time points in the presence of ATMi. These data suggest that ATM is not required for HR in these cells and that the persisting RAD51 foci are likely to represent persisting DSBs serving as a substrate for HR. More recent data points to ATM-dependent end-processing required for a subfraction of (approx. 10%) of DSBs repaired by NHEJ induced by IR (Lobrich and Jeggo 2005). Our data demonstrating inhibition of DSB repair by KU55933 is similar to, though not as great, as the defect seen in cells deficient for NHEJ (V3-3 cells, see Chapter 4). To this end, ATM has been shown to be essential for DNA-PKcs phosphorylation following IR and this is critical for its role in DSB repair (Chen, Uematsu et al. 2007). It is possible that incomplete phosphorylation of DNA-PKcs by ATM may impair the NHEJ pathway. This provides a possible mechanism for direct involvement of ATM in NHEJ mediated DSB repair and hence the dramatic effect of KU55933 on DSB repair seen here (Chen, Uematsu et al. 2007).

Following DNA damage, ATM not only activates signalling pathways for DNA repair but also cell cycle checkpoints mainly via p53 and Chk2 thereby controlling the G1/S and G2/M checkpoints. Inhibition of these checkpoints allows damaged cells to move to the mitotic phase without undergoing proper DNA repair, leading to mitotic catastrophe, which is currently considered a main cause of cell death induced by radiotherapy (Eriksson and Stigbrand 2010; Postiglione, Chiaviello et al. 2010). It has been shown previously that CHO cells may harbour mutations in p53 that

abrogates the ability to arrest in G1 without affecting the G2 checkpoint (Lee, Larner et al 1997). Our data show that the addition of ATMi to WT cells results in loss of sparing effect of fractionated IR. The loss of cell cycle checkpoint control and redistribution into more sensitive phases of the cell cycle with each fraction of IR may account for the increased radiosensitivity as well as loss of fractionation sensitivity. This is consistent with studies of ATM deficient cells, which suffer both cell cycle checkpoint abrogation and persistent residual DSBs even after very low doses of IR and show hardly any delayed plating recovery and low dose-rate sparing (Kuhne, Riballo et al. 2004).

Precise cellular responses to DNA DSBs require efficient recognition of the damaged DNA sites and organised activation of the signalling pathways leading to DNA repair and cell cycle checkpoints. Numerous preclinical studies have shown that ATM and the MRN complex play critical roles in this response, which indicates that these molecules are promising targets for radiosensitisation. In fact, the ATM inhibitors described above have exhibited profound radiosensitising effects in preclinical studies. Our data confirms the radiosensitising effect even with fractionated IR over 3 weeks. The next step would be to test these inhibitors with radiotherapy in the clinical setting, but to our knowledge, none of them have entered clinical trials so far. One of the factors that could impede the success of ATM complex inhibitors in clinical trials is tumour selectivity. The expression and functions of the ATM complex do not appear to differ much in cancer cells and normal cells, which means that unless these inhibitors are delivered to tumours selectively, severe adverse events may occur when they are combined with radiotherapy. Recent developments in the field of drug delivery could have remarkable outcomes when combined with developments in the field of drug discovery. For example, nanomedicine has revolutionized drug delivery, and nanosized carriers such as liposomes, polymers, and micelles increase the stability of therapeutic drugs in the

bloodstream (Peer, Karp et al. 2007). Moreover, these carriers can acquire tumour-targeting potential by being equipped with antibodies or peptides that target biomarkers that are overexpressed in tumours (Majumdar, Peng et al. 2010).

5.3 DNA-PK as a Target for Radiosensitisation

The core NHEJ machinery consists of the Ku70/80 heterodimer and the catalytic subunit of DNA-dependent protein kinase (DNA-PK_{CS}), which together make the active DNA-PK, XRCC4, ligase IV, and the endonuclease artemis. Ku locates at the break first, recruiting DNA-PK_{CS} to bring about synapsis of the ends. Artemis processes the DNA ends, and the final ligation of the juxtaposed ends is accomplished by the XRCC4/ligase IV complex (Weterings and van Gent 2004; Collis, DeWeese et al. 2005). DNA-PK has been shown to phosphorylate several cellular proteins *in vivo*, including itself and the variant histone H2AX (Collis, DeWeese et al. 2005). Cells deficient in components of the NHEJ pathway are defective in DSB repair and highly sensitive to ionizing radiation and topoisomerase II poisons (Jeggo, Caldecott et al. 1989; Caldecott and Jeggo 1991; Tanaka, Yamagami et al. 1993; Gu, Jin et al. 1997; Smith and Jackson 1999; Veuger, Curtin et al. 2003). Moreover, overexpression of DNA-PK_{CS} can accelerate the repair of ionizing radiation–induced, etoposide-induced, and doxorubicin-induced DNA DSBs and confer resistance to these agents (Shen, Schultz et al. 1998; Hansen, Lundin et al. 2003). DNA-PK may also be responsible for chemoresistance and radioresistance in the clinical setting: studies have shown that DNA-PK protein expression correlates with sensitivity to etoposide in human chronic lymphocytic leukemia samples (Eriksson, Lewensoh et al. 2002). Inhibition of NHEJ is therefore an attractive approach to modulating resistance to therapeutically induced DNA DSBs.

5.3.1 Inhibitors of DNA-PK

DNA-PK is a member of the phosphatidylinositol-3 kinase (PI3K)–related protein kinase (PIKK) family of enzymes. These DNA damage-activated serine/threonine protein kinases include DNA-PK, ATM, and ATR (Durocher and Jackson 2001). Inhibitors of PI3K, such as wortmannin and LY294002, also inhibit DNA-PK in a noncompetitive and competitive manner, respectively. Both wortmannin and LY294002 have been reported to retard DSB repair and enhance the cytotoxicity of ionizing radiation and etoposide, which has largely been attributed to inhibition of DNA-PK_{CS} (Boulton, Kyle et al. 1996; Rosenzweig, Youmell et al. 1997). Using LY294002 as a lead, a more potent and specific inhibitor of DNA-PK_{CS}, NU7026 (2-(morpholin-4-yl)-benzo[h]chromen-4-one), was developed, which also increased the cytotoxicity of both ionizing radiation and topoisomerase II poisons and retarded DSB repair (Veuger, Curtin et al. 2003; Willmore, de Caux et al. 2004). NU7026 has been shown to be selective for DNA-PK (IC_{50} of 0.23 µM) with a 60-fold greater potency against this enzyme than PI 3-K and inactive against both ATM and ATR (Kurimasa, Kumano et al. 1999; Veuger, Curtin et al. 2003). NU7026 at 10 µM completely inhibited purified DNA-PK activity, while having no effect on PARP-1 activity (Veuger, Curtin et al. 2003). We therefore wanted to study the effects of DNA-PK inhibition with NU7026 in the context of fractionated irradiation as it is delivered in the clinical setting and study DNA DSB repair kinetics with each fraction.

5.3.2 Results

5.3.2.1 Western blot testing the DNA-PK inhibitor NU7026 (KU51777)

To determine DNA-PK activity and inhibition in intact wild type CHO cells (AA8), we measured DNA-PK- specific autophosphorylation at serine 2056 in response to IR by western blot analysis. Autophosphorylation at serine 2056 is considered the most

robust and specific target of DNA-PK activity (Uematsu, Weterings et al. 2007). Using an anti-DNA-PKcs (phospho S2056) antibody, we confirmed that DNA-PKcs is rapidly phosphorylated at this residue in response to 10 Gy IR. In the presence of the DNA-PK inhibitor NU7026 at 10 μM (added 60 minutes prior to IR) this autophosphorylation is significantly reduced after IR, although the band at 460kDA does not completely disappear **(Figure 5.7).** At this concentration NU7026 has previously shown complete inhibition of DNA-PK activity in purified enzyme assays and maximum potentiation of IR (Veuger, Curtin et al. 2003; Bryant and Helleday 2006). Hence 10 μM was used for all experiments below.

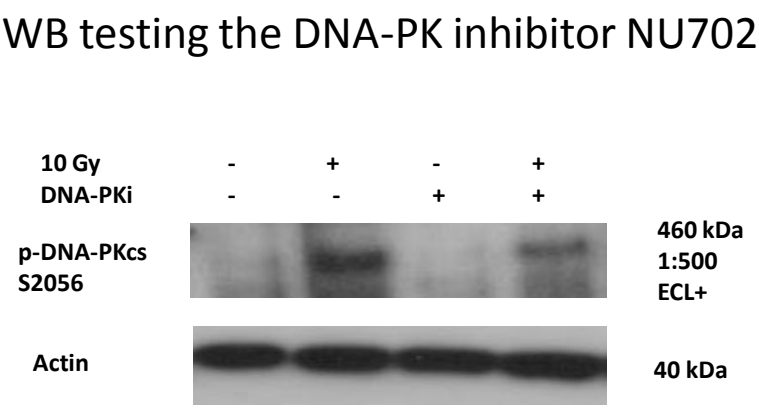


Figure 5.7: Western Blot testing the DNA-PK inhibitor NU7026. The DNA-PK inhibitor NU7026 at 10 μM concentration for 1 h significantly reduces the phosphorylation of DNA-PKcs at serine 2056 in response to 10 Gy of irradiation in wild type CHO cells.

5.3.2.2 Clonogenic cell survival following radiation in wild type CHO cells (AA8) with or without DNAPKcs inhibitor

5.3.2.2.1 Single radiation dose clonogenic survival curves

It has been shown previously that NU7026 increases ionising radiation-induced cytotoxicity as studied by single dose in vitro clonogenic assays in DNA-PK proficient V3 CHO cells (V3YAC -transfected with human DNA-PKcs gene) but has no effect in V3 cells defective in DNA-PKcs gene (Veuger, Curtin et al. 2003). It was found to maximally potentiate radiation-induced cell killing at a concentration of 10 μM and hence was used at this dose in our experiments. At concentrations < 50 μM the drug alone does not reduce clonogenic survival (Veuger, Curtin et al. 2003). We found that NU7026 sensitises AA8 cells to the effect of ionising radiation at higher doses **(Figure 5.8)**. The sensitiser enhancement ratio at 4 and 8 Gy was 1.6 and 2.4 respectively. On comparing the radiation response with the V3-3 cells (DNA-PKcs defective) we found that the genetically mutant cell line was significantly more radiosensitive compared to DNA-PK inhibited wild type cells.

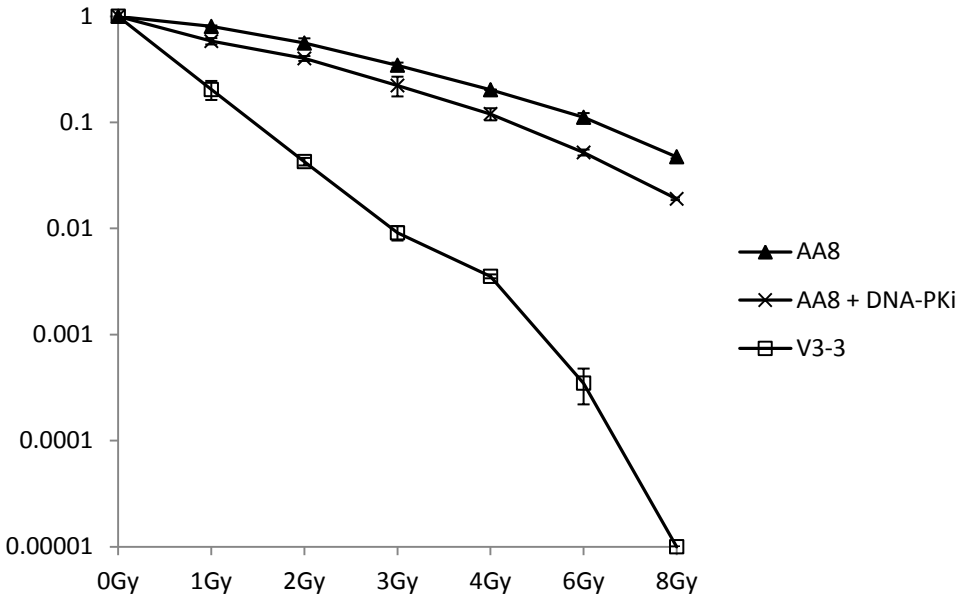


Figure 5.8: Acute dose clonogenic survival curves (semi-log) comparing WT AA8 cells with or without the DNA-PKi (NU7026) and NHEJ mutant V3-3 cells at doses of 0, 1, 2, 3, 4, 6 and 8 Gy. Error bars show SEM of 3 repeats in triplicate.

5.3.2.2.2 Fractionated irradiation clonogenic survival curves – 1 Gy/day

As clinical radiotherapy is given in small fractional doses each day (usually 1.8-2 Gy per day) over several weeks with a gap over the weekend, we wanted to test the effect of adding a DNA-PKi to fractionated IR. We tested 1 Gy/day given from Monday to Friday for 3 weeks to a total dose of 16 Gy. Surprisingly we found no radiosensitisation with the addition of NU7026 to AA8 cells during the first week of IR as seen in **Figure 5.9.** During the second week there was some decreased clonogenic survival, with further sensitisation during the third week of IR. Although all media and washings were saved and added to the final trypsinised pellet, it is possible that some loss of non-viable cells contributed to higher survival despite the presence of the drug. As with acute dose survival curves, radiosensitivity was significantly greater in the genetically deficient NHEJ mutant compared to the DNA-PK inhibited WT cells.

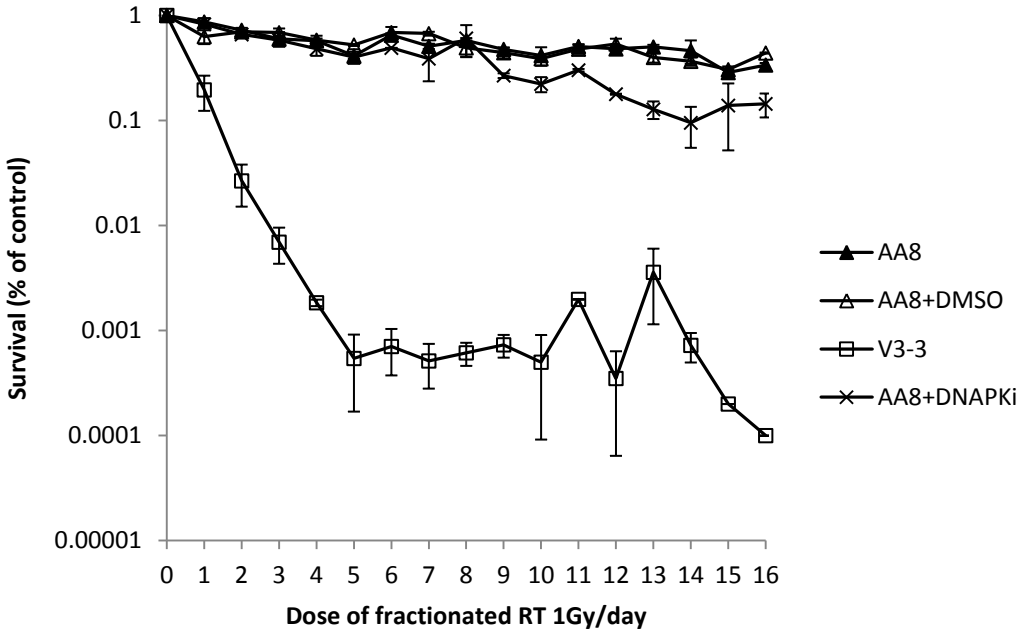


Figure 5.9: Fractionated IR clonogenic survival curves testing 1 Gy/day in WT AA8 cells with or without the DNA-PKi (NU7026) and NHEJ mutant V3-3 cells. 1 Gy given daily Monday to Friday with weekend breaks to a total of 16 Gy. Error bars show SEM of 3 repeats in triplicate.

5.3.2.3 Sensitivity to changes in dose per fraction as measured by clonogenic survival in AA8 cells with or without DNA-PKi

In order to see if addition of DNA-PKi altered the fraction size sensitivity of the WT cell line, we compared survival following 2 Gy as a single fraction (high dose per fraction) versus 2 fractions of 1 Gy each (low dose per fraction) and 1x3 Gy versus 3x1 Gy **(Figure 5.10)**. We found that the addition of DNA-PKi to AA8 maintained the sparing effect of fractionation seen in these wild type cells. For example there was a 2.7 and 2.8 fold decrease in survival following 4 GyX1 versus 1 Gyx4 in AA8 cells with or without DNA-PKi respectively. This is in contrast to our earlier finding (in Chapter 4) that the genetically NHEJ deficient V3-3 cells show no sparing effect from fractionation **(Figure 4.3 and Figure 5.10)**.

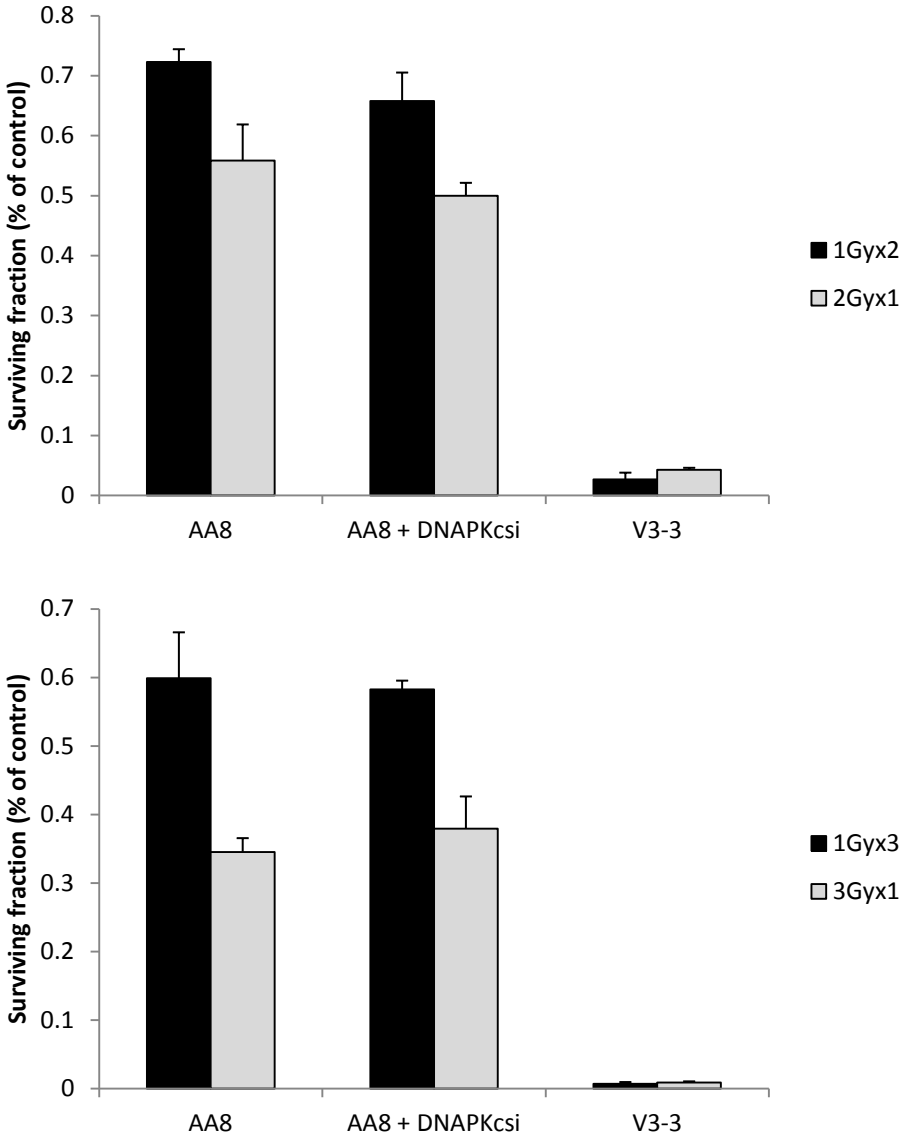
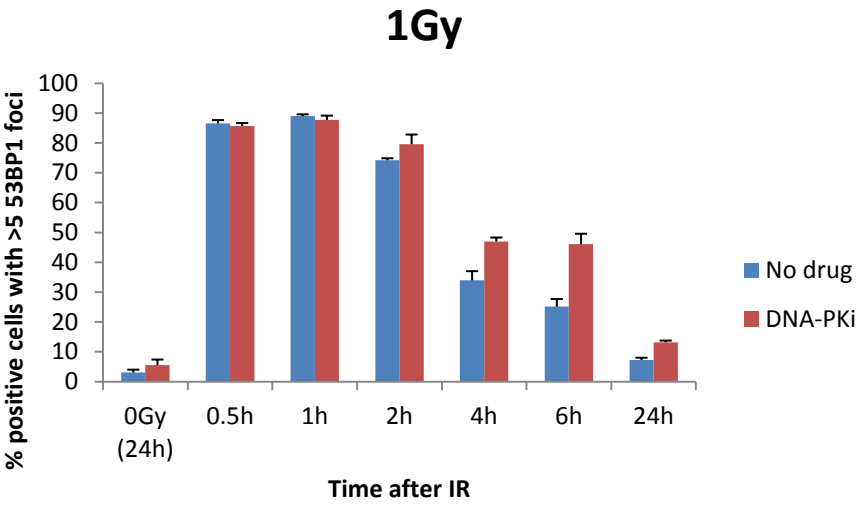
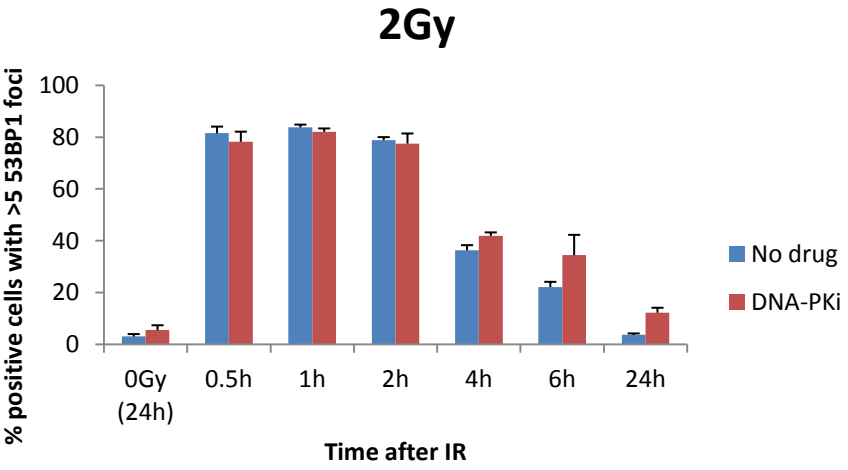


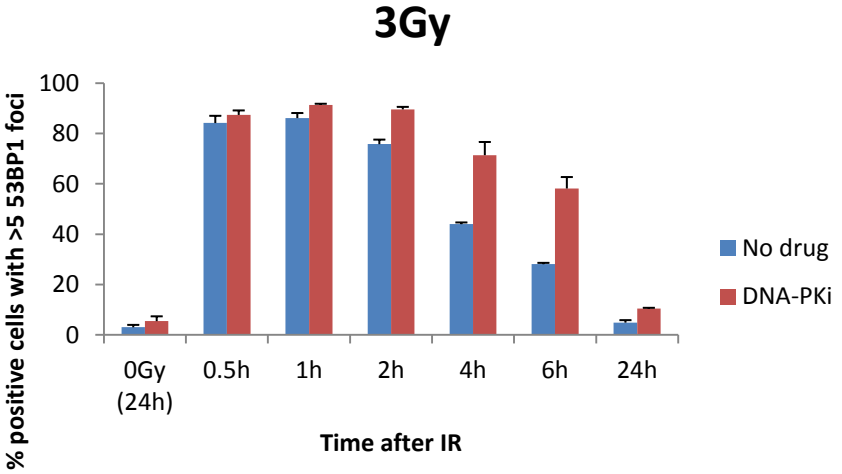
Figure 5.10: Comparison of survival between high dose per fraction vs low dose per fraction with or without DNA-PKi (NU7026). A & B. The WT AA8 cells show increased sensitivity to higher dose per fraction even with the addition of DNA-PKi, when comparing 2 Gy as a single fraction vs 2 fractions of 1 Gy or 3 Gyx1 fraction vs 1 Gyx3 fractions. This is in contrast to the response of the NHEJ mutant cell line which shows no sparing effect from smaller fractions (Chapter 4). Error bars show SEM of 3 repeats in triplicate.

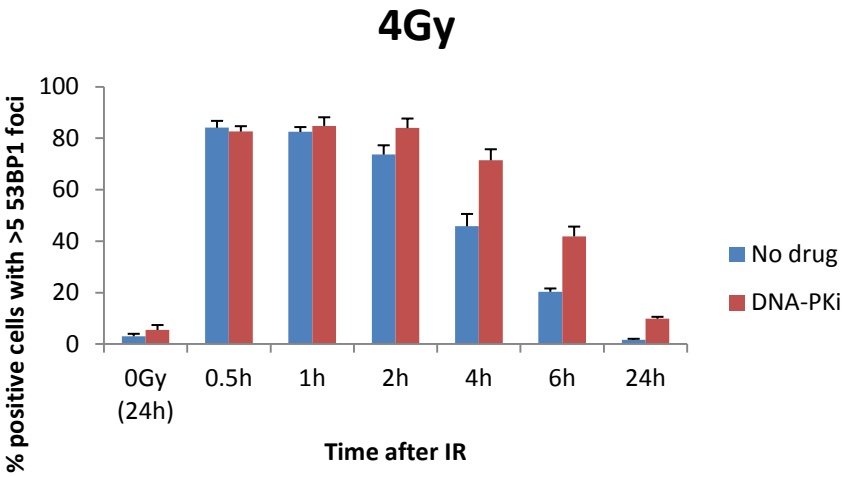
5.3.2.4 DNA DSB repair kinetics during fractionated IR in AA8 cells with or without DNA-PKi

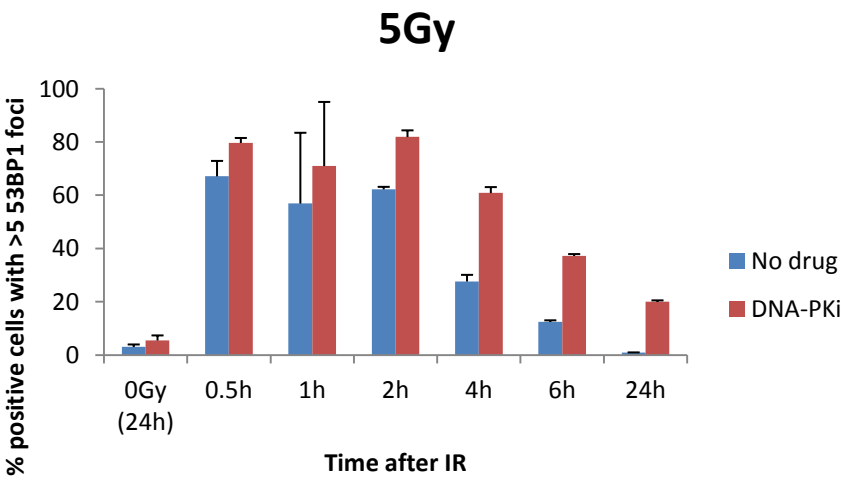
It has been shown previously that NU7026 inhibits DNA DSB repair using the neutral elution assay in NHEJ competent cells albeit at supralethal doses of 75 Gy (Veuger, Curtin et al. 2003; Veuger, Hunter et al. 2009). No additional inhibitory effect was seen when the drug was added to the genetically DNA-PK defective V3 cells. We wanted to study DSB repair kinetics using 53BP1 foci analysis at various time points (0.5, 1, 2, 4, 6 and 24 hours) after each daily 1 Gy fraction of IR to a total dose of 10 Gy over 2 weeks with or without the DNA-PKi **(Figure 5.11).** The 96 well plate format was used as described earlier and percentage of cells with >5 53BP1 foci were analysed as positive. Initially there was no increase in 53BP1 foci induction at 0.5 and 1 h with the addition of DNA-PKi during the first week of irradiation. Although resolution of 53BP1 foci at 24 h was impaired towards the end of the first week, there was a significant increase in the number of 53BP1 foci at all time points in the second week of IR with the addition of DNA-PKi **(Figure 5.11)**.

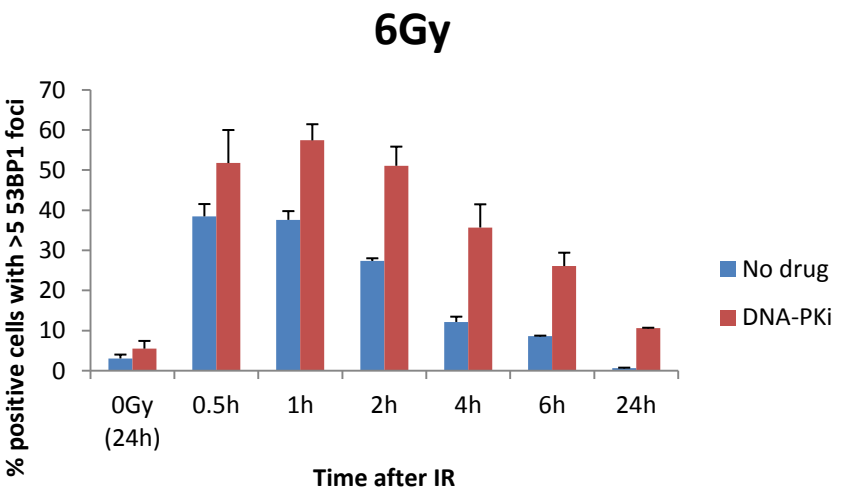

1Gy
% positive cells with >5 53BP1 foci
100
90
80
70
60
50
40
30
20
10
0
0Gy (24h)
0.5h
1h
2h
4h
6h
24h
Time after IR
No drug
DNA-PKi

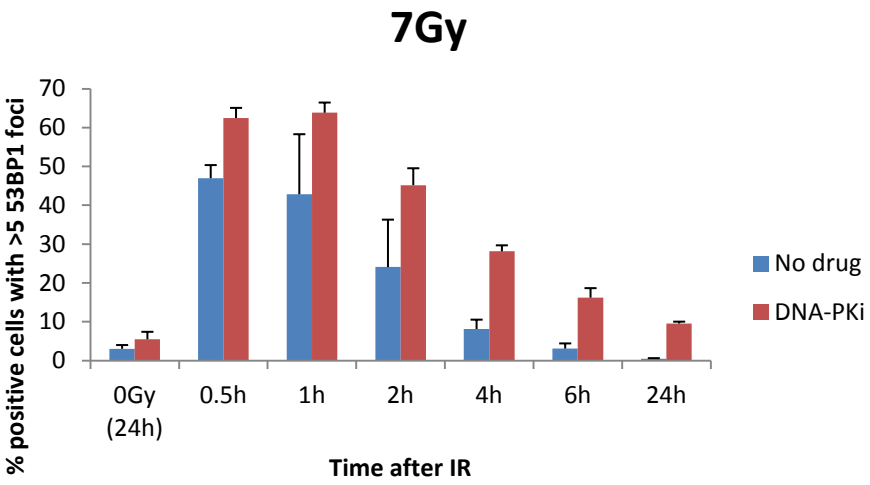

2Gy
% positive cells with >5 53BP1 foci
100
80
60
40
20
0
0Gy (24h)
0.5h
1h
2h
4h
6h
24h
Time after IR
No drug
DNA-PKi

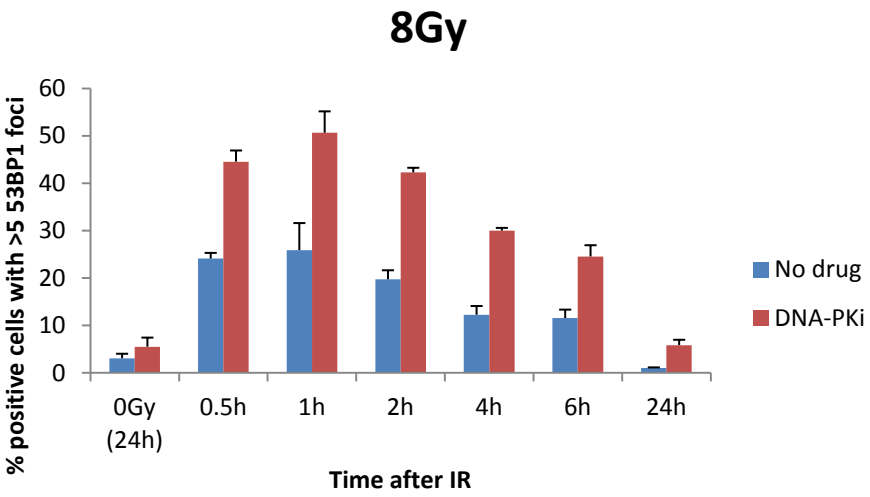

3Gy
% positive cells with >5 53BP1 foci
100
80
60
40
20
0
0Gy (24h)
0.5h
1h
2h
4h
6h
24h
Time after IR
No drug
DNA-PKi

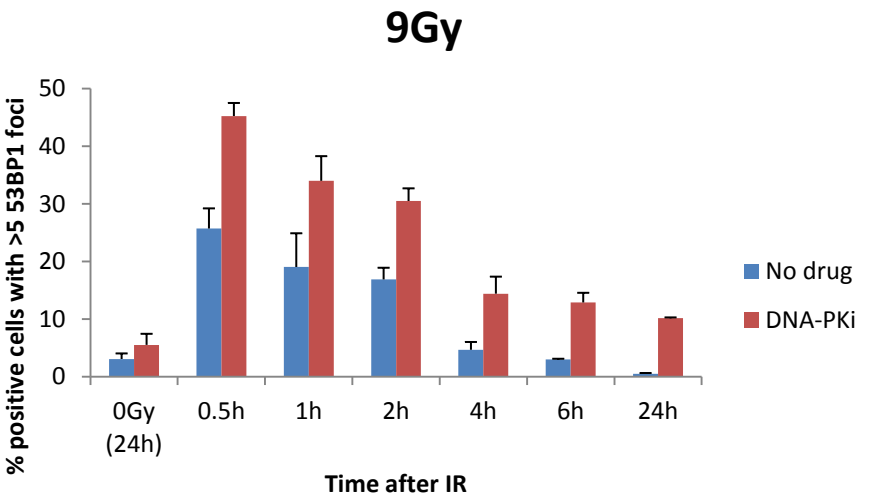

4Gy
% positive cells with >5 53BP1 foci
100
80
60
40
20
0
0Gy (24h)
0.5h
1h
2h
4h
6h
24h
Time after IR
No drug
DNA-PKi


5Gy
% positive cells with >5 53BP1 foci
100
80
60
40
20
0
0Gy (24h)
0.5h
1h
2h
4h
6h
24h
Time after IR
No drug
DNA-PKi


6Gy
% positive cells with >5 53BP1 foci
70
60
50
40
30
20
10
0
0Gy (24h)
0.5h
1h
2h
4h
6h
24h
Time after IR
No drug
DNA-PKi


7Gy
% positive cells with >5 53BP1 foci
70
60
50
40
30
20
10
0
0Gy (24h)
0.5h
1h
2h
4h
6h
24h
Time after IR
No drug
DNA-PKi


8Gy
% positive cells with >5 53BP1 foci
60
50
40
30
20
10
0
0Gy (24h)
0.5h
1h
2h
4h
6h
24h
Time after IR
No drug
DNA-PKi


9Gy
% positive cells with >5 53BP1 foci
50
40
30
20
10
0
0Gy (24h)
0.5h
1h
2h
4h
6h
24h
Time after IR
No drug
DNA-PKi

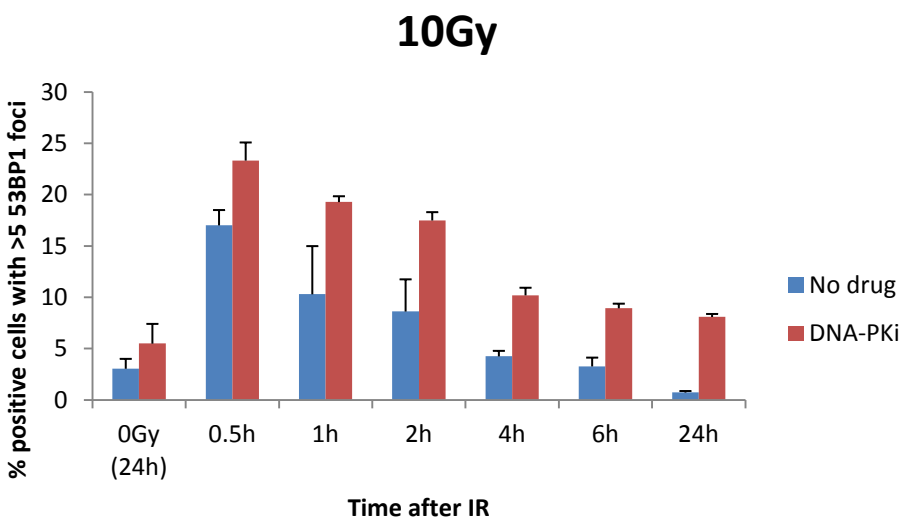
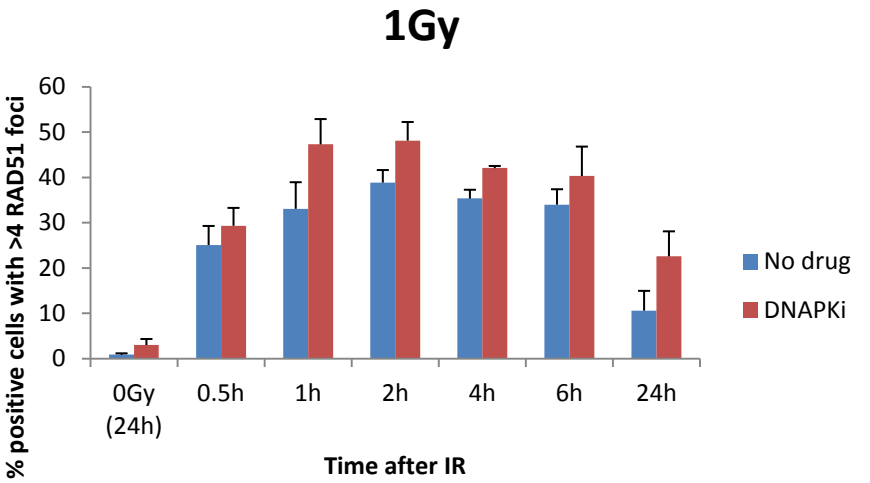
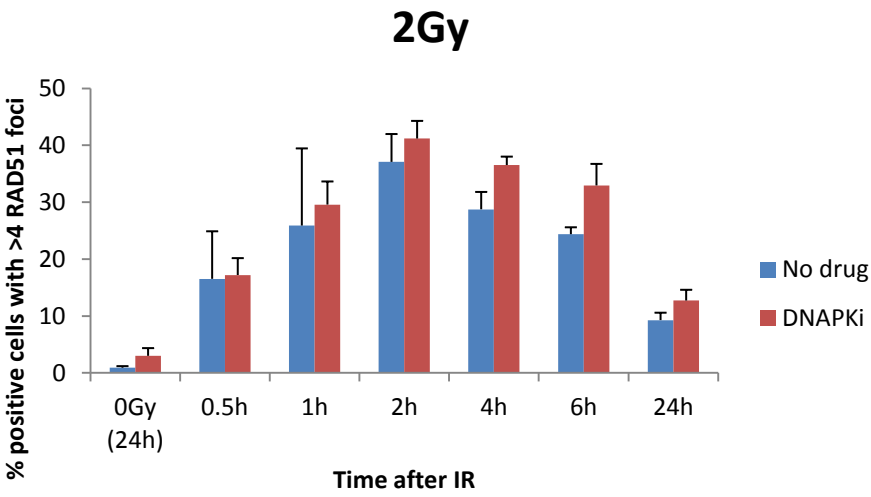


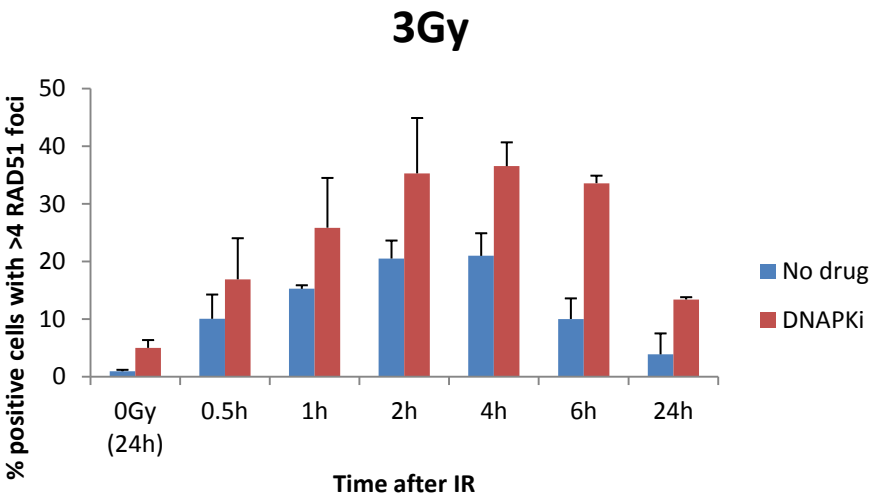
Figure 5.11: DNA DSB repair kinetics using 53BP1 foci analysis during fractionated IR in AA8 cells with or without DNA-PKi (NU7026). Measured as percentage positive cells with >5 53BP1 foci at 0.5, 1, 2, 4, 6 and 24 h after each fraction of 1 Gy given daily over 2 weeks (with a weekend gap), to a total dose of 10 Gy. Error bars represent SEM of 3 experiments in duplicate.

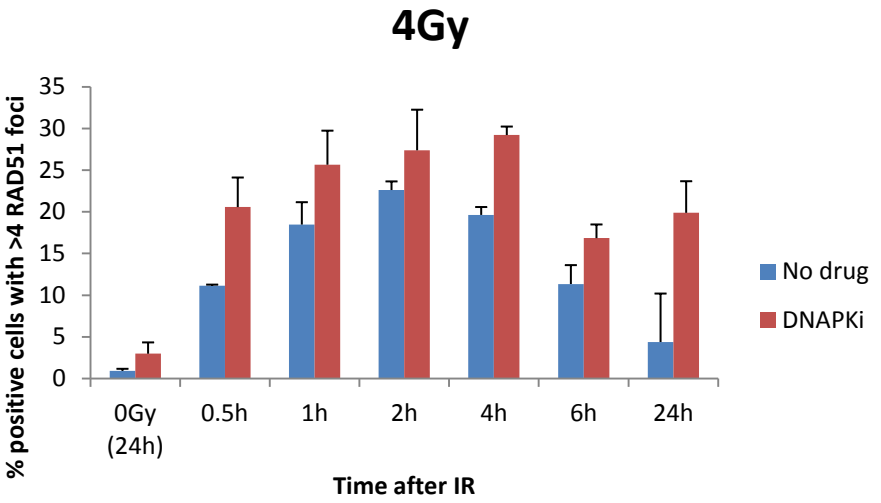
5.3.2.5 Homologous recombination repair kinetics in AA8 cells with or without DNAPKcsi during fractionated IR

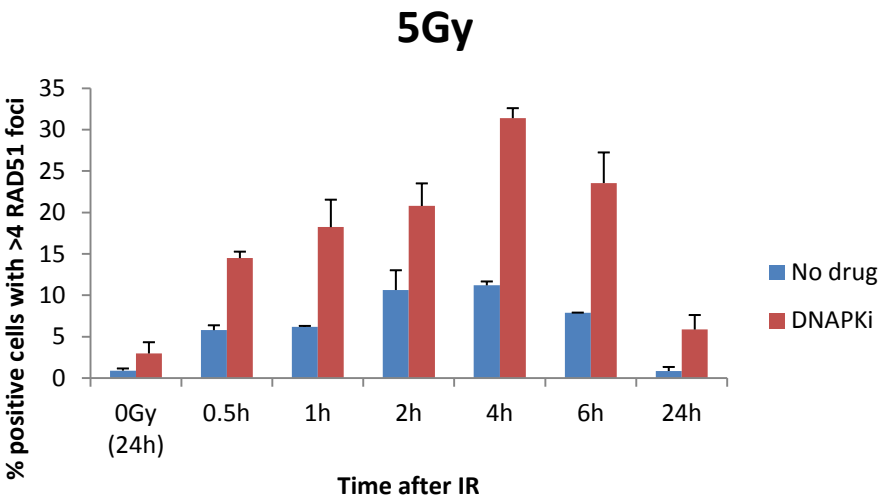
To study the effect of NU7026 on HR repair we analysed RAD51 foci levels at various time points (0.5, 1, 2, 4, 6 and 24 hours) after each daily 1 Gy fraction of IR to a total dose of 10 Gy with or without the DNA-PKi **(Figure 5.6).** During HR, the protein RAD51 forms a nucleoprotein filament that facilitates strand invasion, and therefore detection of RAD51 foci can be used to evaluate HR activity. We found higher levels of RAD51 positive cells at all time points after IR with the addition of the DNA-PKi inhibitor compared to wild type cells alone. The peak induction of RAD51 foci was usually seen at the 2 h time point in WT cells, and this was similar in the presence of the drug.

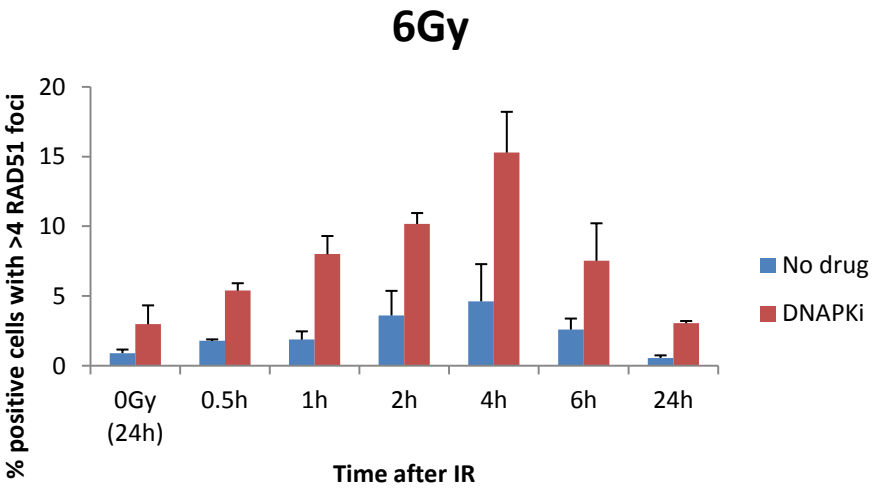

1Gy
% positive cells with >4 RAD51 foci
60
50
40
30
20
10
0
0Gy (24h)
0.5h
1h
2h
4h
6h
24h
Time after IR
No drug
DNAPKi

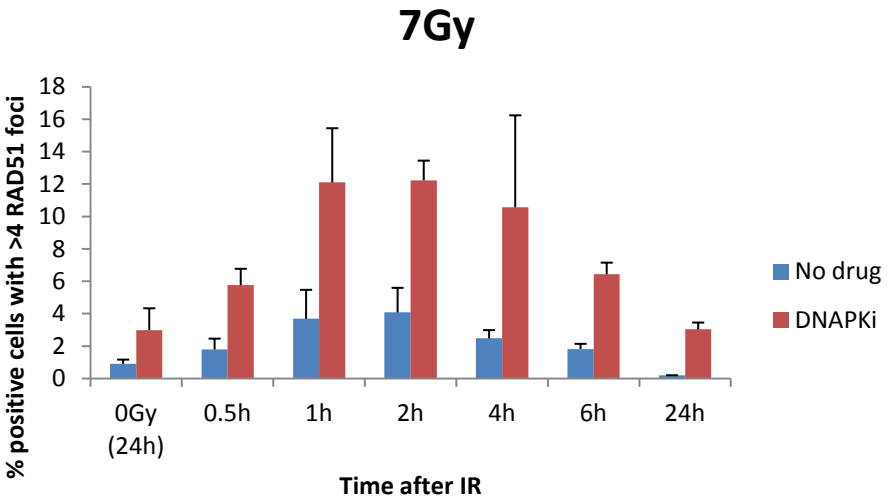

2Gy
% positive cells with >4 RAD51 foci
50
40
30
20
10
0
0Gy (24h)
0.5h
1h
2h
4h
6h
24h
Time after IR
No drug
DNAPKi

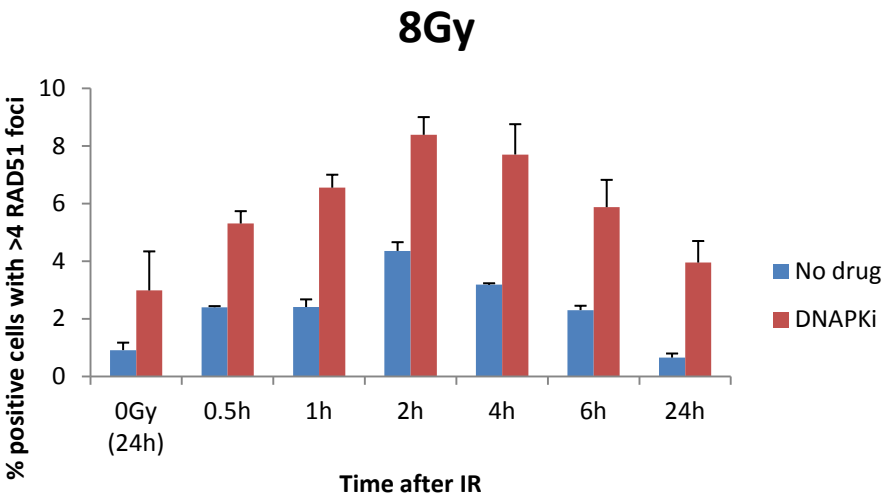

3Gy
% positive cells with >4 RAD51 foci
50
40
30
20
10
0
0Gy (24h)
0.5h
1h
2h
4h
6h
24h
Time after IR
No drug
DNAPKi

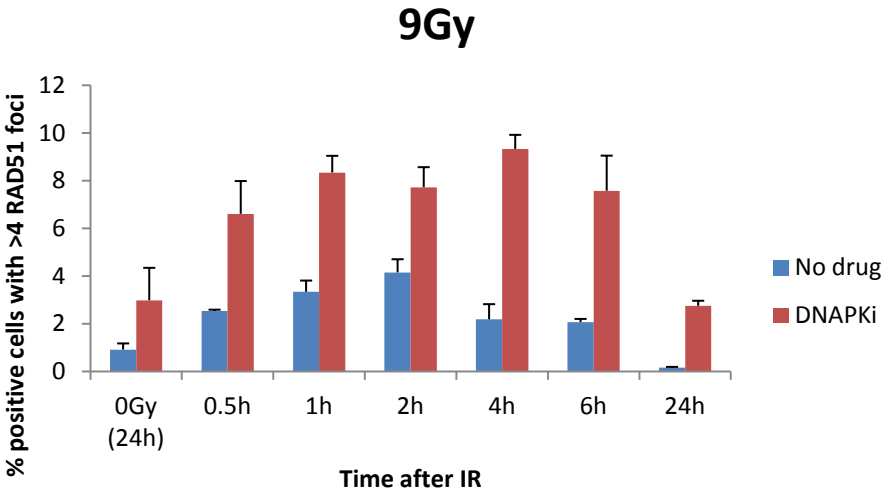

4Gy
% positive cells with >4 RAD51 foci
35
30
25
20
15
10
5
0
0Gy (24h)
0.5h
1h
2h
4h
6h
24h
Time after IR
No drug
DNAPKi


5Gy
% positive cells with >4 RAD51 foci
35
30
25
20
15
10
5
0
0Gy (24h)
0.5h
1h
2h
4h
6h
24h
Time after IR
No drug
DNAPKi


6Gy
% positive cells with >4 RAD51 foci
20
15
10
5
0
0Gy (24h)
0.5h
1h
2h
4h
6h
24h
Time after IR
No drug
DNAPKi


7Gy
% positive cells with >4 RAD51 foci
18
16
14
12
10
8
6
4
2
0
0Gy (24h)
0.5h
1h
2h
4h
6h
24h
Time after IR
No drug
DNAPKi


8Gy
% positive cells with >4 RAD51 foci
10
8
6
4
2
0
0Gy (24h)
0.5h
1h
2h
4h
6h
24h
Time after IR
No drug
DNAPKi


9Gy
% positive cells with >4 RAD51 foci
12
10
8
6
4
2
0
0Gy (24h)
0.5h
1h
2h
4h
6h
24h
Time after IR
No drug
DNAPKi

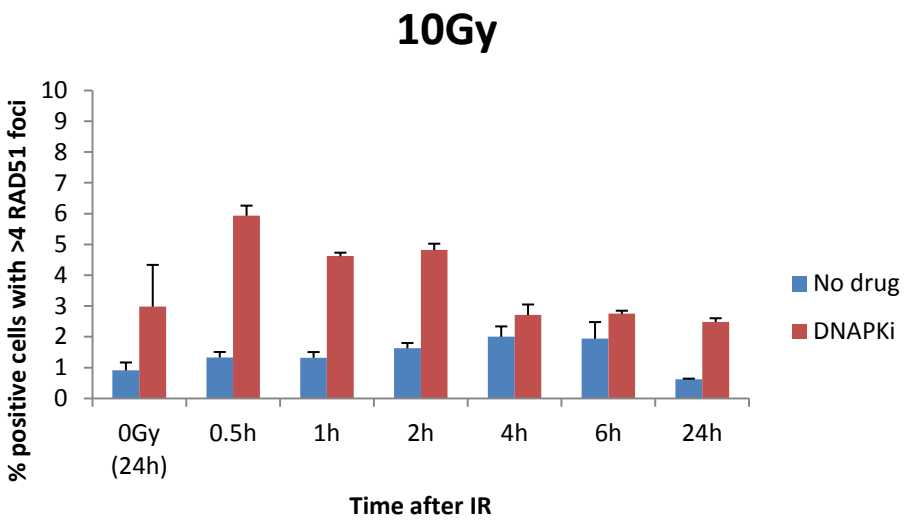


Figure 5.12: Homologous recombination repair kinetics in AA8 cells with or without DNAPKi (NU7026) during fractionated IR. Measured as percentage positive cells with >4 RAD51 foci at 0.5, 1, 2, 4, 6 and 24 h after each fraction of 1 Gy given daily over 2 weeks (with a weekend gap), to a total dose of 10 Gy. Error bars represent SEM of 3 experiments in duplicate.

5.3.3 Discussion

Our data suggests that the DNA-PK inhibitor NU7026 does not decrease clonogenic survival during fractionated daily IR (1 Gy/day) during the first week of irradiation when added to WT CHO cells **(Figure 5.9)**. Radiosensitisation is seen during the second week of treatment with NU7026, but this is not as dramatic as the radiosensitivity of the genetically DNA-PK deficient V3-3 cells. We also found that the addition of DNA-PKi to AA8 maintained the sparing effect of fractionation seen in these wild type cells in contrast to our earlier finding that the genetically NHEJ deficient CHO cells show no sparing effect from fractionation **(Figure 4.3 and Figure 5.10)**. It is likely that NU7026 only causes partial inhibition of enzyme and 100% inhibition maybe required for equivalent effect. In any case, only inhibiting the enzymatic activity as opposed to removing DNA-PK may have very different effects as the inhibited DNA-PK protein will bind DNA ends, potentially stabilising them. Similar findings of reduced radiosensitivity have been observed in other isogenic cells proficient in DNA-PK (M059-Fus1) when treated with a DNA-PK inhibitor compared to their genetically deficient counterparts (M059 J) (Tavecchio, Munck et al. 2012). It has been previously shown that NU7026 completely inhibits DNA-PK activity in purified enzyme assays (Veuger, Curtin et al. 2003; Bryant and Helleday 2006) but when we measured activity in intact wild type CHO cells (AA8), we found only partial inhibition of DNA-PK- specific autophosphorylation at serine 2056 in response to IR by western blot analysis. It should also be mentioned that the phospho-specific antibody to DNA-PK has been reported to cross react with other sites. Another important consideration maybe the minimum exposure to drug required for a radiosensitisation effect. Nutley et al when investigating the preclinical pharmacokinetics and metabolism of NU7026 have shown that at least a 4 h exposure at 10 μM is required to see a radiosensitisation effect in CH1 human ovarian carcinoma cell line (Nutley, Smith et al. 2005). In fact a 24 h exposure prior

to IR produced an even greater effect (Veuger, Curtin et al. 2003; Nutley, Smith et al. 2005). They postulated that this requirement may be dependent on the kinetics of cellular uptake of the drug, the k_{on} and k_{off} of the inhibitor as well as the kinetics of DSB repair. This may have relevance to our findings in that radiosensitisation increased with longer duration of exposure to drug during the second week of fractionated IR and was not seen earlier.

We then wanted to see if the results from the clonogenic survival experiments were reflected in the DNA DSB repair kinetics. It has been shown previously that NU7026 inhibits DNA DSB repair using the neutral elution assay in NHEJ competent cells albeit at supralethal doses of 75 Gy (Veuger, Curtin et al. 2003; Veuger, Hunter et al. 2009). In the DNA-PK complemented V3 cells (V3YAC), NU7026 was shown to inhibit DSB repair by 56% at 60 minutes post IR compared with the drug free control. No additional inhibitory effect was seen when the drug was added to the genetically DNA-PK defective V3 cells. At 24 hours after IR these authors showed that 96% of DSBs were rejoined in the V3YAC cells compared with 60% when treated with the DNA-PKi (Veuger, Curtin et al. 2003). In our experiments there was no difference in 53BP1 foci levels at 0.5, 1 and 2 h with the addition of DNA-PKi during the first week of irradiation (1 Gy/day) **(Figure 5.11)**. This may explain the findings of the clonogenic survival assays in that we found no radiosensitisation with the addition of NU7026 during the first week. However, there was a significant increase in the number of 53BP1 foci at all time points in the second week of IR with the addition of DNA-PKi which correlates with the increased radiosensitivity seen later.

We postulated that when DNA-PK was defective or inhibited, cells would be more reliant on HR for DNA DSB repair. This hypothesis is supported by published

observation of higher levels of both DSB-induced and spontaneous HR in DNA-PK defective cells (Allen, Kurimasa et al. 2002; Delacote, Han et al. 2002; Shrivastav, Miller et al. 2009). A number of lines of evidence also indicate that although DNA-PKcs highly stimulates the NHEJ pathway, in its absence, a slower repair pathway still operates (DiBiase, Zeng et al. 2000; Ferguson, Sekiguchi et al. 2000). The slower component of repair is probably mediated by DNA-PKcs-independent NHEJ but may also involve HRR, which requires a complex of DNA repair proteins, including RAD51, BRCA1, BRCA2, XRCC2, and ATM (Jackson 2002). In keeping with this, we found higher levels of RAD51 positive cells at all time points after IR with the addition of NU7026 compared to wild type cells alone **(Figure 5.12)**. Interestingly, other authors have reported lower IR-induced RAD51 foci in the presence of a DNA-PKi (NU7441) in the glioblastoma cell line M059-Fus-1 (transfected with DNA-PK gene) (Tavecchio, Munck et al. 2012). However, they also noted lower basal RAD51 levels in the isogenic DNA-PK deficient M059 J cells, with no induction by IR or change with NU7441. This may be due to lower ATM activity in these cell lines or reflect co-operation between DNA-PK and ATM for HR action. In any case, inhibited DNA-PK is likely to have very different effect to lost DNA-PK. It has been suggested that inhibition of DNA-PK blocks the enzyme onto the DSB and the overall effect on HR appears to differ depending on which of the >40 phosphorylation sites on DNA-PK are affected (Neal, Dang et al. 2011). Hence, it is important to understand how inhibition will affect HR.

Recently newer and more potent inhibitors of DNA-PK have been identified and characterised such as NU7441 (Leahy, Golding et al. 2004; Zhao, Thomas et al. 2006; Tavecchio, Munck et al. 2012). NU7441 (2-N-morpholino-8-dibenzothiophenyl-chromen-4-one) is a potent (IC_{50} = 12 nM) ATP-competitive DNAPK inhibitor developed from the PI3 K inhibitor LY294002. It has been shown to

cause increased cytotoxicity with IR and etoposide in DNA-PK proficient versus deficient cell lines. NU7441 substantially retarded the repair of IR induced DSBs and increased G2 accumulation induced by IR after a single fraction of 2 or 4 Gy (Zhao, Thomas et al. 2006; Tavecchio, Munck et al. 2012). In the glioblastoma cell line M059-Fus-1 (transfected with DNA-PK gene) NU7441 delayed the peak of γH2AX focus formation and their disappearance after 4 Gy, with 32% of the foci remaining at 24 h (Zhao, Thomas et al. 2006; Tavecchio, Munck et al. 2012). Shaheen et al have also shown that targeting the DNA repair machinery by a combination of the ATMi KU55933 and DNA-PKi NU7441 further enhances chemo- and radiosensitivity in prostate cancer cells by increasing cell death, alteration of cell cycle profile and DNA DSBs (Shaheen, Znojek et al. 2011). Clearly these molecules show immense promise and need to be evaluated further in the context of fractionated RT (including animal models) before moving towards clinical trials. However, one must bear in mind the implications for normal tissue toxicity when combining a DNA-PKi with RT as NHEJ remains the most important pathway for repair of radiation induced DNA damage in normal tissues as well as perhaps tumours.

5.4 PARP as a target for radiosensitisation

5.4.1 PARP-1 and DNA repair

PARP-1 is a 113 kDa nuclear metalloenzyme and was the first identified member of the PARP superfamily which currently contains 18 proteins (Schreiber, Dantzer et al. 2006). PARP-1 and its structural homologues, PARP-2 and PARP-3, are the only members that actively participate in DNA repair. The signature β–α–loop-β–α NAD+ fold is variably conserved among the PARP members which play important roles in DNA repair, transcription, mitotic segregation, telomere homeostasis and cell death (Mortusewicz, Ame et al. 2007). PARP-1 binds to DNA via zinc fingers contained within the DNA binding domain to catalyze the polymerisation of APD-ribose from NAD+ on target proteins, a process known as poly(ADP-ribosyl)ation. Once PARP-1 is hyper(ADP-ribosyl)ated it is highly negatively charged causing it to be repulsed by DNA and hence inactivated. The polymer is rapidly degraded with a half-life less than 10 min and poly(ADP-ribose) glycohydrolase (PARG) hydrolyses the polymers present on PARP which is subsequently recycled (Davidovic, Vodenicharov et al. 2001). This ‘‘PARP cycling” allows access of DNA repair enzymes to the DNA strand breaks in order to facilitate their repair (Smulson, Istock et al. 1994).

The most well-characterised role for PARP-1 is in sensing single-strand DNA breaks (SSB) to which it binds via the two zinc fingers located at its NH_2-terminus (Benjamin and Gill 1980). This binding facilitates dimerisation of PARP-1 which in turn leads to polymerisation of linear or branched chains of poly(ADP-ribose) onto its targets, enabling it to perform a pivotal role in DNA damage repair. Thousands of SSB occur each hour and if left unrepaired can develop into potentially lethal DSBs due to collapse of DNA replication forks during S phase of the cell cycle. Most SSB are repaired by a rapid and efficient global SSB repair process which involves binding of PARP-1 to damaged DNA and the resultant poly(ADP-ribosyl)ation

(Caldecott 2003). In addition, PARP-1 is thought to recruit repair proteins such as the molecular scaffold protein, X-ray repair cross complementing group 1 (XRCC1) which is involved in BER. The next step is to remove the damaged termini of the DNA backbone in order to facilitate restoration of 3'-hydroxy and 5'-phosphate end groups which can act as primers for DNA polymerases. Usually a single nucleotide is lost at the site of SSB and this is replaced by gap filling by DNA polymerase-β and the process is known as short patch repair (Dianov, Price et al. 1992). The final step in repairing SSB is performed by DNA ligase III which seals the gap in the DNA strand and this too is bound and stabilised by XRCC1 thus providing a physical link with DNA polymerase-β. A smaller proportion of SSB repair involves insertion of multiple nucleotides (long patch repair), a process thought to occur during S phase of the cell cycle as many of the required enzymes are core components of the replication machinery, although DNA polymerase-β and hence PARP-1 have been implicated in this process (Caldecott 2008).

5.4.1.1 PARP inhibition as a therapeutic strategy

The recent upsurge in interest in PARP inhibitors has stemmed from the discovery that breast cancer associated (BRCA) protein 1 and 2 deficient cells are extremely sensitive to PARP inhibition (Bryant, Schultz et al. 2005; Farmer, McCabe et al. 2005). BRCA-1 and -2 are breast cancer susceptibility proteins which are involved in the repair of DSBs by homologous recombination (HR). Cells which lack BRCA proteins are forced to repair defects by more error prone pathways which in turn lead to genomic instability (Tutt, Bertwistle et al. 2001). PARP inhibition impairs the repair of SSB which, as a result, are converted to DSB during replication and this, in turn, increases the burden for repair by HR. In BRCA-deficient cells, which are defective in HR, the damage cannot be repaired and consequently cell cycle arrest, chromosome instability and cell death results (synthetic lethality). Proof-of-principle

for this therapeutic action of PARP inhibitors has recently been demonstrated with phase 1 and 2 trials with olaparib (a novel orally active PARP inhibitor) in BRCA-1 and -2-associated familial cancers (Fong, Boss et al. 2009; Audeh, Carmichael et al. 2010).

5.4.1.2 PARP inhibitors as radiosensitisers

Several PARP inhibitors have been identified and refined over time to become more specific and effective (Calvert and Azzariti 2011). The majority of PARP inhibitors are derived from the benzamide structure and act by competitively inhibiting the catalytic domain of the PARP enzyme. Despite the newer generation of PARP inhibitors being more specific for the PARP family, it is likely that they inhibit both PARP-1 and PARP-2 due to the similarity in the structure of their catalytic domains. As PARP-1 has been specifically shown to bind DNA strand breaks formed by ionizing radiation to facilitate repair, it as an attractive target for radiation enhancement (Powell, Mikropoulos et al. 2010).

Several authors have shown that PARP inhibitors are radiosensitising agents in vitro using single or a few split doses of radiation in rodent and human tumour cell lines (Little, Ueno et al. 1989; Utsumi and Elkind 1994; Brock, Milas et al. 2004; Chalmers, Johnston et al. 2004; Dungey, Loser et al. 2008). Data also exists for potential radiosensitisation in mouse xenograft models showing up to 2-fold tumour growth delay with the addition of a PARPi to radiation (Calabrese, Almassy et al. 2004; Russo, Kwon et al. 2009).

AG14699 {8-Fluoro-2-(4-methylaminomethyl-phenyl)-1,3,4,5-tetrahydro-azepino (5,4,3-cd)indol-6-one phosphate} also known as Rucaparib was the first PARPi to enter clinical trials (Thomas, Calabrese et al. 2007; Plummer, Jones et al. 2008; Ali,

Telfer et al. 2009). It was identified by Thomas *et al* as a potent PARP-1 inhibitor (Ki=1.4 nM) with potential chemosensitising, radiosensitising and antineoplastic activities (Thomas, Calabrese et al. 2007; Plummer, Jones et al. 2008; Ali, Telfer et al. 2009). We therefore wanted to study the effects of PARP inhibition with AG14699 in the context of continuous fractionated irradiation and study DNA DSB repair kinetics and fraction size sensitivity.

5.4.2 Results

5.4.2.1 PARP inhibitor activity assay

PARP1 is an abundant nuclear protein that rapidly binds to DNA single-strand breaks and catalyses the formation of PAR polymers from NAD^+ (Satoh and Lindahl 1992), attached primarily on glutamic acid residues on acceptor proteins. PARP activity in CHO cells and inhibition by the PARP inhibitor AG14699 (at 0.4 µmol/L) was tested by assessing PAR levels using the Trevigen Universal chemiluminescent PARP assay kit (data not shown). These experiments were kindly performed by Drs Ponnari Gottipati and Barbara Vischioni in the Helleday lab at Oxford and have been published (Gottipati, Vischioni et al. 2010). It has also been shown previously that AG14699 at 0.4 µmol/L completely inhibits human full length recombinant PARP-1 by [^{32}P]NAD^+ incorporation with a K_i value of only 1.7 nmol/L (Thomas, Calabrese et al. 2007). These authors showed that at this concentration the PARPi alone did not cause growth inhibition or cytotoxicity and selected this for chemopotentiation and radiopotentiation studies. We have therefore used AG14699 at 0.4 µmol/L added 1 hour prior to radiation for the experiments below.

5.4.2.2 Clonogenic cell survival following radiation in wild type CHO cells (AA8) with or without PARP inhibitor

5.4.2.2.1 Single dose clonogenic survival

To study the effect of AG14699 on clonogenic survival in WT CHO cells we added the drug at 0.4 µmol/L, 1 hour prior to radiation. We found no significant radiosensitisation at doses of 1 to 4 Gy with addition of PARPi. This was in contrast to the CHO cell line genetically defective in BER (EM9) as shown in **Fig 5.13**.

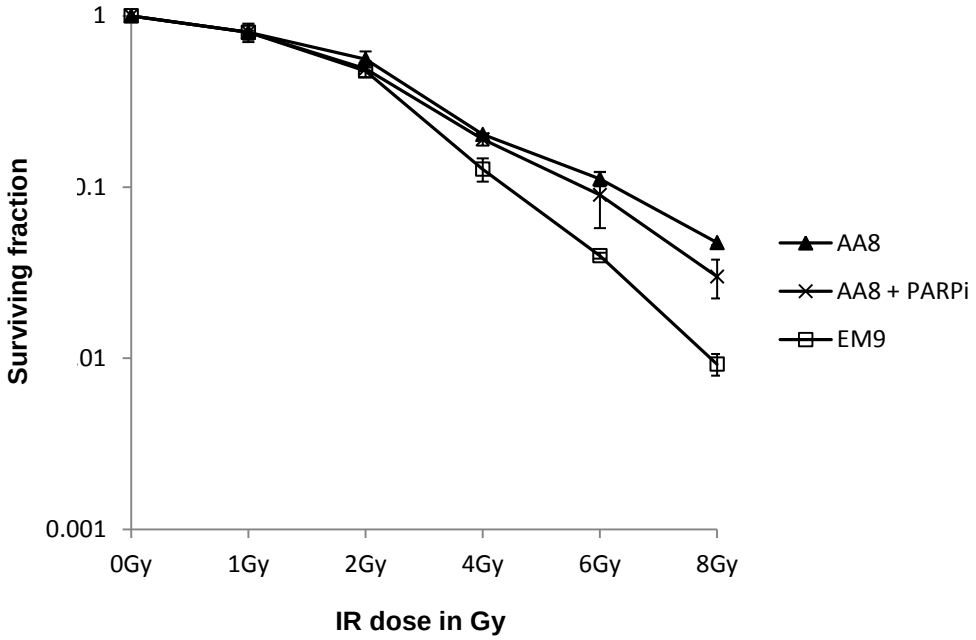


Figure 5.13: Acute dose clonogenic survival curves comparing WT AA8 cells with or without the PARPi (AG14699) and BER mutant EM9 cells at doses of 0, 1, 2, 4, 6 and 8 Gy. Error bars show SEM of 3 repeats in triplicate.

5.4.2.2.2 Fractionated irradiation clonogenic survival curves – 1 Gy/day

As clinical radiotherapy is given in small fractional doses each day over several weeks with a gap over the weekend, we wanted to test the effect of adding a PARPi to fractionated IR in wild type CHO cells. We tested 1 Gy/day given from Monday to Friday for 3 weeks to a total dose of 16 Gy. We found no significant radiosensitisation with the addition of AG14699 to AA8 cells throughout the course of IR as seen in **Figure 5.14.** This was consistent with our results in the genetically BER defective CHO cell line EM9 **(Figure 5.14 and Chapter 4)**.

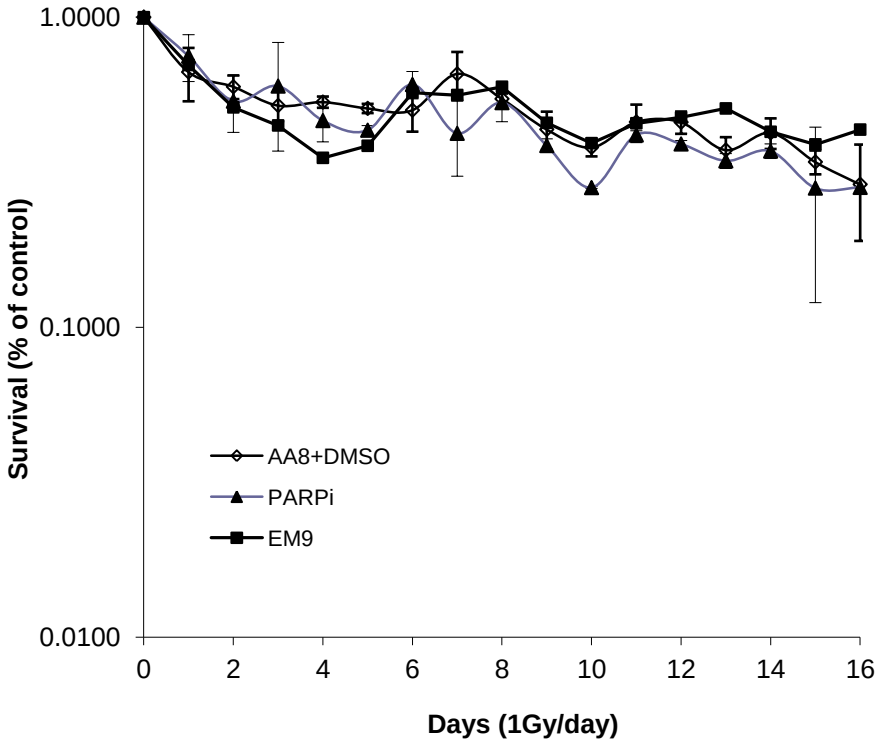


Figure 5.14: Fractionated IR survival curves testing 1 Gy/day in WT AA8 cells with or without the PARPi (AG14699) and BER mutant EM9 cells. 1 Gy given daily Monday to Friday with weekend breaks to a total of 16 Gy. Error bars show SEM of 3 repeats in triplicate.

5.4.2.2.3 Sensitivity to changes in dose per fraction as measured by clonogenic survival in AA8 cells with or without PARPi

In order to see if addition of PARPi altered the fraction size sensitivity of the WT cell line, we compared survival following 2 Gy as a single fraction (high dose per fraction) versus 2 fractions of 1 Gy each (low dose per fraction) and 1 fraction of 4 Gy versus 4 fractions of 1 Gy **(Figure 5.15)**. We found that the addition of PARPi did not alter the sparing effect of fractionation seen in these wild type cells. For example there was a 2.4 and 2.6 fold decrease in survival following 4 GyX1 versus 1 Gyx4 in AA8 cells with or without PARPi respectively. The BER defective EM9 cells also show sparing with lower doses per fraction as shown in Chapter 4 **(Figure 4.3 and Figure 5.15)**.

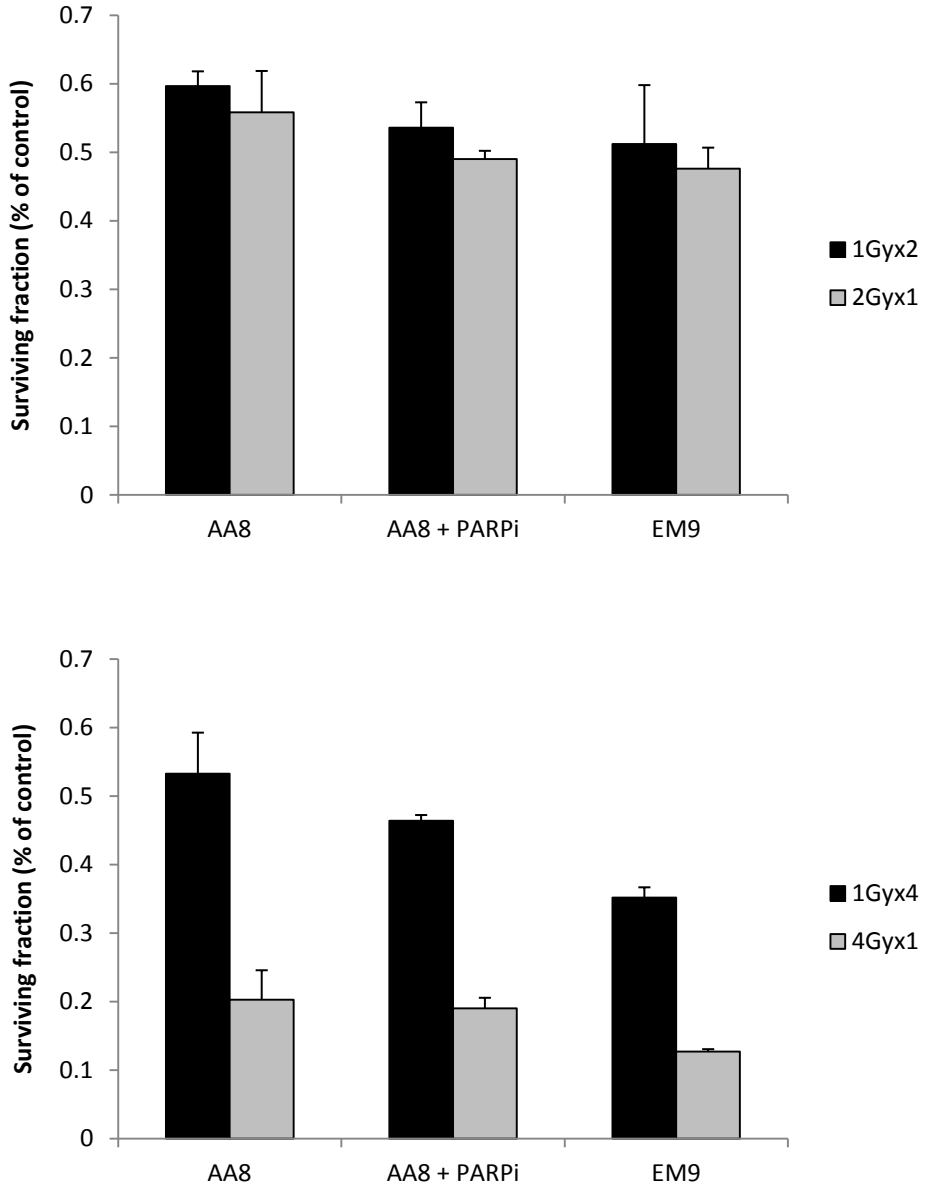
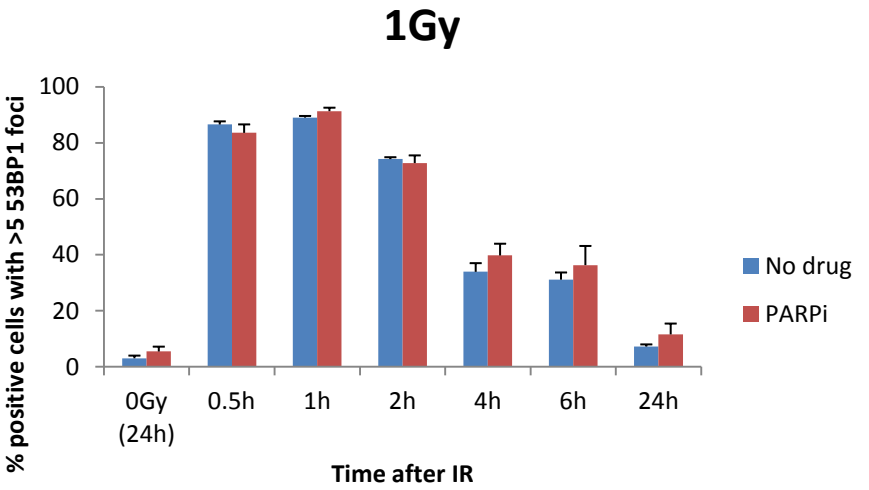
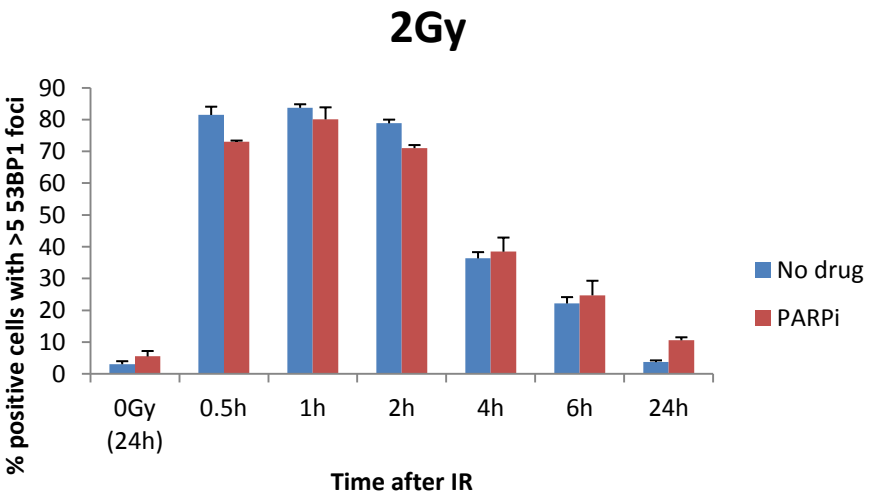


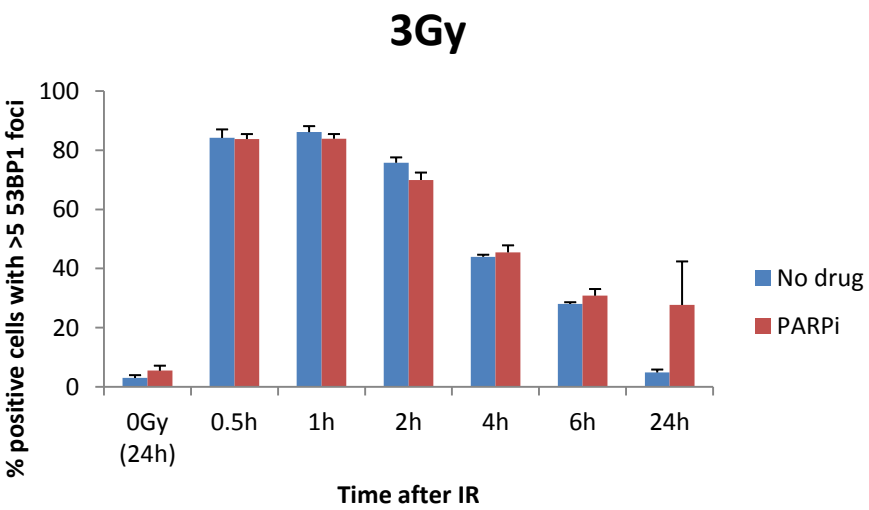
Figure 5.15: Comparison of survival between high dose per fraction vs low dose per fraction without PARPi (AG14699). A & B. The WT (AA8) and EM9 (BER-) cell lines showed increased sensitivity to higher dose per fraction. The addition of PARPi to WT cells maintains the sparing effect with fractionation, when comparing 2 Gy as single fraction vs 1 Gy in 2 fractions or 4 Gyx1 vs 1 Gyx4. Error bars show SEM of 3 repeats in triplicate.

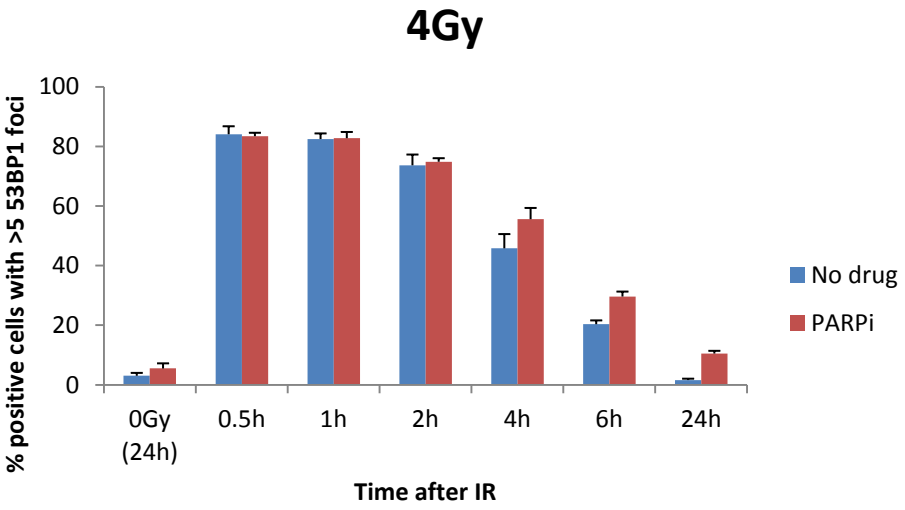
5.4.2.3 DNA DSB repair kinetics during fractionated IR in AA8 cells with or without PARPi

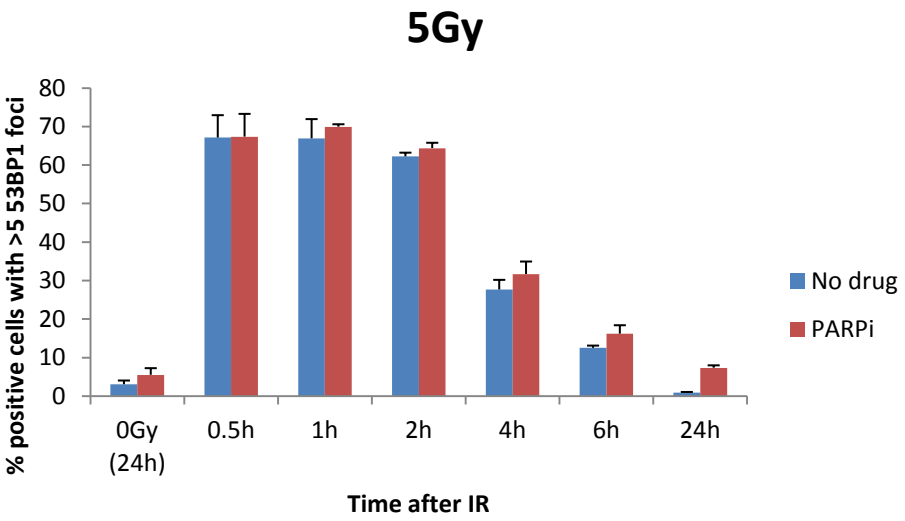
We wanted to study the effect of adding a PARPi to DSB repair kinetics by using 53BP1 foci analysis at various time points (0.5, 1, 2, 4, 6 and 24 hours) after each daily 1 Gy fraction of IR to a total dose of 10 Gy over 2 weeks **(Figure 5.16).** The 96 well plate format was used as described earlier and percentage of cells with >5 53BP1 foci were analysed as positive. We found that addition of AG14699 to WT cells made no difference to the induction and resolution of 53BP1 foci throughout the 2 weeks of irradiation compared to WT cells alone **(Figure 5.16)**.

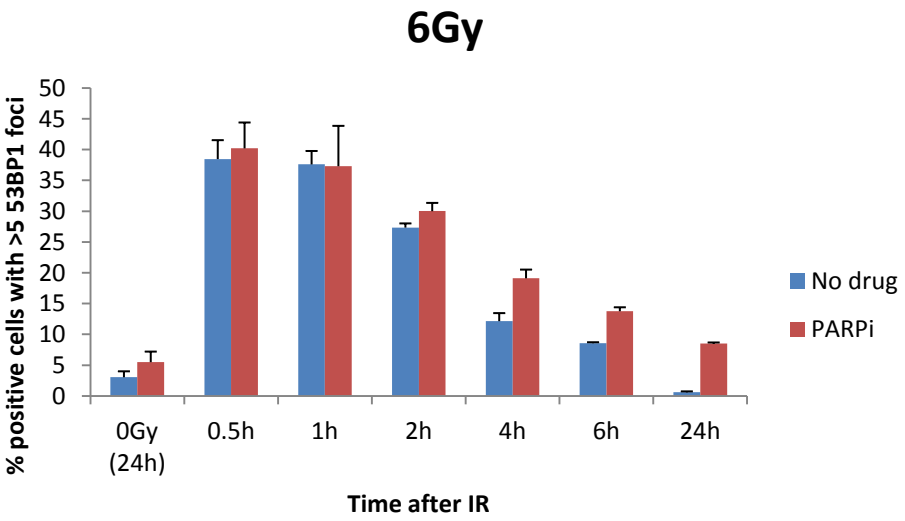

1Gy
% positive cells with >5 53BP1 foci
100
80
60
40
20
0
0Gy (24h)
0.5h
1h
2h
4h
6h
24h
Time after IR
No drug
PARPi

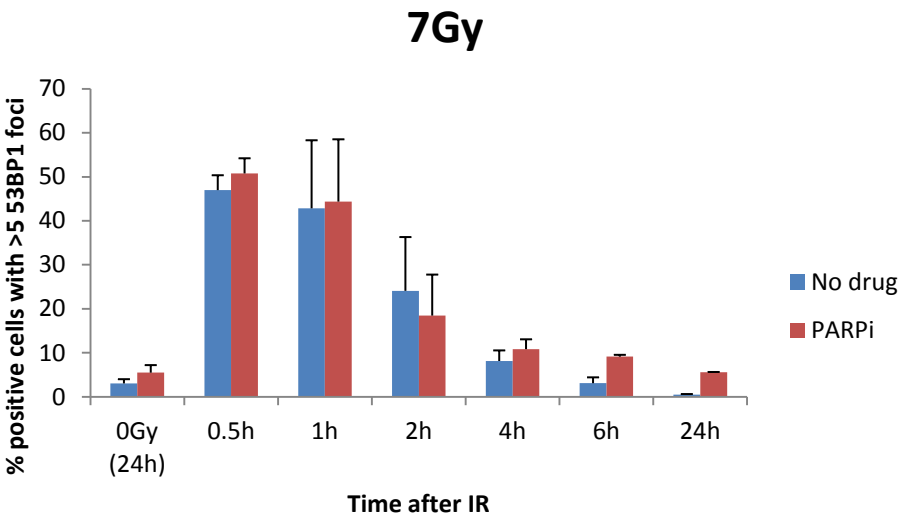

2Gy
% positive cells with >5 53BP1 foci
90
80
70
60
50
40
30
20
10
0
0Gy (24h)
0.5h
1h
2h
4h
6h
24h
Time after IR
No drug
PARPi

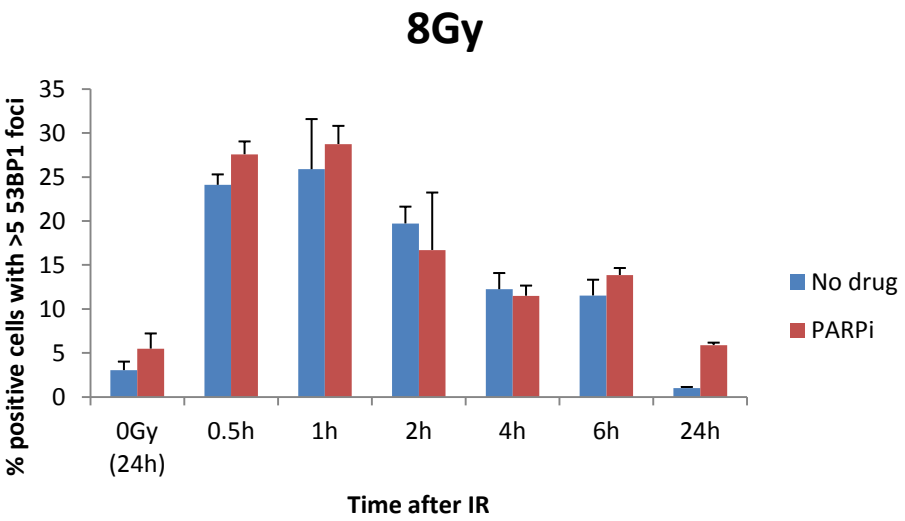

3Gy
% positive cells with >5 53BP1 foci
100
80
60
40
20
0
0Gy (24h)
0.5h
1h
2h
4h
6h
24h
Time after IR
No drug
PARPi

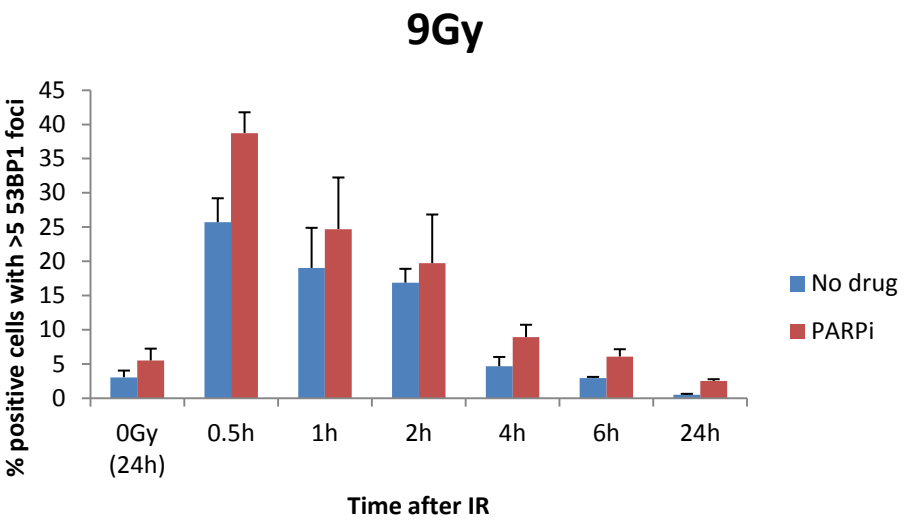

4Gy
% positive cells with >5 53BP1 foci
100
80
60
40
20
0
0Gy (24h)
0.5h
1h
2h
4h
6h
24h
Time after IR
No drug
PARPi


5Gy
% positive cells with >5 53BP1 foci
80
70
60
50
40
30
20
10
0
0Gy (24h)
0.5h
1h
2h
4h
6h
24h
Time after IR
No drug
PARPi


6Gy
% positive cells with >5 53BP1 foci
50
45
40
35
30
25
20
15
10
5
0
0Gy (24h)
0.5h
1h
2h
4h
6h
24h
Time after IR
No drug
PARPi


7Gy
% positive cells with >5 53BP1 foci
70
60
50
40
30
20
10
0
0Gy (24h)
0.5h
1h
2h
4h
6h
24h
Time after IR
No drug
PARPi


8Gy
% positive cells with >5 53BP1 foci
35
30
25
20
15
10
5
0
0Gy (24h)
0.5h
1h
2h
4h
6h
24h
Time after IR
No drug
PARPi


9Gy
% positive cells with >5 53BP1 foci
45
40
35
30
25
20
15
10
5
0
0Gy (24h)
0.5h
1h
2h
4h
6h
24h
Time after IR
No drug
PARPi

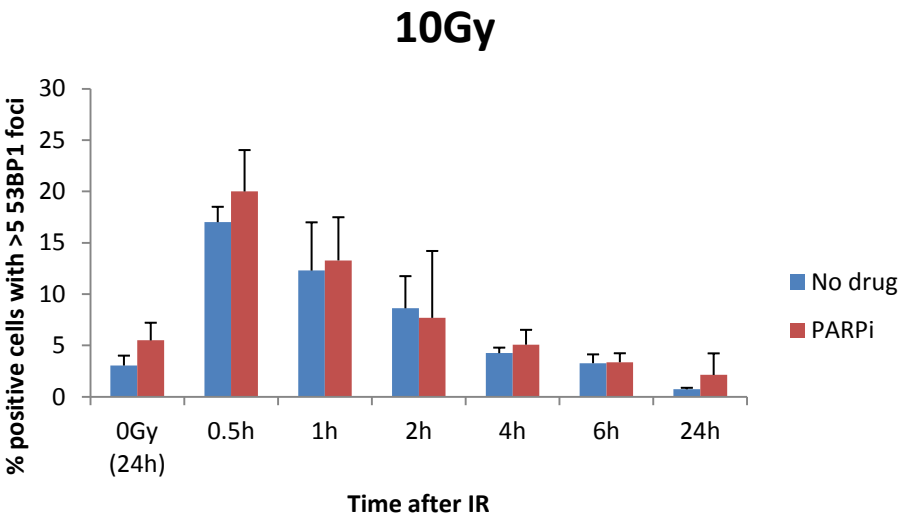
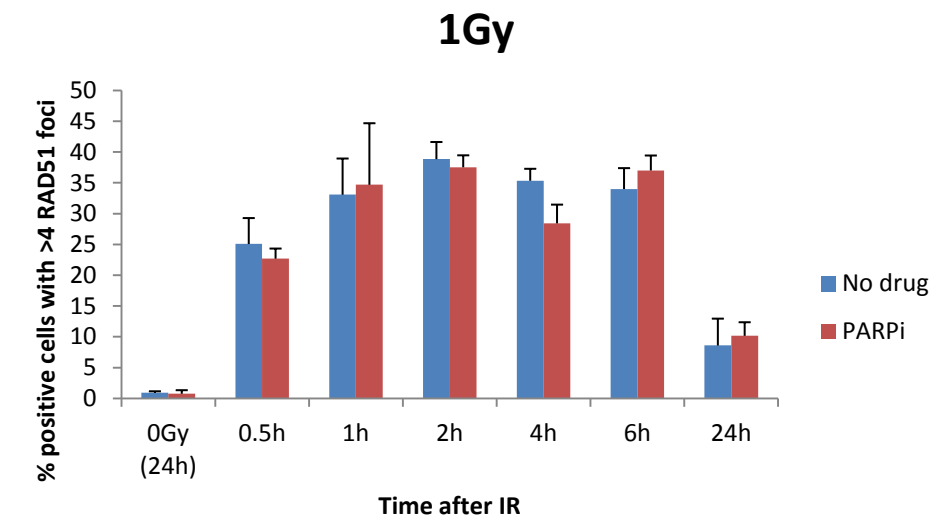
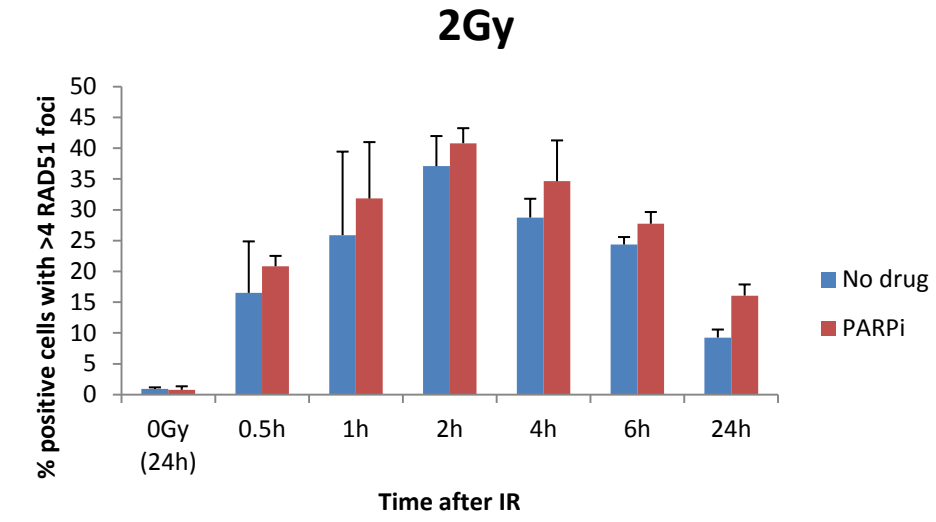


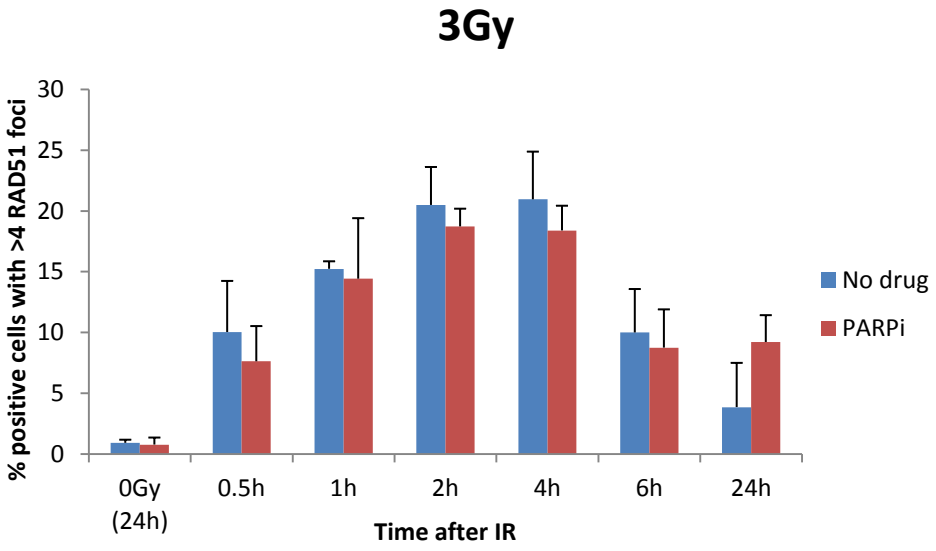
Figure 5.16: DNA DSB repair kinetics using 53BP1 foci analysis during fractionated IR in AA8 cells with or without PARPi (AG14699). Measured as percentage positive cells with >5 53BP1 foci at 0.5, 1, 2, 4, 6 and 24 h after each fraction of 1 Gy given daily over 2 weeks (with a weekend gap), to a total dose of 10 Gy. Error bars represent SEM of 3 experiments in duplicate.

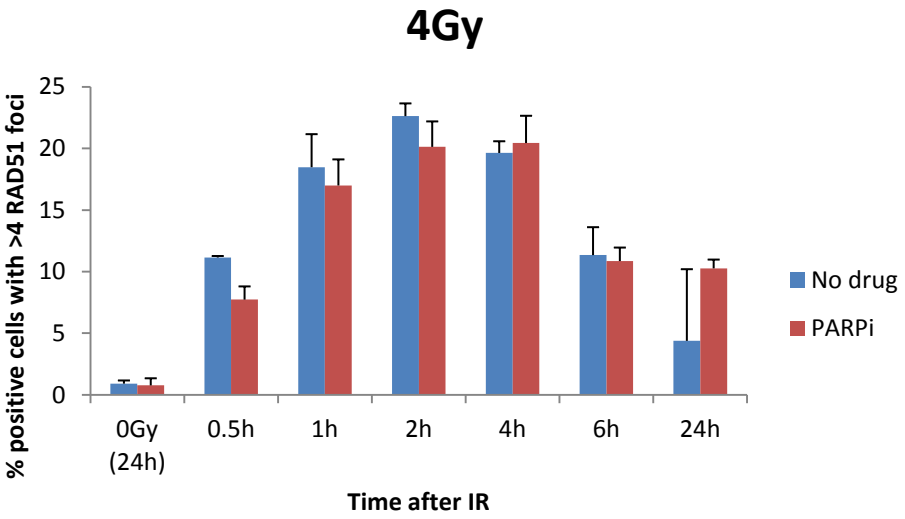
5.4.2.4 Homologous recombination repair kinetics in AA8 cells with or without PARPi during fractionated IR

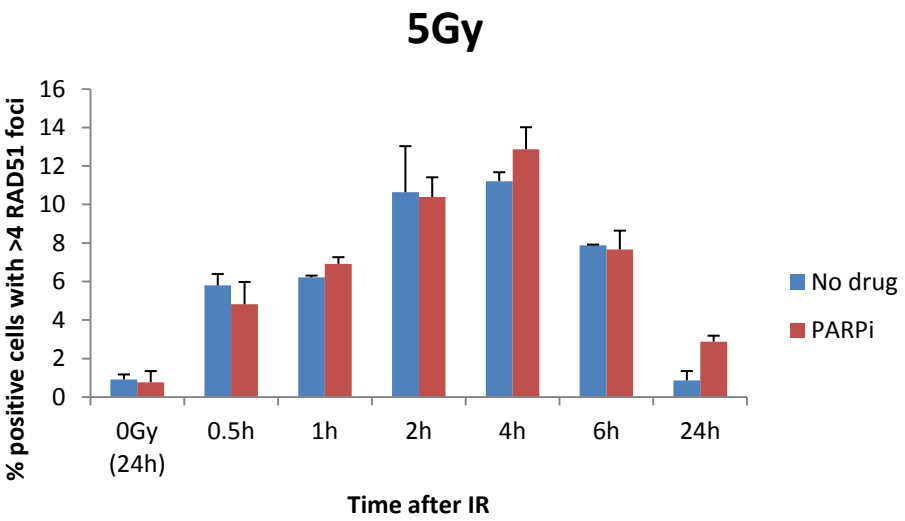
To study the effect of AG14699 on HR repair we analysed RAD51 foci levels at various time points (0.5, 1, 2, 4, 6 and 24 hours) after each daily 1 Gy fraction of IR to a total dose of 10 Gy with or without the PARPi **(Figure 5.17).** Again, we found no significant difference in the induction or resolution of RAD51 foci at all time points after IR with the addition of the PARPi compared to wild type cells alone. The peak induction of RAD51 foci was usually seen at the 2 h time point in WT cells, and this was similar in the presence of the drug.

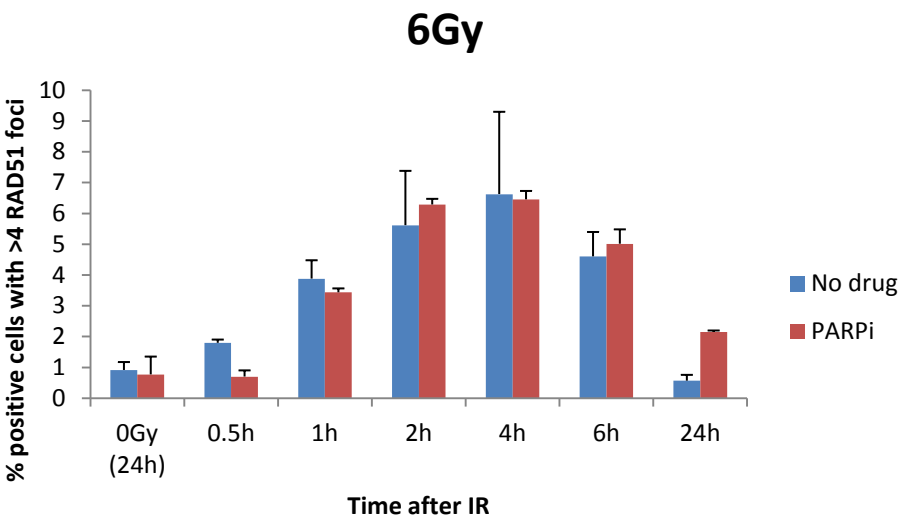

1Gy
% positive cells with >4 RAD51 foci
50
45
40
35
30
25
20
15
10
5
0
0Gy (24h)
0.5h
1h
2h
4h
6h
24h
Time after IR
No drug
PARPi

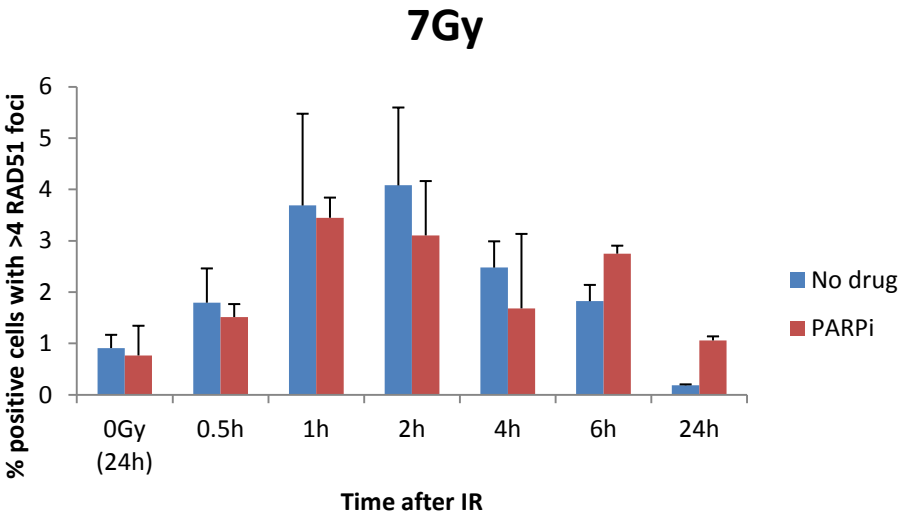

2Gy
% positive cells with >4 RAD51 foci
50
45
40
35
30
25
20
15
10
5
0
0Gy (24h)
0.5h
1h
2h
4h
6h
24h
Time after IR
No drug
PARPi

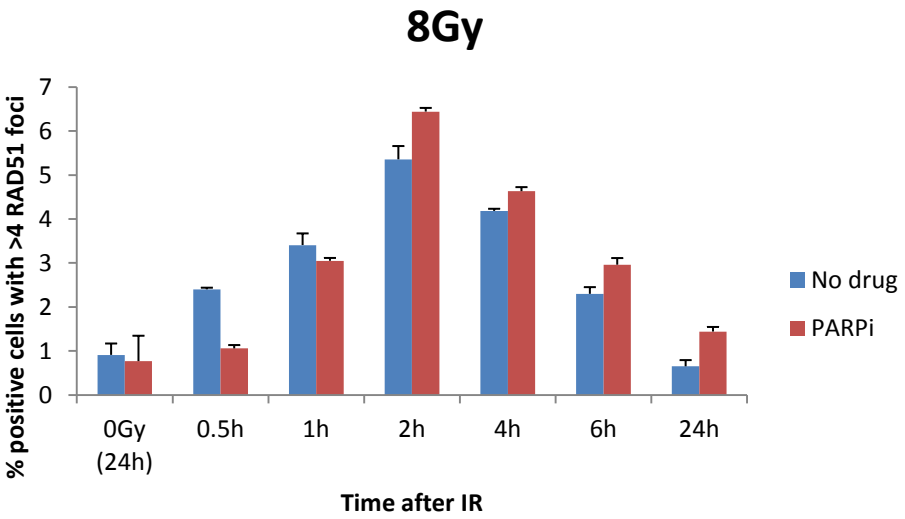

3Gy
% positive cells with >4 RAD51 foci
30
25
20
15
10
5
0
0Gy (24h)
0.5h
1h
2h
4h
6h
24h
Time after IR
No drug
PARPi

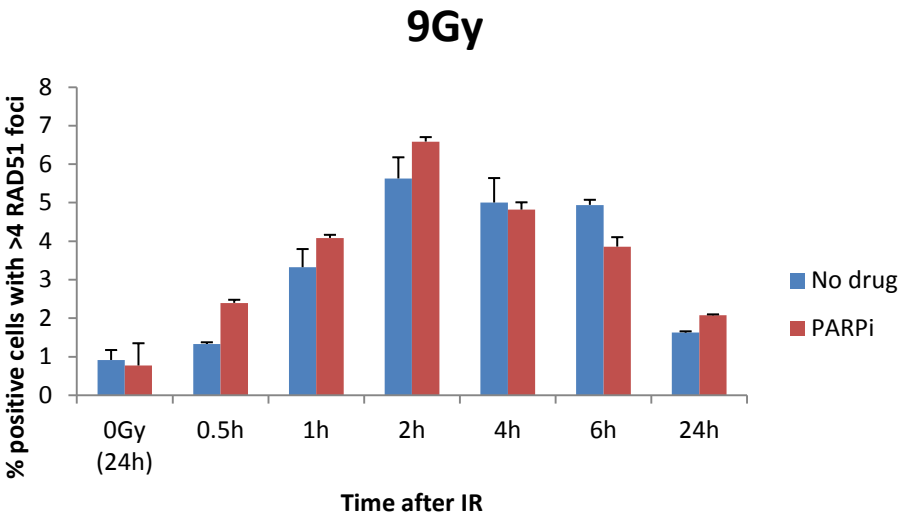

4Gy
% positive cells with >4 RAD51 foci
25
20
15
10
5
0
0Gy (24h)
0.5h
1h
2h
4h
6h
24h
Time after IR
No drug
PARPi


5Gy
% positive cells with >4 RAD51 foci
16
14
12
10
8
6
4
2
0
0Gy (24h)
0.5h
1h
2h
4h
6h
24h
Time after IR
No drug
PARPi


6Gy
% positive cells with >4 RAD51 foci
10
9
8
7
6
5
4
3
2
1
0
0Gy (24h)
0.5h
1h
2h
4h
6h
24h
Time after IR
No drug
PARPi


7Gy
% positive cells with >4 RAD51 foci
0
1
2
3
4
5
6
0Gy (24h)
0.5h
1h
2h
4h
6h
24h
Time after IR
No drug
PARPi


8Gy
% positive cells with >4 RAD51 foci
0
1
2
3
4
5
6
7
0Gy (24h)
0.5h
1h
2h
4h
6h
24h
Time after IR
No drug
PARPi


9Gy
% positive cells with >4 RAD51 foci
0
1
2
3
4
5
6
7
8
0Gy (24h)
0.5h
1h
2h
4h
6h
24h
Time after IR
No drug
PARPi

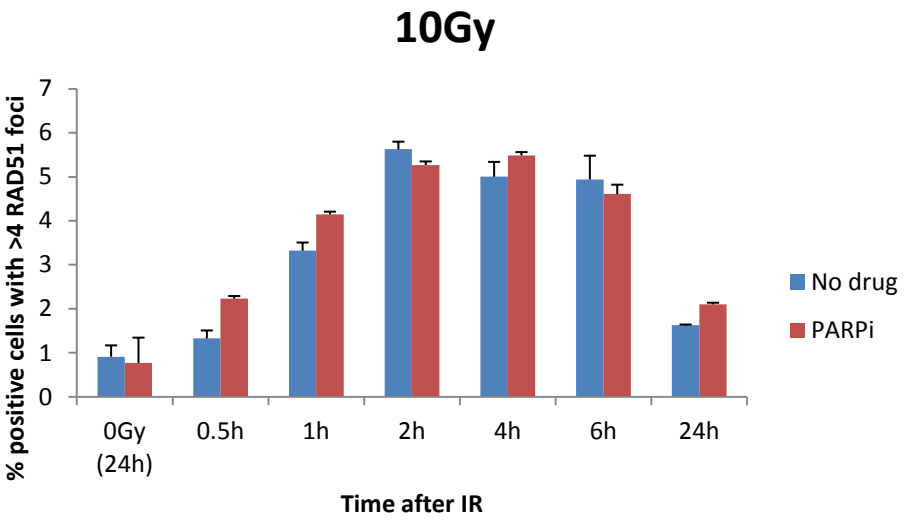


Figure 5.17: Homologous recombination repair kinetics in AA8 cells with or without PARPi (AG14699) during fractionated IR. Measured as percentage positive cells with >4 RAD51 foci at 0.5, 1, 2, 4, 6 and 24 h after each fraction of 1 Gy given daily over 2 weeks (with a weekend gap), to a total dose of 10 Gy. Error bars represent SEM of 3 experiments in duplicate.

5.4.3 Discussion

It is well established that PARP may affect both HR induced at replication forks and a backup pathway for NHEJ in the absence of Ku70 or Ku80 (Helleday 2011). PARP inhibitors have also been shown previously to selectively sensitise cells in the S phase of the cell cycle and not sensitise cells in the G1 phase of the cell cycle (Dungey, Loser et al. 2008; Chalmers 2009). Chalmers et al showed that when cell populations had been confluent for 24 h and were confirmed to be arrested in G1, the radiosensitisation of PARP inhibitor PJ34 on the T98G glioma cell line was lost (Chalmers, Johnston et al. 2004). Here, we find no additional effect with PARP inhibitors on response to fractionated IR. This is unlikely to represent failure to inhibit PARP under the conditions used here. The underlying reason could be that the daily IR dose is too small to make a difference. Indeed, scrutinising the published literature, it appears that sensitisation after IR with PARP inhibitors appears to occur at higher doses (Dungey, Loser et al. 2008). It has been shown that PARP-$1^{-/-}$ knockout mouse cells showed sensitivity only to radiation doses >1.5 Gy in contrast to cells cultured with PARP inhibitors which are not specific for PARP-1. The results from preliminary immunofluorescence data support the hypothesis that PARP-2 can compensate for a lack of PARP-1 after low-dose radiation but not after higher radiation doses where greater levels of DNA damage are present (Chalmers, Johnston et al. 2004).

We also wanted to study the effect of PARP inhibition on fraction size sensitivity. Previously Brock et al treated exponentially growing CHO cells with 2 split doses of 4 Gy versus a single 8 Gy dose with or without the PARPi INO-1001 (Brock, Milas et al. 2004). They found that addition of the PARPi to the split dose regimen reduced the recovery ratio from 5.3 to 2.2 compared to radiation alone, suggesting that PARP inhibition may block a significant proportion of DNA repair that occurs

between fractions. We found that AG14699 did not alter the sparing effect from fractionation in AA8 cells. It is likely that at small doses per fraction used here (1 Gy) potentially lethal damage is effectively repaired in WT cells despite inhibition of PARP1.

The challenge in combining radiation with novel agents is in augmenting its ability to kill tumour cells without worsening normal tissue toxicity. There is evidence showing accumulation of γH2AX foci in plucked eyebrow-hair follicles in the phase 1 trial of olaparib in BRCA mutation carriers (Fong, Boss et al. 2009). This raises concerns that long-term PARP inhibition may lead to an accumulation of DNA damage in normal tissues. Our data show that WT CHO cells recover very well from daily fractionated IR at 1 Gy/day over 3 weeks despite the prolonged inhibition with PARPi which is reflected in the DSB repair kinetics. This suggests that normal cells within the radiation field may be able to recover well when exposed to small daily fractions of RT over several weeks even in the presence of PARP inhibition. This presents an exciting therapeutic advantage which needs to be explored further in pre-clinical and clinical models.

CHAPTER SIX

Final Discussion

6.1 Cell and molecular basis of fractionation sensitivity

Every cell function is an elaborately branched signalling network mediated by receptors, ligands and small molecules that can activate DNA repair, alter chromatin organisation, switch on cell cycle checkpoints and modulate various cellular metabolic processes (Shiloh and Lehmann 2004). Most radiobiology models place DNA damage, in particular double-strand breaks, as the pivotal event within a cell that initiates the radiation response and subsequent effects. We have attempted to elucidate the cell and molecular determinants of sensitivity to fraction size in this thesis. There is a tight association between proliferative indices and the timing of normal tissue responses after radiotherapy (Stewart and Van der Kogel 2002). Normal tissues that respond early (within days of radiotherapy) have high proliferative indices and low sensitivity to fraction size and vice versa for those that respond late (years later). This association is so tight as to offer clues to mechanisms.

We have used human epidermis as a model system to test the association between fractionation sensitivity, cell proliferation and DNA repair. The sensitivity of early skin reactions (erythema and desquamation) to fraction size varies over a 5-week course of radiotherapy, being greatest at the start of radiotherapy and losing sensitivity during weeks 4 & 5 (Turesson and Thames 1989; Hopewell, Nyman et al. 2003). Our data show that a 10-fold increase in the use of homologous recombination (HR) to repair radiation-induced DNA double-strand breaks (DSB) towards the end of RT correlates with the loss of fractionation sensitivity seen clinically (Somaiah, Yarnold et al. 2012). This observation is consistent with loss of fractionation sensitivity in

CHO cell lines defective in non-homologous end joining (NHEJ) which rely on HR repair (Thacker and Wilkinson 1995). We have shown that a cell line defective in EJ and relying on HR for repair of radiation-induced DSB loses sensitivity to fractionation with cells accumulating in S/G2 phase (Somaiah, Yarnold et al. 2012). NHEJ is error prone and sensitive to DNA damage levels (fraction size), in marked contrast to the high fidelity of HR that is independent of DNA damage levels (Rothkamm, Kruger et al. 2003). Our model based on these observations is that fractionation sensitivity reflects NHEJ repair, which is greatest in tissues having the lowest proliferative indices and the highest percentage of cells in G0/1 phase.

Another mechanism contributing to loss of fraction size sensitivity in S/G2 could be via cohesin, which facilitates more efficient DSB repair in replicated chromatin (Bauerschmidt, Arrichiello et al. 2010) and may enhance correct DSB repair at high doses in S/G2 in an HR-independent manner (Kruger, Rothkamm et al. 2004). The tightly bound chromatid in S/G2 might serve as a scaffold to hold break ends in place and thus avoid loss or rearrangement of chromosome material. Without such a scaffold (i.e. in G0/G1), break ends would be able to move more freely, repair would be slower and more frequently result in 'wrong' ends being joined, especially at higher doses (or dose per fraction) when breaks are in close proximity. Whatever mechanisms are involved, cells in S/G2 appear to have a high fidelity for repair that is independent of DNA damage levels, explaining insensitivity to fraction size and mediating resistance to radiation (Utsumi and Elkind 2001; Rothkamm, Kruger et al. 2003). Thus a higher proportion of cells in S/G2 phase of the cell cycle (allowing greater use of high fidelity DSB repair) is more likely to influence fractionation sensitivity than proliferation per se (as determined by Ki67 staining). This model however does not exclude a role for HR in enhancing repair fidelity and insensitivity to fraction size in S/G2 phase cells.

6.2 The proposed model of fractionation sensitivity

Based on our findings we would propose the following simple model of fraction size sensitivity **(Figure 6.1)**. Tissues with high proliferative indices with majority of cells in S/G2 phase and/or those using HR to repair RT induced DSB are fraction size insensitive and vice versa for cells in G0/G1 and/or relying on NHEJ repair. However, the situation in tumours is likely to be more complex as discussed below.

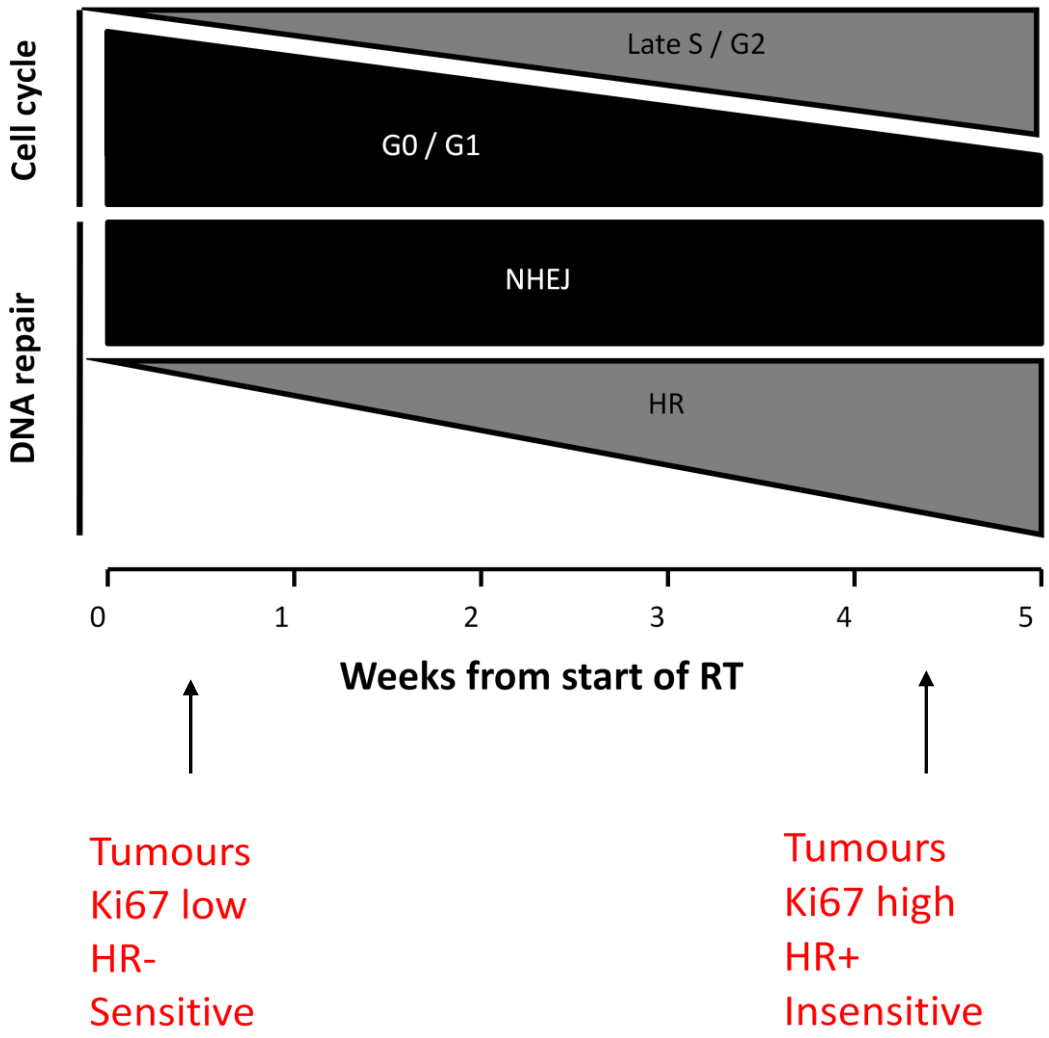


Figure 6.1. Model of fractionation sensitivity

6.3 Deregulation of cell cycle controls and DNA damage responses modify the fractionation sensitivity of cancer

Models of fractionation sensitivity applicable to normal tissues may not be directly relevant to cancers, which are commonly defective for components of the DNA damage response (Bartek and Lukas 2003; Bartkova, Horejsi et al. 2005; Gorgoulis, Vassiliou et al. 2005). In this context, mutations and reduced expression of BRCA1, BRCA2, p53, ATM, Chk2, MDC1 and 53BP1 have been observed in subsets of human breast cancers (Bartek and Lukas 2003; Turner, Tutt et al. 2004; Nevanlinna and Bartek 2006; Ribeiro-Silva, Moutinho et al. 2006; Bartkova, Horej Sbreve et al. 2007). In addition, radiation induced G1/S arrest and subsequent non-homologous end joining repair is a p53-dependent process and, thus, is lacking in many tumour cells (Ferguson, Sekiguchi et al. 2000). It has been shown that cancer cells defective in p53 accumulate in the G2 phase of the cell cycle after DNA damage (Kastan, Onyekwere et al. 1991). Thus, tumours with low proliferative indices, intact cell cycle checkpoints and/or loss of functional HR are predicted be more sensitive to fraction size than tumours with high proliferative indices, abrogated cell cycle checkpoints and/or functional HR.

There are other cancer-specific features that may be relevant. Ionising radiation activates epidermal growth factor receptor (EGFR), inducing a range of cyto-protective responses including increased cell proliferation, reduced apoptosis and enhanced DNA repair (Schmidt-Ullrich, Contessa et al. 2003; Baumann, Krause et al. 2007). It has also been shown that EGFR membrane receptor signalling enhances repair of radiation-induced DNA DSB mainly via the NHEJ pathway (Toulany and Rodemann 2010). It is, therefore, possible that upregulated EGFR signalling seen in many tumours may affect fractionation sensitivity (Rodemann, Dittmann et al. 2007). These observations are relevant to the extent that drugs

targeting plasma membrane receptor signalling pathways are increasingly incorporated in experimental radiotherapy (Bonner, Harari et al. 2006).

6.4 Influence of hypoxia on fractionation sensitivity

It is also possible that oxygenation status plays an important part in the fractionation sensitivity of tumours. Each fraction interval gives opportunities for the tumour tissue to re-oxygenate and therefore be more sensitive to RT. This would compensate for the sparing effect of fractionation which allows the cells to repair the DNA damage. It is known that rapidly proliferating tumours like head and neck squamous cell carcinomas have a high hypoxic component and such tumours generally have a high α/β ratio. Therefore it is possible that tumour α/β ratio is sensitive to the degree of oxygenation. Re-oxygenation during fractionation may result in a changing tumour α/β ratio. If this were true, a well oxygenated tumour or a hypoxic tumour given an anti-hypoxic treatment such as nicotinamide/carbogen, would have a lower α/β ratio and the sparing effect of fractionation would be higher. The differential fractionation effect between tumour and normal tissue would be lower and the necessity to use fractionated treatment may also be lower.

On the contrary, several groups have reported that the expression and function of homologous recombination proteins, including RAD51, BRCA1 and BRCA2 are compromised under hypoxic conditions (Meng, Jalali et al. 2005; Chan, Koritzinsky et al. 2008; Chan, Pires et al. 2010). These studies also observed that the decreased HR gene expression was independent of p53 and cell cycle distribution. In addition there is recent data suggesting activation of DNA-PK by hypoxia (Bouquet, Ousset et al. 2011). Given our findings that cells relying on NHEJ are more sensitive to fraction size, it is possible that hypoxic cells may in actual fact be sensitive to fraction size whilst being radioresistant due to the oxygen effect. Poor

tumour oxygenation has also been shown to affect DNA damage checkpoint activation and suppress DNA mismatch repair (Rodriguez-Jimenez, Moreno-Manzano et al. 2008). In response to anoxia, cell-cycle checkpoint-proficient cells activate ataxia telangiectasia mutated (ATM) and ataxia telangiectasia and Rad3-related (ATR) DNA-damage kinase-mediated intra-S-phase arrest of DNA replication. When reoxygenated, cells can generate reactive oxygen species and DNA breaks, which lead to a CHK2-dependent, G2 arrest and attempted repair of ROS-mediated DNA damage (Hammond, Freiberg et al. 2006; Bindra, Crosby et al. 2007). In contrast, diffusion-limited, chronically hypoxic cells may slowly adapt to increasingly low oxygen conditions and bypass these checkpoints. These proliferating hypoxic cells may then be prone to DNA replicative errors (Bristow and Hill 2008). Therefore, tumour hypoxia can be both spatially and temporally heterogeneous with dynamic gradients of oxygenation, and lead to differential biology with respect to signalling and repair of DNA damage that may influence fractionation sensitivity and needs to be explored further.

6.5 Modelling the change in fractionation sensitivity with time during radiotherapy.

As discussed earlier, the α/β ratio (describing fractionation sensitivity) is used in many practical clinical situations including comparing different fractionation schedules, for correcting both dose delivery errors and unintended treatment interruptions, as well as being useful in the assessment of dose rate effects and when linear energy transfer is changed (Jones, Dale et al. 2001). When using the linear quadratic model of radiation effect and the biological effective dose (BED) concept, it is assumed that the α/β values used are constant over a treatment or reflect averaged values (Jones, Dale et al. 2001). For slowly proliferating tumours and late reacting tissues the α/β ratios are likely to remain stable, but in epithelial

tissues and some rapidly growing tumours, apparent acceleration of repopulation with time during radiotherapy has been recognised (Turesson and Thames 1989; Hopewell, Nyman et al. 2003). Such a process would imply that the α/β ratio may also increase in proportion to the change in the proliferative indices. There is evidence that this may be the case for normal tissues such as skin where the α/β ratio can change from 5 to 15 to 35 Gy during weeks 1-2, 3-4 and 5-6 respectively of radiotherapy in animal and human tissues (Turesson and Thames 1989; Hopewell, Nyman et al. 2003) . This in turn correlates well with observed cellular repopulation rates and also a measured reduction in fractionation sensitivity (Turesson and Thames 1989; Hopewell, Nyman et al. 2003).

Molecular studies have clearly shown that HR appears to occur during the later phases of the cell cycle (S/G2). This form of repair appears not to be associated with a sub-lethal form so that there is no split dose recovery: this leads to a dependency on dose with effect without a major dependency on dose per fraction. In the remainder of the cell cycle (which predominates in slowly proliferating cell systems), NHEJ repair occurs and confers fraction sensitivity due to repair of sub-lethal damage components during and after treatment. In terms of the LQ model, the α parameter is the non-fractionation dependent parameter, which increases substantially in rapidly proliferating cells. The β parameter is assumed to be relatively stable. It follows that increased proliferation during radiotherapy will be followed by an increase in the α/β ratio, which in turn implies reduced fractionation sensitivity. Thus problems may emerge in treatment comparisons, especially due to the dynamic change in α/β ratios, since BED equations comparisons of two fractionation schedules can only be allowed when the α/β ratio is the same. This problem may explain some examples where BED correlations with clinical effects have, in some instances, not been as good as expected.

Our data shows that HR increases during radiotherapy, which is clinically associated with a loss in fractionation sensitivity. Therefore, tentative modelling may be devised, which allows α to change in this way with time. The use of fractionation schedules that are sufficiently short does not allow these changes to occur. Also, tumour systems that have lost significant repair capacity will not show such a marked change in fractionation sensitivity with time. It may be possible in the future to include these effects when comparing normal tissue tolerances for acute and late reacting tissues. Estimations of acute tolerance doses based on BED or Gy per week also could be reassessed for such effects. Consequential reactions may also be influenced by these changes and further prospective long-term analysis of patients treated by modern techniques is indicated.

CHAPTER SEVEN

Future Directions

Biomarkers of sensitivity to fraction size in curative radiotherapy

7.1 Aims and Objectives

The aims of further research arising from this thesis will be:

1. To further evaluate cell and molecular determinants of sensitivity to radiotherapy fraction size
2. To identify biomarkers of fraction size sensitivity for evaluation in clinical trials testing individualisation of fraction size
3. To investigate the modifying effects of small molecule inhibitors of DNA repair, cell cycle checkpoints and growth factor signalling on fractionation responses

The long-term goal of aims 1 & 2 will be to test the clinical benefit of incorporating tumour biomarkers of fractionation sensitivity into current algorithms used to select radiotherapy dose prescriptions. The long-term goal of aim 3 will be to test what changes in fractionation sensitivity of tumour and normal tissues are expected as a result of combining biological and radiation therapies and to define the potential to improve the therapeutic index by selection of appropriate individualised dose prescriptions.

7.2 Hypotheses

7.2.1 Hypothesis 1

Reduced sensitivity to radiotherapy fraction size in tissues with high proliferative indices is dependent on the DSB repair system used in S/G2 phase cells.

7.2.2 Hypothesis 2

Sensitivity to fraction size is dependent on cell cycle phase distribution.

In both cases, abrogated cell cycle checkpoints will act to further reduce sensitivity to fraction size. The following table summarises the predicted expression of biomarkers consistent with the above hypotheses:

Table 7.1: Possible biomarkers of fractionation sensitivity

Cellular Property	Biomarker	Postulated Status of Biomarker	
		Tumours insensitive to fraction size	Tumours sensitive to fraction size
Cell proliferation	Ki67	High	Low
	S/G2 fraction (Cyclin A)	High	Low
	Cohesin	High	Low
Cell cycle checkpoints	p53	Mutant	Normal
	Chk1/Chk2	Functional	Defective *
DNA repair	EJ- Ku70, Ku80, DNAPKcs	Defective	Functional
	HR- BRCA1/2, ATM, PTEN, RAD51	Functional	Defective
Growth Factor signalling	EGFR (via effect on EJ)	Defective	Upregulated/ Functional
Hypoxia	Pimonidazole	High	Low

*depending on functional G1/S checkpoint

7.3 Future translational research plan

7.3.1 *In vitro* studies

7.3.1.1 Testing hypothesis 1:

Our data show that HR defective CHO cells are moderately radiosensitive compared to wild-type and retain fraction size sensitivity, whereas NHEJ defective cells are very radiosensitive compared to wild-type and lose fraction size sensitivity (Somaiah, Yarnold et al. 2012). Although proof-of-principle has been established in CHO cell lines, these are all defective in p53. Therefore the effect of loss of functional HR on fractionation sensitivity needs to be tested in a more clinically relevant panel of isogenic cell lines (Tutt, Bertwistle et al. 2001; Foray, Marot et al. 2003; Farmer, McCabe et al. 2005). In addition the specific effects of cell cycle checkpoint controls on fraction size sensitivity can be investigated in p53 wild-type/null isogenic cell lines using similar experimental designs as described in this thesis (Borst, McLaughlin et al. 2012).

7.3.1.2 Testing hypothesis 2:

It is possible that the tight binding of chromatin by cohesin in late G2/S phase cells facilitates high fidelity repair whether achieved by HR or NHEJ. If so, the loss of fractionation sensitivity in late G2/S phase cells may not depend primarily on HR.

This model of fractionation sensitivity can be tested using wild-type (AA8) and HR- (irs1SF) CHO cells, comparing clonogenic survival of cells arrested in G0/G1 (serum starvation) with aphidicolin-synchronised S/G2 phase cells after low dose rate (1-2 cGy/min) or high dose rate irradiation (1-2 Gy/minute). If the above hypothesis is true, then cells in S/G2 phase will lose low dose rate sparing relative to G0/G1 cells.

7.3.1.3 Testing the effect of small molecule inhibitors on radiotherapy fractionation response:

Increasingly inhibitors of DNA repair pathways, checkpoint and growth factor signalling are being used as radiation sensitisers in clinical trials with fractionated RT (for example DNA-PK inhibitors, EGFR inhibitors (gefitinib/cetuximab), HER2 inhibitors (lapatinib) and Chk1 inhibitors (SAR-020106)). Currently we do not know how these drugs modulate fraction size sensitivity and this needs to be evaluated further if we want to exploit the interaction between drugs and radiation for maximum therapeutic gain. It is quite possible that certain interventions on molecular pathways could have an influence on the α/β ratio and thus, on the need to use high or low dose per fraction. Our data has shown the feasibility of testing the effect of various small molecule inhibitors on fractionated IR responses in CHO cells. This needs to be evaluated further in a more clinically relevant panel of p53 wild-type/null cell lines.

7.3.2 Implications for translational research:

If results from the above experiments suggest that sensitivity to fraction size is a function of HR repair and/or cell cycle phase and an intact G1/S checkpoint, this would generate a relatively simple model of fractionation sensitivity and provide a strong steer for biomarker development and clinical exploitation (as outlined in **Table 6.1**). If biological agents are shown to modify the fractionation response this raises the possibility of improving therapeutic index by selection of appropriate individualised dose prescriptions.

7.3.3 Molecular pathology

7.3.3.1 Identification of human tumour biomarkers:

Randomised clinical trials testing different fraction sizes are a unique resource for investigating biomarkers of fraction size sensitivity. We are currently undertaking a correlative study (Trans-FRACTION: Royal Marsden CCR 3079, NRES 08/H0801/53) analysing primary tumour blocks of 213 patients with local tumour relapse in the START pilot and START A breast hypofractionation trials. Tumour immunohistochemistry offers reliable measures of tumour proliferation (Ki67, Cyclin A), cell cycle checkpoint activation (p53, p21, CHK1/2), DNA damage response markers (BRCA1/2, ATM, PTEN) and growth factor signalling pathways (EGFR, HER2). The primary analysis compares the Ki67 distribution of primary tumours which relapse locally after radiotherapy fractions of 2.0 Gy with that of primary tumours relapsing after fractions >2.0 Gy. Other markers being studied include those of DNA repair, growth factor signalling and cell cycle checkpoints mentioned above. Although these are baselines samples it would be possible to enrich for HR defects based on ER, PR and HER2 with majority of triple negative tumours lacking functional HR (Graeser, McCarthy et al. 2010).

The UK national prostate cancer CHHIP trial testing hypofractionation versus standard fractionation is currently banking tissue microarrays from primary prostate tumours, funded by CRUK (>3000 expected in 2 years) . This will provide an invaluable resource to validate markers identified in Trans-FRACTION.

7.3.4 Clinical evaluation- prospective randomised trial

The long-term goal of this research will be to exploit biomarkers of fractionation sensitivity in curative radiotherapy. There is modest variation between patients in fractionation sensitivity of dose-limiting normal tissues (dose-response curves are

very steep), so the focus of this personalised approach will be tumour response. If robust biomarkers are identified this would translate in to a prospective randomised clinical trial testing low versus high dose per fraction based on baseline tumour biomarker profile, moving away from the ‘one fraction size fits all’ approach.

PUBLICATIONS ARISING FROM THIS WORK

1. **The relationship between homologous recombination repair and the sensitivity of human epidermis to the size of daily doses over a 5-week course of breast radiotherapy.** Navita Somaiah, John Yarnold, Frances Daley, Ann Pearson, Lone Gothard, Kai Rothkamm and Thomas Helleday. Clinical Cancer Research 2012 Aug 1; 18:5479-5488. PMID: 22855580. **Selected by Editor as 'Highlights of the issue'**

Cancer Therapy: Clinical

Clinical Cancer Research

The Relationship Between Homologous Recombination Repair and the Sensitivity of Human Epidermis to the Size of Daily Doses Over a 5-Week Course of Breast Radiotherapy

Navita Somaiah[1,2], John Yarnold[2], Frances Daley[2], Ann Pearson[2], Lone Gothard[2], Kai Rothkamm[3], and Thomas Helleday[4]

Abstract

Purpose: A molecular understanding of tissue sensitivity to radiotherapy fraction size is missing. Here, we test the hypothesis that sensitivity to fraction size is influenced by the DNA repair system activated in response to DNA double-strand breaks (DSB). Human epidermis was used as a model in which proliferation and DNA repair were correlated over 5 weeks of radiotherapy.

Experimental design: Radiotherapy (25 fractions of 2 Gy) was prescribed to the breast in 30 women with early breast cancer. Breast skin biopsies were collected 2 hours after the 1st and 25th fractions. Samples of contralateral breast skin served as controls. Sections were coimmunostained for Ki67, cyclin A, p21, RAD51, 53BP1, and β1-integrin.

Results: After 5 weeks of radiotherapy, the mean basal Ki67 density increased from 5.72 to 15.46 cells per millimeter of basement membrane ($P = 0.002$), of which the majority were in S/G2 phase, as judged by cyclin A staining ($P < 0.0003$). The p21 index rose from 2.8% to 87.4% ($P < 0.0001$) after 25 fractions, indicating cell cycle arrest. By week 5, there was a 4-fold increase ($P = 0.0003$) in the proportion of Ki67-positive cells showing RAD51 foci, suggesting increasing activation of homologous recombination.

Conclusions: Cell cycle arrest in S/G2 phase in the basal epidermis after a 5-week course of radiotherapy is associated with greater use of homologous recombination for repairing DSB. The high fidelity of homologous recombination, which is independent of DNA damage levels, may explain the low-fractionation sensitivity of tissues with high-proliferative indices, including self-renewing normal tissues and many cancers. *Clin Cancer Res; 18(19); 5479–88.* ©2012 AACR.



Colorectal Patient-Derived Tumor Models

Julien *et al.* _____ **Page 5314**

The work of Julien and colleagues represents the joint effort of a public/private consortium to characterize a new collection of patient-derived colorectal cancer models and evaluate drug sensitivity as a means to improve the standard of care. Maintenance of this repository of clinical features, even with the highly heterogeneous colorectal cancers, is allowing correlation with drug sensitivity and patient clinical history. Beyond the cetuximab sensitivity shown to be associated with *KRAS* status, this collection opens up new avenues to evaluate new targeted therapies or biomarkers in experimental phase II trials. Moreover, the occurrence of metastases emphasizes the value of patient-derived xenograft models as preclinical models relevant for translational research.

PET Imaging of xC⁻ Transporter in Lung and Breast Cancer

Baek *et al.* _____ **Page 5427**

System xC⁻ plays an important role in growth and progression of cancer and glutathione-based drug resistance. The xCT subunit of system xC⁻ is stabilized by CD44 enabling better regulation of redox status. Baek and colleagues conducted an exploratory clinical trial with (4S)-4-(3-[^{18}F]fluoropropyl)-L-glutamate ([^{18}F]FSPG) in patients with non–small cell lung or breast cancer. The authors observed a high cancer detection rate of [^{18}F]FSPG positron emission tomography (PET) and a correlation of [^{18}F]FSPG uptake with the expression of the xCT subunit of system xC⁻ together with CD44. These findings suggest that [^{18}F]FSPG PET can be used to assess xC⁻ transporter activity in cancer patients.

Effects of Mixed Bacterial Vaccine

Karbach *et al.* _____ **Page 5449**

Mixed bacterial vaccine (MBV; Coley's toxins) is a historical, vaguely defined preparation of heat-inactivated *Streptococcus pyogenes* and *Serratia marcescens* used as nonspecific immunotherapy in the treatment of cancer. Karbach and colleagues revisit Coley's toxins with a phase I clinical trial examining the immune-modulatory and clinical effects of a new, biochemically well-defined and cGMP-compliant MBV preparation. The study shows safety and evidence of *in vivo* MBV effects through the production of inflammatory cytokines. These findings clearly indicate that a strong "danger signal" evokes measurable inflammatory immune responses that render MBV as a potent adjuvant treatment in combination with different strategies to treat cancer, including cancer vaccines.

Homologous Recombination and Fraction Size Sensitivity

Somaiah *et al.* _____ **Page 5479**

Normal tissues are typically more sensitive to the size of daily doses (fractions) of radiotherapy than cancers are. However, recent evidence indicates that breast and prostate cancer are more sensitive to fraction size than is commonly assumed. Using human epidermis as a model, Somaiah and colleagues show that homologous recombination repair of radiation-induced DNA breaks is progressively activated during a course of radiotherapy. This finding correlates with the loss of fractionation sensitivity seen clinically. Adoption of homologous recombination, due to its high fidelity, may explain the loss of fractionation sensitivity in rapidly cycling normal and malignant tissues and suggests a potential approach to individualized treatment.

2. **Homologous recombination mediates cellular resistance and fraction size sensitivity to radiation therapy.** Navita Somaiah, John Yarnold, Anne Lagerqvist, Kai Rothkamm and Thomas Helleday. Radiotherapy and Oncology 2013;108(1):155-61.
3. **A New DNA Damage Checkpoint Regulating the G0 – G1 Transition.** Christina Bauerschmidt, Navita Somaiah, Michael Woodcock, Eric O'Neil, and Thomas Helleday. (Manuscript in preparation)
4. **The effect of different small molecule inhibitors of DNA repair on fractionated radiation responses.** Navita Somaiah, Anne Lagerqvist, Mamun, Kai Rothkamm, John Yarnold and Thomas Helleday. (Manuscript under review by Radiotherapy and Oncology)

REFERENCES

"CHHIP Trial. ISRCTN97182923. A randomised phase III multi-centre trial of Conventional or Hypofractionated High dose Intensity modulated radiotherapy for Prostate cancer. Further information from chhip-icrctsu@icr.ac.uk."

"IMPORT HIGH. ISRCTN47437448. Randomised trial testing dose escalated intensity modulated radiotherapy in women with higher than average local tumour recurrence risk after breast conservation therapy for early breast cancer. Protocol information can be found at: http://www.controlled-trials.com/ISRCTN47437448/import+high."

"RTOG 1005 Protocol. A Phase III Trial Of Accelerated Whole Breast Irradiation With Hypofractionation Plus Concurrent Boost Versus Standard Whole Breast Irradiation Plus Sequential Boost For Early-Stage Breast Cancer. Protocol information is available at : http://www.rtog.org/ClinicalTrials/ProtocolTable/StudyDetails.aspx?study=1005."

"RTQA, *ART DECO* study details http://rttrialsqa.dnsalias.org/ART-DECO/artdeco_web-siteMar2011_summary.htm."

"UKCRN, *ART DECO* study protocol. http://public.ukcrn.org.uk/search/StudyDetail.aspx?StudyID=9562."

(2011). "First results of the randomised UK FAST Trial of radiotherapy hypofractionation for treatment of early breast cancer (CRUKE/04/015)." Radiother Oncol **100**(1): 93-100.

Abbas, T. and A. Dutta (2009). "p21 in cancer: intricate networks and multiple activities." Nat Rev Cancer **9**(6): 400-414.

Alao, J. P. and P. Sunnerhagen (2009). "The ATM and ATR inhibitors CGK733 and caffeine suppress cyclin D1 levels and inhibit cell proliferation." Radiat Oncol **4**: 51.

Ali, M., B. A. Telfer, et al. (2009). "Vasoactivity of AG014699, a clinically active small molecule inhibitor of poly(ADP-ribose) polymerase: a contributory factor to chemopotentiation in vivo?" Clin Cancer Res **15**(19): 6106-6112.

Allen, C., J. Halbrook, et al. (2003). "Interactive competition between homologous recombination and non-homologous end joining." Mol Cancer Res **1**(12): 913-920.

Allen, C., A. Kurimasa, et al. (2002). "DNA-dependent protein kinase suppresses double-strand break-induced and spontaneous homologous recombination." Proc Natl Acad Sci U S A **99**(6): 3758-3763.

Ambler, C. A. and A. Maatta (2009). "Epidermal stem cells: location, potential and contribution to cancer." J Pathol **217**(2): 206-216.

Arai, T., T. Kuroishi, et al. (1994). "Tumor doubling time and prognosis in lung cancer patients: evaluation from chest films and clinical follow-up study. Japanese Lung Cancer Screening Research Group." Jpn J Clin Oncol **24**(4): 199-204.

Asakawa, H., H. Koizumi, et al. (2010). "Prediction of breast cancer sensitivity to neoadjuvant chemotherapy based on status of DNA damage repair proteins." Breast Cancer Res **12**(2): R17.

Audeh, M. W., J. Carmichael, et al. (2010). "Oral poly(ADP-ribose) polymerase inhibitor olaparib in patients with BRCA1 or BRCA2 mutations and recurrent ovarian cancer: a proof-of-concept trial." Lancet **376**(9737): 245-251.

Badie, C., G. Alsbeih, et al. (1996). "Dose-rate effects on the survival of irradiated hypersensitive and normal human fibroblasts." Int J Radiat Biol **70**(5): 563-570.

Bakkenist, C. J. and M. B. Kastan (2003). "DNA damage activates ATM through intermolecular autophosphorylation and dimer dissociation." Nature **421**(6922): 499-506.
Banath, J. P. and P. L. Olive (2003). "Expression of phosphorylated histone H2AX as a surrogate of cell killing by drugs that create DNA double-strand breaks." Cancer Res **63**(15): 4347-4350.
Banin, S., L. Moyal, et al. (1998). "Enhanced phosphorylation of p53 by ATM in response to DNA damage." Science **281**(5383): 1674-1677.
Bao, S., Q. Wu, et al. (2006). "Glioma stem cells promote radioresistance by preferential activation of the DNA damage response." Nature **444**(7120): 756-760.
Barendsen, G. W. (1982). "Dose fractionation, dose rate and iso-effect relationships for normal tissue responses." Int J Radiat Oncol Biol Phys **8**(11): 1981-1997.
Bartek, J. and J. Lukas (2003). "Chk1 and Chk2 kinases in checkpoint control and cancer." Cancer Cell **3**(5): 421-429.
Bartkova, J., I. Z. Horej Sbreve, et al. (2007). "DNA damage response mediators MDC1 and 53BP1: constitutive activation and aberrant loss in breast and lung cancer, but not in testicular germ cell tumours." Oncogene.
Bartkova, J., Z. Horejsi, et al. (2005). "DNA damage response as a candidate anti-cancer barrier in early human tumorigenesis." Nature **434**(7035): 864-870.
Bates, T. and R. G. Evans (1995). "Audit of brachial plexus neuropathy following radiotherapy." Clin Oncol (R Coll Radiol) **7**(4): 236.
Bauerschmidt, C., C. Arrichiello, et al. (2010). "Cohesin promotes the repair of ionizing radiation-induced DNA double-strand breaks in replicated chromatin." Nucleic Acids Res **38**(2): 477-487.
Baumann, M., M. Krause, et al. (2007). "EGFR-targeted anti-cancer drugs in radiotherapy: Preclinical evaluation of mechanisms." Radiother Oncol **83**(3): 238-248.
Begg, A. C., F. A. Stewart, et al. (2011). "Strategies to improve radiotherapy with targeted drugs." Nat Rev Cancer **11**(4): 239-253.
Bekker-Jensen, S., C. Lukas, et al. (2006). "Spatial organization of the mammalian genome surveillance machinery in response to DNA strand breaks." J Cell Biol **173**(2): 195-206.
Benjamin, R. C. and D. M. Gill (1980). "Poly(ADP-ribose) synthesis in vitro programmed by damaged DNA. A comparison of DNA molecules containing different types of strand breaks." J Biol Chem **255**(21): 10502-10508.
Bentzen, S. M. (2006). "Preventing or reducing late side effects of radiation therapy: radiobiology meets molecular pathology." Nat Rev Cancer **6**(9): 702-713.
Bentzen, S. M., R. K. Agrawal, et al. (2008). "The UK Standardisation of Breast Radiotherapy (START) Trial A of radiotherapy hypofractionation for treatment of early breast cancer: a randomised trial." Lancet Oncol **9**(4): 331-341.
Bentzen, S. M., R. K. Agrawal, et al. (2008). "The UK Standardisation of Breast Radiotherapy (START) Trial B of radiotherapy hypofractionation for treatment of early breast cancer: a randomised trial." Lancet **371**(9618): 1098-1107.
Bentzen, S. M., J. J. Christensen, et al. (1988). "Some methodological problems in estimating radiobiological parameters from clinical data. Alpha/beta ratios and electron RBE for cutaneous reactions in patients treated with postmastectomy radiotherapy." Acta Oncol **27**(2): 105-116.
Bentzen, S. M., P. M. Harari, et al. (2007). "Exploitable mechanisms for combining drugs with radiation: concepts, achievements and future directions." Nat Clin Pract Oncol **4**(3): 172-180.

Bentzen, S. M., J. Overgaard, et al. (1989). "Clinical radiobiology of malignant melanoma." Radiother Oncol **16**(3): 169-182.
Bentzen, S. M. and M. Overgaard (1991). "Relationship between early and late normal-tissue injury after postmastectomy radiotherapy." Radiother Oncol **20**(3): 159-165.
Bentzen, S. M., M. Overgaard, et al. (1989). "Fractionation sensitivity of a functional endpoint: impaired shoulder movement after post-mastectomy radiotherapy." Int J Radiat Oncol Biol Phys **17**(3): 531-537.
Bentzen, S. M. and M. A. Ritter (2005). "The alpha/beta ratio for prostate cancer: What is it, really?" Radiother Oncol **76**(1): 1-3.
Bentzen, S. M., M. I. Saunders, et al. (1999). "Repair halftimes estimated from observations of treatment-related morbidity after CHART or conventional radiotherapy in head and neck cancer." Radiother Oncol **53**(3): 219-226.
Bentzen, S. M., J. Z. Skoczylas, et al. (2000). "Quantitative clinical radiobiology of early and late lung reactions." Int J Radiat Biol **76**(4): 453-462.
Bentzen, S. M., I. Turesson, et al. (1990). "Fractionation sensitivity and latency of telangiectasia after postmastectomy radiotherapy: a graded-response analysis." Radiother Oncol **18**(2): 95-106.
Bernier, J. (2005). "Alteration of radiotherapy fractionation and concurrent chemotherapy: a new frontier in head and neck oncology?" Nat Clin Pract Oncol **2**(6): 305-314.
Bernier, J. and S. M. Bentzen (2003). "Altered fractionation and combined radio-chemotherapy approaches: pioneering new opportunities in head and neck oncology." Eur J Cancer **39**(5): 560-571.
Beucher, A., J. Birraux, et al. (2009). "ATM and Artemis promote homologous recombination of radiation-induced DNA double-strand breaks in G2." EMBO J **28**(21): 3413-3427.
Bindra, R. S., M. E. Crosby, et al. (2007). "Regulation of DNA repair in hypoxic cancer cells." Cancer Metastasis Rev **26**(2): 249-260.
Blunt, T., N. J. Finnie, et al. (1995). "Defective DNA-dependent protein kinase activity is linked to V(D)J recombination and DNA repair defects associated with the murine scid mutation." Cell **80**(5): 813-823.
Bonner, J. A., P. M. Harari, et al. (2006). "Radiotherapy plus cetuximab for squamous-cell carcinoma of the head and neck." N Engl J Med **354**(6): 567-578.
Borst, G. R., M. McLaughlin, et al. (2012). "Targeted Radiosensitization by the Chk1 Inhibitor SAR-020106." Int J Radiat Oncol Biol Phys.
Boulton, S., S. Kyle, et al. (1996). "Wortmannin is a potent inhibitor of DNA double strand break but not single strand break repair in Chinese hamster ovary cells." Carcinogenesis **17**(11): 2285-2290.
Bouquet, F., M. Ousset, et al. (2011). "A DNA-dependent stress response involving DNA-PK occurs in hypoxic cells and contributes to cellular adaptation to hypoxia." J Cell Sci **124**(Pt 11): 1943-1951.
Bourhis, J., J. Overgaard, et al. (2006). "Hyperfractionated or accelerated radiotherapy in head and neck cancer: a meta-analysis." Lancet **368**(9538): 843-854.
Bristow, R. G. and R. P. Hill (2008). "Hypoxia and metabolism. Hypoxia, DNA repair and genetic instability." Nat Rev Cancer **8**(3): 180-192.
Brock, W. A., L. Milas, et al. (2004). "Radiosensitization of human and rodent cell lines by INO-1001, a novel inhibitor of poly(ADP-ribose) polymerase." Cancer Lett **205**(2): 155-160.
Bryant, H. E. and T. Helleday (2006). "Inhibition of poly (ADP-ribose) polymerase activates ATM which is required for subsequent homologous recombination repair." Nucleic Acids Res **34**(6): 1685-1691.

Bryant, H. E., N. Schultz, et al. (2005). "Specific killing of BRCA2-deficient tumours with inhibitors of poly(ADP-ribose) polymerase." Nature **434**(7035): 913-917.
Burma, S., B. P. Chen, et al. (2001). "ATM phosphorylates histone H2AX in response to DNA double-strand breaks." J Biol Chem **276**(45): 42462-42467.
Calabrese, C. R., R. Almassy, et al. (2004). "Anticancer chemosensitization and radiosensitization by the novel poly(ADP-ribose) polymerase-1 inhibitor AG14361." J Natl Cancer Inst **96**(1): 56-67.
Caldecott, K. and P. Jeggo (1991). "Cross-sensitivity of gamma-ray-sensitive hamster mutants to cross-linking agents." Mutat Res **255**(2): 111-121.
Caldecott, K. W. (2003). "Protein-protein interactions during mammalian DNA single-strand break repair." Biochem Soc Trans **31**(Pt 1): 247-251.
Caldecott, K. W. (2008). "Single-strand break repair and genetic disease." Nat Rev Genet **9**(8): 619-631.
Calvert, H. and A. Azzariti (2011). "The clinical development of inhibitors of poly(ADP-ribose) polymerase." Ann Oncol **22 Suppl 1**: i53-59.
Chadha, M., R. Woode, et al. (2009). "Results using 3-week accelerated whole-breast (WB) radiation
therapy (RT) and concomitant boost for early-stage node negative breast cancer." Int J Radiat Oncol Biol Phys **75**: S77.
Chalmers, A., P. Johnston, et al. (2004). "PARP-1, PARP-2, and the cellular response to low doses of ionizing radiation." Int J Radiat Oncol Biol Phys **58**(2): 410-419.
Chalmers, A. J. (2009). "The potential role and application of PARP inhibitors in cancer treatment." Br Med Bull **89**: 23-40.
Chalmers, A. J., E. M. Ruff, et al. (2009). "Cytotoxic effects of temozolomide and radiation are additive- and schedule-dependent." Int J Radiat Oncol Biol Phys **75**(5): 1511-1519.
Chan, N., M. Koritzinsky, et al. (2008). "Chronic hypoxia decreases synthesis of homologous recombination proteins to offset chemoresistance and radioresistance." Cancer Res **68**(2): 605-614.
Chan, N., I. M. Pires, et al. (2010). "Contextual synthetic lethality of cancer cell kill based on the tumor microenvironment." Cancer Res **70**(20): 8045-8054.
Chen, B. P., N. Uematsu, et al. (2007). "Ataxia telangiectasia mutated (ATM) is essential for DNA-PKcs phosphorylations at the Thr-2609 cluster upon DNA double strand break." J Biol Chem **282**(9): 6582-6587.
Chen, G., S. S. Yuan, et al. (1999). "Radiation-induced assembly of Rad51 and Rad52 recombination complex requires ATM and c-Abl." J Biol Chem **274**(18): 12748-12752.
Cohen, L. (1952). "Radiotherapy in breast cancer I. The dose-time relationship theoretical considerations." Br J Radiol **25**(300): 636-642.
Collette, S., L. Collette, et al. (2008). "Predictors of the risk of fibrosis at 10 years after breast conserving therapy for early breast cancer: a study based on the EORTC Trial 22881-10882 'boost versus no boost'." Eur J Cancer **44**(17): 2587-2599.
Collis, S. J., T. L. DeWeese, et al. (2005). "The life and death of DNA-PK." Oncogene **24**(6): 949-961.
Collis, S. J., M. J. Swartz, et al. (2003). "Enhanced radiation and chemotherapy-mediated cell killing of human cancer cells by small inhibitory RNA silencing of DNA repair factors." Cancer Res **63**(7): 1550-1554.
Coquerelle, T. M., K. F. Weibezahn, et al. (1987). "Rejoining of double strand breaks in normal human and ataxia-telangiectasia fibroblasts after exposure to 60Co gamma-rays, 241Am alpha-particles or bleomycin." Int J Radiat Biol Relat Stud Phys Chem Med **51**(2): 209-218.

Cordes, N. and V. Meineke (2003). "Cell adhesion-mediated radioresistance (CAM-RR). Extracellular matrix-dependent improvement of cell survival in human tumor and normal cells in vitro." Strahlenther Onkol **179**(5): 337-344.
Cordes, N. and V. Meineke (2004). "Integrin signalling and the cellular response to ionizing radiation." J Mol Histol **35**(3): 327-337.
Cornforth, M. N. and J. S. Bedford (1985). "On the nature of a defect in cells from individuals with ataxia-telangiectasia." Science **227**(4694): 1589-1591.
Courdi, A., C. Ortholan, et al. (2006). "Long-term results of hypofractionated radiotherapy and hormonal therapy without surgery for breast cancer in elderly patients." Radiother Oncol **79**(2): 156-161.
Coutard, H. (1937). "The Results and Methods of Treatment of Cancer by Radiation." Ann Surg **106**(4): 584-598.
Davidovic, L., M. Vodenicharov, et al. (2001). "Importance of poly(ADP-ribose) glycohydrolase in the control of poly(ADP-ribose) metabolism." Exp Cell Res **268**(1): 7-13.
Delacote, F., M. Han, et al. (2002). "An xrcc4 defect or Wortmannin stimulates homologous recombination specifically induced by double-strand breaks in mammalian cells." Nucleic Acids Res **30**(15): 3454-3463.
Denham, J. W., Q. J. Walker, et al. (1996). "Mucosal regeneration during radiotherapy. Trans Tasman Radiation Oncology Group (TROG)." Radiother Oncol **41**(2): 109-118.
Deschavanne, P. J., B. Fertil, et al. (1980). "Radiosensitivity and repair of radiation damage in human HF19 fibroblasts." Int J Radiat Biol Relat Stud Phys Chem Med **38**(2): 167-177.
Dewar, J. A., S. Benhamou, et al. (1988). "Cosmetic results following lumpectomy, axillary dissection and radiotherapy for small breast cancers." Radiother Oncol **12**(4): 273-280.
Di Leonardo, A., S. P. Linke, et al. (1994). "DNA damage triggers a prolonged p53-dependent G1 arrest and long-term induction of Cip1 in normal human fibroblasts." Genes Dev **8**(21): 2540-2551.
Dianov, G., A. Price, et al. (1992). "Generation of single-nucleotide repair patches following excision of uracil residues from DNA." Mol Cell Biol **12**(4): 1605-1612.
DiBiase, S. J., Z. C. Zeng, et al. (2000). "DNA-dependent protein kinase stimulates an independently active, nonhomologous, end-joining apparatus." Cancer Res **60**(5): 1245-1253.
Dische, S., W. M. Martin, et al. (1981). "Radiation myelopathy in patients treated for carcinoma of bronchus using a six fraction regime of radiotherapy." Br J Radiol **54**(637): 29-35.
Dische, S. and M. I. Saunders (1999). "The CHART regimen and morbidity." Acta Oncol **38**(2): 147-152.
Donovan, E., N. Bleakley, et al. (2007). "Randomised trial of standard 2D radiotherapy (RT) versus intensity modulated radiotherapy (IMRT) in patients prescribed breast radiotherapy." Radiother Oncol.
Dorr, W. (1997). "Three A's of repopulation during fractionated irradiation of squamous epithelia: Asymmetry loss, Acceleration of stem-cell divisions and Abortive divisions." Int J Radiat Biol **72**(6): 635-643.
Dorr, W. and J. H. Hendry (2001). "Consequential late effects in normal tissues." Radiother Oncol **61**(3): 223-231.
Douglas, B. G. and J. R. Castro (1984). "Novel fractionation schemes and high linear energy transfer." Prog Exp Tumor Res **28**: 152-165.
Douglas, B. G. and J. F. Fowler (1976). "The effect of multiple small doses of x rays on skin reactions in the mouse and a basic interpretation." Radiat Res **66**(2): 401-426.

Dubray, B., M. Henry-Amar, et al. (1995). "Radiation-induced lung damage after thoracic irradiation for Hodgkin's disease: the role of fractionation." Radiother Oncol **36**(3): 211-217.
Dungey, F. A., D. A. Loser, et al. (2008). "Replication-dependent radiosensitization of human glioma cells by inhibition of poly(ADP-Ribose) polymerase: mechanisms and therapeutic potential." Int J Radiat Oncol Biol Phys **72**(4): 1188-1197.
Durocher, D. and S. P. Jackson (2001). "DNA-PK, ATM and ATR as sensors of DNA damage: variations on a theme?" Curr Opin Cell Biol **13**(2): 225-231.
El Sharouni, S. Y., H. B. Kal, et al. (2003). "Accelerated regrowth of non-small-cell lung tumours after induction chemotherapy." Br J Cancer **89**(12): 2184-2189.
Elkind, M. M., H. Sutton-Gilbert, et al. (1967). "Sub-lethal and lethal radiation damage." Nature **214**(5093): 1088-1092.
Elkind, M. M. and H. Sutton (1959). "X-ray damage and recovery in mammalian cells in culture." Nature **184**: 1293-1295.
Elkind, M. M. and H. Sutton (1960). "Radiation response of mammalian cells grown in culture. 1. Repair of X-ray damage in surviving Chinese hamster cells." Radiat Res **13**: 556-593.
Ellis, F. (1969). "Dose, time and fractionation: a clincal hypothesis." Clinical Radiology **20**: 1-7.
Eriksson, A., R. Lewensoh, et al. (2002). "DNA-dependent protein kinase in leukaemia cells and correlation with drug sensitivity." Anticancer Res **22**(3): 1787-1793.
Eriksson, D. and T. Stigbrand (2010). "Radiation-induced cell death mechanisms." Tumour Biol **31**(4): 363-372.
Farmer, H., N. McCabe, et al. (2005). "Targeting the DNA repair defect in BRCA mutant cells as a therapeutic strategy." Nature **434**(7035): 917-921.
Fei, P. and W. S. El-Deiry (2003). "P53 and radiation responses." Oncogene **22**(37): 5774-5783.
Ferguson, D. O., J. M. Sekiguchi, et al. (2000). "The nonhomologous end-joining pathway of DNA repair is required for genomic stability and the suppression of translocations." Proc Natl Acad Sci U S A **97**(12): 6630-6633.
Ferguson, D. O., J. M. Sekiguchi, et al. (2000). "The interplay between nonhomologous end-joining and cell cycle checkpoint factors in development, genomic stability, and tumorigenesis." Cold Spring Harb Symp Quant Biol **65**: 395-403.
Ferguson, P. C., E. L. Boynton, et al. (1999). "Intradermal injection of autologous dermal fibroblasts improves wound healing in irradiated skin." J Surg Res **85**(2): 331-338.
Fertil, B., P. J. Deschavanne, et al. (1988). "Correlation between PLD repair capacity and the survival curve of human fibroblasts in exponential growth phase: analysis in terms of several parameters." Radiat Res **116**(1): 74-88.
Flatt, P. M., J. O. Price, et al. (1998). "Differential cell cycle checkpoint response in normal human keratinocytes and fibroblasts." Cell Growth Differ **9**(7): 535-543.
Fletcher, G. H. (1991). "Hypofractionation: lessons from complications." Radiother Oncol **20**(1): 10-15.
Fong, P. C., D. S. Boss, et al. (2009). "Inhibition of poly(ADP-ribose) polymerase in tumors from BRCA mutation carriers." N Engl J Med **361**(2): 123-134.
Foray, N., D. Marot, et al. (2003). "A subset of ATM- and ATR-dependent phosphorylation events requires the BRCA1 protein." EMBO J **22**(11): 2860-2871.

Foray, N., A. Priestley, et al. (1997). "Hypersensitivity of ataxia telangiectasia fibroblasts to ionizing radiation is associated with a repair deficiency of DNA double-strand breaks." Int J Radiat Biol **72**(3): 271-283.
Formenti, S. C., D. Gidea-Addeo, et al. (2007). "Phase I-II trial of prone accelerated intensity modulated radiation therapy to the breast to optimally spare normal tissue." J Clin Oncol **25**(16): 2236-2242.
Fornace, A. J., Jr. and J. B. Little (1980). "Normal repair of DNA single-strand breaks in patients with ataxia telangiectasia." Biochim Biophys Acta **607**(3): 432-437.
Fowler, J., R. Chappell, et al. (2001). "Is alpha/beta for prostate tumors really low?" Int J Radiat Oncol Biol Phys **50**(4): 1021-1031.
Fowler, J. F. (1983). "Dose response curves for organ function or cell survival." Br J Radiol **56**(667): 497-500.
Fowler, J. F. (1984). "Review: total doses in fractionated radiotherapy--implications of new radiobiological data." Int J Radiat Biol Relat Stud Phys Chem Med **46**(2): 103-120.
Fowler, J. F. (1989). "The linear-quadratic formula and progress in fractionated radiotherapy." Br J Radiol **62**(740): 679-694.
Fowler, J. F. (2005). "The radiobiology of prostate cancer including new aspects of fractionated radiotherapy." Acta Oncol **44**(3): 265-276.
Frankenberg, D., M. Frankenberg-Schwager, et al. (1984). "Split-dose recovery is due to the repair of DNA double-strand breaks." Int J Radiat Biol Relat Stud Phys Chem Med **46**(5): 541-553.
Freedman, G. M., P. R. Anderson, et al. (2007). "Four-week course of radiation for breast cancer using hypofractionated intensity modulated radiation therapy with an incorporated boost." Int J Radiat Oncol Biol Phys **68**(2): 347-353.
Fuller, L. F. and R. B. Painter (1988). "A Chinese hamster ovary cell line hypersensitive to ionizing radiation and deficient in repair replication." Mutat Res **193**(2): 109-121.
Ganguly, N. and S. P. Parihar (2009). "Human papillomavirus E6 and E7 oncoproteins as risk factors for tumorigenesis." J Biosci **34**(1): 113-123.
Gauter, B., O. Zlobinskaya, et al. (2002). "Rejoining of radiation-induced DNA double-strand breaks: pulsed-field electrophoresis analysis of fragment size distributions after incubation for repair." Radiat Res **157**(6): 721-733.
Geh, J. I., S. J. Bond, et al. (2006). "Systematic overview of preoperative (neoadjuvant) chemoradiotherapy trials in oesophageal cancer: evidence of a radiation and chemotherapy dose response." Radiother Oncol **78**(3): 236-244.
Golding, S. E., E. Rosenberg, et al. (2009). "Improved ATM kinase inhibitor KU-60019 radiosensitizes glioma cells, compromises insulin, AKT and ERK prosurvival signaling, and inhibits migration and invasion." Mol Cancer Ther **8**(10): 2894-2902.
Gorgoulis, V. G., L. V. Vassiliou, et al. (2005). "Activation of the DNA damage checkpoint and genomic instability in human precancerous lesions." Nature **434**(7035): 907-913.
Gorodetsky, R., W. H. McBride, et al. (1991). "Effect of fibroblast implants on wound healing of irradiated skin: assay of wound strength and quantitative immunohistology of collagen." Radiat Res **125**(2): 181-186.
Gottipati, P., B. Vischioni, et al. (2010). "Poly(ADP-ribose) polymerase is hyperactivated in homologous recombination-defective cells." Cancer Res **70**(13): 5389-5398.
Graeser, M., A. McCarthy, et al. (2010). "A marker of homologous recombination predicts pathologic complete response to neoadjuvant chemotherapy in primary breast cancer." Clin Cancer Res **16**(24): 6159-6168.

Gu, Y., S. Jin, et al. (1997). "Ku70-deficient embryonic stem cells have increased ionizing radiosensitivity, defective DNA end-binding activity, and inability to support V(D)J recombination." Proc Natl Acad Sci U S A **94**(15): 8076-8081.
Guha, C., U. Guha, et al. (2000). "Antisense ATM gene therapy: a strategy to increase the radiosensitivity of human tumors." Gene Ther **7**(10): 852-858.
Guha, C., A. Sharma, et al. (1999). "Amelioration of radiation-induced liver damage in partially hepatectomized rats by hepatocyte transplantation." Cancer Res **59**(23): 5871-5874.
Hammond, E. M., R. A. Freiberg, et al. (2006). "The roles of Chk 1 and Chk 2 in hypoxia and reoxygenation." Cancer Lett **238**(2): 161-167.
Hansen, L. T., C. Lundin, et al. (2003). "DNA repair rate and etoposide (VP16) resistance of tumor cell subpopulations derived from a single human small cell lung cancer." Lung Cancer **40**(2): 157-164.
Haustermans, K. M., I. Hofland, et al. (1997). "Cell kinetic measurements in prostate cancer." Int J Radiat Oncol Biol Phys **37**(5): 1067-1070.
Helleday, T. (2011). "The underlying mechanism for the PARP and BRCA synthetic lethality: clearing up the misunderstandings." Mol Oncol **5**(4): 387-393.
Helleday, T., J. Lo, et al. (2007). "DNA double-strand break repair: from mechanistic understanding to cancer treatment." DNA Repair (Amst) **6**(7): 923-935.
Hendry, J. H. (1992). "Treatment acceleration in radiotherapy: the relative time factors and dose-response slopes for tumours and normal tissues." Radiother Oncol **25**(4): 308-312.
Hewitt, G., D. Jurk, et al. (2012). "Telomeres are favoured targets of a persistent DNA damage response in ageing and stress-induced senescence." Nat Commun **3**: 708.
Hickson, I., Y. Zhao, et al. (2004). "Identification and characterization of a novel and specific inhibitor of the ataxia-telangiectasia mutated kinase ATM." Cancer Res **64**(24): 9152-9159.
Higgins, G. S., R. Prevo, et al. (2010). "A small interfering RNA screen of genes involved in DNA repair identifies tumor-specific radiosensitization by POLQ knockdown." Cancer Res **70**(7): 2984-2993.
Hlatky, L., M. Olesiak, et al. (1996). "Measurement of potential doubling time for human tumor xenografts using the cytokinesis-block method." Cancer Res **56**(7): 1660-1663.
Holloway, C. L., V. Panet-Raymond, et al. (2010). "Hypofractionation should be the new 'standard' for radiation therapy after breast conserving surgery." Breast **19**(3): 163-167.
Hopewell, J. W., J. Nyman, et al. (2003). "Time factor for acute tissue reactions following fractionated irradiation: a balance between repopulation and enhanced radiosensitivity." Int J Radiat Biol **79**(7): 513-524.
Hoskin, P. J., A. Sibtain, et al. (2004). "The immunohistochemical assessment of hypoxia, vascularity and proliferation in bladder carcinoma." Radiother Oncol **72**(2): 159-168.
Jackson, S. P. (2002). "Sensing and repairing DNA double-strand breaks." Carcinogenesis **23**(5): 687-696.
Jazayeri, A., J. Falck, et al. (2006). "ATM- and cell cycle-dependent regulation of ATR in response to DNA double-strand breaks." Nat Cell Biol **8**(1): 37-45.
Jeggo, P. A., K. Caldecott, et al. (1989). "Sensitivity of Chinese hamster ovary mutants defective in DNA double strand break repair to topoisomerase II inhibitors." Cancer Res **49**(24 Pt 1): 7057-7063.
Jeggo, P. A., V. Geuting, et al. (2011). "The role of homologous recombination in radiation-induced double-strand break repair." Radiother Oncol **101**(1): 7-12.
Jensen, U. B., S. Lowell, et al. (1999). "The spatial relationship between stem cells and their progeny in the basal layer of human epidermis: a new view based

on whole-mount labelling and lineage analysis." Development **126**: 2409-2418.
Jensen, U. B., S. Lowell, et al. (1999). "The spatial relationship between stem cells and their progeny in the basal layer of human epidermis: a new view based on whole-mount labelling and lineage analysis." Development **126**(11): 2409-2418.
Jiang, G. L., S. L. Tucker, et al. (1994). "Radiation-induced injury to the visual pathway." Radiother Oncol **30**(1): 17-25.
Jones, B., R. G. Dale, et al. (2001). "The role of biologically effective dose (BED) in clinical oncology." Clin Oncol (R Coll Radiol) **13**(2): 71-81.
Jones, B., R. G. Dale, et al. (2000). "Biological equivalent dose assessment of the consequences of hypofractionated radiotherapy." Int J Radiat Oncol Biol Phys **47**(5): 1379-1384.
Jones, P. H., S. Harper, et al. (1995). "Stem cell patterning and fate in human epidermis." Cell **80**(1): 83-93.
Judas, L., S. M. Bentzen, et al. (1996). "Proliferative response of mouse spermatogonial stem cells after irradiation: a quantitative model analysis of experimental data." Cell Prolif **29**(2): 73-87.
Kastan, M. B. and D. S. Lim (2000). "The many substrates and functions of ATM." Nat Rev Mol Cell Biol **1**(3): 179-186.
Kastan, M. B., O. Onyekwere, et al. (1991). "Participation of p53 protein in the cellular response to DNA damage." Cancer Res **51**(23 Pt 1): 6304-6311.
Kirova, Y. M., F. Campana, et al. (2009). "Breast-conserving treatment in the elderly: long-term results of adjuvant hypofractionated and normofractionated radiotherapy." Int J Radiat Oncol Biol Phys **75**(1): 76-81.
Kogelnik, H. D. (1997). "Inauguration of radiotherapy as a new scientific speciality by Leopold Freund 100 years ago." Radiother Oncol **42**(3): 203-211.
Kozlov, S. V., M. E. Graham, et al. (2006). "Involvement of novel autophosphorylation sites in ATM activation." EMBO J **25**(15): 3504-3514.
Krempler, A., D. Deckbar, et al. (2007). "An imperfect G2M checkpoint contributes to chromosome instability following irradiation of S and G2 phase cells." Cell Cycle **6**(14): 1682-1686.
Kruger, I., K. Rothkamm, et al. (2004). "Enhanced fidelity for rejoining radiation-induced DNA double-strand breaks in the G2 phase of Chinese hamster ovary cells." Nucleic Acids Res **32**(9): 2677-2684.
Kuhne, M., E. Riballo, et al. (2004). "A double-strand break repair defect in ATM-deficient cells contributes to radiosensitivity." Cancer Res **64**(2): 500-508.
Kuhne, M., K. Rothkamm, et al. (2000). "No dose-dependence of DNA double-strand break misrejoining following alpha-particle irradiation." Int J Radiat Biol **76**(7): 891-900.
Kurimasa, A., S. Kumano, et al. (1999). "Requirement for the kinase activity of human DNA-dependent protein kinase catalytic subunit in DNA strand break rejoining." Mol Cell Biol **19**(5): 3877-3884.
Kuroda, S., Y. Urata, et al. (2012). "Ataxia-telangiectasia mutated and the Mre11-Rad50-NBS1 complex: promising targets for radiosensitization." Acta Med Okayama **66**(2): 83-92.
Lambin P, W., B (2004). "Molecular explanation of variation in the alpha/beta ratio." ESTRO News **58**: 13.
Leahy, J. J., B. T. Golding, et al. (2004). "Identification of a highly potent and selective DNA-dependent protein kinase (DNA-PK) inhibitor (NU7441) by screening of chromenone libraries." Bioorg Med Chem Lett **14**(24): 6083-6087.
Lee, H., J. M. Larner, et al. (1997). "Cloning and characterization of Chinese hamster p53 cDNA." Gene **184**(2): 177-183.

Lee, S. P., M. Y. Leu, et al. (1995). "Biologically effective dose distribution based on the linear quadratic model and its clinical relevance." Int J Radiat Oncol Biol Phys **33**(2): 375-389.
Lee, W. R., G. E. Hanks, et al. (1995). "Observations of pretreatment prostate-specific antigen doubling time in 107 patients referred for definitive radiotherapy." Int J Radiat Oncol Biol Phys **31**(1): 21-24.
Legg, J., U. B. Jensen, et al. (2003). "Role of melanoma chondroitin sulphate proteoglycan in patterning stem cells in human interfollicular epidermis." Development **130**(24): 6049-6063.
Li, A., P. J. Simmons, et al. (1998). "Identification and isolation of candidate human keratinocyte stem cells based on cell surface phenotype." Proc Natl Acad Sci U S A **95**(7): 3902-3907.
Lievens, Y. (2010). "Hypofractionated breast radiotherapy: financial and economic consequences." Breast **19**(3): 192-197.
Lind, P. A., B. Wennberg, et al. (2006). "ROC curves and evaluation of radiation-induced pulmonary toxicity in breast cancer." Int J Radiat Oncol Biol Phys **64**(3): 765-770.
Lindell, R. M., T. E. Hartman, et al. (2007). "Five-year lung cancer screening experience: CT appearance, growth rate, location, and histologic features of 61 lung cancers." Radiology **242**(2): 555-562.
Little, J. B., A. M. Ueno, et al. (1989). "Differential response of human and rodent cell lines to chemical inhibition of the repair of potentially lethal damage." Radiat Environ Biophys **28**(3): 193-202.
Liu, N., J. E. Lamerdin, et al. (1998). "XRCC2 and XRCC3, new human Rad51-family members, promote chromosome stability and protect against DNA cross-links and other damages." Mol Cell **1**(6): 783-793.
Lobrich, M. and P. A. Jeggo (2005). "Harmonising the response to DSBs: a new string in the ATM bow." DNA Repair (Amst) **4**(7): 749-759.
Lobrich, M., M. Kuhne, et al. (2000). "Joining of correct and incorrect DNA double-strand break ends in normal human and ataxia telangiectasia fibroblasts." Genes Chromosomes Cancer **27**(1): 59-68.
Lou, Z., K. Minter-Dykhouse, et al. (2006). "MDC1 maintains genomic stability by participating in the amplification of ATM-dependent DNA damage signals." Mol Cell **21**(2): 187-200.
Lukas, C., J. Falck, et al. (2003). "Distinct spatiotemporal dynamics of mammalian checkpoint regulators induced by DNA damage." Nat Cell Biol **5**(3): 255-260.
Maciejewski, B., J. M. Taylor, et al. (1986). "Alpha/beta value and the importance of size of dose per fraction for late complications in the supraglottic larynx." Radiother Oncol **7**(4): 323-326.
Maciejewski, B., H. R. Withers, et al. (1989). "Dose fractionation and regeneration in radiotherapy for cancer of the oral cavity and oropharynx: tumor dose-response and repopulation." Int J Radiat Oncol Biol Phys **16**(3): 831-843.
Majumdar, D., X. H. Peng, et al. (2010). "The medicinal chemistry of theragnostics, multimodality imaging and applications of nanotechnology in cancer." Curr Top Med Chem **10**(12): 1211-1226.
Matsuoka, S., B. A. Ballif, et al. (2007). "ATM and ATR substrate analysis reveals extensive protein networks responsive to DNA damage." Science **316**(5828): 1160-1166.
Matsuoka, S., G. Rotman, et al. (2000). "Ataxia telangiectasia-mutated phosphorylates Chk2 in vivo and in vitro." Proc Natl Acad Sci U S A **97**(19): 10389-10394.
McGale, P. and S. C. Darby (2005). "Low doses of ionizing radiation and circulatory diseases: a systematic review of the published epidemiological evidence." Radiat Res **163**(3): 247-257.

Meistrich, M. L., N. R. Hunter, et al. (1978). "Gradual regeneration of mouse testicular stem cells after exposure to ionizing radiation." Radiat Res **74**(2): 349-362.
Meng, A. X., F. Jalali, et al. (2005). "Hypoxia down-regulates DNA double strand break repair gene expression in prostate cancer cells." Radiother Oncol **76**(2): 168-176.
Miescher, G. (1935). "Tierexperimentelle Untersuchungen über den Einfluβ der Fraktionierung auf den Späteffekt." Acta Radiol **16**: 25-38.
Miralbell, R., S. A. Roberts, et al. (2012). "Dose-fractionation sensitivity of prostate cancer deduced from radiotherapy outcomes of 5,969 patients in seven international institutional datasets: alpha/beta = 1.4 (0.9-2.2) Gy." Int J Radiat Oncol Biol Phys **82**(1): e17-24.
Morgan, M. A., L. A. Parsels, et al. (2010). "Mechanism of radiosensitization by the Chk1/2 inhibitor AZD7762 involves abrogation of the G2 checkpoint and inhibition of homologous recombinational DNA repair." Cancer Res **70**(12): 4972-4981.
Morris, G. M. and J. W. Hopewell (1986). "Changes in the cell kinetics of pig epidermis after repeated daily doses of X rays." Br J Radiol Suppl **19**: 34-38.
Morrison, C., E. Sonoda, et al. (2000). "The controlling role of ATM in homologous recombinational repair of DNA damage." EMBO J **19**(3): 463-471.
Mortusewicz, O., J. C. Ame, et al. (2007). "Feedback-regulated poly(ADP-ribosyl)ation by PARP-1 is required for rapid response to DNA damage in living cells." Nucleic Acids Res **35**(22): 7665-7675.
Moulder, J. E., M. E. Robbins, et al. (1998). "Pharmacologic modification of radiation-induced late normal tissue injury." Cancer Treat Res **93**: 129-151.
Nakajima, M., S. Nakasu, et al. (1998). "Estimation of volume doubling time and cell loss in an experimental rat glioma model in vivo." Acta Neurochir (Wien) **140**(6): 607-612; discussion 612-603.
Nam, J. M., Y. Chung, et al. (2009). "beta1 integrin targeting to enhance radiation therapy." Int J Radiat Biol **85**(11): 923-928.
Neal, J. A., V. Dang, et al. (2011). "Inhibition of homologous recombination by DNA-dependent protein kinase requires kinase activity, is titratable, and is modulated by autophosphorylation." Mol Cell Biol **31**(8): 1719-1733.
Nevanlinna, H. and J. Bartek (2006). "The CHEK2 gene and inherited breast cancer susceptibility." Oncogene **25**(43): 5912-5919.
Nutley, B. P., N. F. Smith, et al. (2005). "Preclinical pharmacokinetics and metabolism of a novel prototype DNA-PK inhibitor NU7026." Br J Cancer **93**(9): 1011-1018.
Nyman, J. and I. Turesson (1994). "Basal cell density in human skin for various fractionation schedules in radiotherapy." Radiother Oncol **33**(2): 117-124.
Nyman, J. and I. Turesson (1995). "Does the interval between fractions matter in the range of 4-8 h in radiotherapy? A study of acute and late human skin reactions." Radiother Oncol **34**(3): 171-178.
Orecchia, R., M. Ciocca, et al. (2005). "Intraoperative electron beam radiotherapy (ELIOT) to the breast: a need for a quality assurance programme." Breast **14**(6): 541-546.
Orton, C. G. (2001). "High-dose-rate brachytherapy may be radiobiologically superior to low-dose rate due to slow repair of late-responding normal tissue cells." Int J Radiat Oncol Biol Phys **49**(1): 183-189.
Owen, J. R., A. Ashton, et al. (2006). "Effect of radiotherapy fraction size on tumour control in patients with early-stage breast cancer after local tumour excision: long-term results of a randomised trial." Lancet Oncol **7**(6): 467-471.
Paterson, R. (1936). "Experiences in Manchester with the Metropolitan-Vickers Tube: (Section of Radiology)." Proc R Soc Med **29**(5): 449-452.

Pawlik, T. M. and K. Keyomarsi (2004). "Role of cell cycle in mediating sensitivity to radiotherapy." Int J Radiat Oncol Biol Phys **59**(4): 928-942.
Peer, D., J. M. Karp, et al. (2007). "Nanocarriers as an emerging platform for cancer therapy." Nat Nanotechnol **2**(12): 751-760.
Peer, P. G., J. A. van Dijck, et al. (1993). "Age-dependent growth rate of primary breast cancer." Cancer **71**(11): 3547-3551.
Plummer, R., C. Jones, et al. (2008). "Phase I study of the poly(ADP-ribose) polymerase inhibitor, AG014699, in combination with temozolomide in patients with advanced solid tumors." Clin Cancer Res **14**(23): 7917-7923.
Postiglione, I., A. Chiaviello, et al. (2010). "Twilight effects of low doses of ionizing radiation on cellular systems: a bird's eye view on current concepts and research." Med Oncol **27**(2): 495-509.
Powell, C., C. Mikropoulos, et al. (2010). "Pre-clinical and clinical evaluation of PARP inhibitors as tumour-specific radiosensitisers." Cancer Treat Rev **36**(7): 566-575.
Powell, S., J. Cooke, et al. (1990). "Radiation-induced brachial plexus injury: follow-up of two different fractionation schedules." Radiother Oncol **18**(3): 213-220.
Prevo, R., E. Deutsch, et al. (2008). "Class I PI3 kinase inhibition by the pyridinylfuranopyrimidine inhibitor PI-103 enhances tumor radiosensitivity." Cancer Res **68**(14): 5915-5923.
Puck, T. T., D. Morkovin, et al. (1957). "Action of x-rays on mammalian cells. II. Survival curves of cells from normal human tissues." J Exp Med **106**(4): 485-500.
Qvarnstrom, O. F., M. Simonsson, et al. (2004). "DNA double strand break quantification in skin biopsies." Radiother Oncol **72**(3): 311-317.
Rachidi, W., G. Harfourche, et al. (2007). "Sensing radiosensitivity of human epidermal stem cells." Radiother Oncol **83**(3): 267-276.
Ragaz, J., I. A. Olivotto, et al. (2005). "Locoregional radiation therapy in patients with high-risk breast cancer receiving adjuvant chemotherapy: 20-year results of the British Columbia randomized trial." J Natl Cancer Inst **97**(2): 116-126.
Rainey, M. D., M. E. Charlton, et al. (2008). "Transient inhibition of ATM kinase is sufficient to enhance cellular sensitivity to ionizing radiation." Cancer Res **68**(18): 7466-7474.
Rancati, T., B. Wennberg, et al. (2007). "Early clinical and radiological pulmonary complications following breast cancer radiation therapy: NTCP fit with four different models." Radiother Oncol **82**(3): 308-316.
Rao, B. S., K. Tano, et al. (2007). "Split dose recovery studies using homologous recombination deficient gene knockout chicken B lymphocyte cells." J Radiat Res (Tokyo) **48**(1): 77-85.
Regaud, C. (1923). "Principes du traitement des épithéliomas épidermoïdes par les radiations. Application aux épidermoïdes de la peau et de la bouche." J Radiol **7**: 297-322.
Regaud, C. (1977). "The influence of the duration of irradiation on the changes produced in the testicle by radium." Int J Radiat Oncol Biol Phys **2**(5-6): 565-567.
Regaud, C. and R. Ferroux (1919). "Durée d'application en radium-thérapie, procédés de notation et de calcul, table pour l'emploi de l'émanation du radium." J Radiol Electrol **3**: 481.
Reisner, A. (1933). "Hauterythem und Röntgenstrahlung." Erg.Med.Strahlenforsch. **6**: 1-60.
Rew, D. A. and G. D. Wilson (2000). "Cell production rates in human tissues and tumours and their significance. Part 1: an introduction to the techniques of measurement and their limitations." Eur J Surg Oncol **26**(3): 227-238.

Rew, D. A. and G. D. Wilson (2000). "Cell production rates in human tissues and tumours and their significance. Part II: clinical data." Eur J Surg Oncol **26**(4): 405-417.

Rezvani, M., C. J. Alcock, et al. (1991). "Normal tissue reactions in the British Institute of Radiology Study of 3 fractions per week versus 5 fractions per week in the treatment of carcinoma of the laryngo-pharynx by radiotherapy." Br J Radiol **64**(768): 1122-1133.

Rezvani, M., J. F. Fowler, et al. (1993). "Sensitivity of human squamous cell carcinoma of the larynx to fractionated radiotherapy." Br J Radiol **66**(783): 245-255.

Rezvani, M., J. W. Hopewell, et al. (1998). "Repair, repopulation and cell cycle redistribution in rat foot skin." Radiother Oncol **46**(2): 193-199.

Riballo, E., M. Kuhne, et al. (2004). "A pathway of double-strand break rejoining dependent upon ATM, Artemis, and proteins locating to gamma-H2AX foci." Mol Cell **16**(5): 715-724.

Ribeiro-Silva, A., M. A. Moutinho, et al. (2006). "Expression of checkpoint kinase 2 in breast carcinomas: correlation with key regulators of tumor cell proliferation, angiogenesis, and survival." Histol Histopathol **21**(4): 373-382.

Rodemann, H. P., K. Dittmann, et al. (2007). "Radiation-induced EGFR-signaling and control of DNA-damage repair." Int J Radiat Biol **83**(11-12): 781-791.

Rodier, F., J. P. Coppe, et al. (2009). "Persistent DNA damage signalling triggers senescence-associated inflammatory cytokine secretion." Nat Cell Biol **11**(8): 973-979.

Rodriguez-Jimenez, F. J., V. Moreno-Manzano, et al. (2008). "Hypoxia causes downregulation of mismatch repair system and genomic instability in stem cells." Stem Cells **26**(8): 2052-2062.

Rosenzweig, K. E., M. B. Youmell, et al. (1997). "Radiosensitization of human tumor cells by the phosphatidylinositol3-kinase inhibitors wortmannin and LY294002 correlates with inhibition of DNA-dependent protein kinase and prolonged G2-M delay." Clin Cancer Res **3**(7): 1149-1156.

Rothkamm, K., I. Kruger, et al. (2003). "Pathways of DNA double-strand break repair during the mammalian cell cycle." Mol Cell Biol **23**(16): 5706-5715.

Rothkamm, K., M. Kuhne, et al. (2001). "Radiation-induced genomic rearrangements formed by nonhomologous end-joining of DNA double-strand breaks." Cancer Res **61**(10): 3886-3893.

Rothkamm, K. and M. Lobrich (2002). "Misrepair of radiation-induced DNA double-strand breaks and its relevance for tumorigenesis and cancer treatment (review)." Int J Oncol **21**(2): 433-440.

Russo, A. L., H. C. Kwon, et al. (2009). "In vitro and in vivo radiosensitization of glioblastoma cells by the poly (ADP-ribose) polymerase inhibitor E7016." Clin Cancer Res **15**(2): 607-612.

Saleh-Gohari, N. and T. Helleday (2004). "Conservative homologous recombination preferentially repairs DNA double-strand breaks in the S phase of the cell cycle in human cells." Nucleic Acids Res **32**(12): 3683-3688.

Sarkaria, J. N., R. S. Tibbetts, et al. (1998). "Inhibition of phosphoinositide 3-kinase related kinases by the radiosensitizing agent wortmannin." Cancer Res **58**(19): 4375-4382.

Satoh, M. S. and T. Lindahl (1992). "Role of poly(ADP-ribose) formation in DNA repair." Nature **356**(6367): 356-358.

Savitsky, K., A. Bar-Shira, et al. (1995). "A single ataxia telangiectasia gene with a product similar to PI-3 kinase." Science **268**(5218): 1749-1753.

Schmidt-Ullrich, R. K., J. N. Contessa, et al. (2003). "ERBB receptor tyrosine kinases and cellular radiation responses." Oncogene **22**(37): 5855-5865.

Schreiber, V., F. Dantzer, et al. (2006). "Poly(ADP-ribose): novel functions for an old molecule." Nat Rev Mol Cell Biol **7**(7): 517-528.
Schultz, L. B., N. H. Chehab, et al. (2000). "p53 binding protein 1 (53BP1) is an early participant in the cellular response to DNA double-strand breaks." J Cell Biol **151**(7): 1381-1390.
Shaheen, F. S., P. Znojek, et al. (2011). "Targeting the DNA double strand break repair machinery in prostate cancer." PLoS One **6**(5): e20311.
Shen, H., M. Schultz, et al. (1998). "Increased expression of DNA-dependent protein kinase confers resistance to adriamycin." Biochim Biophys Acta **1381**(2): 131-138.
Shibamoto, Y., O. Ike, et al. (1998). "Proliferative activity and micronucleus frequency after radiation of lung cancer cells as assessed by the cytokinesis-block method and their relationship to clinical outcome." Clin Cancer Res **4**(3): 677-682.
Shiloh, Y. and A. R. Lehmann (2004). "Maintaining integrity." Nat Cell Biol **6**(10): 923-928.
Shimomatsuya, T., N. Tanigawa, et al. (1991). "Proliferative activity of human tumors: assessment using bromodeoxyuridine and flow cytometry." Jpn J Cancer Res **82**(3): 357-362.
Shrivastav, M., L. P. De Haro, et al. (2008). "Regulation of DNA double-strand break repair pathway choice." Cell Res **18**(1): 134-147.
Shrivastav, M., C. A. Miller, et al. (2009). "DNA-PKcs and ATM co-regulate DNA double-strand break repair." DNA Repair (Amst) **8**(8): 920-929.
Singh, K. (1978). "Two regimes with the same TDF but differing morbidity used in the treatment of stage III carcinoma of the cervix." Br J Radiol **51**(605): 357-362.
Smith, G. C. and S. P. Jackson (1999). "The DNA-dependent protein kinase." Genes Dev **13**(8): 916-934.
Smulson, M., N. Istock, et al. (1994). "Deletion mutants of poly(ADP-ribose) polymerase support a model of cyclic association and dissociation of enzyme from DNA ends during DNA repair." Biochemistry **33**(20): 6186-6191.
So, S., A. J. Davis, et al. (2009). "Autophosphorylation at serine 1981 stabilizes ATM at DNA damage sites." J Cell Biol **187**(7): 977-990.
Somaiah, N., J. Yarnold, et al. (2012). "Homologous recombination mediates cellular resistance and fraction size sensitivity to radiation therapy." (Submitted for publication).
Somaiah, N., J. R. Yarnold, et al. (2012). "The relationship between homologous recombination repair and sensitivity of human epidermis to the size of daily doses over a 5-week course of breast radiotherapy." Clin Cancer Res.
Spratt, J. S., J. S. Meyer, et al. (1996). "Rates of growth of human neoplasms: Part II." J Surg Oncol **61**(1): 68-83.
Stamato, T. D., R. Weinstein, et al. (1983). "Isolation of cell cycle-dependent gamma ray-sensitive Chinese hamster ovary cell." Somatic Cell Genet **9**(2): 165-173.
Steel, G. G. (1991). "The ESTRO Breur lecture. Cellular sensitivity to low dose-rate irradiation focuses the problem of tumour radioresistance." Radiother Oncol **20**(2): 71-83.
Steel, G. G., T. J. McMillan, et al. (1989). "The picture has changed in the 1980s." Int J Radiat Biol **56**(5): 525-537.
Stephens, P. J., P. S. Tarpey, et al. (2012). "The landscape of cancer genes and mutational processes in breast cancer." Nature **486**(7403): 400-404.
Stewart, F. A. and A. Van der Kogel (2002). Proliferative and cellular organization of normal tissues. Basic Clinical Radiobiology. G. G. Steel. London, Arnold**:** 23-29.

Strandqvist, M. (1944). "Studien über die kumulative Wirkung der Röntgenstrahlen bei Fraktionierung. Erfahrungen aus dem Radiumhemmet an 280 Haut- und Lippenkarzinomen." Acta Radiol (Suppl.) **55**: 1-300.

Stucki, M. and S. P. Jackson (2006). "gammaH2AX and MDC1: anchoring the DNA-damage-response machinery to broken chromosomes." DNA Repair (Amst) **5**(5): 534-543.

Sturgeon, C. M., Z. A. Knight, et al. (2006). "Effect of combined DNA repair inhibition and G2 checkpoint inhibition on cell cycle progression after DNA damage." Mol Cancer Ther **5**(4): 885-892.

Stuschke, M. and H. D. Thames (1999). "Fractionation sensitivities and dose-control relations of head and neck carcinomas: analysis of the randomized hyperfractionation trials." Radiother Oncol **51**(2): 113-121.

Supiot, S., S. Shubbar, et al. (2008). "A phase I trial of pre-operative radiotherapy for prostate cancer: clinical and translational studies." Radiother Oncol **88**(1): 53-60.

Tanaka, T., T. Yamagami, et al. (1993). "The scid mutation in mice causes defects in the repair system for both double-strand DNA breaks and DNA cross-links." Mutat Res **288**(2): 277-280.

Tavecchio, M., J. M. Munck, et al. (2012). "Further characterisation of the cellular activity of the DNA-PK inhibitor, NU7441, reveals potential cross-talk with homologous recombination." Cancer Chemother Pharmacol **69**(1): 155-164.

Taylor, A. M., D. G. Harnden, et al. (1975). "Ataxia telangiectasia: a human mutation with abnormal radiation sensitivity." Nature **258**(5534): 427-429.

Taylor, C. W., A. Nisbet, et al. (2007). "Cardiac exposures in breast cancer radiotherapy: 1950s-1990s." Int J Radiat Oncol Biol Phys **69**(5): 1484-1495.

Thacker, J. and R. E. Wilkinson (1995). "The genetic basis of cellular recovery from radiation damage: response of the radiosensitive irs lines to low-dose-rate irradiation." Radiat Res **144**(3): 294-300.

Thames, H. D., S. M. Bentzen, et al. (1989). "Fractionation parameters for human tissues and tumors." Int J Radiat Biol **56**(5): 701-710.

Thames, H. D., S. M. Bentzen, et al. (1990). "Time-dose factors in radiotherapy: a review of the human data." Radiother Oncol **19**(3): 219-235.

Thames, H. D. and J. H. Hendry (1987). Fractionation in radiotherapy. London, Taylor and Francis.

Thames, H. D., Jr., H. R. Withers, et al. (1982). "Changes in early and late radiation responses with altered dose fractionation: implications for dose-survival relationships." Int J Radiat Oncol Biol Phys **8**(2): 219-226.

Thames, H. D. and H. D. Suit (1986). "Tumor radioresponsiveness versus fractionation sensitivity." Int J Radiat Oncol Biol Phys **12**(4): 687-691.

Thomas, H. D., C. R. Calabrese, et al. (2007). "Preclinical selection of a novel poly(ADP-ribose) polymerase inhibitor for clinical trial." Mol Cancer Ther **6**(3): 945-956.

Thompson, L. H., K. W. Brookman, et al. (1982). "A CHO-cell strain having hypersensitivity to mutagens, a defect in DNA strand-break repair, and an extraordinary baseline frequency of sister-chromatid exchange." Mutat Res **95**(2-3): 427-440.

Thompson, L. H., S. Fong, et al. (1980). "Validation of conditions for efficient detection of HPRT and APRT mutations in suspension-cultured Chinese hamster ovary cells." Mutat Res **74**(1): 21-36.

Thompson, L. H. and D. Schild (2001). "Homologous recombinational repair of DNA ensures mammalian chromosome stability." Mutat Res **477**(1-2): 131-153.

Toulany, M. and H. P. Rodemann (2010). "Membrane receptor signaling and control of DNA repair after exposure to ionizing radiation." Nuklearmedizin **49 Suppl 1**: S26-30.

Trott, K. R. (1986). "What can the experience of radiation therapy teach us about accidents?" Br J Radiol Suppl **19**: 28-30.
Trott, K. R. (1999). "The mechanisms of acceleration of repopulation in squamous epithelia during daily irradiation." Acta Oncol **38**(2): 153-157.
Trott, K. R., B. Maciejewski, et al. (1984). "Dose-response curve and split-dose recovery in human skin cancer." Radiother Oncol **2**(2): 123-129.
Turesson, I., R. Bernefors, et al. (2001). "Normal tissue response to low doses of radiotherapy assessed by molecular markers--a study of skin in patients treated for prostate cancer." Acta Oncol **40**(8): 941-951.
Turesson, I., J. Nyman, et al. (1996). "Prognostic factors for acute and late skin reactions in radiotherapy patients." Int J Radiat Oncol Biol Phys **36**(5): 1065-1075.
Turesson, I., J. Nyman, et al. (2010). "A low-dose hypersensitive keratinocyte loss in response to fractionated radiotherapy is associated with growth arrest and apoptosis." Radiother Oncol **94**(1): 90-101.
Turesson, I. and H. D. Thames (1989). "Repair capacity and kinetics of human skin during fractionated radiotherapy: erythema, desquamation, and telangiectasia after 3 and 5 year's follow-up." Radiother Oncol **15**(2): 169-188.
Turner, N., A. Tutt, et al. (2004). "Hallmarks of 'BRCAness' in sporadic cancers." Nat Rev Cancer **4**(10): 814-819.
Tutt, A., D. Bertwistle, et al. (2001). "Mutation in Brca2 stimulates error-prone homology-directed repair of DNA double-strand breaks occurring between repeated sequences." EMBO J **20**(17): 4704-4716.
Uematsu, N., E. Weterings, et al. (2007). "Autophosphorylation of DNA-PKCS regulates its dynamics at DNA double-strand breaks." J Cell Biol **177**(2): 219-229.
Utsumi, H. and M. M. Elkind (1994). "Inhibitors of poly (ADP-ribose) synthesis inhibit the two types of repair of potentially lethal damage." Int J Radiat Oncol Biol Phys **29**(3): 577-578.
Utsumi, H. and M. M. Elkind (2001). "Requirement for repair of DNA double-strand breaks by homologous recombination in split-dose recovery." Radiat Res **155**(5): 680-686.
Vaidya, J. S., M. Baum, et al. (2010). "Long-term Results of Targeted Intraoperative Radiotherapy (Targit) Boost during Breast-conserving Surgery." Int J Radiat Oncol Biol Phys.
van den Aardweg, G. J. and J. W. Hopewell (1992). "The kinetics of repair for sublethal radiation-induced damage in the pig epidermis: an interpretation based on a fast and a slow component of repair." Radiother Oncol **23**(2): 94-104.
Veuger, S. J., N. J. Curtin, et al. (2003). "Radiosensitization and DNA repair inhibition by the combined use of novel inhibitors of DNA-dependent protein kinase and poly(ADP-ribose) polymerase-1." Cancer Res **63**(18): 6008-6015.
Veuger, S. J. and B. W. Durkacz (2011). "Persistence of unrepaired DNA double strand breaks caused by inhibition of ATM does not lead to radio-sensitisation in the absence of NF-kappaB activation." DNA Repair (Amst) **10**(2): 235-244.
Veuger, S. J., J. E. Hunter, et al. (2009). "Ionizing radiation-induced NF-kappaB activation requires PARP-1 function to confer radioresistance." Oncogene **28**(6): 832-842.
Vogelstein, B., D. Lane, et al. (2000). "Surfing the p53 network." Nature **408**(6810): 307-310.
Weterings, E. and D. C. van Gent (2004). "The mechanism of non-homologous end-joining: a synopsis of synapsis." DNA Repair (Amst) **3**(11): 1425-1435.

Whelan, T., R. MacKenzie, et al. (2002). "Randomized trial of breast irradiation schedules after lumpectomy for women with lymph node-negative breast cancer." J Natl Cancer Inst **94**(15): 1143-1150.
Whelan, T. J., J. P. Pignol, et al. (2010). "Long-Term Results of Hypofractionated Radiation Therapy for Breast Cancer." N Engl J Med **362**(6): 513-520.
White, O., J. A. Eisen, et al. (1999). "Genome sequence of the radioresistant bacterium Deinococcus radiodurans R1." Science **286**(5444): 1571-1577.
Whitmore, G. F., A. J. Varghese, et al. (1989). "Cell cycle responses of two X-ray sensitive mutants defective in DNA repair." Int J Radiat Biol **56**(5): 657-665.
Willers, H., A. G. Taghian, et al. (2009). "Utility of DNA repair protein foci for the detection of putative BRCA1 pathway defects in breast cancer biopsies." Mol Cancer Res **7**(8): 1304-1309.
Williams, M. V., J. Denekamp, et al. (1985). "A review of alpha/beta ratios for experimental tumors: implications for clinical studies of altered fractionation." Int J Radiat Oncol Biol Phys **11**(1): 87-96.
Willmore, E., S. de Caux, et al. (2004). "A novel DNA-dependent protein kinase inhibitor, NU7026, potentiates the cytotoxicity of topoisomerase II poisons used in the treatment of leukemia." Blood **103**(12): 4659-4665.
Wilson, P. F., J. M. Hinz, et al. (2010). "Influence of homologous recombinational repair on cell survival and chromosomal aberration induction during the cell cycle in gamma-irradiated CHO cells." DNA Repair (Amst) **9**(7): 737-744.
Withers, H. R. (1975). "The four R's of radiotherapy." Adv. Radiat. Res. **15**: 241-247.
Withers, H. R. (1989). "Failla memorial lecture. Contrarian concepts in the progress of radiotherapy." Radiat Res **119**(3): 395-412.
Withers, H. R. (1992). Biologic basis of radiation therapy. Principles and practice of radiation oncology. C. A. Perez and L. W. Brady. Philadelphia, J.B. Lippincott Co**:** 64-96.
Withers, H. R., H. D. Thames, Jr., et al. (1983). "A new isoeffect curve for change in dose per fraction." Radiother Oncol **1**(2): 187-191.
Won, J., M. Kim, et al. (2006). "Small molecule-based reversible reprogramming of cellular lifespan." Nat Chem Biol **2**(7): 369-374.
Yamamoto, A., T. Taki, et al. (1996). "Cell cycle-dependent expression of the mouse Rad51 gene in proliferating cells." Mol Gen Genet **251**(1): 1-12.
Yarnold, J., A. Ashton, et al. (2005). "Fractionation sensitivity and dose response of late adverse effects in the breast after radiotherapy for early breast cancer: long-term results of a randomised trial." Radiother Oncol **75**(1): 9-17.
Yarnold, J. and J. Haviland (2010). "Hypofractionated adjuvant whole breast radiotherapy: progress and prospects." Acta Oncol **49**(8): 1288-1292.
Zhao, Y., H. D. Thomas, et al. (2006). "Preclinical evaluation of a potent novel DNA-dependent protein kinase inhibitor NU7441." Cancer Res **66**(10): 5354-5362.
Zhou, B. B., P. Chaturvedi, et al. (2000). "Caffeine abolishes the mammalian G(2)/M DNA damage checkpoint by inhibiting ataxia-telangiectasia-mutated kinase activity." J Biol Chem **275**(14): 10342-10348.